MOLECULAR MECHANISMS REGULATING PLURIPOTENCY AND DIFFERENTIATION OF HUMAN EMBRYONIC STEM CELLS

by

ANGELOS PAPADOPOULOS

A thesis submitted to

The University of Birmingham

for the degree of

DOCTOR OF PHILOSOPHY

School of Biosciences

College of Life and Environmental Sciences

University of Birmingham

March 2018

UNIVERSITY OF
BIRMINGHAM

University of Birmingham Research Archive

e-theses repository

This unpublished thesis/dissertation is copyright of the author and/or third parties. The intellectual property rights of the author or third parties in respect of this work are as defined by The Copyright Designs and Patents Act 1988 or as modified by any successor legislation.

Any use made of information contained in this thesis/dissertation must be in accordance with that legislation and must be properly acknowledged. Further distribution or reproduction in any format is prohibited without the permission of the copyright holder.

To my beloved parents for their unconditional love and support

To my mentors for showing me the way

ABSTRACT

Dr James A. Thomson and co-workers reached a milestone discovery in 1998, as they managed to isolate and in vitro expand embryonic stem cells originating from ‘’fresh or frozen cleavage stage human embryos’’. These had been ‘’produced by in vitro fertilization (IVF) for clinical purposes and donated by individuals after informed.” Since then, along with mouse embryonic stem (mES) cells, human embryonic stem (hES) cells have served as excellent tools used for the understanding and evaluation of a plethora of events that take place during mammalian embryogenesis. A full and comprehensive analysis of the molecular mechanisms that regulate both pluripotency and differentiation procedures will ultimately allow these cells to be utilised for therapeutic purposes. A first and decisive step in that direction would be to elucidate the action of TGFβ superfamily members, Activin A and BMP4, as they constitute key ligands that influence the fate of hES cells.

The first part of the present thesis is dedicated to investigating the implication of ADP-Ribosylation Factor 6 (ARF6) in TGFβ superfamily signalling. ARF6 is a low molecular weight GTPase involved in many cellular functions including membrane trafficking, adhesion, abscission and lipid homeostasis. Our preliminary data indicate that ARF6 interacts with SMAD4, the co-SMAD that facilitates the transition of phosphorylated SMADs to the nucleus, where they regulate transcription. Building on that, we uncover novel interactions of ARF6 with proteins SMAD2/3 and the interconnection between nucleotide status and downstream signalling events.

The connection between ARF6 and TGFβ signalling led us to hypothesize a role for the GTPase in hES cells. In that system, we characterise the effects of ARF6

activation or knockout on both Activin A and BMP4 signalling. In addition, we uncover a role for the GTPase during mesendoderm specification as it is found to influence the expression levels of BRACHYURY, a transcription factor upregulated during the early stages of differentiation.

In the last part of the thesis, we utilise a broad transcriptomic approach to reveal novel candidates that are implicated in early differentiation of hES cells to mesendoderm. The assay has been carried out using a novel, versatile culture system that is based on the ability of Activin A to preserve pluripotency and BMP4 to initiate differentiation.

CONTENTS

Thesis Aims and Contributions *16*

1.1 Aims and Experimental Approach **16**

1.2 Contributions **17**

Introduction *18*

2.1 Stem Cells: An Overview **18**

2.1.1 Stem Cell Classification Based on Differentiation Potency 18

2.1.2 Stem Cell Classification Based on Origin 19

2.1.3 Stem Cell Therapeutic Potential and Reported Cases 24

2.2 Human Embryonic Stem Cells **25**

2.2.1 Human Early Embryogenesis 25

2.2.2 Major Pluripotency Transcription Factors in hES cells 33

2.2.3 Major Signalling Pathways in hES cells 36

2.3 Signalling and Trafficking of TGFβ Superfamily Members **41**

2.3.1 TGFβ Superfamily Components 41

2.3.1.1 TGFβ Superfamily Ligands 41

2.3.1.2 TGFβ Superfamily Ligand Binding Factors 42

2.3.1.3 TGFβ Superfamily Receptors and Co-Receptors 43

2.3.2 SMAD Signalling Pathways 45

2.3.2.1 SMAD Proteins 45

2.3.2.2 SMAD Machinery Regulation 49

2.3.2.3 SMAD Transcriptional Regulation 51

2.3.3 Non-SMAD Signalling Pathways 54

2.3.3.1 MAPK/ERK Signalling Pathway 54

2.3.3.2 JNK and p38 Signalling Pathways 55
2.3.3.3 Rho-like GTPases Signalling Pathways 55
2.3.3.4 PI3K/AKT Signalling Pathway 56
2.3.4 Trafficking of TGFβ Family Receptors 57
2.3.4.1 Endocytic Routes 57
2.3.4.2 Endocytic Compartments 60
2.3.4.3 Endocytic Routes of TGFβ Receptors 64
2.3.4.4 Endocytic Routes of Activin Receptors 65
2.3.4.5 Endocytic Routes of BMP Receptors 66
2.4 ARF6: An Overview 68
2.4.1 ARF6 Structure and Mutants 69
2.4.2 ARF6 Activation Machinery 71
2.4.3 ARF6 Inactivation Machinery 72
2.4.4 ARF6 in Endocytosis and Trafficking 74
2.5 Thesis Organisation and Objectives 76
2.5.1 Chapter 3: Elucidating the Role of ARF6 in Activin A / TGFβ Signalling 76
2.5.2 Chapter 4: Elucidating the Role of ARF6 in Human Embryonic Stem Cell Signalling 77
2.5.3 Chapter 5: Identifying Novel Molecules Implicated in Early Mesendoderm Specification by a Broad Transcriptomic Approach 77
Elucidating the Role of ARF6 in Activin A / TGFB Signalling 78
3.1 Introduction 78
3.2 Results 81
3.2.1 Activated ARF6 Interacts with the C-Terminal Tail of SMAD4 81
3.2.2 Activated ARF6 Interacts with the C-Terminal Tails of SMAD2/3 85
3.2.3 ARF6 is Implicated in Activin A / TGFβ Mediated SMAD2/3 Phosphorylation 88
3.2.4 Activin A / TGFβ Signalling Promotes ARF6 GTP – GDP Exchange 92

3.2.5 ARF6GAP SMAP1 Interacts Specifically with ACVR1B 94

3.2.6 SMAP1 CRISPR Knock-Out in HEK-293 Cells 96

3.2.7 SMAP1 is Responsible for the Activin A / TGFβ Mediated ARF6 GTP – GDP Exchange 99

3.3 Discussion 101

Elucidating the Role of ARF6 in Human Embryonic Stem Cell Signalling 104

4.1 Introduction 104

4.2 Results 106

4.2.1 Generation and Characterisation of the Fast Cycling ARF6 and GFP Control Stable H1 Cell Lines ... 106

4.2.2 ARF6 Activation Increases the Activin A Mediated SMAD2/3 Phosphorylation in H1 Cells 113

4.2.3 ARF6 Activation Increases the BMP4 Mediated SMAD1/5/9 Phosphorylation in H1 Cells 115

4.2.4 ARF6 Activation Reduces the Expression of BRACHYURY upon Mesendoderm Induction 117

4.2.5 Generation and Characterisation of ARF6 CRISPR Knock-Out H1 Cell Lines 121

4.2.6 ARF6 Knock-out Reduces the Activin A Mediated SMAD2/3 Phosphorylation in H1 Cells 129

4.2.7 ARF6 Knock-out Reduces the BMP4 Mediated SMAD1/5/9 Phosphorylation in H1 Cells 131

4.2.8 ARF6 Knock-out Increases the Expression of BRACHYURY upon Mesendoderm Induction 133

4.2.9 Activin A / BMP4 Signalling Promotes ARF6 GTP – GDP Exchange in H1 Cells 139

4.3 Discussion 141

Identifying Novel Molecules Implicated in Early Mesendoderm Specification by a Broad Transcriptomic Approach 145

5.1 Introduction 145

5.2 Results 147

5.2.1 H1 Cells Cultured in Activin A Based Media Remain Pluripotent 147

5.2.2 H1 Cells in Activin A mTeSR are Karyotypically Normal and Form Teratomas in NOD/SCID Mice ... 150

5.2.3 BMP4 Transcriptomics in H1 Cells Cultured in Activin A mTeSR 153

5.2.4 Molecular Pathways and Functions Enriched after BMP4 Treatment 156

5.3 Discussion 169

Conclusions and Future Directions 173

Materials and Methods 180

7.1 Cellular Biology Methods 180

7.1.1 Transformed Cells 180

7.1.1.1 Cell Culture 180

7.1.1.2 Plasmid / siRNA Transfections 181

7.1.2 Human Embryonic Stem Cells 183

7.1.2.1 Cell Culture 183

7.1.2.2 Plasmid Transfections 184

7.1.2.3 Cell Differentiation 185

7.2 Biochemical Methods 186

7.2.1 SDS-PAGE Electrophoresis and Western Blotting 186

7.2.2 GST Protein Amplification and Purification 188

7.2.3 GST Pull - Down 189

7.2.4 Co-Immunoprecipitation 189

7.2.5 Immunofluorescence 190

7.2.6 Karyotype Analysis 191

7.3 In Vivo Assays 192

7.3.1 Teratoma Formation 192

List of References 193

Appendix 214

LIST OF FIGURES

Figure 2.1: Stem Cell Hierarchy and Potency 22

Figure 2.2: Types of Stem Cell Division 23

Figure 2.3: Human Blastocyst Representation at Day 7 of Development 29

Figure 2.4: Human Blastocyst Representation at Day 8 of Development 30

Figure 2.5: Human Blastocyst Representation at Days 14-16 of Development 31

Figure 2.6: Timeline of Human Early Development 31

Figure 2.7: Human Developmental Ontology Tree 32

Figure 2.8: OCT4, NANOG and SOX2 in hES Cell Pluripotency 36

Figure 2.9: Major Signalling Pathways Regulating Pluripotency and Differentiation in hES cells 40

Figure 2.10: TGFβR Type I and II Structure 44

Figure 2.11: Structure of SMAD Proteins 48

Figure 2.12: Overview of TGF Signalling Components 49

Figure 2.13: Canonical TGF Signalling Cascades 53

Figure 2.14 Endocytic Compartments 63

Figure 2.15 ARF6 Structure in GDP/GTP Forms 70

Figure 3.1: Interaction of the Activated ARF6 with SMAD4 83

Figure 3.2: Mapping the Interaction of Activated ARF6 with SMAD4 84

Figure 3.3: Interaction of Activated ARF6 with SMAD2 and SMAD3 86

Figure 3.4: Immunoprecipitations of Activated ARF6 with SMAD2 and SMAD3 87

Figure 3.5: Effect of ARF6 Activation on SMAD2/3 Phosphorylation 90

Figure 3.6: Effect of ARF6 Knock-Down on SMAD2/3 Phosphorylation 91

Figure 3.7: Effect of Activin A / TGFβ on ARF6-GTP Loading 93

Figure 3.8: Interaction of SMAP1 with the Wild Type ACVR1B 95

Figure 3.9: CRISPR/CAS9 Vector Design for the Knock-out of SMAP1 97

Figure 3.10: SMAP1 CRISPR Knock-out in HEK-293 cells 98

Figure 3.11: Effect of Activin A / TGFβ Signalling on ARF6-GTP Loading in SMAP1KO Cells 100

Figure 4.1: Design of H1 ARF6T157A-GFP Stable Cell Lines 108

Figure 4.2: Expression of Pluripotency Factors in H1 ARF6T157A-GFP Cells and GFP Control Cells 111

Figure 4.3: Levels of Pluripotency Factors in H1 ARF6T157A-GFP Cells 112

Figure 4.4: Effect of ARF6 Activation on SMAD2/3 Phosphorylation 114

Figure 4.5: Effect of ARF6 Activation on SMAD1/5/9 Phosphorylation 116

Figure 4.6: Effect of ARF6 Activation on BRACHYURY Expression upon Mesendoderm Induction 118

Figure 4.7: Effect of ARF6 Activation on the Timing of BRACHYURY Expression upon Mesendoderm Induction 120

Figure 4.8: CRISPR/CAS9 Vector Design for the Knock-out of ARF6 123

Figure 4.9: Generation of HEK-293 and H1 ARF6KO Cell Lines 124

Figure 4.10: Expression of Pluripotency Factors in H1 ARF6KO Cells 127

Figure 4.11: Levels of Pluripotency Factors in H1 ARF6KO Cells 128

Figure 4.12: Effect of ARF6 Knock-out on SMAD2/3 Phosphorylation 130

Figure 4.13: Effect of ARF6 Knock-out on SMAD1/5/9 Phosphorylation 132

Figure 4.14: Effect of ARF6 Knock-out on BRACHYURY Expression upon Mesendoderm Induction 134

Figure 4.15: Effect of ARF6 Knock-out on the Timing of BRACHYURY Expression upon Mesendoderm Induction 136

Figure 4.16: Effect of ARF6 Knock-out on the Percentage of Cells Expressing BRACHYURY upon Mesendoderm Induction 138

Figure 4.17: Effect of Activin A / BMP4 Signalling on ARF6-GTP Loading 140

Figure 5.1: Expression Levels of Pluripotency Factors in H1 Cells Cultured in Activin A Based mTeSR 149

Figure 5.2: Karyotypic Analysis of H1 Cells Cultured in Activin A Based mTesR 151

Figure 5.3: Teratoma Formation Assay of H1 Cells Cultured in Activin A mTeSR 152

Figure 5.4: Overlap of Identified Transcripts 155

Figure 5.5: Enriched Biological Pathways (1hr BMP4 – UP transcripts) 158

Figure 5.6: Enriched Molecular Functions (1hr BMP4 – UP transcripts) 159

Figure 5.7: Deregulated KEGG Pathways (1hr BMP4 – UP transcripts) 161

Figure 5.8: Enriched Biological Pathways (4hrs BMP4 – UP transcripts) 163

Figure 5.9: Enriched Molecular Functions (4hrs BMP4 – UP transcripts) *164*

Figure 5.10: Deregulated KEGG Pathways (4hrs BMP4 – UP transcripts) *166*

Figure 5.11: Enriched Biological Pathways (4hrs BMP4 – DOWN transcripts) *168*

Figure 6.1: Proposed Model *174*

Supplementary Figure 1: Raw Data of Figure 3.1 (B) *214*

Supplementary Figure 2: Raw Data of Figure 3.4 (A) *214*

Supplementary Figure 3: Raw Data of Figure 3.4 (B) *215*

Supplementary Figure 4: Raw Data of Figure 3.4 (C) *215*

Supplementary Figure 5: Raw Data of Figure 3.4 (D) *216*

Supplementary Figure 6: Raw Data of Figure 3.8 (B) *217*

Supplementary Figure 7: Interaction of SMAP1 with the Wild Type ACVR1B *218*

LIST OF TABLES

Table 5.1 Quantity and Purity of RNA Used for RNA-Sequencing *154*

Table 7.1 Summary of Plasmids Used in Chapter 3 ..... *182*

Table 7.2 Summary of Plasmids Used in Chapter 4 ..... *185*

Table 7.3 Western Blotting Primary Antibodies *187*

Table 7.4 Western Blotting Secondary Antibodies *187*

Table 7.6 Immunofluorescence Primary Antibodies *190*

Table 7.7 Immunofluorescence Secondary Antibodies *191*

CONVENTIONS

The level of statistical significance in all the figures included is depicted by the use of significance stars.

* ⟶ $p < 0.05$

** ⟶ $p < 0.01$

*** ⟶ $p < 0.001$

**** ⟶ $p < 0.0001$

ABBREVIATIONS

ACVR1B	Activin A Receptor Type 1B
AMH	Anti-Müllerian hormone
ALP	Alkaline Phosphatase
ARF	ADP Ribosylation Factor
ARHGAP	Rho GTPase Activating Protein
AS	Adult Stem
BAMBI	BMP and Activin Membrane-Bound Inhibitor
bFGF	basic Fibroblast Growth Factor
BMP	Bone Morphogenetic Protein
CAG	Chicken β-ACTIN promoter
CAS9	CRISPR Associated Protein 9
cDNA	Complementary DNA
CME	Clathrin-Mediated Endocytosis
CLIC	Clathrin-Independent Carriers
CRISPR	Clustered Regularly Interspaced Short Palindromic Repeats
DMEM	Dulbecco`s Modified Eagle Media
DMSO	Dimethyl Sulfoxide
DNA	Deoxyribonucleic Acid
ECD	Extracellular Domain
EDTA	Ethylenediaminetetraacetic Acid
EMT	Epithelial to Mesenchymal Transition
ES	Embryonic Stem
ER	Endoplasmic Reticulum
ERK	Extracellular signal-Regulated Kinase
FCS	Foetal Calf Serum
FEME	Fast Endophilin-Mediated Endocytosis
FGF	Fibroblast Growth Factor
GAP	GTPase Activating Protein

GDP	Guanosine Diphosphate
GEEC	GPI-Enriched Early Endosomal Compartment
GEF	Guanine Nucleotide Exchange Factor
GFP	Green Fluorescence Protein
GPI-AP	Glycosylphosphatidylinositol-Anchored Proteins
gRNA	guide RNA
GST	Glutathione S-Transferase
GTP	Guanosine Triphosphate
GVHD	Graft-Versus Host Disease
HEK-293 cells	Human Embryonic Kidney – 293 cells
hES	human Embryonic Stem
HGF	Hepatocyte Growth Factor
HMG	High Mobility Group
HRP	Horseradish Peroxidase
iPS	induced Pluripotent Stem
IPTG	Isopropyl β-D-1-Thiogalactopyranoside
IRES	Internal Ribosome Entry Site
KEGG	Kyoto Encyclopaedia of Genes and Genomes
LAP	Latency-Associated Peptide
LIF	Leukaemia Inhibitor Factor
LB	Luria Broth
MCS	Multi Cloning Site
MDCK cells	Madin-Darby Canine Kidney cells
mES	mouse Embryonic Stem
MHC	Major Histocompatibility Complex
MS	Mesenchymal Stem
NLS	Nuclear Localisation Signal
NOD	Non-Obese Diabetic
OCT	Octamer-Binding Transcription Factor
PAGE	Polyacrylamide Gel Electrophoresis
PAM	Protospacer Adjacent Motif

PBS	Phosphate Buffered Saline
PLD	Phospholipase D
PMSF	Phenylmethylsulfonyl Fluoride
RNA	Ribonucleic Acid
ROCK	Rho-Associated Protein Kinase
SAD	SMAD4 Activation Domain
SARA	SMAD-Anchor for Receptor Activation
SCID	Severe Combined Immunodeficiency
SDS	Sodium Dodecyl Sulfate
siRNA	small interfering RNA
SMAD	Mothers Against Decapentaplegic Homolog
SMAP	Small ARFGAP
SOX	Sex Determining Region Y – Box
SPF	Specific Pathogen Free
S/TKD	Serine/Threonine Kinase Domain
TBS	Tris Buffered Saline
TBS-T	Tris Buffered Saline – Tween 20
TGF	Transforming Growth Factor
TGN	Trans-Golgi Network
TMD	Transmembrane Domain
TRIS–HCl	Tris Buffered Saline – Hydrochloric Acid

CHAPTER 1

THESIS AIMS AND CONTRIBUTIONS

1.1 Aims and Experimental Approach

The present thesis is devoted to deciphering the molecular mechanisms that regulate pluripotency and differentiation in hES cells. More specifically, we are interested in the regulation of TGFβ superfamily pathways by ARF6.

Pilot experiments conducted by our lab have yielded a potential interaction between SMAD4 and ARF6. Using HEK-293 cells, we validated this interaction and investigated new ones by performing pull-down and co-immunoprecipitation assays. Overexpression of activated mutants, RNA interference and the novel CRISPR technique were used to reveal potential alterations in signalling upon induction with different growth factors of the TGFβ superfamily.

The aforementioned gain and loss of function experiments were replicated in the versatile hES cell system. To overcome the limited transfection efficiency, we generated stable cell lines and CRISPR knock-outs. These lines were initially characterised by confocal microscopy and western blotting for the expression of key pluripotency factors. Potential effects during differentiation to mesendoderm were also examined.

In the last part of the thesis, we generated a novel medium for the culture of hES cells, based on the ability of Activin A to promote self-renewal under pluripotent conditions. Cells cultured in that system were used in an RNA sequencing screening,

after induction with BMP4, aiming to reveal novel candidates that are implicated in the onset of differentiation to mesendoderm.

1.2 Contributions

In the 3rd chapter of the present thesis we explored the role of ARF6 in TGFβ / Activin A signalling. We reported three novel interactions between ARF6 and proteins SMAD2, SMAD3 and SMAD4. In addition, we investigated the results of ARF6 activation or knock-down on SMAD2/3 phosphorylation and the outcome of TGFβ / Activin A signalling on the status of ARF6 GTP – loading. Last, we identified SMAP1 as a novel partner of ACVR1B that is responsible for the inactivation of the GTPase after activation of the TGFβ or Activin A signalling pathway.

In the 4th chapter, we investigated the role of ARF6 in hES cell signalling. We successfully generated novel activated ARF6 stable cell lines and CRISPR knock-outs. Initially, we demonstrated the result of ARF6 cycle status on SMAD2/3 and SMAD1/5/9 phosphorylation upon treatment with Activin A or BMP4, respectively. Using the same cell lines, we revealed a novel, undocumented role for ARF6 during differentiation of hES cells towards mesendoderm.

In the 5th chapter, we reported the development of a novel medium for the culture of hES cells. Utilising that, we managed to preserve cells in a pluripotent state based on the action of Activin A. Cells grown in that system were induced with BMP4 in two different time points and RNA sequencing was performed. The results yielded interesting new transcripts involved in the specification to mesendoderm.

CHAPTER 2

INTRODUCTION

2.1 Stem Cells: An Overview

Recent scientific findings revealed that the human body is comprised of approximately 37.2 billion cells (Bianconi et al., 2014). Each and every one of them is a direct offspring of the fertilised egg that carries all the necessary information to form an adult and fertile individual. During development, this massive amount of information is subsequently subdivided through consecutive rounds of cell division and specification. Gradually, this results in formation of specialised tissues comprised of cells with unique functions and narrow lifespans. The distinctive cellular property that drives this process is known as ‘’stemness’’.

Stemness is the ability of a cell to self-renew and differentiate into other cell types. Cells that demonstrate this ability are known as stem cells. Stem cells are indispensable to human physiology, both during development driving tissue formation, and throughout adulthood maintaining tissue homeostasis.

2.1.1 Stem Cell Classification Based on Differentiation Potency

Based on their differentiation capacity, stem cells can be characterised as totipotent, pluripotent, multipotent, oligopotent or unipotent (Kolios and Moodley, 2013). Totipotent cells are characterised by their ability to give rise to a fully functioning, fertile organism. In the case of mammalian embryogenesis only the fertilised oocyte and the two identical cells arising from the first mitotic division have that capacity (Condic,

2014). Pluripotent cells have the ability to differentiate into all germ layers (endoderm – mesoderm – ectoderm) including the germ line, i.e. primordial germ cells set aside early in embryogenesis (Condic, 2014). Multipotent cells reside in most adult tissues and have the capacity to differentiate into all cell types of a specific germ layer (Ratajczak et al., 2012). The most well studied cells in that category are mesenchymal stem (MS) cells. These have the potential to give rise to adipose or muscle tissue, bone and cartilage (Kfoury and Scadden, 2015). Oligopotent cells are able to self-renew and differentiate into at least 2 cell types of a single germ layer. The most prominent members of that category are haematopoietic stem (HS) cells that can give rise to both myeloid and lymphoid lineages. Being able to produce only T and B cells, lymphoid cells are known as bipotent (Pietras et al., 2011). Lastly, unipotent cells can only differentiate into a single cell type. Muscle stem cells are a typical example of unipotent cells (Bentzinger et al., 2013). The hierarchy of stem cells based on their differentiation potential is depicted in **Figure 2.1**.

2.1.2 Stem Cell Classification Based on Origin

Stem cells can be further segregated into groups based on their origin (Kolios and Moodley, 2013). Embryonic stem (ES) cells are derived from the inner cell mass (ICM) of the pre-implantation blastocyst and are thus considered to be pluripotent. Mouse embryonic stem (mES) cells were isolated and *in vitro* expanded for the first time in 1981 (Martin, 1981), with hES cells following almost two decades afterwards (Thomson et al., 1998). Signalling in both lines is mainly characterised by the expression of specific transcription factors such as NANOG, OCT4 and SOX2. These factors cooperate to inhibit differentiation and promote self-renewal (Saunders et al., 2013).

Interestingly, the same transcription factors have been found to possess separate roles during differentiation as well. For instance, SOX2 has been reported to be associated with the neuroectodermal fate (Kopp et al., 2008) and NANOG to affect the outcome of BMP4 induced differentiation, favouring mesendoderm (Yu et al., 2011). Additionally to the ICM, pre-morula blastomeres as well as the epiblast can also be sources of ES cells. However, mES cells originating from blastomeres or the ICM exhibit a distinct pluripotency state (naïve) to that of epiblast mES cells (primed). Also, the signalling profile of hES cells originating from either of the above sources resembles that of epiblast mES cells and are thus considered as ‘’primed’’, reviewed in: (De Los Angeles et al., 2015). Compared to ‘’naïve’’ mES cells, hES cells exhibit increased DNA methylation, X-chromosome inactivation, low cloning efficiency and favouring of glycolysis over oxidative phosphorylation. In addition, they rely on FGF2 and NODAL signalling for pluripotency maintenance, in contrast with ‘’naïve’’ mES cells that depend on LIF (Davidson et al., 2015). Reverting hES cells back to a ‘’naïve’’ state has been proven possible by supplementing culture media with a specific cocktail of factors and pathway inhibitors (Gafni et al., 2013).

The major limitations for using ES cells therapeutically are their availability and the ethical concerns arising from their foetal origin. These issues can be bypassed by cellular reprogramming, a technique that won the 2012 Nobel prize in Physiology or Medicine for Dr. Shinya Yamanaka. By introducing a combination of transcription factors (OCT4, SOX2, KLF4, c-MYC) Takahashi and Yamanaka were able to reprogram terminally differentiated mouse cells back to a pluripotent state (Takahashi and Yamanaka, 2006). Ever since, induced pluripotent stem (iPS) cells have been extensively researched and applications in the fields of drug screening and disease

modelling have been developed (Grskovic et al., 2011). The subsequent reprogramming of somatic human cells to pluripotency (Yu et al., 2007) created new possibilities in the fields of regenerative medicine and stem cell research. These cells constitute a source of patient-specific pluripotent stem cells that bypass autoimmune rejection concerns and any ethical considerations. However, the methodology for generating human induced pluripotent stem (hiPS) cell lines usually entails the use of retro- or lenti- viruses to deliver the transgenes in the somatic cells. These viruses are known to integrate in the genome and in some instances activate oncogenes. For instance, in one study, mice developed tumours after being transplanted with iPS cells originating from somatic cells reprogrammed with viruses (Duinsbergen et al., 2009). The above concerns lead to the research for novel techniques of cellular reprogramming. Now, iPS cells can be generated using non-integrating viruses (Fusaki et al., 2009), non-integrating episomes (Yu et al., 2009), recombinant proteins (Zhou et al., 2009), mRNA (Warren et al., 2010), or small molecules (Obokata et al., 2014). The novel CRISPR method has also been used with positive results, as a research team managed to activate a single endogenous gene (*OCT4* or *SOX2*) that initiated the reprogramming cascade (Liu et al., 2018).

Last, adult stem (AS) cells reside in specific tissues and organs in the adult organism having the ability to self-renew and differentiate in response to external stimuli such as injury (Passier and Mummery, 2003). The fine balance between self-renewal and differentiation is controlled by the microenvironment or ‘’niche’’ which the AS cells inhabit. The niche is generated by a combination of extracellular matrix signalling and soluble factors that regulate stem cell proliferation, migration, differentiation and apoptosis (Watt and Hogan, 2000). In addition, the type of division

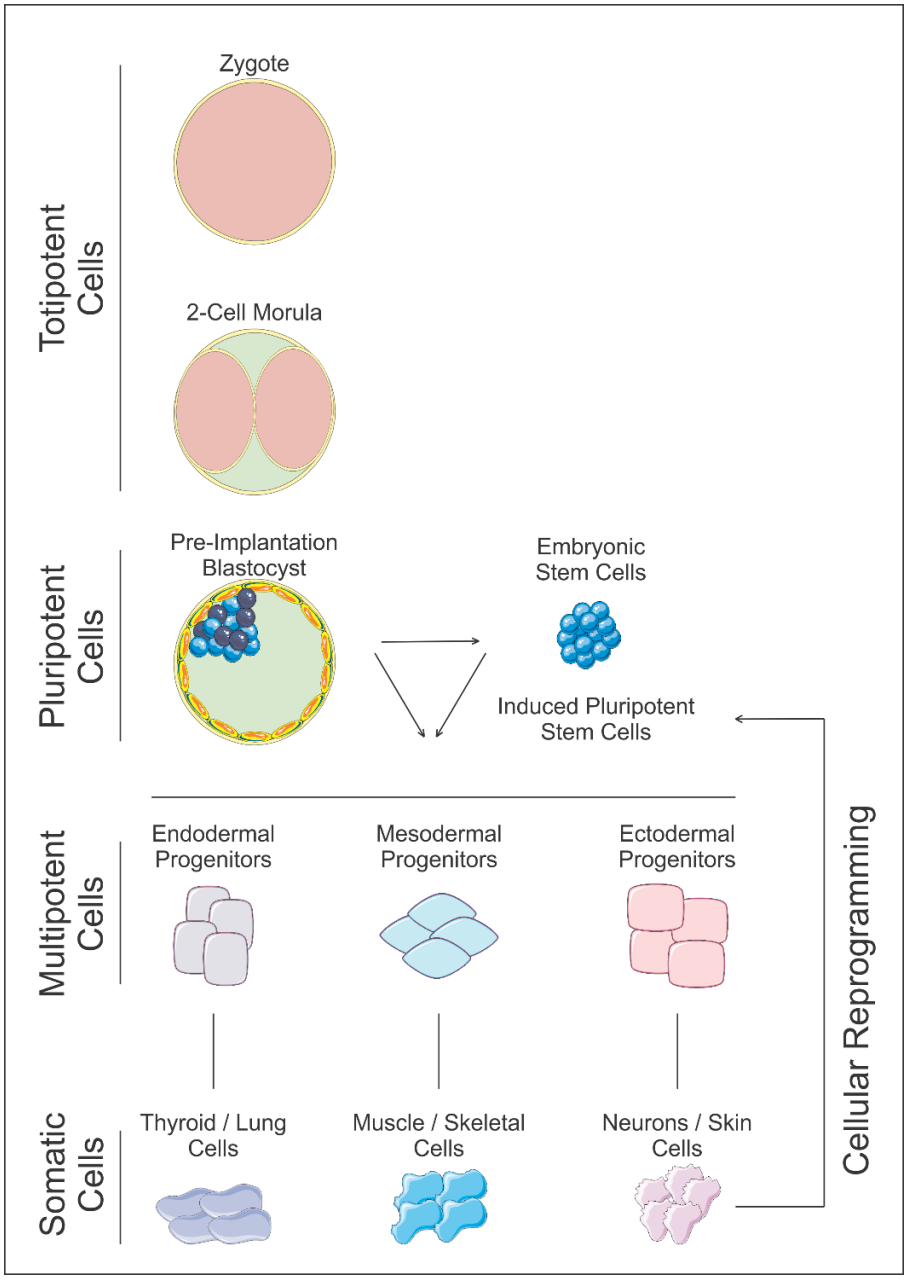


Figure 2.1: Stem Cell Hierarchy and Potency

Stem cells can be clustered into different categories based on their differentiation capacity or origin of isolation. The zygote and the two blastomeres arising from the first mitotic division are the only ones characterised as totipotent. ICM cells of the pre-implantation blastocyst are pluripotent, since they can differentiate into progenitors of the three germ layers or generate ES cell lines *in vitro*. Even though the ICM at this developmental stage demonstrates a mosaic of future epiblast (blue) and hypoblast (dark blue) cells, hES lines isolated exhibit mainly epiblast signalling profiles. The germ layer progenitors can produce terminally differentiated cells that form the tissues and organs of the adult organism. Somatic cells can be reprogrammed back to pluripotency by introduction of a specific cocktail of transcription factors.

these cells undergo is also influenced by the niche. In homeostasis, asymmetric divisions maintain the stem cell numbers intact. In the event of injury, proliferation symmetric divisions replenish the stem cell population and differentiation divisions repair the tissue (Fuchs, 2009).The hierarchy of stem cells based on their origin is depicted in **Figure 2.1**. The three types of divisions are depicted in **Figure 2.2**.

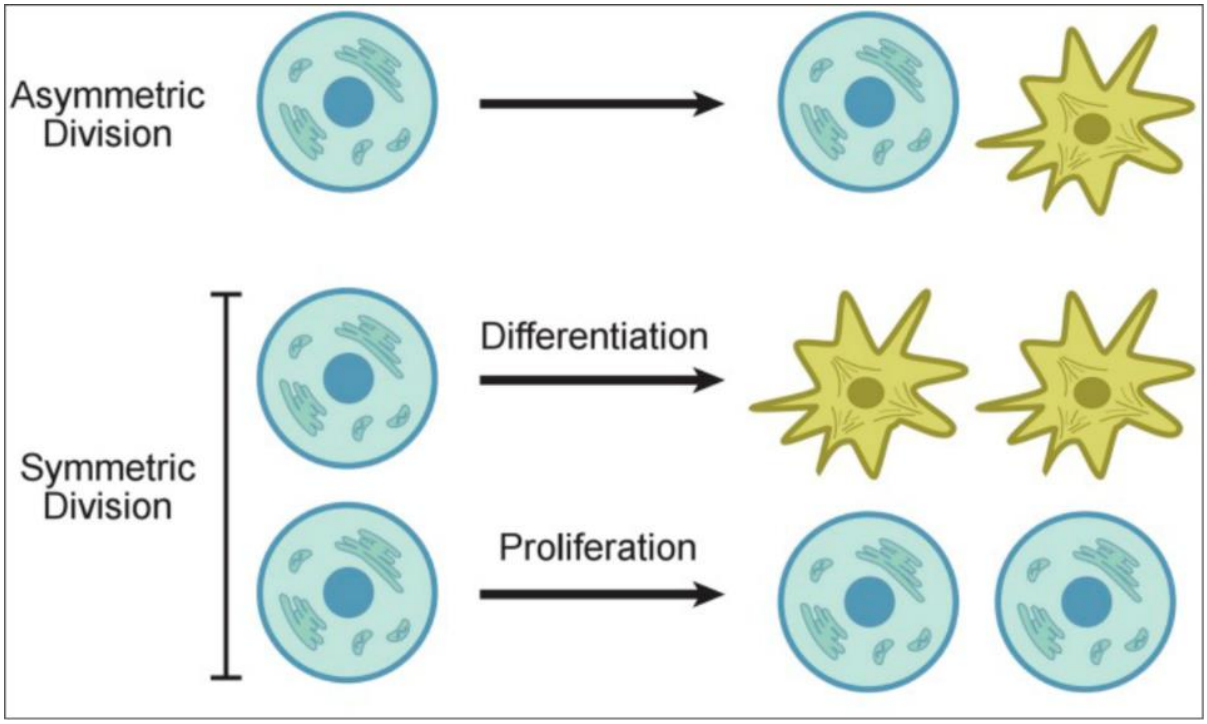


Figure 2.2: Types of Stem Cell Division

AS cells undergo either symmetric or asymmetric cell divisions. An asymmetric division entails the generation of a stem cell and a differentiated daughter cell. Symmetric divisions give rise to either two stem cells or two differentiated cells (Yang et al., 2015).

2.1.3 Stem Cell Therapeutic Potential and Reported Cases

To date, there has been a considerable number of attempts to utilise a variety of stem cell types for therapeutic purposes with encouraging results. This section will be focused on ES cells and MS cells.

In 2010, oligodendrocytes originating from hES cells were used in a clinical trial aiming to reverse spinal cord injury. The five patients that volunteered tolerated the transplantation with no adverse effects. However, limited motor neuron improvement resulted in the discontinuation of the study (Kimbrel and Lanza, 2016). In 2011, in a separate clinical trial, hES cell-derived retinal pigment epithelial cells were transplanted in patients with age-related macular degeneration. The cells were shown to engraft and survive with no adverse effects for the subjects. Vision quality was documented to be improved in approximately 50% of the patients (Schwartz et al., 2012). In 2014, a study was initiated with diabetic patients being transplanted with a subcutaneous drug delivery device that consists of hES cell-derived pancreatic cells. While the results will not be available until 2021, preclinical experiments showed that the pancreatic cells start producing insulin that successfully regulated blood sugar levels in mice (Kroon et al., 2008). Lastly, a clinical trial that involves the transplantation of hES cell-derived cardiac progenitors in patients with ischemic heart disease has also been approved. The progenitor cells will be enclosed in a fibrin scaffold that will be engrafted on the epicardium. Data in primate and rodent models have shown that following transplantation cardiac function improves, possibly due to the graft's paracrine signalling that promotes activation of endogenous regeneration (Bellamy et al., 2015; Blin et al., 2010).

MS cells have also been utilised clinically to treat a considerable number of diverse medical conditions. The first clinical trial conducted in 1995 demonstrated that transplanting patients with MS cells presents no adverse effects (Lazarus et al., 1995). Since then, more than 200 clinical studies have been conducted for acute disorders like myocardial infarction (Behfar et al., 2010), stroke (Honmou et al., 2011), liver cirrhosis (Zhang et al., 2012) and amyotrophic lateral sclerosis (Connick et al., 2012). In addition, clinical trials have demonstrated that MS cells can treat patients with steroid-resistant acute graft-versus-host disease (GVHD) (Le Blanc et al., 2004). Also, their ability to mitigate T-cell immunoresponse is under investigation with direct applications in various autoimmune conditions (Tse et al., 2003).

2.2 Human Embryonic Stem Cells

The term hES cells refers to a pool of pluripotent stem cells typically isolated from the ICM of the pre-implantation blastocyst. These have the ability to self-renew indefinitely under specific conditions *in vitro*, while maintaining their differentiation potential towards all the germ layers (endoderm, mesoderm and ectoderm), the germline (Condic, 2014) and some extraembryonic lineages (Amita et al., 2013). The developmental process of human embryogenesis that describes the origins and functional purpose of hES cells is summarised below.

2.2.1 Human Early Embryogenesis

The term ‘’embryogenesis’’ refers to the elaborate and highly regulated process that dictates the biological steps implicated in the formation of an embryo from a fertilised egg or ‘’zygote’’.

Following fertilisation in the ampulla of the oviduct, the zygote undergoes a series of mitotic divisions in a process known as ‘’cleavage’’. In human development, these divisions are 12 to 24 hours apart and lead to the generation of eight identical cells or ‘’blastomeres’’, by the end of day 2. Interestingly, blastomeres occupy the same space as the zygote, which suggests that after every division, daughter cells are significantly smaller. Also, they are surrounded by a veil of glycoproteins known as ‘’zona pellucida’’, that participates in the sperm acrosome reaction and prevents polyspermy and ectopic or tubal pregnancy **Figure 2.6**.

Following cleavage, the newly formed blastomeres or ‘’morula’’ enter the phase of ‘‘compaction’’. This process entails the formation of tight junctions between the cells of the outer layer due to the expression of adhesion molecules like E-Cadherin. The cells residing inside the morula form gap junctions that allow the flow of small molecules and ions. (Aghion et al., 1994). These two distinct cell populations are the products of the first differentiation event in embryogenesis. The outer layer of cells forms the trophoblast (trophoectoderm) which expresses the characteristic transcription factor CDX2 and the inner layer forms the ICM that is positive for OCT4 and NANOG (Strumpf et al., 2005). Data acquired by time-lapse photo-microscopy suggest that the cell’s differentiation decision towards trophoectoderm or ICM is completely stochastic (Dard et al., 2009). An alternative theory adequately explaining this segregation is known as the ‘’micro-environment hypothesis’’. This model suggests that blastomeres apically facing the acellular zona pellucida are subjected to signalling cues inhibiting the Hippo pathway, which results in upregulation of CDX2. In contrast, blastomeres that reside centrally in the morula are protected from the above signals and upregulate OCT4 and NANOG (Nishioka et al., 2009). The process of compaction

at the morula stage is accompanied by the activation of the zygotes genome. That event takes place on the 4th day of development **Figure 2.6** (Rossant and Tam, 2017).

The trophoectoderm cells have been found to carry active sodium pumps on their membranes. Secretion of sodium cations in the extracellular space is stimulated by oviduct cells (Xu et al., 2004) and leads to accumulation of water by osmosis (Kawagishi et al., 2004). In a process known as ‘’cavitation’’, water accumulation creates a cavity in the blastocoel and reasonably the ICM polarises in a niche space, still being attached to the trophoectoderm cells. This new structure, formed in humans by day 5, is referred to as an ‘’early blastocyst’’ **Figure 2.6**.

The generation and continuous enlargement of the blastocoelic cavity increases the volume of the early blastocyst and the tension imposed on the zona pellucida. By day 6, this leads to the ‘’hatching’’ of the blastocyst from the protective membrane which will eventually disintegrate (Seshagiri et al., 2009). Since the trophoblast layer is no longer confined by the surrounding zona pellucida, cells are able to bind to the uterine collagen, fibronectin and laminin through their integrins (Carson et al., 1993). Also, interaction with the endometrium leads to the trophoblasts secreting several extracellular proteases, such as collagenase, stromelysin and plasminogen activator. These proteins digest components of the endometrium and allow the implantation of the blastocyst in the endometrial tissue **Figure 2.6** (Staun-Ram and Shalev, 2005).

Human blastocyst implantation usually occurs 7 days after fertilisation. At that point, the trophoblastic layer of cells differentiate into two separate formations, the cytotrophoblast and the syncytiotrophoblast. The former invades and digests the uterine walls paving a path for the blastocyst. The latter supports the forming embryo

by providing nutrients directly from the endometrium, until nourishment can be available directly from the maternal blood vessels (Bischof and Campana, 1996). In parallel, a second differentiation event takes place. The cells constituting the ICM segregate into two distinct populations, the epiblast which expresses the marker NANOG and the hypoblast or primitive endoderm which is positive for GATA6 (Chazaud et al., 2006). The hypoblast cells will eventually migrate from the ICM and decorate the cavity of the blastocyst creating the extraembryonic endoderm, which will develop into the yolk sac. The epiblast cells are further separated into two populations, the embryonic epiblast that forms all the adult tissues and the amnionic ectoderm or epithelium. The latter cells are attached on the trophoblasts creating a space known as the ‘’amnionic cavity’’ which contains amnionic fluid and serves as a shock absorber for the forming embryo **Figure 2.3, Figure 2.6, Figure 2.7**.

On day 8, the embryonic epiblast differentiates into an ectodermal and an endodermal germ layer. The two populations are in contact, forming the ‘’bilaminar germ disk’’. The ectodermal cells are facing the amnionic cavity and the endodermal cells, the blastocoel. The tissue that develops between the trophoblastic and the hypoblastic cell layer is mesodermal. Even though its origins are still subject for debate, data suggests that it demonstrates similar characteristics to the hypoblast **Figure 2.4**, **Figure 2.6, Figure 2.7** (Enders and King, 1988).

Gastrulation is the final event of early embryogenesis. It takes place between days 12 to 16 and involves the differentiation of the embryonic epiblast to the three germ layers that give rise to all the embryonic tissues. During gastrulation, the bilaminar germ disk is transformed into a trilaminar disk due of the formation of the mesodermal germ layer. The primitive streak is a structure appearing approximately at

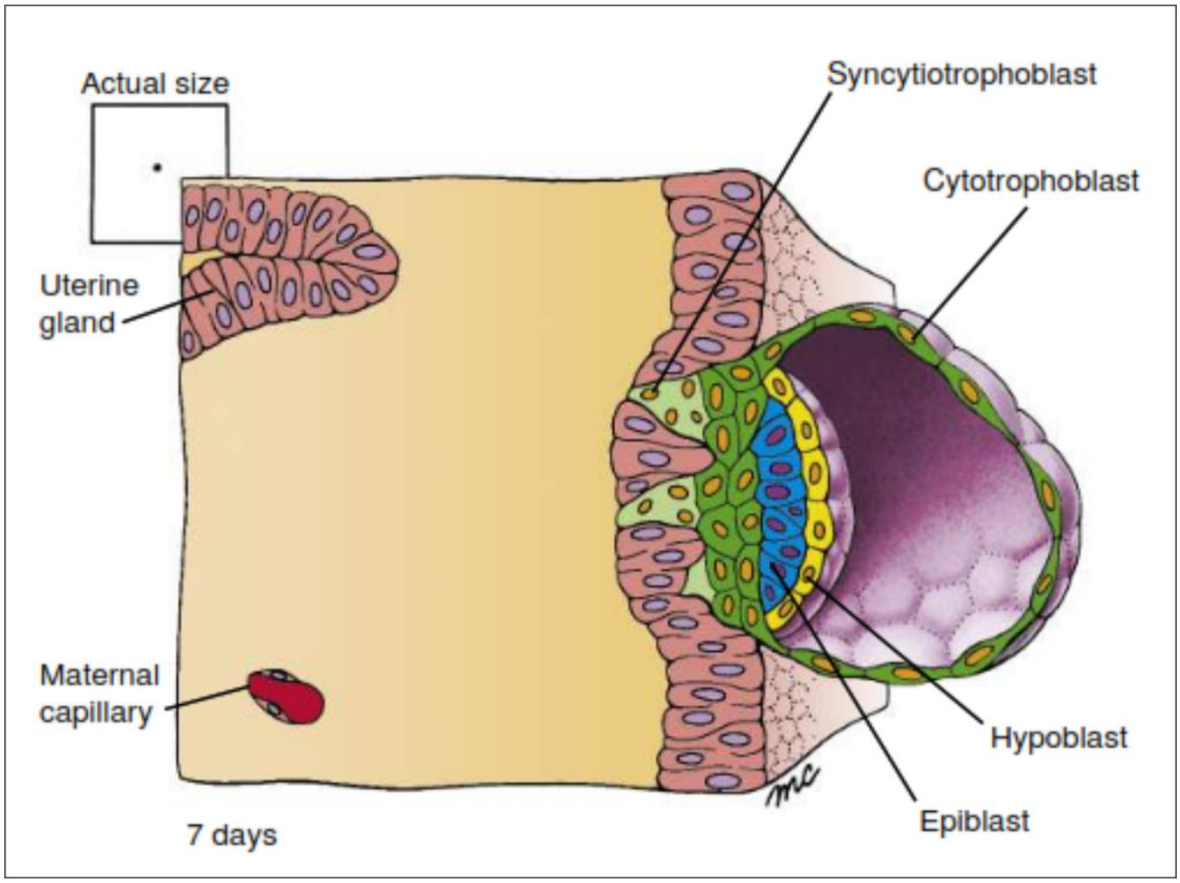


Figure 2.3: Human Blastocyst Representation at Day 7 of Development

At day 7 of embryogenesis the pre-implantation human blastocyst consists of an outer layer of trophoblastic cells surrounding the blastocystic cavity. Cells of the ICM are polarised and in contact with the trophoblasts. The trophoblasts have segregated into two distinct cell layers, the cytotrophoblast and the syncytiotrophoblast. Both act to digest the extracellular matrix of the uterine wall, attempting to attach the blastocyst in the endometrium while feeding the forming embryo. In parallel, the ICM differentiates into the epiblast and the hypoblast (embryonic endoderm). Adapted from (Gary C Schoenwolf, Steven B Bleyl, Philip R Brauer, 2015).

day 14 of development and resembles an elongated groove creating a pit on the surface of the epiblast. On day 15, epiblast cells migrate through the primitive streak and into the cavity formed in the space between the embryonic epiblast and the hypoblast. These cells undergo an epithelial to mesenchymal transition and displace the hypoblast cells forming the definitive endoderm. On day 16, a second pool of cells

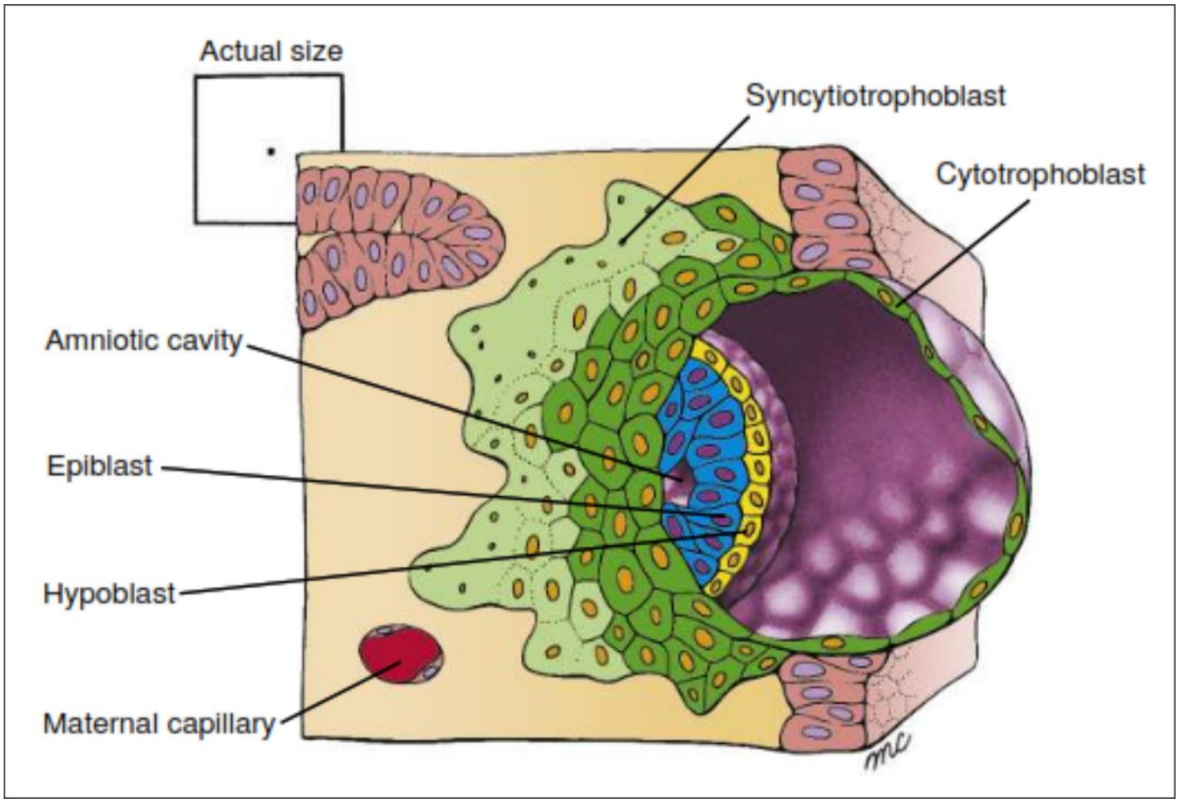


Figure 2.4: Human Blastocyst Representation at Day 8 of Development

At day 8 of embryogenesis the human blastocyst has infiltrated the uterine wall. At the same time, the embryonic epiblast has given rise to the amnionic endoderm and a cavity has formed between the two cell types. Also, at this stage the bilaminar germ disk is observed, formed by cells of the epiblast and the hypoblast that are in close contact. Adapted from (Gary C Schoenwolf, Steven B Bleyl, Philip R Brauer, 2015).

originating from the epiblast, enters the primitive streak and colonises the space between the epiblast and the primitive endoderm, forming the embryo's mesodermal progenitors with a potency to differentiate into fibroblasts, blood cells, muscle etc. The remaining epiblastic cells seize their migration and form the ectoderm, thus completing the trilaminar germ disk **Figure 2.5, Figure 2.6, Figure 2.7**.

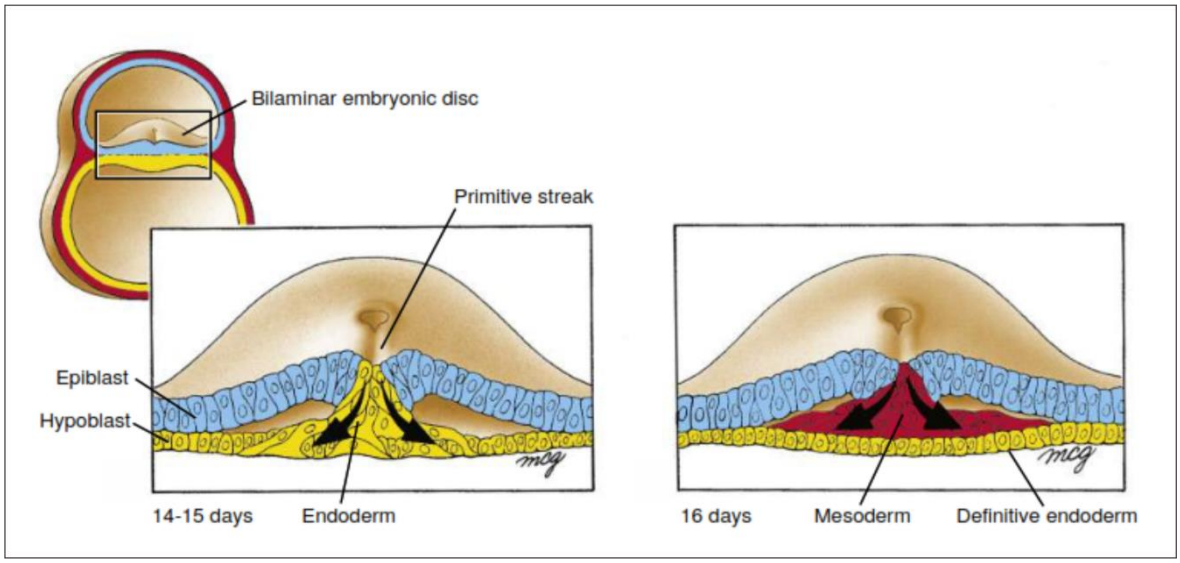


Figure 2.5: Human Blastocyst Representation at Days 14-16 of Development

At day 14 of human embryogenesis the primitive streak develops. This is a structure that appears like an elongated grove ending in a pit and forming on the epiblastic cell layer. Epiblast cells start migrating through the pit and colonising the cavity formed between their layer and the hypoblast. These cells differentiate and form the definitive endoderm and mesoderm. The cells that remain in the epiblast differentiate into the ectoderm, completing the formation of the trilaminar germ disk. Adapted from (Gary C Schoenwolf, Steven B Bleyl, Philip R Brauer, 2015).

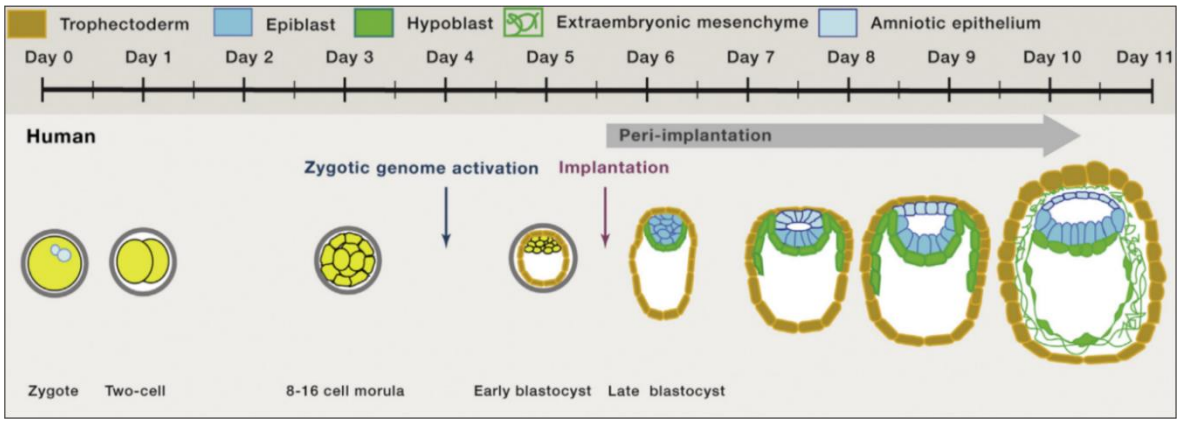


Figure 2.6: Timeline of Human Early Development

During the first 3 days of embryogenesis the zygote undergoes three cleavages that result in the formation of 8 identical blastomeres called morula. The morula will then undergo compaction, a process that entails the formation of tight junctions between the outer cell layer and gap junctions between the inner cells. At day 4, the endogenous

zygotic genome of the morula cells is activated, with them no longer relying on maternally inherited cytoplasmic RNA and proteins for their function. Next, cells of the formula differentiate into two distinct populations, the ICM and the trophoblastic layer. That segregation leads to the formation of the early blastocyst that increases in volume, hatches from the zona pellucida and implants in the uterine wall. Following implantation at day 6, the ICM further differentiates into the epiblast and the hypoblast. The former will give rise to the 3 germ layers and the amnionic epithelium. The latter will create the yolk sac and the extraembryonic mesoderm. Adapted from (Wu and Izpisua Belmonte, 2016).

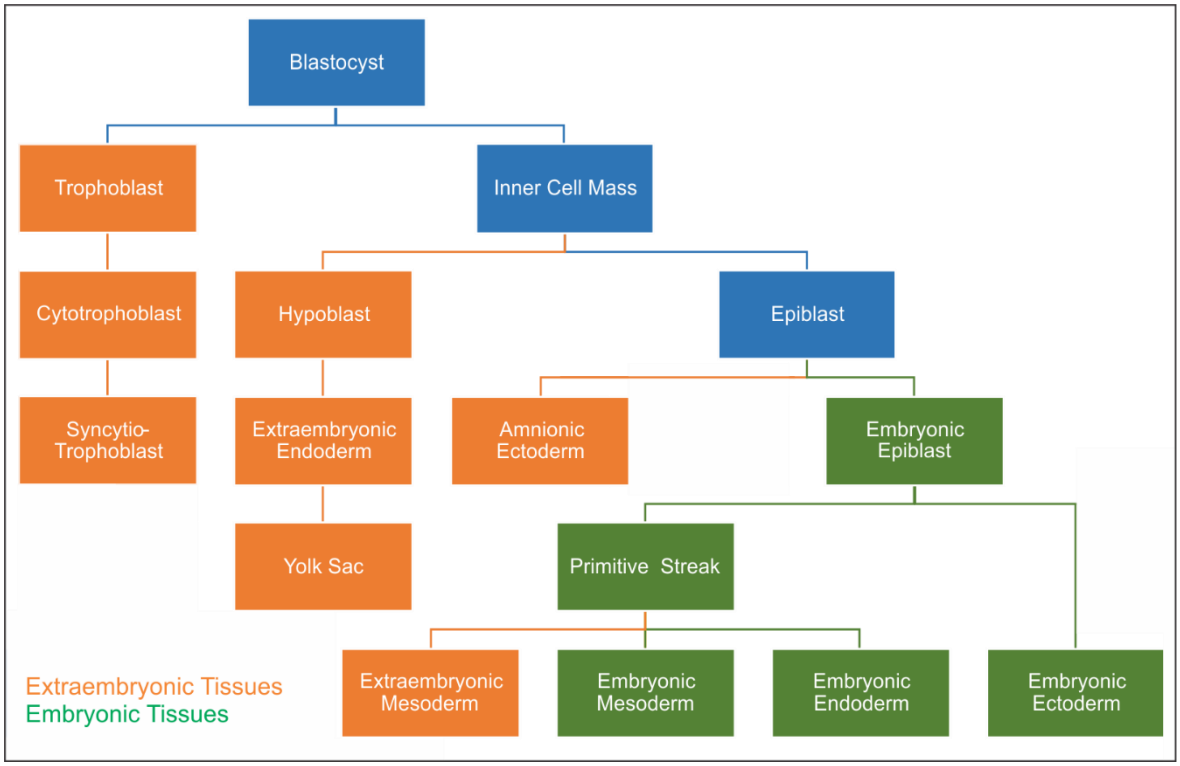


Figure 2.7: Human Developmental Ontology Tree

Graphical representation of tissue development during early embryogenesis in the human embryo. The information of the differentiation events spans from day 4 and the segregation of the blastocyst till day 15 and the generation of the trilaminar germ disk.

2.2.2 Major Pluripotency Transcription Factors in hES cells

hES cell pluripotency is regulated by an elaborate network of transcription factors that downregulate the expression of genes promoting differentiation while maintaining others involved in self-renewal. To date, there has been a vast number of genes reported to be involved in that complicated network. In this section, the function of *NANOG*, *OCT4* and *SOX2* will be summarised, as these have been proven indispensable for the maintenance of pluripotency regardless of the culture system (Wang et al., 2012), (Zhang et al., 2014), (Zhang and Cui, 2014). Several studies have also associated these factors with somatic cellular reprogramming (Liao et al., 2008), (Chiu et al., 2015).

Octamer-binding transcription factor 4 (OCT4) is a POU-homeodomain containing transcription factor, encoded by *POU5F1* gene. OCT4 binds target genes via two subdomains of the POU domain. Each consists of a helix-turn-helix structure and are interconnected with a linker region (Schöler, 1991). Both the N- and C-terminal tails of OCT4 have found to be important for gene transactivation (Vigano and Staudt, 1996). The POU domain, though important in DNA binding, can be replaced without affecting the transactivation potency of the protein (Brehm et al., 1997). OCT4 has been found to be indispensable during embryonic development. *OCT4* knock-out has an embryonic lethal phenotype in mice, as they fail to develop a normal ICM in the blastocyst stage (Nichols et al., 1998). Normally, it is expressed in the blastomeres and restricted during the first differentiation of cells to the ICM, and during the second, to the epiblast, meaning that the trophoectoderm and hypoblast are negative for the transcription factor (Pesce and Schöler, 2000). In ES cells, *OCT4* has been found to

regulate both pluripotency and differentiation. Adequate levels of OCT4 have been found to sustain pluripotency and are a prerequisite for somatic cell reprogramming (Wang et al., 2012). On the other hand, high or low expression of OCT4 is linked with differentiation towards extraembryonic lineages (Niwa et al., 2000).

NANOG is a homeodomain transcription factor, initially discovered for its ability to maintain mES cells in pluripotency, in the absence of LIF (Chambers et al., 2003). The homeodomain structure of NANOG that promotes DNA binding, involves three α-helices close to the N-terminal tail which are connected by loops (Gehring et al., 1994). *NANOG* knock-out has been demonstrated as embryonic lethal in mice (Mitsui et al., 2003). During early embryogenesis, after the first differentiation event, the expression of NANOG is confined to the cells of the ICM, while the trophoblastic layer is positive for CDX2 (Niakan and Eggan, 2013). At the same time, the ICM cells do not express NANOG at the same level. Interestingly, cells with a high expression of NANOG demonstrate low expression of GATA6 and vice versa (Chazaud et al., 2006). Following hatching of the blastocyst and segregation of the ICM to the epiblast and hypoblast layers, NANOG expression is confined to the former and GATA6 to the latter (Roode et al., 2012). This is evidence that during embryogenesis NANOG is implicated in both fate decisions. In culture, NANOG expression levels of both hES and mES cells fluctuate significantly. This fluctuation appears to be stochastic and creates a highly heterogenic population within the same colony that comprises of NANOG high and low cells. The former appear to be less and the latter more prone to differentiation signals (Abranches et al., 2014).

Sex determining region Y box 2 (SOX2) is a member of the *SOX* gene family with a characteristic high mobility group (HMG) DNA binding domain. SOX2 has been

found to closely cooperate with OCT4 and form heterodimers in order to bind and regulate transcriptional targets (van den Berg et al., 2010). The heterodimers bind via their POU and HMG domains specific motifs within the DNA with the conserved sequences ATGAAAT (OCT4) and CATTGTC (SOX2) (Reményi et al., 2003). Additionally, SOX2 is also capable of forming a heterodimeric complex with NANOG. The sequence within SOX2 responsible for this interaction consists of a triple repeated SXS/TY motif. Mutation of this motif within SOX2 in mES, leads to increased differentiation, thus highlighting the importance of this interaction for the preservation of pluripotency (Gagliardi et al., 2013). *SOX2* knock-out in mice has a lethal phenotype. More specifically, blastocyst formation is impaired because the ICM fails to form the epiblastic layer (Campolo et al., 2013). During early development, expression of SOX2 is detected since the morula stage and gets gradually confined to the ICM and then the epiblast. In hES and mES cells, knockdown of SOX2 has been shown to favour differentiation to trophoectoderm while compromising pluripotency (Fong et al., 2008). SOX2 is still present in later development with a clear role in the developing central nervous system (Zhang and Cui, 2014).

The transcription factors summarised above are known to safeguard hES cell pluripotency against differentiation cues. Not only can these factors positively regulate their own genes, but they have the capability to cooperatively influence the activity of 2360 target genes **Figure 2.8**. These targets include key components of pluripotency whose expression is upregulated, comprising the indispensable WNT and TGFβ signalling pathways. In addition, all three proteins have the ability to repress transcription of genes involved in differentiation towards all germ layers and extraembryonic lineages (Boyer et al., 2005).

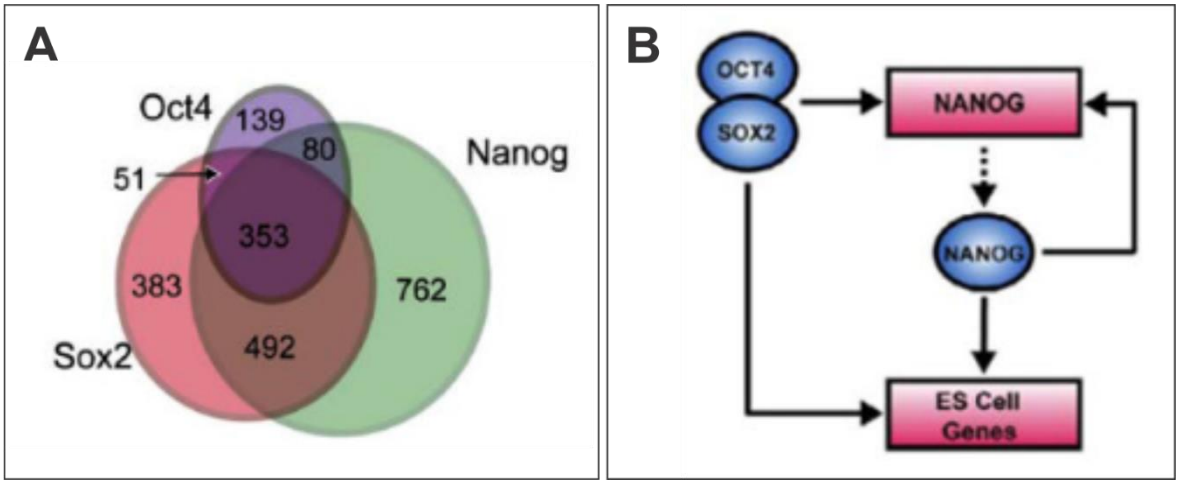


Figure 2.8: OCT4, NANOG and SOX2 in hES Cell Pluripotency

(A) OCT4, NANOG and SOX2 are responsible for the regulation of 2360 genes. Interestingly, all three factors form a complex that influences the transcription of 353 genes. (B) OCT4 and SOX2 complex to upregulate the transcription of *NANOG* and other ES cell genes. NANOG will subsequently promote ES cell gene expression resulting in a feed forward loop. Data presented above data have been obtained via mapping of genome-wide binding sites of the respective transcription factors. Adapted from (Boyer et al., 2005).

2.2.3 Major Signalling Pathways in hES cells

There is a plethora of signalling pathways that intersect and form an elaborate network that sustains pluripotency and regulates differentiation in hES cells. Below, the function of the most important ones is summarised.

FGF2 is an important growth factor supplemented in nearly all the available media employed to sustain hES cell cultures. The ligand binds to an FGF receptor on the plasma membrane and promotes autophosphorylation of its intracellular domain tyrosine residues. In hES cells, this mainly leads to activation of two signalling cascades (PI3K-AKT and MEK-ERK) that promote cell proliferation and self-renewal (Armstrong et al., 2006; Kang et al., 2005). Interestingly, these two pathways cross-

talk, with PI3K maintaining ERK activation to pluripotency-compatible levels. This fact explains how both low (<10ng/mL) and high (>50ng/mL) levels of FGF2 have the same effect on hES cells, preserving pluripotency. In brief, low doses of the growth factor moderately activate ERK1/2, while high doses also activate PI3K-AKT, which in turn suppresses ERK1/2 activity (Singh et al., 2012). Recent research implicates FGF signalling in mesoderm differentiation by acting through MEK-ERK to sustain NANOG expression upon induction with BMP4. In the absence of FGF2, NANOG is quickly downregulated and BMP4 drives hES cells to extraembryonic lineages (Yu et al., 2011). Additionally, activation of the FGF pathway is essential for the tight regulation of Activin A - SMAD2/3 signalling. Activation of the latter pathway is context dependent and can lead to either pluripotency or endodermal differentiation. However, in the presence of FGF2 and PI3K-AKT induction, ERK and WNT signalling is suppressed and SMAD2/3 activates a specific group of genes implicated in pluripotency. On the other hand, inactivation of PI3K-AKT leads to activation of the WNT pathway and its effectors such as β-catenin and SNAIL, which cooperate with SMAD2/3 to induce genes involved in early differentiation **Figure 2.9** (Singh et al., 2012).

WNT ligands initiate signalling by binding to FRIZZLED and LRP6 receptors on the plasma membrane. Downstream pathway events include the deconstruction of the GSK3β – AXIN – APC – CK1 complex that phosphorylates cytosolic β-catenin, resulting in its ubiquitination and proteasomal degradation. In the absence of that complex, β-catenin is stabilized and translocates to the nucleus where it exerts signalling in concert with other transcription factors (Kühl and Kühl, 2013). There has been a considerable number of conflicting publications involving WNT pathway and its implication in the regulation of hES cells (Sato et al., 2004; James et al., 2005; Xiao et

al., 2006; Villa-Diaz et al., 2009; Ding et al., 2010; Sumi et al., 2008). Apart from different culture conditions, growth media, substrates and cell lines, which are factors that indeed contribute to variations in the results, recent research argues that different pools of GSK3β complexes exist in separate cellular compartments, exerting different signals. Chemical inhibition of all GSK3β pools has been shown to lead to β-catenin activation, which acts in concert with SMAD2/3 to initiate hES cell differentiation (Sumi et al., 2008). On the other hand, low doses of GSK3β inhibitors sustain pluripotency through stabilization of the pluripotency gene c-MYC (Singh et al., 2012). The core pluripotency factor OCT4 has also been implicated in WNT signalling, as it has been found to mitigate β-catenin-related differentiation cues **Figure 2.9** (Davidson et al., 2012).

Given their many pleotropic roles in embryo development, it comes to no surprise that TGFβ superfamily members can contribute to both pluripotency and differentiation. More specifically, in concert with PI3K-AKT signalling, TGFβ or Activin A ligands sustain hES cells pluripotency in vitro through moderate activation of the SMAD2/3 pathway (Singh et al., 2012). The SMAD2/3/4 complex that is formed translocates into the nucleus and physically interacts with the promoter of the *NANOG* gene, increasing its transcriptional activity (Xu et al., 2008). The fact that NANOG overexpression maintains hES cell pluripotency suggests that Activin A / TGFβ achieve the same result by sustaining NANOG expression at high levels. In that state, NANOG physically interacts with SMAD2/3, reduces their transcriptional activity and suspends their drive for endodermal differentiation (Vallier et al., 2009). Additionally, NANOG also interacts with the promoter regions of transcription factors SOX2 and OCT4.

Collectively these factors collaborate and form an autoregulatory network that preserves pluripotency in hES cells **Figure 2.9** (Boyer et al., 2005).

BMP4 pathway effector proteins SMAD1/5/9 seem to suppress the expression of genes that are directly implicated in hES cell pluripotency. SMAD1 physically interacts with the promoter of *NANOG* resulting in its downregulation (Xu et al., 2008). The outcome of BMP4 induced differentiation depends on the state of ERK activation. As stated above, activation of ERK leads to sustained NANOG expression during the intial steps of differentiation that drives cells to acquire a mesodermal fate. BMP4 signalling in the absence of ERK drives cells to extraembryonic lineages (Yu et al., 2011). Recent research in mES cells suggests that BMP4 acts through ERK and subsequently KLF2 to safeguard pluripotency. Also, SMAD1 physically interacts with KLF4 with the complex formed suppresesing SMAD1 activity (Morikawa et al., 2011, 2016). Therefore, Kruppel Like factors could potentially be targets of BMP signalling in hES cells, thus expanding the effect of the ligand in that system.

Interestingly, induction with BMP4 has also been associated with the upregulation of the Epithelial to Mesenchymal Transition (EMT) regulator SLUG and the EMT marker MSX2. Activated SMAD1/5/9 proteins have been reported to bind directly to the promoters of the above factors and upregulate their expression. This suggests that BMP4 signalling is directly involved in EMT, a process important in the formation of the primitive streak that marks the onset of gastrulation **Figure 2.9**.

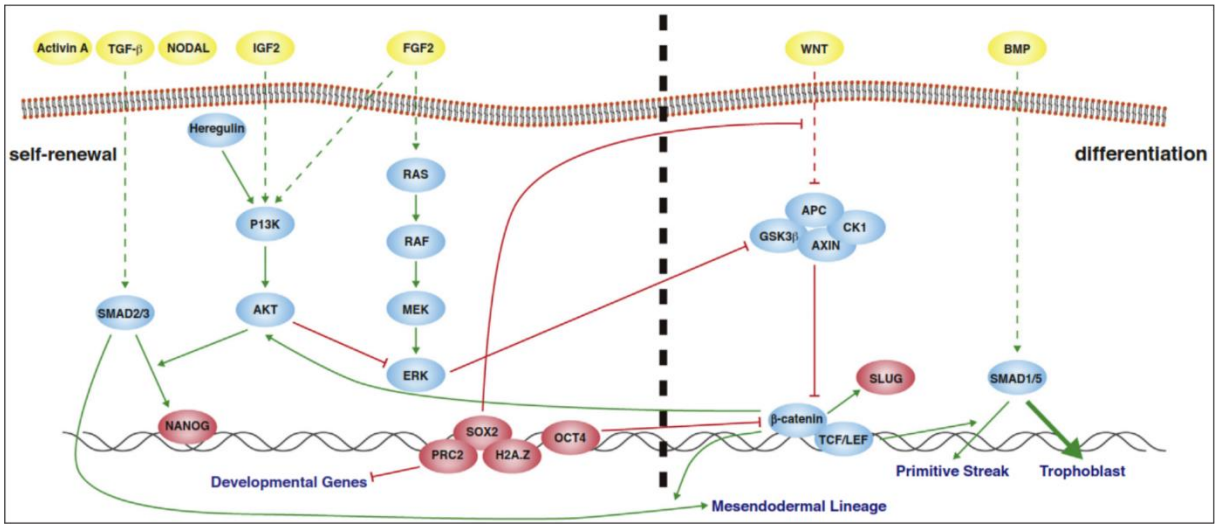


Figure 2.9: Major Signalling Pathways Regulating Pluripotency and Differentiation in hES cells

FGF2 / IGF2 signalling promotes activation of the PI3K-AKT and MEK-ERK pathways with the former maintaining the latter in pluripotency compatible levels. PI3K-AKT works in concert with TGFβ / Activin A to activate SMAD2/3 causing the upregulation of NANOG. NANOG forms an autoregulatory loop with OCT4 and SOX2 to sustain pluripotency in hES cells. PI3K-AKT activation also promotes cell proliferation and inhibit the pool of GSK3β involved in the destabilization of c-MYC. Deactivation of PI3K-AKT, leads to inhibition of GSK3β by ERK1/2 and activation of the WNT / β-catenin cascade. In that context, TGFβ / Activin A induced SMAD2/3 proteins cooperate with WNT components to drive differentiation towards endoderm. BMP4 acts through SMAD1/5/9 to downregulate NANOG and differentiate cells to extraembryonic lineages. FGF2 induced ERK signalling prolongs NANOG expression and switches the fate of differentiation from trophoectoderm to mesoderm. Adapted from (Zhao and Jin, 2017).

2.3 Signalling and Trafficking of TGFβ Superfamily Members

The TGFβ superfamily is comprised of at least 30 different proteins in vertebrates which are subdivided into the TGFβ and BMP groups. The former includes Activins, Inhibins, Nodals and a few Growth and Differentiation Factors (GDFs). The latter contains BMPs, the majority of GDFs and the Anti-Mullerian Hormone (AMH). TGFβ superfamily members are known to regulate a diverse range of cellular processes that include proliferation, adhesion, migration, differentiation and apoptosis. Knock-out of either ligands or receptors of the family has detrimental effects in the development of mouse embryos (Gordon and Blobe, 2008). In addition, TGFβ members are also implicated in various human diseases, including autoimmune conditions and cancer (Gordon and Blobe, 2008; Massagué, 2008).

2.3.1 TGFβ Superfamily Components

2.3.1.1 TGFβ Superfamily Ligands

TGFβ superfamily proteins are originally translated as precursor molecules that carry a large N-terminal prodomain, a convertase cleavage sequence and a C-terminal region that includes the active ligand. Intracellularly, the prodomain folds and binds the C-terminally located active ligand thus preserving its dimerization competency. Furins and other convertases recognise and chop the cleavage sequence situated between the prodomain and the active ligand. Interestingly, in the case of TGFβ ligands, the two structures remain in a complex known as the Latency Associated Protein (LAP) following cleavage (Harrison et al., 2011; Constam, 2014). Release of the active ligand will occur only after secretion and processing by a wide range of extracellular-matrix

proteases. Furthermore, interesting research conducted in chick embryos revealed that unprocessed Nodal (pro-Nodal), which still carries its prodomain, participates in the activation of different pathways compared to the mature ligand. More specifically, pro-Nodal synergizes with FGFR3 to promote prechordal mesoderm formation by suppressing Bmp signalling. In the same system, mature Nodal is unable to convey the same results, suggesting that unprocessed TGFβ superfamily ligands could possess additional functions to ligand maturation (Ellis et al., 2015).

Mature TGFβ superfamily ligands are characterized by a structure referred to as the ‘’cysteine knot’’ which is formed by six conserved cysteine residues interconnected with disulphide bonds. This structure promotes dimerization of the homomeric ligand that allows for its association with TGFβ superfamily receptors (Sun and Davies, 1995). Notably, GDF3, GDF9, BMP15 and LEFTY1/2 lack one of the cysteine residues that stabilizes the intermolecular disulphide bond and thus exist as monomers (Mueller and Nickel, 2012). Studies in flies and zebrafish have shown that TGFβ ligands can also form heterodimers *in vivo* (Schmid et al., 2000; Shimmi et al., 2005). Even though this observation increases the complexity of TGFβ superfamily signalling, such evidence is not available for mammals (O’Connor et al., 2006).

2.3.1.2 TGFβ Superfamily Ligand Binding Factors

As mentioned in the previous section, TGFβ is secreted from cells in complex with its large prodomain, thus forming the LAP. In some instances, the LAP can be associated with proteins with a role in mediating interactions with specific integrin receptors situated in the extracellular matrix. These proteins are known as Latent TGFβ-Binding Proteins (LTBPs) (Harrison et al., 2011). The first LTBP identified for TGFβ was LTBP-1. LTBP-1 expression is regulated by TGFβ signalling and it functions by

modulating the ligand's processing, secretion and correct targeting to the extracellular matrix (Saharinen et al., 1999).

Contrary to LTBPs that assist TGFβ ligands in their functions, several TGFβ antagonists have also been identified. The first fully characterized Activin A antagonist was Follistatin, with several BMP antagonists like Noggin, Chordin and Twisted Gastrulation, following. These proteins are known to physically bind ligands in the extracellular space and attenuate their signalling **Figure 2.12** (Umulis et al., 2009).

2.3.1.3 TGFβ Superfamily Receptors and Co-Receptors

Ligands of the TGFβ superfamily recognise and bind specific transmembrane type I and type II Serine/Threonine kinase receptors to form heteromeric complexes. To date, seven type I and five type II receptors have been identified in vertebrates. Their structure consists of an N-terminal ligand-binding domain, a transmembrane domain and a C-terminal Serine/Threonine kinase domain. Type I receptors include a separate characteristic SGSGSG sequence (GS domain), situated between the kinase and transmembrane domains. GS domains are transphosphorylated by type II receptors in response to ligand binding (Kretzschmar and Massagué, 1998). It should be noted that type II receptors are constitutively active kinases, whereas type I require transphosphorylation to be able to act as kinases **Figure 2.10**. In addition, binding to receptors differs between the two groups within the TGFβ family. All TGFs initially form complexes with type II receptors. This causes a transformational change on type II receptors that facilitates their association with type I receptors (Groppe et al., 2008). On the other hand, it has been demonstrated that BMP ligands have a higher affinity for type I receptors (Groppe et al., 2008), with events downstream of receptor phosphorylation being the same between groups **Figure 2.12, Figure 2.13**.

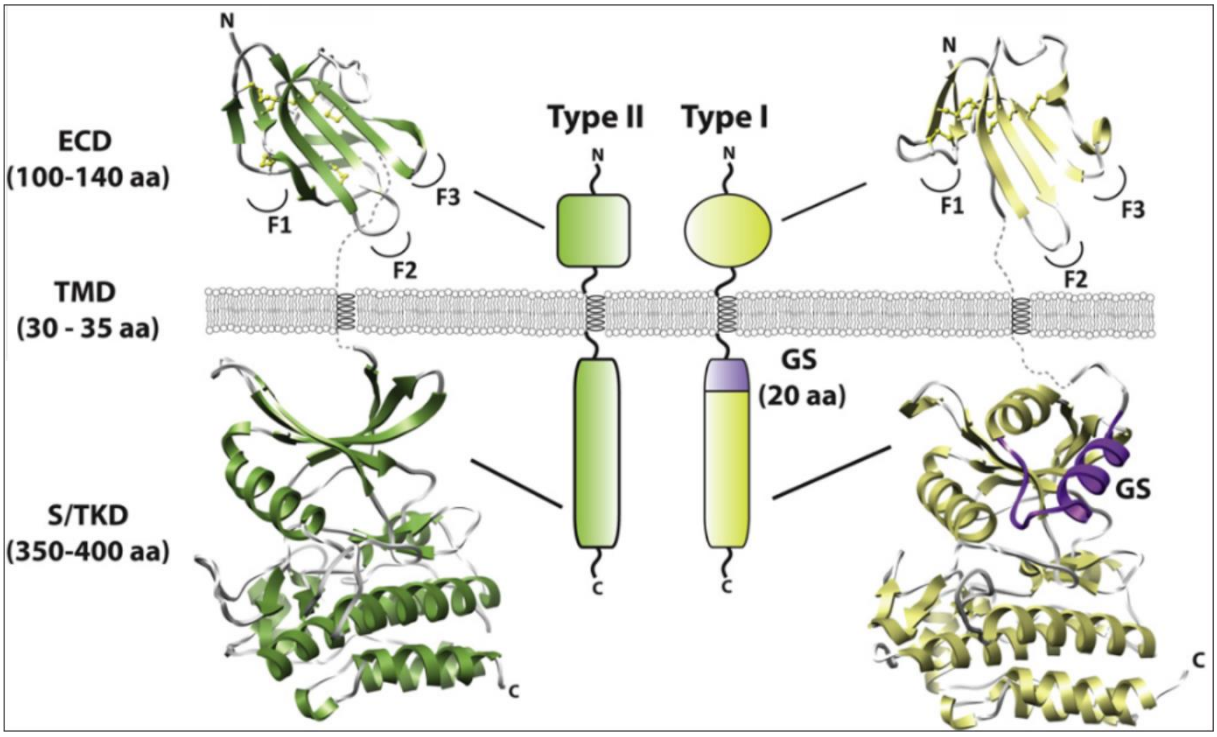


Figure 2.10: TGFβR Type I and II Structure

TGFβR1 and TGFβRII are comprised of three separate domains. An extracellular domain (ECD) that binds the ligand, a small transmembrane domain (TMD) and a cytoplasmic Serine/Threonine kinase domain (S/TKD). TGFβRI also contains a GS domain that is transphosphorylated by TGFβRI, upon ligand binding and complex formation. Adapted from (Hinck, 2012).

TGFβ signalling is further regulated by the binding of ligands to plasma membrane-localised co-receptors. This extra measure of control can function in a binary way. Having their extracellular domains intact, co-receptors facilitate the binding of ligands to type I or II receptors by increasing affinity. However, if cleaved, their extracellular domains can work as molecular traps, binding available ligands with high affinity and mitigating their signalling. This mechanism of signalling attenuation can have various implications in several pathological conditions, including cancer **Figure 2.12** (Bernabeu et al., 2009).

Lastly, a group of proteins that complexes with type I or II receptors in order to block signalling has also been identified. A well-characterized member of that group is the BMP and Activin Membrane-Bound Inhibitor (BAMBI). BAMBI is a pseudoreceptor that lacks the intracellular kinase domain and forms non-functional complexes with type II receptors on the membrane, thus terminating the signalling cascade (Onichtchouk et al., 1999).

2.3.2 SMAD Signalling Pathways

2.3.2.1 SMAD Proteins

TGFβ superfamily signal transduction is initiated by the formation of ligand-receptor complexes that lead to transphosphorylation and activation of type I receptors. Further signal propagation relies primarily on a family of proteins, known as SMADs, named after their homologs in *Caenorhabditis elegans* (SMA) and *Drosophila melanogaster* (Mad) (Raftery et al., 1995; Sekelsky et al., 1995). In vertebrates, SMAD proteins are separated into three categories: the Receptor-regulated (R-SMADs), the Common-mediator (Co-SMAD) and the Inhibitory (I-SMADs) (Moustakas and Heldin, 2009).

R-SMADs are the first ones recruited to the ligand-receptor complexes in direct response to type I receptor phosphorylation. SMAD2/3 proteins respond to ligands of the TGFβ subgroup and SMAD1/5/9 proteins to ligands of the BMP subgroup. R-SMADs are comprised of approximately 500 aminoacids and their structure includes the C- and N- terminal Mad Homology domains (MH1 and MH2), coupled by a linker region. The MH1 domain contains a β-hairpin (βH) sequence that is important for DNA binding. Interestingly, all R-SMADs except for SMAD2 have the capacity to bind directly

to DNA. This is attributed to an extra sequence upstream of the βH domain of SMAD2 that interferes with that function. However, SMAD2(ΔE3) which is an alternative splicing product of the *SMAD2* gene, is completely capable of exerting TGFβ signalling, due to acetylation of a Lysine residue (Lys19) (Simonsson et al., 2006). The Serine and Proline rich linker region carries sites that are targets of phosphorylation by MAPKs, GSK3β and CDKs, thus crosslinking TGFβ signalling with other cascades (Fuentealba et al., 2007; Kretzschmar et al., 1997). Within the linker region, the PPXY motif is recognized by E3 ubiquitin ligases such as SMURF1/2 that attenuate signalling by promoting SMAD-ubiquitination. The MH2 domain is involved in SMAD oligomerisation and also carries a sequence termed as the L3 loop that establishes specificity between R-SMADs and type I receptors. The last N-terminal amino acids form the SSXS motif which carries the two serine residues which are phosphorylated by type I receptors **Figure 2.11, Figure 2.12, Figure 2.13** (Shi and Massagué, 2003).

SMAD4 is the only member of the co-SMAD group, and is able to partner with R-SMADs of both subgroups so as to propagate signalling. SMAD4 structure is similar to the R-SMADs, containing the MH1 / MH2 motifs and a linker region. Within the linker region, SMAD4 contains an additional element termed as SMAD Activation Domain (SAD), which is indispensable for transcriptional activation. Knock-out mutants retain their ability to form complexes with R-SMADs and transcription factors but are unable to mediate transcription (de Caestecker et al., 2000). It should also be noted that SMAD4 does not carry an N-terminal SSXS motif and therefore is not phosphorylated **Figure 2.11, Figure 2.12, Figure 2.13** (Shi and Massagué, 2003).

SMAD6 and SMAD7 comprise the I-SMAD group and their function is to mitigate signalling by interacting with phosphorylated type I receptors and R-SMADs. SMAD7

is capable of inhibiting both TGF and BMP subgroup signalling cascades by interacting with a broad range of type I receptors (Hanyu et al., 2001). Contrary to SMAD7, SMAD6 demonstrates increased receptor specificity and can interfere only with BMP subgroup related signalling pathways (Goto et al., 2007). The C-terminal MH2 domain of all SMADs is conserved, the only difference being that I-SMADs and SMAD4 do not include the characteristic SSXS motif and are thus not sensitive to phosphorylation by type I receptors. In addition, I-SMADs also contain the PPXY motif that attracts E3 ubiquitin ligases. However, the C-terminal and linker regions of I-SMADs significantly differ from the rest of the SMAD proteins **Figure 2.11** (Schmierer and Hill, 2007). In order to mitigate TGFβ signalling, I-SMADs can employ a diverse range of strategies. By physically binding type I receptors via their MH2 domains, I-SMADs can compete with R-SMADs. Recruitment of effector proteins like the SMURF1/2 E3 ligases or the GADD34 / PP1c complex leads to receptor degradation or dephosphorylation, respectively. Interaction with R-SMADs prevents their oligomerisation with SMAD4. Last, interfering with the formation of SMAD-DNA complexes in the nucleus inhibits transcriptional activation, **Figure 2.13** (Miyazawa and Miyazono, 2017).

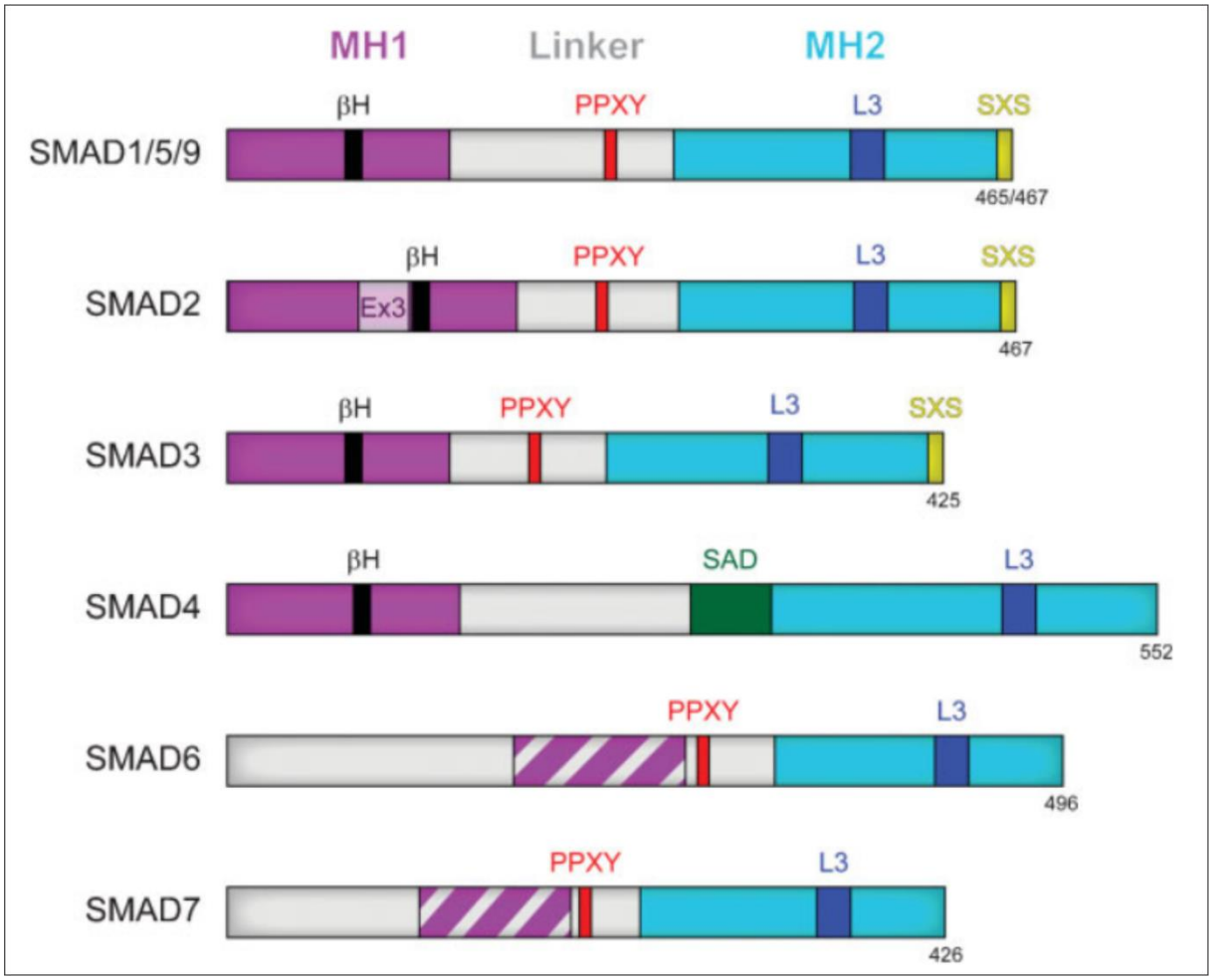


Figure 2.11: Structure of SMAD Proteins

R-SMADs (SMAD2/3, SMAD1/5/9) and SMAD4 are comprised of the highly conserved MH1 and MH2 domains separated by a linker region. The MH1 domains contain a βH motif that is indispensable for DNA binding. SMAD2 does not have DNA binding capacity due to an extra sequence upstream of the βH motif. In their linker region, R-SMADs and I-SMADs encode the PPXY motif which is a target of different E3 ligases and SMAD4 carries the SAD domain that confers transcriptional activation. The MH2 domain of all SMADs is highly conserved and contains the L3 loop which increases their affinity for the TGFβ type I receptors. The last N-terminal aminoacids of the R-SMADs comprise the SSXS motif that includes the Serine residues which are phosphorylated by the receptors. Adapted from (Weiss and Attisano, 2013).

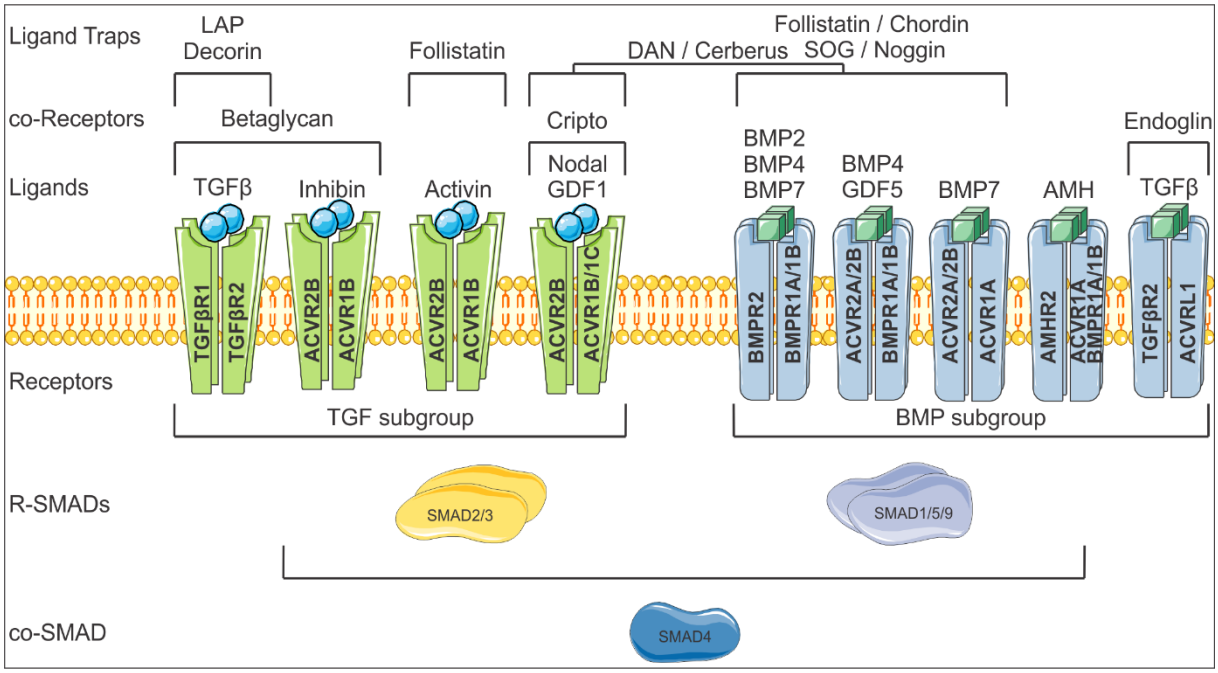


Figure 2.12: Overview of TGF Signalling Components

TGFβs, Inhibins, Activins, Nodals and GDF1 exert their signalling by binding specific receptors on the plasma membrane that will activate SMAD2/3 proteins to affect transcription. BMPs, most GDFs and AMH bind their own receptors that activate SMAD1/5/9 to affect separate pathways. Interestingly, aided by the accessory receptor Endoglin, TGFβ can activate the BMP-related R-SMADs and propagate signal via their cascade. Betaglycan facilitates Inhibin binding to Activin receptors therefore attenuating Activin signalling. Cripto has been found to mediate the interaction of Nodal and GDF1 to Activin receptors, enabling signal propagation. Ligand binding proteins such as Follistatin and LAP and Noggin serve as traps, sequestering TGF and BMP ligands away from receptors and attenuating signalling.

2.3.2.2 SMAD Machinery Regulation

As mentioned in the previous sections, TGF signalling is initiated by ligand binding to an appropriate receptor on the plasma membrane. This interaction causes a conformational change that facilitates the heterodimerisation of type I and type II receptors with the former being phosphorylated by the latter in its GS domain. Subsequently, type I receptors are able to bind R-SMADs via their phosphorylated GS domains that interact with a positively charged sequence within the MH2 domains (Wu

et al., 2000). This is demonstrated by the fact that mutation of that sequence within the MH2 domain of SMAD2 leads to reduced binding affinity with TGFβR2 and limited phosphorylation (Huse et al., 2001). Even though this interaction facilitates binding of R-SMADs to type I receptors, it is not responsible for SMAD specificity since it is conserved among all SMADs. Type I receptors are able to locate and activate their own SMAD target proteins via an L45 loop domain that is situated close to the GS domain and binds the L3 loop in the R-SMAD MH2 domain (Chen et al., 1998). Recognition of R-SMADs by the receptors is also assisted by proteins such as SMAD-Anchor for Receptor Activation (SARA) and Endofin. SARA interacts with specific hydrophobic sequences in SMAD2/3 proteins, carrying them to the early endosomes via a separate phospholipid binding domain (FYVE domain) **Figure 2.13** (Tsukazaki et al., 1998). Endofin exhibits a 48% similarity with SARA and has been hypothesized to function in a similar way and recruit SMAD1/5/9 proteins to BMPRs. However, recent findings have shown that knock-down of SARA or Endofin exhibits minimum effects on the phosphorylation of SMAD2/3 and SMAD1/5/9, respectively (Bakkebø et al., 2012).

SMAD2 phosphorylation by activated type I receptors on the plasma membrane reduces its affinity for SARA, due to a conformational change in the MH2 domain (Wu et al., 2000). In addition, the phosphorylated SSXS motif that is formed on the C-terminal tail of a SMAD2 monomer exhibits high affinity for a positively charged pocket region of an adjacent phosphorylated SMAD2 molecule with the binding being stabilized by hydrogen bonds (Shi, 2001). This pocket is primarily comprised of four residues that are conserved in all R-SMADs and also SMAD4, indicating that the same mechanism underlies the oligomerisation of R-SMADs with the co-SMAD in the

cytoplasm after activation (Wu et al., 2001). In addition, R-SMADs dephosphorylation is dependent on the action of specific phosphatases, such as PPM1A and the small C-terminal phosphatases (SCPs). These enzymes can terminate signalling by modifying phosphorylated SSXS motifs either in the nucleus or cytoplasm (Wrighton and Feng, 2008).

2.3.2.3 SMAD Transcriptional Regulation

Accumulation of phosphorylated SMADs in the nucleus entails their dissociation from the activated type I receptors located on the plasma membrane and early endosomes. This dissociation is made possible because the C-terminal phosphorylated SSXS motifs compete with receptor GS domains for the binding of the MH2 located L3 loop (Wu et al., 2001). In a resting state R-SMADs are primarily cytoplasmic, I-SMADs nuclear and the co-SMAD continuously shuttles between the two compartments. Relocation of SMAD2/3 to the nucleus has been shown to rely on a Nuclear Localisation Sequence (NLS) within the MH2 domain that facilitates binding to nucleoporins, Nup214 and Nup153 (Xu et al., 2002). In addition, SMAD4 nuclear transport is partly based on complexing with R-SMADs and partly on a NLS comprised of residues in the MH2 domain and the βH motif (Pierreux et al., 2000). SMAD4 also contains a nuclear export sequence situated in the linker domain **Figure 2.13** (Inman et al., 2002).

R-SMADs and SMAD4 have been found to recognise specific DNA sequences in order to regulate transcription. The only exception is SMAD2 which does not demonstrate DNA binding capabilities due to an extra region of aminoacids adjacent to the βH domain. Removal of that sequence has been demonstrated to restore the DNA binding ability of SMAD2 (Yagi et al., 1999). The DNA sequences recognized by

SMADs are known as SMAD-Binding Elements (SBEs) and are comprised of the 5'-GTCT-3', 5'-AGAC-3' and 5'-GNCN-3' sequences as well as GC-rich regions (Zawel et al., 1998; Labbé et al., 1998; Kim et al., 1997; Shi et al., 1998; Morikawa et al., 2011). As these sequences confer only a weak interaction between SMADs and DNA, the former have to rely on the action of partner proteins to increase specificity. SMADs recruit chromatin remodeling complexes such as the histone acetyltransferases CBP/p300 to activate transcription and the histone deacetylases HDAC1/3/4/5/6 to inhibit it (Moustakas and Heldin, 2009; Feng and Derynck, 2005). FOXH1, a chromatin remodeler able to bind condensed chromatin, was the first SMAD2/3 partner identified in mammals, required for the regulation of the *GSC* promoter. This promoter contains a SMAD4 binding element and needs SMAD4 activity for activation. Interestingly, in this case, SMAD2-SMAD4 complexes positively influence transcription while SMAD3-SMAD4 complexes have a negative effect. This is attributed to the MH1 domain of SMAD3 that complexes with SMAD4 and impairs its binding to *GSC* (Labbé et al., 1998). In hES cells, SMAD2/3 complexes with the transcription factor NANOG to upregulate its own activity in an autoregulatory loop and the transcription of pluripotency genes such as OCT4 and SOX2 (Vallier et al., 2009). Interestingly, during the initial stages of definitive endoderm specification, the same SMAD2/3-NANOG complex activates EOMES. EOMES will ultimately interact with SMAD2/3 for differentiation to progress **Figure 2.13** (Teo et al., 2011).

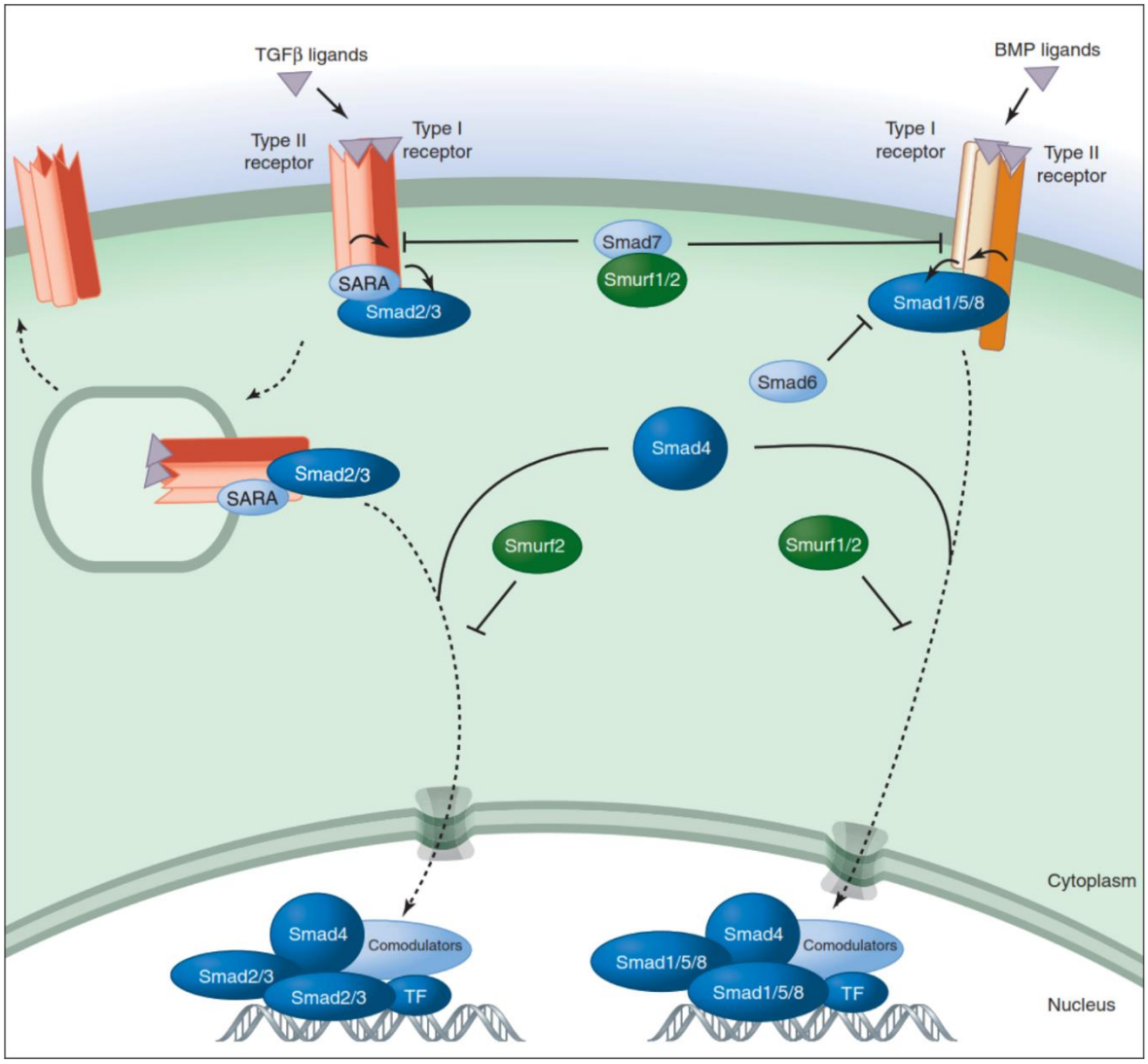


Figure 2.13: Canonical TGF Signalling Cascades

TGFβ ligands bind to the extracellular domain of type II receptors triggering the recruitment of type I receptors and the formation of a heterotetrameric complexes. This leads to the phosphorylation and activation of the type I receptor which enables it to phosphorylate SMAD2/3 that are recruited to the complex by SARA. SMAD2/3 will oligomerise with SMAD4 (co-SMAD) in the cytoplasm and translocate to the nucleus. There, SMADs interact with transcription factors and chromatin regulators such as histone acetylases and deacetylases to regulate gene transcription. BMP ligands follow a similar pathway. Two distinct differences are that they initially bind type I receptors on the plasma membrane and SMAD1/5/9 is phosphorylated as a result. SMAD6/7 mitigate TGF signalling by competing with R-SMADs for receptor binding or recruiting E3 ligases like SMURF1/2 that ubiquitinate R-SMADs. Interestingly, SMAD7 is a general TGF pathway inhibitor, whereas SMAD6 preferentially inhibits the BMP pathway. Adapted from (Wrana, 2013).

2.3.3 Non-SMAD Signalling Pathways

TGFβ signalling can progress via the canonical SMAD-dependent cascades, or non-canonical SMAD-independent pathways. The latter involve small Rho-like GTPases, MAPKs and PI3K/AKT.

2.3.3.1 MAPK/ERK Signalling Pathway

TGFβ stimulation has been found responsible for the activation of the MAPK/ERK cascade. Interestingly, kinetics of ERK phosphorylation differ significantly between cell lines. Late ERK activation (2hrs after ligand induction) can be attributed to a secondary response tied to a SMAD-dependent cascade. However, early ERK phosphorylation (5-10min after ligand induction) can only be a direct effect of TGFβ on the MAPK cascade (Olsson et al., 2001; Simeone et al., 2001). The mechanism involves the initial phosphorylation of ShcA by TGFβR1 which leads to the former complexing with Grb2. Grb2 is an adaptor of SOS and is therefore recruiting it to the plasma membrane where it acts by catalyzing the GDP-GTP exchange on RAS. Activated RAS initiates a linear activation cascade that involves MEK1, RAF and leads to phosphorylation of ERK. Despite being a non-canonical pathway, activation of ERK by TGFβ is indispensable during early development as it is involved in EMT (Davies et al., 2005). BMP ligands and Activin A are also implicated in the pathway. BMP-induced activation of ERK has been detected in several cell lines including osteoblasts, endothelial cells, and cancer cells (Lai and Cheng, 2002; Zhou et al., 2007; Le Page et al., 2009) . Similar to TGFβ, in specific cell lines BMP induced ERK at a later timepoint, suggesting an indirect mechanism of activation. Activin A induction is known to increase phosphorylation levels of ERK in K562 cells, thus inducing their differentiation (Huang et al., 2004).

2.3.3.2 JNK and p38 Signalling Pathways

TGFβ can also stimulate the activation of JNK and p38 in a SMAD-independent manner. This was supported by the fact that TGFβR1 with a mutated L45 loop was able to activate the two aforementioned pathways in response to TGFβ induction (Itoh et al., 2003). This cascade is initiated by TRAF6, a protein that interacts with TGFβR2 via its C-terminal TRAF domain. Upon ligand induction, lysine 63 within this domain gets polyubiquitinated by E3 ligases. Interestingly, in this case ubiquitination does not lead to degradation but propagates signalling by recruiting TAK1. TAK1 is an effector, indispensable during development as knockout mice embryos fail to form a functioning yolk sac. Recruitment of TAK1 leads to activation of p38 through MKK3/6 and JNK through MKK4 (Yamashita et al., 2008). In the *Xenopus* model, TAK1 is implicated in the BMP-related induction of mesoderm (Shibuya et al., 1998). In AR42J-B13 cells, Activin A is reported to act via the TAK1-MKK3-p38 cascade and upregulate *NEUROG3* (Ogihara et al., 2003). Collectively these facts indicate that BMP and Activin A function similarly to TGFβ to activate the JNK and p38 pathways.

2.3.3.3 Rho-like GTPases Signalling Pathways

RAC and CDC42 are GTPases involved in mediating TGFβ signalling in tight junctions between cells. There, upon ligand induction and receptor complex formation, TGFβR2 is known to coordinate with the GTPases and phosphorylate specific serine residues of PAR6, a protein modulating cellular polarity. Phosphorylated PAR6 recruits SMURF1 ligase to the tight junctions. This relocation is regulated by PKC, an effector of the CDC42/RAC-PAR6 complex that physically binds SMURF1. Once localized at the tight junctions, SMURF1 leads to the proteasomal degradation of RhoA, thus promoting cytoskeleton reorganization and EMT (Ozdamar et al., 2005). A separate

mechanism affecting the cytoskeleton has been attributed to BMPR2, as it has been found to interact with LIMK1. LIMK1 together with the receptor cooperates with CDC42 to rearrange ACTIN filaments (Foletta et al., 2003). Last, in keratinocytes, Activin has been found to mediate migration and promote the formation of ACTIN stress fibers. The mechanism involves phosphorylation of JNK and c-Jun by MEKK1, with the function of the latter being dependent on activation of RhoA by Activin signalling (Zhang et al., 2005).

2.3.3.4 PI3K/AKT Signalling Pathway

TGFβ stimulation initiates a cascade which leads to AKT phosphorylation. AKT is a serine/threonine kinase and effector of the PI3K pathway that contributes to proliferation, growth, metabolism and EMT. In a resting state, TGFβR2 is associated with the p85 subunit of PI3K, which interacts with TGFβR2 only upon ligand induction (Yi et al., 2005). Induction leads to phosphorylation of PI3K and AKT and subsequent signalling through activation of mechanistic Target Of Rapamycin (mTOR) complex 1 and 2. Activation and signalling though the two complexes is indispensable for EMT. mTORC1 contributes to processes like protein synthesis and invasion while mTORC2 to migration and cytoskeletal reorganization (Lamouille and Derynck, 2007; Lamouille et al., 2012). Apart from the mTOR pathway, AKT regulates EMT by phosphorylating GSK3β and TWIST1. The former leads to prolonged expression of the EMT-related factors NF-kb and SNAIL, whereas the latter creates a feed forwarding loop for AKT by stimulating the expression of TGFβ2 (Xue et al., 2012; Julien et al., 2007). BMP ligands have also been implicated in the activation of PI3K and AKT. BMP2 has been demonstrated to promote gastric tumor metastasis by inducing PI3K/AKT and MAPKs

(Kang et al., 2011). In chondrocytes, BMP2 promotes survival by inducing NF-kb through the same pathway (Sugimori et al., 2005).

2.3.4 Trafficking of TGFβ Family Receptors

2.3.4.1 Endocytic Routes

Ligand/receptor complexes can be internalised via many pathways which are separated to Clathrin-Mediated (CME) and Clathrin-Independent Endocytosis (CIE) as well as Caveolae-Mediated Endocytosis (CavME). Cargo entering via these different routes is transported to intracellular compartments such as Early Endosomes (EEs). From there, cargo can be recycled back to the cell surface via Recycling Endosomes (RE) or be forwarded to Late Endosomes (LEs), Multivesicular Bodies (MVBs) and lysosomes to undergo degradation.

To date, CME is the best characterised form of endocytosis, functional in all eukaryotic cells. The process of CME is initiated by polymerisation of Clathrin monomers, known as triskelia, which form hexagons or pentagons and decorate invaginations of the plasma membrane that harbour cargo. Binding of Clathrin to the membrane is not direct, but instead facilitated by adaptor proteins that are recruited in pre-existing plasma membrane curvatures and comprise the nucleation module which is comprised of FCH domain only containing proteins, Eps15 and intersectins (Henne et al., 2010). This module recruits AP2, an adaptor protein that interacts both with cargo and plasma membrane units. AP2 binds $PI(4,5)P_2$ as well as the cytoplasmic tails of receptors via its μ- and σ-subunits (Collins et al., 2002). Furthermore, several other accessory proteins such as AP180 and Epsin, have been found to contribute to membrane curving by interacting both with membrane subunits and cargo, thus

increasing internalisation specificity (Ford et al., 2001, 2002). In addition, AP2 and accessory proteins cooperatively recruit Clathrin to the budding vesicle, with the latter polymerizing and stabilizing the structure. Clathrin-coated vesicle fission is facilitated by Dynamin, a GTPase that is recruited to the neck of the forming pit and separates it from the membrane while undergoing GTP hydrolysis (Hinshaw and Schmid, 1995). Dynamin is recruited there by proteins such as endophilin and sorting nexin 9 (SNX9) that interact with its proline rich motifs. Vesicle fission is facilitated by Auxilin which binds to non-polymerised triskelia and recruits HSC70, an ATPase that facilitates Clathrin uncoating (Xing et al., 2010). Uncoated vesicles are then able to fuse with EEs where cargo sorting is initiated.

CavME is another well-understood endocytic pathway, indispensable for processes such as mechanosensing, lipid homeostasis and endothelial transcytosis (Parton and Simons, 2007). CavME is characterised by the formation of invaginations at the plasma membrane known as Caveolae. In non- skeletal muscle cells, Caveolae construction relies on proteins Caveolin-1 (CAV1) and Caveolin-2 (CAV2) that coordinate with a complex of membrane effectors that includes Cavin1,2 and 3 (Parton and del Pozo, 2013). In skeletal muscle cells, Caveolin-4 (CAV4) substitutes CAV1/2 and Cavin4 is added to the complex (Bastiani et al., 2009). Similarly to CME, cytosolic accessory proteins are recruited to Caveolae and aid in vesicle budding and fission. The ATPase EHD2 has been demonstrated to localise on the neck of the forming buds and inhibit CavME, possibly by interacting with ACTIN filaments (Stoeber et al., 2012). Contrary to EHD2, Dynamin promotes Caveolae fission from the membrane acting in a manner similar to CME. Last, an interactor of EHD2, called Pacsin2 is able to bind both Dynamin and CAV1 to regulate CavME by influencing membrane curving

mechanically. Interestingly, Pacsin2 has been found to be regulated by PKC via direct phosphorylation, an event that reduces its membrane association capacity and negatively impacts endocytosis (Senju et al., 2015).

While CME and CavME rely on Dynamin for vesicle fission from the plasma membrane, CIE pathways can be either into Dynamin- dependent or independent. Fast Endophilin-Mediated Endocytosis (FEME) is a recently characterized pathway that mediates internalisation of various G-Protein Coupled Receptors (GPCRs) and Receptor-Tyrosine Kinases (RTKs). FEME relies on the action of Endophilin, a binding partner of Dynamin and Synaptojanin that was originally identified as an accessory protein for CME. Following research showed that Endophilin contributes to a unique endocytic pathway that acts on the leading edge of cells and rapidly internalizes vesicles upon ligand stimulation (Boucrot et al., 2015).

Glycosylphosphatidyinositol-Anchored Proteins (GPI-APs) are usually internalised in a Clathrin and Dynamin independent manner. The resulting GPI-AP Enriched Early Endosomal Compartments (GEECs) are formed due to the action of Clathrin Independent Carriers (CLICs) and thus the pathway is known as CLIC /GEEC (CG). In addition to GPI-APs, the CG pathway is used by various other transmembrane proteins such as CD44. The activation machinery relies on ACTIN polymerization, a process that is tightly regulated by CDC42 GTPase. CDC42 cycling is regulated by ARHGAP10, a GTPase-Activating Protein (GAP) that catalyzes its hydrolysis. ARHGAP10 is recruited to the membrane by ARF1-GTP, a GTPase that is activated by Guanine Exchange Factor (GEF), GBF1 (Kumari and Mayor, 2008). A separate method of cargo delivery to the GEECs involves the action of GRAF1, a RhoGAP that substitutes ARHGAP10 in regulating CDC42. Interestingly, GRAF1 carries a BAR and

an SH3 domain. The former can contribute to membrane curving while the latter is capable of binding and recruiting Dynamin (Lundmark et al., 2008).

Above, three major pathways of CIE are summarized, while the pathway of ARF6 is discussed further on. In addition, several other endocytic routes that involve different effector proteins have recently emerged. A common denominator of all these pathways is the dependence on the ACTIN machinery for vesicle formation, abscission from the membrane and subsequent trafficking (Römer et al., 2010).

2.3.4.2 Endocytic Compartments

Post internalisation via any of the pathways described above, vesicles undergo multiple rounds of homotypic fusion and ultimately form EEs. From EEs, cargo can be recycled back to the plasma membrane via REs, forwarded to the Trans-Golgi Network (TGN) or be destined for lysosomal degradation. Even though REs can be formed directly from EEs, trafficking along each of the other two pathways requires the formation of LEs and MVBs in a process known as endosomal maturation. This process is accompanied by a gradual endosomal acidification due to H+ pumped into the endosomal lumen by membrane H+/ATPases (Mellman et al., 1986). Endosomal identity is also regulated by tweaking of the membrane phosphorylated phosphatidylinositols (PIPs) as well as the action and activation state of specific RAB GTPases **Figure 2.14**.

RABs constitute a subfamily of RAS GTPases with countless implications in endosomal trafficking. As all GTPases, they cycle between an activated GTP-bound and an inactivated GDP-bound state. Cycling between the two states is catalyzed by specific GEFs and GAPs (Müller and Goody, 2017). In most cases, endocytic effector

proteins recognise and interact with GTP-bound, activated RABs. In addition, several RAB effectors also include Phosphorylated Phosphatidylinositol (PIP) binding motifs. This allows them to limit their action to appropriate endocytic compartments, as each one has a unique PIP composition. For instance, the plasma membrane is enriched for $PI(4,5)P_{2,}$ whereas EEs for PI(3)P. PIPs involved in endocytic compartments can be modulated by the action of a set of kinases and phosphatases that are hence involved in the endosomal maturation process **Figure 2.14** (Di Paolo and De Camilli, 2006).

The process of sorting EE cargo depends on several aspects discussed below. Acidification is an important factor contributing to endosomal maturation and thus, cargo sorting. It has been demonstrated that EEs are slightly acidic (ph 6.8 - 6.1), LEs and MVBs acidic (ph 6.0 - 4.8) and lysosomes highly acidic (ph ~4.5) (Maxfield and Yamashiro, 1987). Modulation of endosomal ph is mainly attributed to the action of V-ATPases which are complex, membrane-bound H+ pumps and assisted by Na+/K+ ATPases and ion channels. These pumps are primarily localised to the spherical compartment of EEs and are therefore enriched in LEs (Lafourcade et al., 2008). The ph gradient formed between compartments (extracellular space / EEs, TGN – LEs) provides receptors the ability to modulate their affinity for ligands (Mellman, 1996). The same mechanism is also utilised by several viruses that are preferentially activated when reaching a specific endocytic compartment with the appropriate acidity (Mercer et al., 2010).

Endosomal geometry is another factor that changes during maturation and is involved in cargo sorting. In most cases, EEs are comprised of a large spherical vacuole as well as several elongated protrusions of their membrane derived from tubulation. The spherical space contains ligands and other cargo that will be forwarded

to LEs, whereas the membrane protrusions carry transmembrane receptors and other molecules that will be returned to the plasma membrane via REs **Figure 2.14** (Maxfield and McGraw, 2004).

Several sorting mechanisms have been identified to act on different endocytic compartments and regulate cargo destination. EE tubulation is partly modulated by proteins that bind both cargo and lipid membrane motifs, thus regulating recycling. A typical example in this category are sorting nexins (SNXs) (van Weering et al., 2012). SNXs are also part of the retromer complex, a cluster of proteins that is recruited to both EEs and LEs in order to transport cargo to the TGN. The retromer consists of both cargo (Vps26 / 29 / 35) and membrane binding agents (SNX 1/2 or SNX 5/6), and is recruited to EEs by association with PI(3)P or LEs by interaction with RAB7 (Burd and Cullen, 2014). Cargo that has undergone ubiquitination often accumulates in sub-endocytic compartments within EEs. Cargo targeting to these Intraluminal Vesicles (ILVs) is facilitated by the ESCRT complex. The latter is composed of sorting proteins (ESCRT -0 / I / II / III) and VPS4, an ATPase that disassembles all components in the end of the process. These vesicles remain in the lumen of EEs throughout all the maturation stages and are degraded once LEs or MVBs fuse with lysosomes **Figure 2.14** (Babst, 2011).

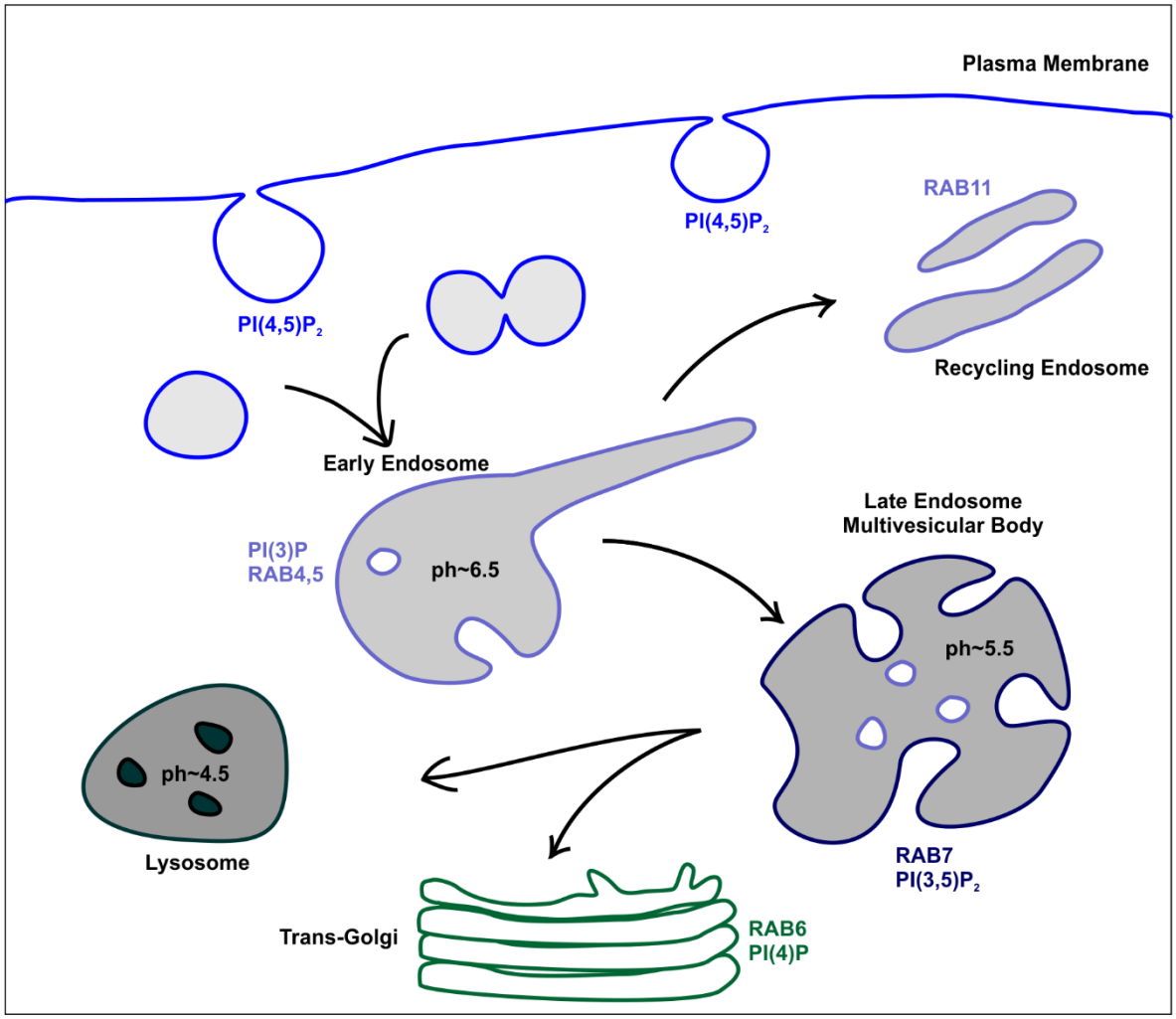


Figure 2.14 Endocytic Compartments

After cargo endocytosis, the vesicles that form undergo homotypic fusion to form the primary sorting endocytic compartment, known as Early Endosome (EE). Acidification, EE geometry and sorting proteins transfer cargo to Recycling Endosomes (RE) or retain it in EEs. Ubiquitinated cargo in EEs is entrapped into Intraluminal Vesicles (ILVs), assisted by the ESCRT complex. EEs gradually mature into Late Endosomes (LEs) and Multivesicular Bodies (MVBs). In LEs and MVBs, other sorting machinery such as the retromer complex, rescues cargo from degradation by transporting it to the Trans-Golgi Network (TGN). The residual cargo undergoes degradation when these compartments fuse with lysosomes. Characteristic RAB GTPases for each compartment as well as the unique phosphorylated phosphatidylinositol (PIP) signature is also depicted.

2.3.4.3 Endocytic Routes of TGFβ Receptors

TGFβR1 and TGFβR2 have been found to be internalised by CME and CavME, reviewed in: (Heldin and Moustakas, 2016). This was demonstrated by inhibiting both pathways separately or together and monitoring receptor internalisation. Inhibition of Dynamin, a GTPase involved in both pathways, completely abolished intracellular receptor localisation. In addition, CME was inhibited by depletion of potassium and CavME by lowering cholesterol levels (Hayes et al., 2002). Interestingly, the endocytic route chosen by the ligand/receptor complexes affects downstream signalling. Internalisation by CME aids in signal propagation, whereas CavME-mediated internalisation promotes ubiquitin-dependent receptor degradation (Di Guglielmo et al., 2003)**.**

CME is initiated by the binding of both TGFβ receptors to β2-Adaptin, an adaptor protein that facilitates their interaction with the Clathrin partner, AP2. More specifically, TGFβRs interact with the N-terminal domain of β2-adaptin via their cytoplasmic tails (Yao et al., 2002). CavME is facilitated by the localisation of receptors to lipid rafts in the plasma membrane (Di Guglielmo et al., 2003). Post-internalisation, TGFβRs localise to the EE, as demonstrated by their colocalisation with RAB5 and EEA1 (Sorkin and von Zastrow, 2009). Even though signalling from the plasma membrane has been shown to be possible, activated TGFβRs primarily signal from the EE. This is facilitated by SMAD Anchor for Receptor Activation (SARA), a FYVE domain-containing accessory protein that binds to the PI(3)P of the EE membrane while recruiting SMAD2 and SMAD3 proteins (Tsukazaki et al., 1998). In the case of membrane signalling, the role of SARA is substituted by other proteins like DAB2 (Hocevar et al., 2001).

The majority of TGFβRs have been found to be recycled back to the plasma membrane via the RAB11-positive RE. Sorting to the RE requires the action of the retromer complex and its VPS26 subunit, which physically interacts with TGFβR2 (Yin et al., 2013). Receptor degradation is dependent on ubiquitination by the E3 ligase SMURF1. Ubiquitination leads to TGFβRs being transferred to ILVs by the ESCRT complex. ILVs accumulate in the MVBs and are degraded upon fusion with the lysosomes (Di Guglielmo et al., 2003). An alternative degradation mechanism involves the protein DPR2. DPR2 exhibits a high affinity for the activated TGFβR1. This, combined with the LE localisation of DPR2, indicates that the protein attenuates signalling by promoting receptor degradation (Chen, 2009).

2.3.4.4 Endocytic Routes of Activin Receptors

To date, knowledge regarding the trafficking of Activin A receptors is very limited. Initial suggestions that Activin A does not require internalisation for signal propagation were quickly disproved by research showing that Activin A internalisation is Dynamin-dependent and essential for signalling. However, the exact endocytic pathway involved was not characterized (Jullien and Gurdon, 2005). As stated above, Dynamin is implicated in several endocytic pathways, including CME, CavME, FEME and others.

Activin Receptor Interacting Proteins (ARIPs) have been found to interact with Activin receptors via a characteristic PDZ domain, thus regulating signalling and trafficking. More specifically, ARIP2 interacts with ACVR2s and modulates their internalisation (Shoji et al., 2000). In addition, ARIP2 binds to RAL Binding Protein I (RALBPI), thus creating a complex that includes ACVR2, RALBP1 and POB1, a RALBP1 partner (Shoji et al., 2000). Previous findings indicated that RALBP1 is a RAL effector protein which facilitates GTP hydrolysis by interacting with a RALGAP.

RALBP1 partner POB1 is directly phosphorylated by EGF and forms a complex with EGF Receptor Pathway Substrate 15 (EPS15), EPS15 Interacting Protein (EPSIN), Adapter Complex 2 and Clathrin to regulate EGF endocytosis. Therefore, ARIP2 controls Activin mediated endocytosis by bridging the interaction between various regulatory proteins involved in the endocytic pathway (Nakashima et al., 1999). All the above indicate that ARIP2 mediates ACVR2s internalisation in a RALA dependent manner. This is also supported by the fact that Activin A induction stimulates RALA activation, probably by recruitment of a RALGDS.

In the absence of ligands, Activin receptors have been found to be rapidly recycled back to the plasma membrane in the *Xenopus* model. This is facilitated by RAP2 which is a member of the RAS GTPases family. The same results were obtained in HeLa cells, where REs carrying Activin receptors were identified as RAB11 positive. Combined with ligand induction, activated RAP2 increased SMAD2 phosphorylation and receptor localisation to the plasma membrane. A separate pathway that involves SMAD7 and SMURF2 leads to receptor ubiquitination and degradation. These two pathways seem to regulate Activin receptor turnover with the exact mechanism still being poorly understood (Choi et al., 2008).

2.3.4.5 Endocytic Routes of BMP Receptors

Similarly to TGFβRs, BMPRs have been found to utilise both CME and CavME for their internalisation. However, it is still unclear whether BMPRs require internalisation for signal propagation. Recent findings demonstrate that inhibition of CME with the inhibitor PitStop did not affect the SMAD pathway (Amsalem et al., 2016). In addition, disruption of Dynamin, a GTPase that contributes to both CME and CavME, using the chemical inhibitor Dynasore resulted only in delayed phosphorylation of SMAD1/5/9

(Heining et al., 2011). Using a dominant negative form of Dynamin combined with BMP4 induction, (Paarmann et al., 2016) were able to demonstrate that R-SMADs are phosphorylated and translocate to the nucleus, normally. Similar results were obtained when using a surface-immobilised BMP2 ligand, unable to undergo internalisation (Schwab et al., 2015). Collectively, the above data suggests that internalisation of BMPRs is dispensable for signalling.

CME has been suggested as the main entry pathway for BMPRs. In agreement to this and similar to TGFβRs, all BMPRs directly interact with critical components of the pathway, such as β-Adaptin, a member of the AP2 machinery (Bragdon et al., 2009). Furthermore, in the model system *C. elegans*, AP2 knock-down results in entrapment of BMPRs at the cell surface, suggesting that CME is the only route of internalisation (Gleason et al., 2014).

Localisation of BMPRs to cholesterol-rich domains on the plasma membrane implicated the receptors in CavME. However, literature regarding the outcome of internalisation through that route is highly contradictory. A study by (Bonor et al., 2012) shows that CavME of BMPRs favors SMAD1/5/9 phosphorylation. Contrary to this, (Hartung et al., 2006) demonstrated that the same entry pathway leads to activation of the non-SMAD, p38 cascade, based on Alkaline Phosphatase (ALP) activity.

Endocytic trafficking of BMPRs and the protein machinery involved is still unclear. A study in *C. elegans* revealed that post internalisation by CME, type I and type II BMPRs follow different recycling routes. More specifically, while SMA-6 (BMPR type I) recycling to the cell surface is associated with subunits of the retromer complex, DAF-4 (BMPR type II) depends on ARF6 GTPase. Interfering with either ARF6 or

retromer components leads to receptors being degraded in the lysosomes (Gleason et al., 2014).

2.4 ARF6: An Overview

ARF6 is a small 20kd protein that belongs to the RAS superfamily of GTPases (D'Souza-Schorey and Chavrier, 2006). There are six mammalian ARFs identified so far, that can be subdivided into three separate classes. Class I consists of ARF1, ARF2 and ARF3 which localise primarily to the Golgi apparatus and Endoplasmic Reticulum (ER) and regulate vesicular trafficking (Bonifacino and Glick, 2004). Class II includes ARF4 and ARF5 that are not currently characterized, except for the latter's potential role in recruiting coating agents to the TGN (Claude et al., 1999). The only member of class III is ARF6, a protein that localises to the plasma membrane, as well as endosomal membranes.

ARF6 exhibits a very diverse role as it is involved in several cellular functions including membrane trafficking (D'Souza-Schorey et al., 1995), adhesion (Balasubramanian et al., 2007), abscission (Schweitzer and D'Souza-Schorey, 2002) and lipid homeostasis (Naslavsky et al., 2004). As all GTPases, ARF6 cycles between an active (GTP-bound) and an inactive (GDP-bound) state through the action of specific effector proteins. GEFs activate ARF6 by catalyzing the exchange of GDP for GTP. In contrast, GAPs hydrolyze GTP to GDP, therefore inactivating the molecule, reviewed in: (Cherfils and Zeghouf, 2013).

Perturbing the expression or cycling of ARF6 has a detrimental phenotype *in vivo*, in different species. In *Drosophila*, overexpression of a dominant negative mutant (see section 2.4.1) resulted in neural malformations and inhibited myoblast fusion

(Onel et al., 2004; Chen et al., 2003). In mice, knockout of ARF6 has a lethal phenotype, mid-gestation, possibly attributed to impaired liver and foetal hepatic cord development (Suzuki et al., 2006). Interestingly, conditional ablation of ARF6 in endothelial cells of mice *in vivo* did not exhibit a lethal phenotype, suggesting that its expression is dispensable in endothelial tissues during development (Hongu et al., 2015).

2.4.1 ARF6 Structure and Mutants

ARF6 is characterised by four distinct regions that contribute to its functionality and subcellular localisation. An amphipathic helix along with a myristoyl group, which is added co-translationally at the amino terminal region, is responsible for the association of the protein with membranes upon GTP binding. Switch I and Switch II domains are responsible for the interaction of ARF6 with specific GAPs and GEFs. These two regions are located centrally in the protein and are separated by a sequence known as the Interswitch (Pasqualato et al., 2001). The above three domains undergo conformational changes upon ARF6 activation and displace the amphipathic helix from a hydrophobic pocket, allowing it to associate with membranes. In addition, the hydrophobic residues that are revealed further strengthen the association of ARF6 with phospholipids **Figure 2.15** (Antonny et al., 1997).

Crystallisation of ARF6 in both the GTP- and GDP- bound forms allowed for the generation of constitutively active, dominant negative and fast cycling mutants that are indispensable to the study of the protein's biology. More specifically, ARF6Q67L exhibits resistance to hydrolysis and ARF6T27N limited activation. Both of these mutations are part of the effector domain of ARF6 and thus interfere with the GTP-GDP

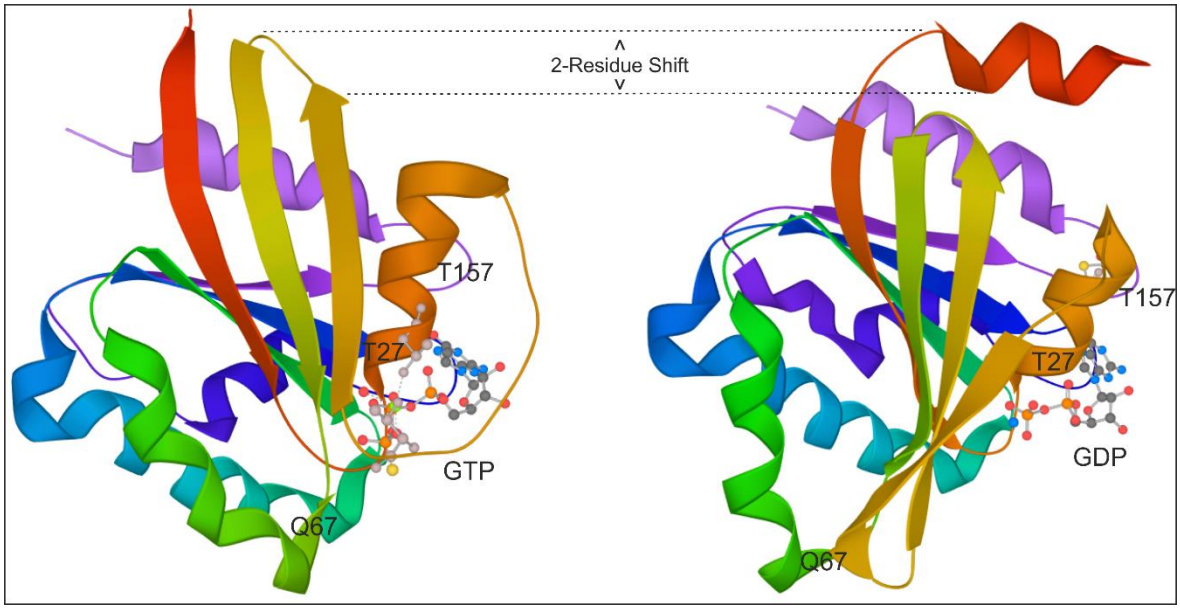


Figure 2.15 ARF6 Structure in GDP/GTP Forms

In the GDP form of ARF6 (Right) Switch I (Orange), Switch II (Green) and the Interswitch (Yellow) regions form a hydrophobic pocket that harbours the N-terminal amphipathic helix (Red). In that state, a conserved aspartic acid residue protrudes from the Switch II domain and along with GDP stabilises the structure. Exchange of GDP for GTP causes a conformational shift on the Interswitch region by exactly two residues. This shift displaces switch I and II regions and allows the protein to bind to GTP, which is available in the cytoplasm. In addition, the movement of the Interswitch dislodges the helix from the pocket with the latter being now able to associate with membranes. Adapted from (Pasqualato et al., 2002)

cycle. However, results extrapolated by using these mutants should be interpreted cautiously because affecting the activation state of ARF6 also interferes with its localisation (D'Souza-Schorey et al., 1995). In addition, ARF6T157A has been shown to rapidly exchange GTP for GDP thus being more active than wild-type AFRF6 while still being able to undergo hydrolysis by GAPs. The function of ARF6T157A is attributed to the limited ability of the alanine residue, located in the binding pocket, to form van der Waals bonds with the guanosine ring (Santy, 2002).

2.4.2 ARF6 Activation Machinery

To date, 15 GEFs have been identified to function in response to cell stimulation by several factors such as hormones and growth factors and promote activation of ARFs. Furthermore, 8 of the above have been found to act specifically on ARF6 and are subdivided into 3 separate families. The Cytohesin family comprises of Cytohesin1, ARNO and GRP1, the EFA6 family of EFA6A /B /C and /D, and the BRAG family of GEP100/BRAG2 (Casanova, 2007). Contrary to the last two families, Cytohesins are not ARF6 specific GEFs but can act on other ARF GTPases, promoting GDP/GTP exchange in a similar manner (Casanova, 2007).The structure of these GEFs includes a 200 amino acid Sec7 domain and a characteristic Pleckstrin Homology (PH) domain. The former includes a conserved glutamate residue that competes with GDP and promotes its dissociation, allowing ARF6 to bind cytosolic GTP. The latter associates with PIPs and other effectors, thus guiding GEFs to appropriate subcellular compartments (Casanova, 2007). In addition, a Coiled-Coil (CC) domain which is present in the structure of all the above GEFs has been implicated in ARF6 activation in response to G protein signalling (Laroche et al., 2007).

GEFs translocate to membranes in order to activate their substrates by interaction of their PH domain with PIPs. Interestingly, association of GEFs with PIPs does not increase their catalytic activity but is indispensable for the precise regulation of ARF6, in response to stimuli, in appropriate subcellular compartments (Paris et al., 1997). Cytohesins have been found to interact with PIP3 which is generated by PI3K in response to membrane receptor signalling (Klarlund et al., 1997). In addition to PIP3 binding, ARNO is recruited to the membrane in response to insulin stimulation. However, it is still unclear whether ARNO-dependent ARF6 activation is related to PIP3

or insulin receptor binding (Li et al., 2003; Jackson et al., 2000b). Furthermore, EFA6 family members bind to PI(4,5)P2 and GEP100 to PI4P, PI(4,5)P2 and PIP3 (Sakagami, 2008; Sakurai et al., 2011). GEP100 has also been found to associate with EGF and VEGF receptors. Both interactions are dependent on ligand stimulation and lead to ARF6 activation. The former is involved in cancer cell invasion and the latter in angiogenesis (Hashimoto et al., 2011; Morishige et al., 2008).

2.4.3 ARF6 Inactivation Machinery

Thus far, 31 GAPs have been identified in the human genome and 10 of them function directly on ARF6, regulating different processes. ARFGAPs include a characteristic 130 amino acid long ARFGAP domain which binds ARF GTPases and is indispensable for hydrolysis of the latter. Within this domain there is a conserved arginine residue that forms an ‘’arginine finger’’ and extends into the GTP-binding pocket of ARFs to stimulate hydrolysis. In addition, a zinc finger motif which is also present in the ARFGAP domain and creates a hydrophobic region within it, is important for the GAP structure and interaction with other partners (Goldberg, 1999).

ARFGAP1 has been found to inactivate ARF6 in an AP-2-dependent manner, thus connecting ARF6 to CME (Bai et al., 2011). ADAP1 and ADAP2 associate with PIPs via their PH domains and regulate ARF6 in specific compartments. ADAP1 binds to PIP3 and arrests ARF6 in endosomes, prohibiting its shuttling to the plasma membrane (Venkateswarlu et al., 2004). ADAP2 has been associated with the ARF6-dependent endocytosis of RNA viruses (Shu et al., 2015). GIT1 and GIT2 GAPs have been found to promote GTP hydrolysis on all mammalian ARFs (Vitale et al., 2000). In addition, GIT1 overexpression leads to reduced internalisation of the

β2-adrenergic receptor, a process in which ARF6 is directly implicated (Premont et al., 1998). ACAP1 and ACAP2 proteins preferentially inactivate ARF6 over other ARFs. Their overexpression inhibits the creation of cellular protrusions, a process in which ARF6 is implicated (Jackson et al., 2000a). ARAP2 and ARAP3 are also involved in ARF6-dependent adhesion processes. ARAP2 promotes focal adhesion growth by inactivating ARF6 and RAC1 (Chen et al., 2013). ARAP3 binds to PIP3 and abrogates RHOA and ARF6 cycling, thus stimulating the formation of lamelipodia (Krugmann et al., 2006).

SMAP1 and SMAP2 are small, 50kd ARFGAPs, characterized by their ability to bind Clathrin heavy chains. To date, SMAP1 alone has been demonstrated as a functional ARF6 GAP. SMAP2 regulates mainly ARF1 activity at the endosomes and TGN where it associates with Clathrin and other Clathrin complex components such as AP-1 (Natsume et al., 2006). Overexpression of SMAP1 had no effect on the ARF6-dependent rearrangement of ACTIN that leads to formation of cell protrusions. However, an effect was noted on CME, as transferrin receptors remained blocked on the plasma membrane. This can be attributed to limited recruitment of AP-2 to Clathrin coated pits. Furthermore, Clathrin-dependent vesicular trafficking between the endosomes and the TGN or lysosomes was not impaired, suggesting that SMAP1 is not involved in the process (Tanabe et al., 2005). In addition, a role for SMAP1 in the internalisation of E-Cadherin has also been demonstrated. In MDCK cells, overexpression of the GAP arrests E-Cadherin on the cell surface. Since E-Cadherin internalisation is known to be Clathrin mediated, SMAP1 inhibits the process by inactivating ARF6 (Kon et al., 2008). Accumulation of E-Cadherin on the cell adherens junctions exhibits a negative effect on EMT. This can explain how increased ARF6

activity correlates with higher aggressiveness of several cancers such as melanoma and lymphoma (Sangar et al., 2014).

2.4.4 ARF6 in Endocytosis and Trafficking

ARF6 is involved in a plethora of cellular functions including the regulation of endocytosis in Clathrin –dependent and –independent manners. It has been demonstrated that ARF6 activates Phosphatidylinositol-4-Phosphate-5-Kinase (PIP5K) and Phospholipase D (PLD). Activating these two factors leads to an increase in the levels of PI(4,5)P2 with the latter functioning cooperatively with activated ARF6 to recruit AP-2, thus promoting CME (Wenk and De Camilli, 2004). This process is tightly regulated by SMAP1, a novel ARF6GAP discussed above that has been shown to interact with Clathrin heavy chains. ARF6 also interacts with the nucleoside diphosphate kinase Nm23-H1. The latter controls Dynamin activity by regulating the supply of GTP and is therefore involved in the Dynamin dependent vesicle fission process (Palacios et al., 2002). In MDCK cells, WNT stimulation has been shown to promote ARF6 activation which leads to E-Cadherin internalisation. Therefore, E-Cadherin is characterised as cargo using the ARF6 and Clathrin –dependent endocytosis pathway (Pellon-Cardenas et al., 2013). In the same cell line, ARF6 was shown to modulate the apical CME of the polymeric immunoglobulin receptor (pIgR), as overexpression of the hydrolysis resistant mutant of the GTPase abolished its internalisation (Hyman et al., 2006).

Apart from CME, ARF6 also regulates the internalisation of cargo independently of Clathrin. This process involves membrane ruffling through activation of RAC and rearrangements in the lipid composition of the plasma membrane. RAC is activated in

response to ARF6 activation, an event catalysed by EFA6 (Franco, 1999). The latter, similar to CME, involves increase of PI(4,5)P2 by sequential activation of ARF6, PLD and PIP5K. PI(4,5)P2-enriched membrane domains act as scaffolds, recruiting ACTIN remodelling enzymes that aid in ruffling (Wenk and De Camilli, 2004). In addition, the forming vesicles which are distinct due to their enrichment in cholesterol, fuse with EEs that also contain CME cargo (Naslavsky et al., 2004). Cargo that enter cells in this manner includes the Major Histocompatibility Complex (MHC) Class I, the M2-muscaranic Acetylcholine receptors, β1 Integrins, the Peripheral Myelin-membrane Protein (PMP22) and others, reviewed in: (Donaldson, 2003).

Cycling of ARF6 is implicated in vesicular trafficking. More specifically, hydrolysis allows for internalisation and vesicle sorting, while subsequent reactivation leads to endosomal recycling (Naslavsky et al., 2004). This is also supported by the fact that hydrolysis resistant mutants of ARF6 lead to the formation of intracellular vacuoles that are enriched for PI(4,5)P2 and F-ACTIN (Brown et al., 2001). ARF6-dependent recycling is associated with tubular endosomes that emanate from the Endocytic Recycling Compartment (ERC) and carry cargo to the cell surface. This is highlighted by the fact that perturbing ARF6 activation by inhibiting ERK leads to REs arrest in the ERC (Robertson et al., 2006). In this process, ARF6 activates Phospholipase D2 (PLD2) and PIP5K. PLD2 catalyses the formation of phosphatidic acid and diacylglycerol, two molecules essential for the fusion of REs with the plasma membrane (Jovanovic et al., 2006). Similar to its role in CME and CIE, PIP5K generates PI(4,5)P2 which acts by recruiting enzymes important in membrane fusion and ACTIN polymerisation (Brown et al., 2001). Fibroblast Growth Factor Receptor (FGFR) has been shown to follow this recycling route, as limited PI(4,5)P2 causes its

endosomal accumulation which leads to impaired cell proliferation (Zimmermann et al., 2005). In addition, Hepatocyte Growth Factor (HGF)- stimulated β1 integrin recycling is also controlled by ARF6 activation, as pharmacological inhibition of ARF6GEFs perturbs integrin trafficking. This is important in cancer drug development, as suppression of ARF6 activation leads to impaired tumor angiogenesis and growth (Hongu et al., 2015).

2.5 Thesis Organisation and Objectives

In the previous introductory sections, we summarised and discussed published material relevant to the nature of this scientific study. Here, we provide an outline of the scientific questions we attempt to answer in the following chapters.

2.5.1 Chapter 3: Elucidating the Role of ARF6 in Activin A / TGFβ Signalling

To date, there is no scientific research conclusively confirming that ARF6 is implicated in Activin A / TGFβ signalling. However, pilot experiments conducted in our lab uncovered a novel interaction between the GTPase and SMAD4. Additionally, ARF6GAP SMAP1 was identified as an interacting partner of ACVR1B, in a proteomics screen. Based on these results, in this chapter we attempt to (1) identify potential interactions of ARF6 with other Activin A / TGFβ pathway components having sequence similarity to SMAD4, (2) examine the effect of the activation state of ARF6 in the progression of Activin A / TGFβ signalling, (3) examine the effect of Activin A / TGFβ signalling on the state of ARF6 activation and (4) test the effect of SMAP1 on the cycle of ARF6, following Activin A / TGFβ cascade induction.

2.5.2 Chapter 4: Elucidating the Role of ARF6 in Human Embryonic Stem Cell Signalling

Several crosslinking signalling pathways are involved in the maintenance of hES cells pluripotency. Deregulation of these and other pathways destabilizes pluripotency and marks the onset and progression of differentiation. Given the importance of Activin A / BMP4 signalling in both processes, as well as our findings that implicate ARF6 in these pathways, we hypothesised a role for the GTPase in hES cell signalling. Therefore, in this chapter we attempt to examine the effect of the state of ARF6 in the (1) maintenance of pluripotency, (2) progression of Activin A / BMP4 signalling and (3) outcome of mesendodermal differentiation.

2.5.3 Chapter 5: Identifying Novel Molecules Implicated in Early Mesendoderm Specification by a Broad Transcriptomic Approach

hES cells pluripotency relies on an elaborate network of interconnected signalling pathways. These are activated or suppressed by compounds and ligands included in all commercially available media used to sustain cells in an undifferentiated state. Even though these media simplify cell culture maintenance, they also restrict research since pathway signalling studies are carried out in a specific background of pre-included compounds. Therefore, in this chapter we attempt to utilise a novel hES cell culture system that allows for substitution, addition or removal of different compounds, thus allowing research on a broader range of signalling cascades. hES cells cultured in this system were induced with a ligand cocktail that initiates mesendoderm specification. Subsequently, RNA sequencing was performed in order to uncover novel transcripts that are deregulated during differentiation to this fate.

CHAPTER 3

ELUCIDATING THE ROLE OF ARF6 IN ACTIVIN A / TGFB SIGNALLING

3.1 Introduction

Current scientific literature suggests that signalling and trafficking of TGFβ superfamily members are tightly regulated and interlinked processes. In the absence of ligand, TGFβRs are continuously internalised via CME (Mitchell et al., 2004). Even though the endocytosis rate is not affected by the presence of ligand, the process itself is indispensable for signalling (Hayes et al., 2002; Penheiter et al., 2002). CME of TGFβ receptors into EEA1 and RAB5 positive endosomes has been associated with signal propagation (Penheiter et al., 2002; Hayes et al., 2002). On the other hand, CavME of TGFβ receptors causes their localisation in SMAD7 and SMURF2 enriched endosomes and results in receptor ubiquitination and degradation leading to signalling termination (Di Guglielmo et al., 2003). However, several other independent studies have questioned the necessity of receptor internalisation for further signalling. Using endocytosis inhibitors, Chen *et al.* reported that TGFβR1 and SARA accumulate on the plasma membrane leading to enhanced TGFβ signalling from that compartment (Chen, 2009). In addition, using internalisation-deficient receptor mutants, Shapira *et al.* demonstrated that endocytosis is dispensable for further signalling (Shapira et al., 2012).

Equally controversial results have been reported for Activin A as well. Experiments using a mutant ACVR1B that is unable to undergo internalisation showed

that signalling in the presence of Activin A is not affected, therefore suggesting that ligand internalisation is dispensable for downstream signalling (Zhou et al., 2004). In support of this, a study in *Xenopus* showed that overexpression of dominant negative RAB5 had no effect on the Activin A cascade. However, in the same model, Jullien *et al.* demonstrated that interfering with Dynamin and thus Activin A internalisation affected downstream signalling (Jullien and Gurdon, 2005).

Several different molecules are involved in the regulation of endocytosis, thus affecting downstream signalling. ARF6 has been implicated in both CME and CIE pathways, mainly by stimulating the formation of PI(4,5)P2 via activation of PLD and PIP5K (Wenk and De Camilli, 2004). Interestingly, PLD is also involved in the activation of mTOR, a complex that phosphorylates the linker domain of SMAD2/3 proteins and limits oligomerisation with SMAD4 (Gadir et al., 2007). In H-RAS transformed cells PLD activity is controlled synergistically by ARF6 and RALA (Xu et al., 2003). RALBP1, an effector of RALA, has been found to interact with ARIP2 (Tsuchida et al., 2004). The latter binds to ACVR2s via its PDZ domain and regulates their internalisation.

ARF6 is involved in various stages of the endocytic pathway with clear roles in the processes of cargo internalisation, vesicle sorting and recycling (Naslavsky et al., 2004). Recent research in *C. elegans* demonstrated that recycling of BMPR2 (DAF-4) occurs through ARF6-dependent REs, whereas BMPR1 (SMA-6) relies on the retromer complex for recycling. It should be noted that full length DAF-4 and SMA-6 were amplified from *C.elegans* genomic DNA, GFP-tagged and used in co-localisation assays in this study (Gleason et al., 2014). In addition, TGFβR2 trafficking has also been associated with the retromer function, with the latter delivering the receptor to

RAB11-positive endosomes, post signalling (Yin et al., 2013). The trafficking routes of TGFβR1 or a potential involvement of ARF6 have not been addressed by the study.

The findings above clearly implicate ARF6 in the regulation of TGFβ superfamily receptor signalling and trafficking. Unpublished results from our lab in collaboration with Phillippe Chavrier indicate that activated ARF6 interacts with SMAD4. In addition, SMAP1, a specific ARF6GAP that contains a Clathrin binding domain, has been identified as an interacting partner of ACVR1B, in a proteomics screen (data not shown). Our initial approach was to validate the above interactions and explore their significance in the outcome of Activin A / TGFβ signalling.

3.2 Results

3.2.1 Activated ARF6 Interacts with the C-Terminal Tail of SMAD4

Preliminary results from a yeast two-hybrid assay, conducted by Dr. Philip Chavrier (Curie Institute, Paris, France) in collaboration with Hybrigenics (Paris, France), yielded a possible interaction between ARF6 and SMAD4. To verify that interaction, recombinant GST-SMAD4 expressed and purified from *E.coli BL21DE* cells was used as bait in a pull-down assay with the wild type, dominant negative (T27N) and constitutively active (Q67L) forms of ARF6 (see section 2.4.1) **Figure 3.1 (A)**. The results of the assay clearly indicated that the interaction between ARF6 and SMAD4 occurs only when ARF6 is activated (GTP-bound form). To further validate that, co-immunoprecipitation experiments between the proteins were performed by overexpressing them both in HEK-293 cells. A weak interaction between HA-ARF6Q67L and GFP-SMAD4 is also apparent from the outcome of the co-immunoprecipitations **Figure 3.1 (B)**.

Next, we investigated whether the interaction observed was restricted to activated ARF6, or if it occurs with other classes of ARF GTPases. To examine that, we performed a pull-down assay using the activated forms of ARF1 (Q71L) and ARF5 (Q71L) as bait for the GST-SMAD4. The activated (Q67L) and the inactive (T27N) forms of ARF6 were used as positive and negative controls, respectively. The results of the assay indicated that the interaction is specific for the activated form of ARF6 (Q67L), as activated ARF1 or ARF5 proteins were not pulled down by GST-SMAD4 **Figure 3.1 (C)**.

Having validated the interaction between ARF6 and SMAD4, we moved on to map the region of the latter that binds the GTPase. In that direction, we generated and purified two different SMAD4 truncated mutants that were used along with the full length protein as baits for activated ARF6 in a pull-down assay. The results traced the interaction to the last 32 amino acids SMAD4 **Figure 3.2 (A)**. The assay was repeated using a new, truncated mutant that lacked the last 43 amino acids. There, the interaction was abolished, definitively proving that ARF6 interacts with a motif located within the last 43 amino acids of SMAD4 **Figure 3.2 (B)**.

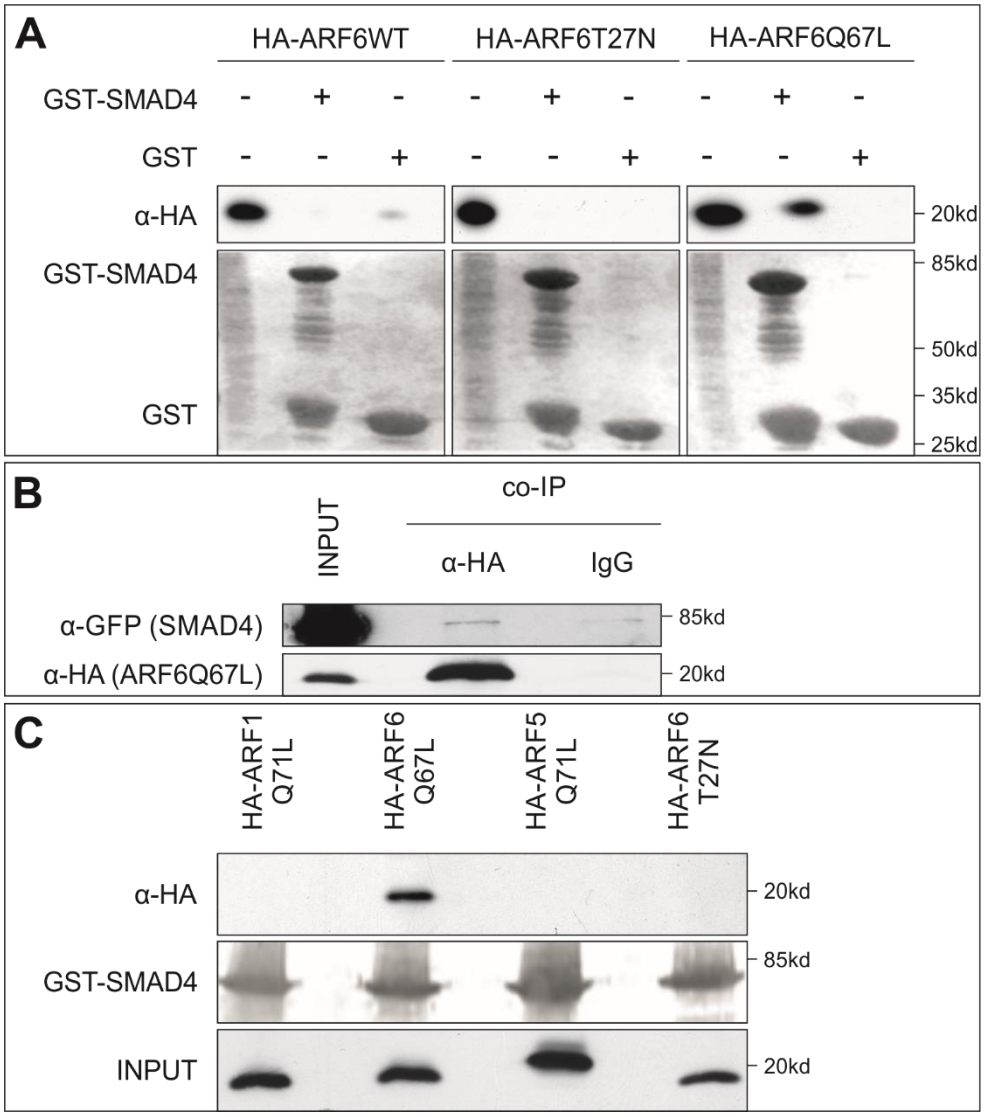


Figure 3.1: Interaction of the Activated ARF6 with SMAD4

(A) HEK-293 cell lysates overexpressing wild type, inactive (T27N) or activated (Q67L) ARF6 were incubated with GST-SMAD4 or GST. The complexes were washed, subjected to SDS-PAGE and immunoblotted with an α-HA antibody. Ponceau staining of GST-SMAD4 and GST is depicted in the lower panel. (B) HA-ARF6Q67L and GFP-SMAD4 were transiently overexpressed in HEK-293 cells and co-immunoprecipitated using α-HA or rat IgG antibodies. Immunocomplexes were washed, subjected to SDS-PAGE and immunoblotted with an α-GFP antibody to confirm GFP-SMAD4 immunoprecipitation. (C) HEK-293 cell lysates overexpressing activated ARF1 (Q71L), ARF6 (Q67L), ARF5 (Q71L) or inactive ARF6 (T27N) were incubated with GST-SMAD4 or GST. The complexes were washed, subjected to SDS-PAGE and immunoblotted with an α-HA antibody. Ponceau staining of GST-SMAD4 is depicted in the middle panel. The input of the proteins probed with an α-HA antibody is depicted in the lower panel. *Results (A) and (C) were produced by a former lab member, Panayiota Chira.*

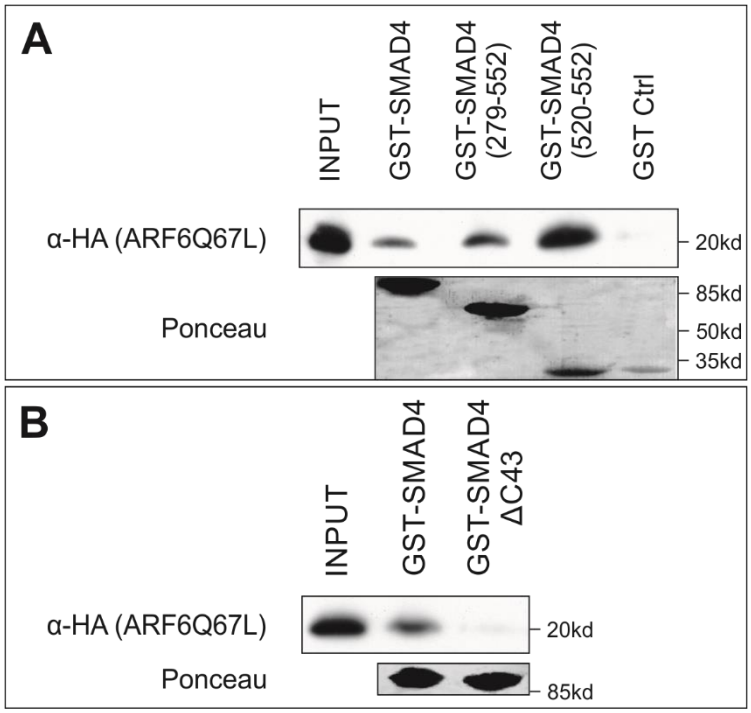


Figure 3.2: Mapping the Interaction of Activated ARF6 with SMAD4

(A) HEK-293 cell lysates overexpressing activated ARF6 (Q67L) were incubated with GST-SMAD4 full length, GST-SMAD4 (279-552), GST-SMAD4 (520-552) or GST. The complexes were washed, subjected to SDS-PAGE and immunoblotted with an α-HA antibody. Ponceau staining of the GST proteins is depicted in the lower panel. (B) HEK-293 cell lysates overexpressing activated ARF6 (Q67L) were incubated with GST-SMAD4 full length or a truncated version of SMAD4 lacking the last 43 amino acids. The complexes were washed, subjected to SDS-PAGE and immunoblotted with an α-HA antibody. Ponceau staining of the GST proteins is depicted in the lower panel. *Results (A) and (B) were produced by a former lab member, Panayiota Chira.*

3.2.2 Activated ARF6 Interacts with the C-Terminal Tails of SMAD2/3

In section 3.2.1, we verified the interaction between SMAD4 and activated ARF6 and traced it to the last 43 amino acids of the former. Having identified that, we examined the sequence of SMAD4 and compared it with proteins SMAD2 and SMAD3 to investigate whether this interaction is conserved among other SMADs, as well. In **Figure 3.3 (A)** we show that there is 50% identity between SMAD2 and SMAD4 and 57% identity between SMAD3 and SMAD4 at their C-terminal tails. Interestingly, part of the L3-Loop domain of SMADs that is responsible for their association with TGFβ type I receptors is encoded within the last 43 amino acids.

In order to investigate whether that similarity has a functional role that relates to ARF6, we GST-tagged and purified the last 40 amino acids of SMAD2 and SMAD3 proteins and used them in a subsequent pull-down assay with wild type (WT), activated (Q67L) or dominant negative (T27N) ARF6. In the same assay, we also used two mutants of the proteins, named SMAD2EDME and SMAD3EDVE, respectively that mimic their phosphorylated forms. GST-SMAD4 was used as a positive control in the experiment. The results clearly showed that both forms of SMAD2 and SMAD3 interact with the activated form of ARF6 **Figure 3.3 (B)**. The interaction also persists, even though weaker, when the wild type ARF6 is used as bait, but is completely abolished in the presence of the dominant negative form of the GTPase.

We further validated the above interactions by co-immunoprecipitation experiments in HEK-293 cells. HA-tagged activated ARF6 was overexpressed with the myc-tagged versions of SMAD2, SMAD2EDME, SMAD3 or SMAD3EDVE. The results of the assays undoubtedly showed that ARF6Q67L interacts with SMAD2 and SMAD3,

both in their wild type **Figure 3.4 (A), (B)** and phosphorylated forms **Figure 3.4 (C), (D)**. No noticeable difference was observed in the intensity of the interaction between activated ARF6 and the wild type or activated forms of the SMAD2/3 proteins.

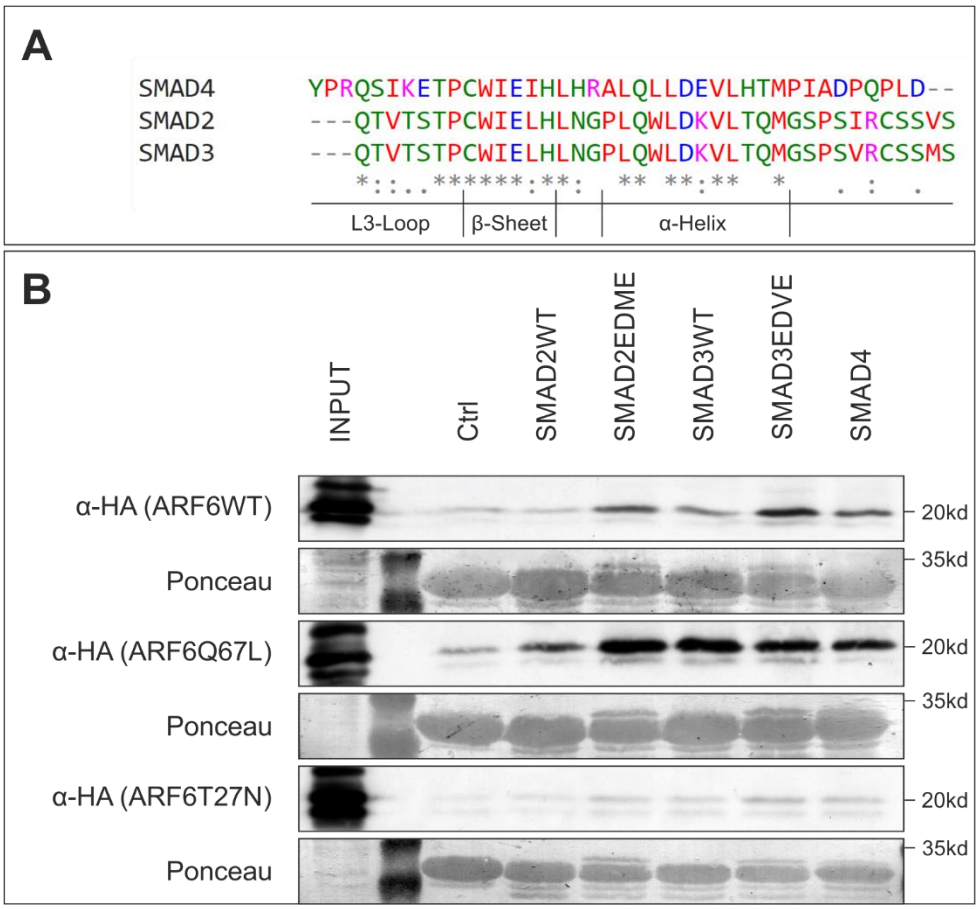


Figure 3.3: Interaction of Activated ARF6 with SMAD2 and SMAD3

(A) Alignment of the C-terminal tails of SMAD4, SMAD2 and SMAD3 proteins. SMAD2 and SMAD3 proteins exhibit a 50% and 57% identity with SMAD4 respectively, in their last 43 amino acids. The SMAD domains involved included in the tails are also depicted. (B) HEK-293 cell lysates overexpressing activated ARF6(Q67L) were incubated with GST proteins encoding the C-terminal tails of SMAD2 and SMAD3 or their phospho-mimicking mutants (SMAD2EDME, SMAD3EDVE), respectively. The complexes were washed, subjected to SDS-PAGE and immunoblotted with an α-HA antibody to detect the pulled-down quantity of HA-ARF6Q67L. The lower panel in each pull-down depicts a ponceau stain of the GST proteins.

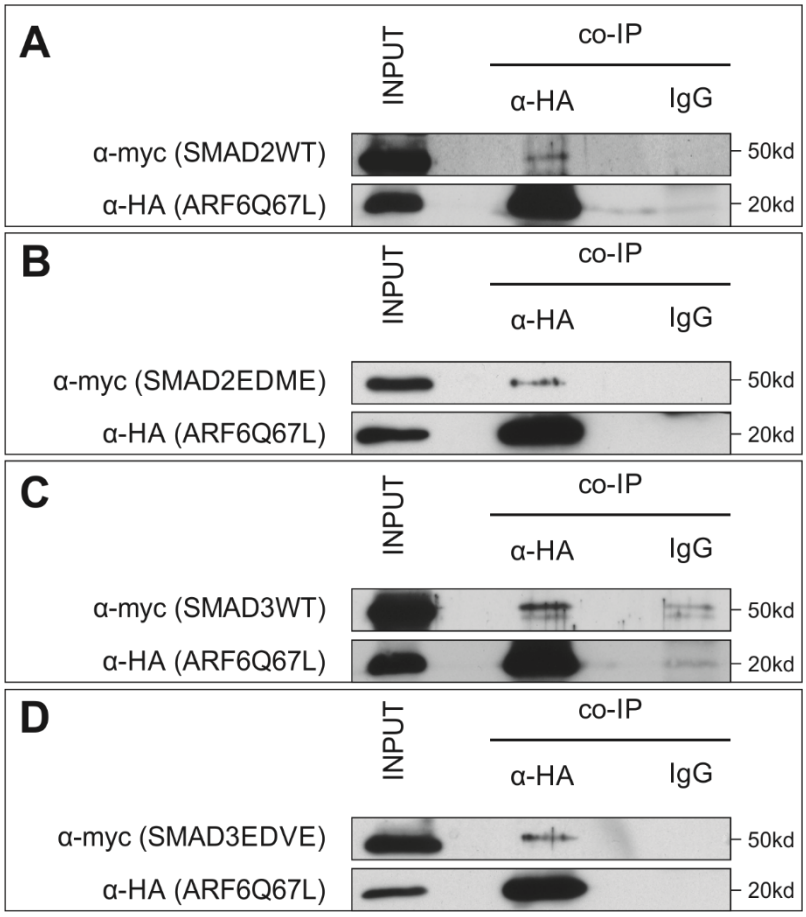


Figure 3.4: Immunoprecipitations of Activated ARF6 with SMAD2 and SMAD3

HEK-293 cells overexpressing HA-ARF6Q67L and (A) myc-SMAD2WT or (B) myc-SMAD2EDME were lysed using 1% Triton X-100 lysis buffer, and subjected to immunoprecipitation using α-HA or rat IgG antibodies. Immunocomplexes were washed, subjected to SDS-PAGE and immunoblotted with an α-myc antibody to confirm myc-SMAD2WT or myc-SMAD2EDME immunoprecipitation. HEK-293 cells overexpressing HA-ARF6Q67L and (C) myc-SMAD3WT or (D) myc-SMAD3EDVE were lysed using 1% Triton X-100 lysis buffer, and subjected to immunoprecipitation using a-HA or rat IgG antibodies. Immunocomplexes were washed, subjected to SDS-PAGE and immunoblotted with an α-myc antibody to confirm myc-SMAD3WT or myc-SMAD3EDVE immunoprecipitation.

3.2.3 ARF6 is Implicated in Activin A / TGFβ Mediated SMAD2/3 Phosphorylation

Upon induction with Activin A or TGFβ, SMAD2 and SMAD3 proteins are known be phosphorylated before interacting with SMAD4. Based on that, we hypothesised that activation of ARF6 might impact the phosphorylation levels of the R-SMADs.

To address this hypothesis, we transfected cells with constitutively active ARF6 (Q67L), a fast cycling mutant (T157A) that rapidly exchanges GDP for GTP, or a GFP control vector. Subsequently, the cells were induced with Activin A or TGFβ for 40min and the lysates were analysed by western blotting using antibodies recognising the phosphorylated forms of SMAD2 and SMAD3 **Figure 3.5 (A)**. The results indicated that activation of ARF6 results in increased phosphorylation levels of SMAD2 and SMAD3. TGFβ induction, in the presence of the fast cycling ARF6, increased the phosphorylation of SMAD2 by 2-fold **Figure 3.5 (B)** and SMAD3 by 1.61-fold **Figure 3.5 (C)**. In the presence of the activated ARF6, TGFβ induction increased the phosphorylation of SMAD2 by 2.6-fold **Figure 3.5 (B)** and SMAD3 by 2.11-fold **Figure 3.5 (C)**. Activin A induction, in the presence of the fast cycling ARF6, increased the phosphorylation of SMAD2 by 1.57-fold **Figure 3.5 (B)** and SMAD3 by 1.38-fold **Figure 3.5 (C)**. In the presence of the activated ARF6 mutant, TGFβ induction increased the phosphorylation of SMAD2 by 1.8-fold **Figure 3.5 (B)** and SMAD3 by 1.48-fold **Figure 3.5 (C)**.

In order to further validate the implication of ARF6 in the phosphorylation of SMAD2/3, we knocked-down the GTPase using an siRNA targeting ARF6 in HEK-293 cells. A scrambled siRNA was used as negative control. Next, the cells were induced with Activin A or TGFβ for 40min, and the lysates were analysed by western blotting

using antibodies recognising the phosphorylated forms of SMAD2 and SMAD3. The phosphorylation levels of both SMAD2 and SMAD3 were observed to be lower in the absence of ARF6 **Figure 3.6 (A)**. TGFβ induction, in the absence of ARF6, decreased SMAD2 phosphorylation by 0.5-fold **Figure 3.6 (B)** and SMAD3 by 0.64-fold **Figure 3.6 (C)** compared to the control. Activin A induction, in the absence of ARF6, decreased SMAD2 phosphorylation by 0.56-fold **Figure 3.6 (B)** and SMAD3 by 0.62-fold **Figure 3.6 (C)** compared to the scrambled control. This result further implicated ARF6 in Activin A and TGFβ signalling pathways.

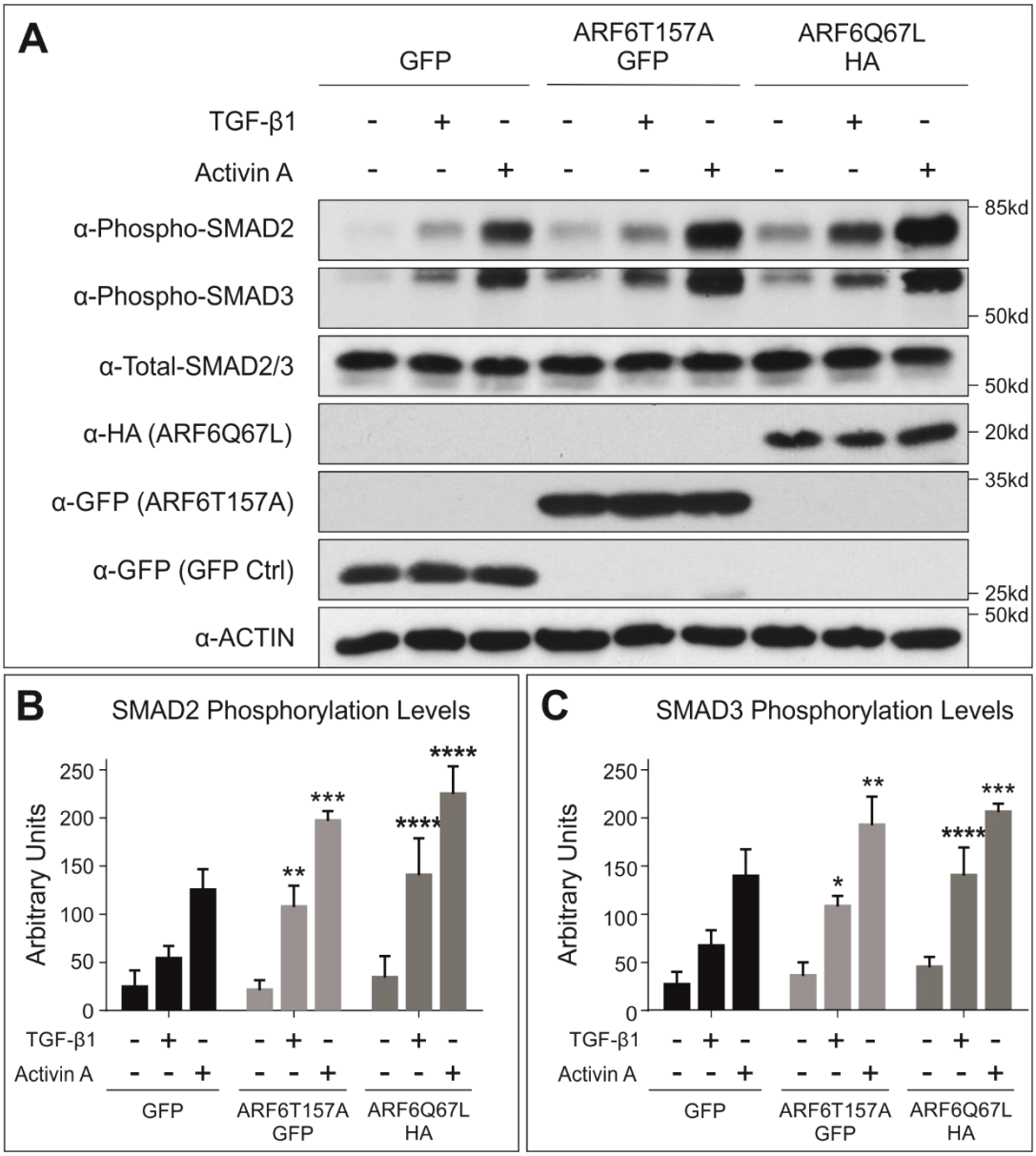


Figure 3.5: Effect of ARF6 Activation on SMAD2/3 Phosphorylation

(A) HEK-293 cells transfected with a GFP control vector, fast cycling ARF6 (GFP-ARF6T157A) or activated ARF6 (HA-ARF6Q67L) were subjected to 3hrs serum starvation followed by induction with 2.5ng/ml TGF-β1 or 50ng/ml Activin A. Cell lysates were subjected to SDS-PAGE and immunoblotted with α-pSMAD2, α-pSMAD3, total SMAD2/3, α-HA, α-GFP and α-ACTIN antibodies. Changes in the phosphorylation levels of (B) SMAD2 and (C) SMAD3 in the presence of the fast cycling (GFP-ARF6T157A) or the activated ARF6 (HA-ARF6Q67L) mutant relative to the GFP transfected control cells. Densitometry was performed using the Image Studio Lite software. Statistical significance was calculated in GraphPad Prism using the non-parametric Mann-Whitney test (N=6).

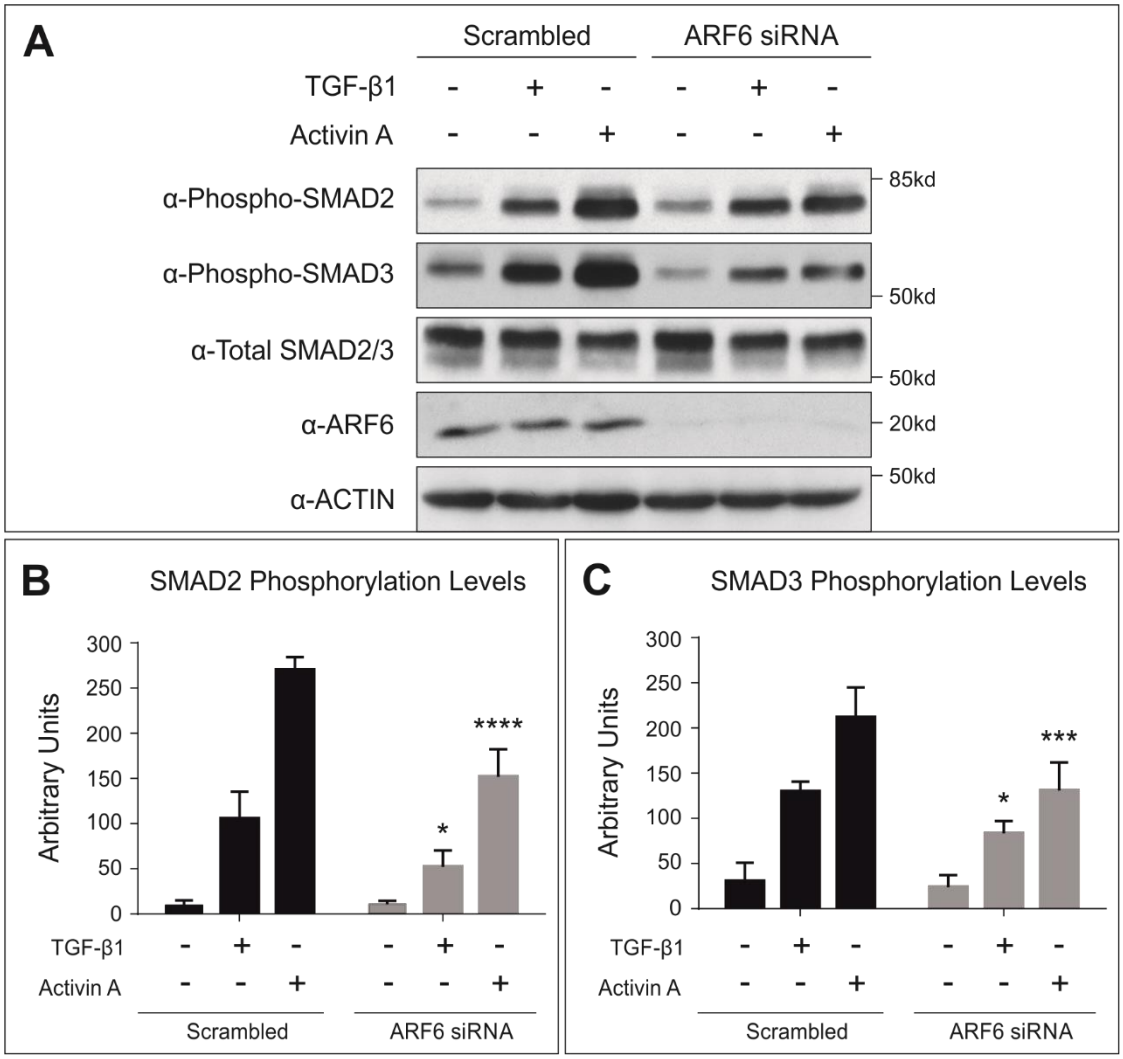


Figure 3.6: Effect of ARF6 Knock-Down on SMAD2/3 Phosphorylation

(A) HEK-293 cells transfected with scrambled or ARF6 specific siRNA were subjected to 3hrs serum starvation followed by induction with 2.5ng/ml TGF-β1 or 50ng/ml Activin A. Cell lysates were subjected to SDS-PAGE and immunoblotted with α-pSMAD2 and α-pSMAD3, total SMAD2/3, α-ARF6 and α-ACTIN antibodies. Changes in the phosphorylation levels of (B) SMAD2 and (C) SMAD3 in the absence of ARF6 relative to the scrambled transfected control cells. Densitometry was performed using the Image Studio Lite software. Statistical significance was calculated in GraphPad Prism using the non-parametric Mann-Whitney test (N=6).

3.2.4 Activin A / TGFβ Signalling Promotes ARF6 GTP – GDP Exchange

All the experiments above confirmed that ARF6 is implicated either directly or indirectly in Activin A and TGFβ signalling. ARF6 physically binds proteins SMAD4, SMAD2, and SMAD3 and affects the phosphorylation of SMAD2/3 upon induction with TGFβ or Activin A. However, it has not yet been examined whether activation of the Activin A or TGFβ pathways has an effect on the ARF6 GTP-GDP cycle.

To address the above, we expressed and purified a GST-tagged GAP domain of ARHGAP10. ARHGAP10 is a GTPase activating protein and a known partner of ARF6 that binds the GTPase only when the latter is activated (GTP-bound form), to catalyze hydrolysis. Therefore, the GAP domain of ARHGAP10 is only capable of binding ARF6-GTP (Dubois et al., 2005). Subsequently, the GST-GAP was used as bait in a pull-down assay with wild-type ARF6. HEK-203 cells were transiently transfected with a construct encoding an HA tagged ARF6. Before lysis, the cells that overexpressed ARF6 had been induced with Activin A or TGFβ for 40min, respectively.

The results of the assay indicated that upon treatment with either ligand, GST-GAP binds a lower quantity of wild-type ARF6 **Figure 3.7 (A)**. That fact suggests that ARF6-GTP has been hydrolyzed to ARF6-GDP in response to the addition of the ligands. More specifically, induction with TGFβ results in a 1.5-fold ARF6 inactivation while treatment with Activin A in a 3-fold inactivation **Figure 3.7 (B)**.

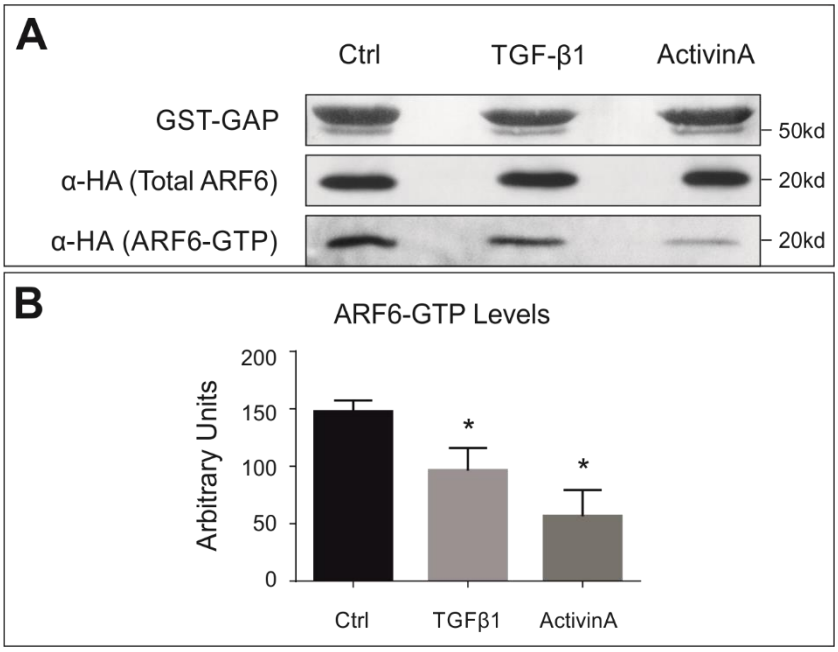


Figure 3.7: Effect of Activin A / TGFβ on ARF6-GTP Loading

(A) The GTP binding domain of an ARF6GAP was tagged with GST and purified from *E. Coli BL21DE* bacteria. HEK-293 cells were transfected with HA-ARF6WT, subjected to 3hrs serum starvation and induced with TGF-β1 (2.5ng/ml) or Activin A (50ng/ml) for 40min. The cell lysates were incubated with GST-GAP for 1hr and GST beads were used to pull-down the ARF6-HA-GTP/GST-GAP complex. HA-ARF6-GTP bound to the beads was detected by western blot using an α-HA antibody. (B) Quantitation of ARF6-GTP levels between control and TGF-β1 or Activin A treated cells. Densitometry was performed using the Image Studio Lite software. Statistical significance was calculated in GraphPad Prism using the non-parametric Mann-Whitney test (N=6).

3.2.5 ARF6GAP SMAP1 Interacts Specifically with ACVR1B

In section 3.2.4 we reported that ARF6 is inactivated in response to Activin A or TGFβ induction. Inactivation of any GTPase can occur due to activation of a GAP or inhibition of a GEF. Unpublished results from a proteomics screen indicated that SMAP1 interacts with the ACVR1B. This assay was carried out in HEK-293 cells using the FLAG-tagged intracellular domain of ACVR1B as bait. In-gel digestion and mass spectrometry were conducted by Prof. Heath's lab (University of Birmingham, UK). This interaction can potentially explain how ligand induction leads to ARF6 inactivation.

To validate the SMAP1 / ACVR1B interaction we carried out a co-immunoprecipitation assay. Initially, FLAG-tagged wild-type, dominant negative (K234R) and constitutively active (T206D) ACVR1B constructs were generated and assessed. Cells were transfected with the aforementioned ACVR1B forms, treated with Activin A for 40min and the lysates were immunoblotted with an antibody against phosphorylated SMAD2. As expected, cells transfected with wild-type ACVR1B had comparable SMAD2 phosphorylation to the non-transfected control. In the presence of ACVR1BK234R, SMAD2 phosphorylation was abolished. Cells transfected with ACVR1BT206D showed increased SMAD2 phosphorylation, even without Activin A induction **Figure 3.8 (A)**.

Co-Immunoprecipitation assays using the constructs above were conducted to validate the SMAP1 / ACVR1B interaction and investigate whether the activation state of the latter affects it. Cells were co-transfected with HA-SMAP1 and FLAG-ACVR1B **Figure 3.8 (B)**, FLAG-ACVR1BK234R **Figure 3.8 (C)** or FLAG-ACVR1BT206D **Figure 3.8 (D)**. The results indicated that only the wild-type form is capable of binding SMAP1.

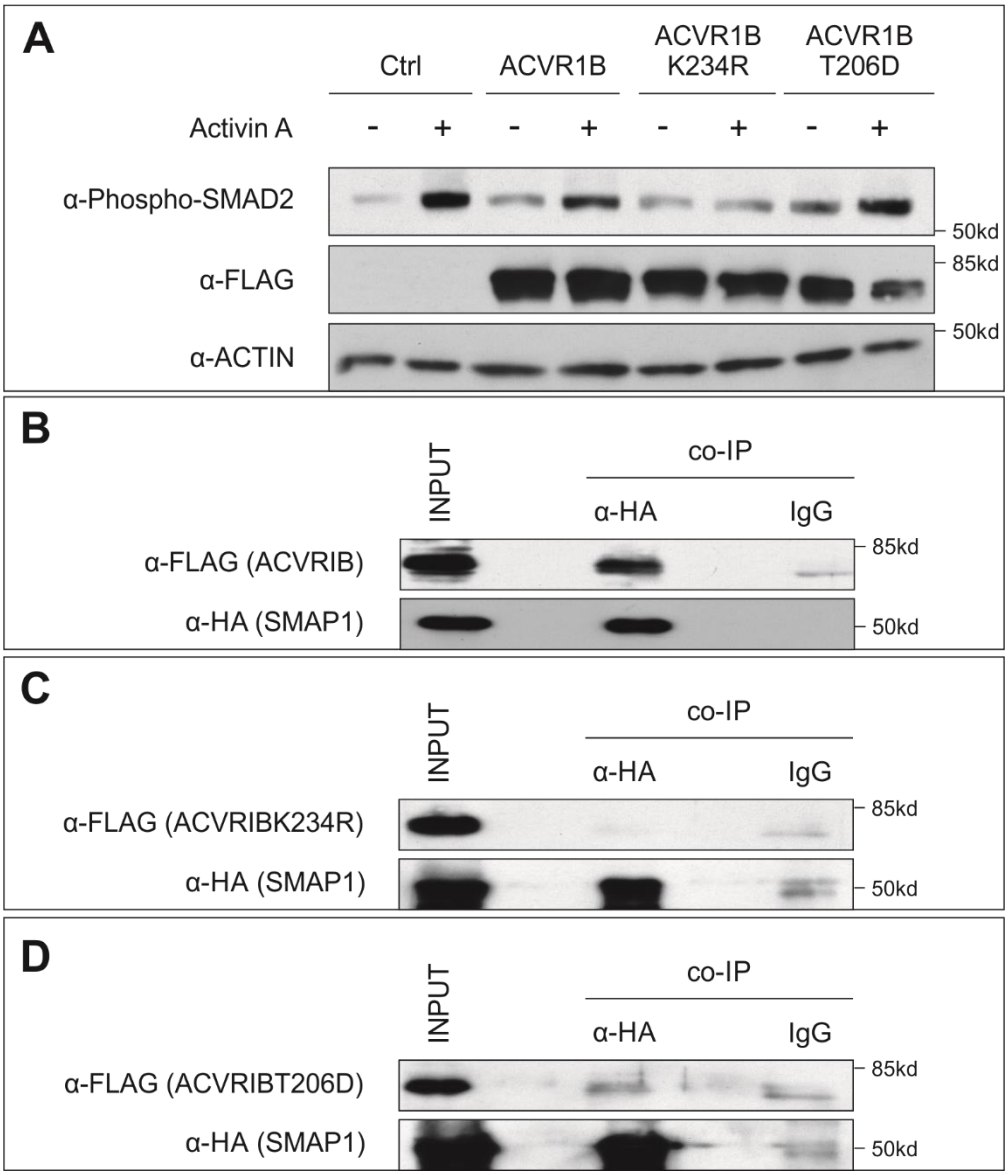


Figure 3.8: Interaction of SMAP1 with the Wild Type ACVR1B

(A) HEK-293 cells transfected with FLAG-ACVR1B, dominant negative ACVR1B (FLAG-ACVR1BK234R) or constitutively active ACVR1B (FLAG-ACVR1BT206D), were subjected to 3hrs serum starvation followed by induction with 50ng/ml of Activin A. Cell lysates were subjected to SDS-PAGE and immunoblotted with an α-pSMAD2 antibody. HEK-293 cells overexpressing HA-SMAP1 and (B) FLAG-ACVR1B, (C) FLAG-ACVR1BK234R or (D) FLAG-ACVR1BT206D were lysed using 1% Triton X-100 lysis buffer and subjected to immunoprecipitation using α-HA or rat IgG antibodies. Immunocomplexes were washed, subjected to SDS-PAGE and immunoblotted with an α-FLAG antibody to confirm the immunoprecipitations. This experiment was also performed using a different co-IP procedure and the results were comparable (see Appendix **Figure 7**)

3.2.6 SMAP1 CRISPR Knock-Out in HEK-293 Cells

In the previous sections we validated the interaction of wild-type ACVR1B with SMAP1 and the inactivation of ARF6 in response to Activin A or TGFβ signalling. Taking together these two results, we hypothesised that SMAP1 is the GAP responsible for the inactivation of ARF6. In order to prove this hypothesis, we generated a SMAP1 knock-out cell line where treatment with Activin A or TGFβ should not be capable of inactivating ARF6.

The CRISPR/CAS9 approach was used to generate the SMAP1 knock-out lines as it constitutes a fast, reliable and cost efficient method of genetic modification. Two different SMAP1 gRNAs were chosen, targeting PAMs close to the translation start site of the SMAP1 protein **Figure 3.9 (A)**. The gRNAs designed exhibited minimum off-target effects based on the Sanger Institute CRISPR platform. The vector used for delivering the gRNAs and the CAS9 endonuclease in the cells, is depicted in **Figure 3.9 (B)**.

Two different constructs, each one of the above gRNAs for SMAP1 were transfected in HEK-293 cells. The cells were subsequently analysed by western blotting using an antibody against SMAP1 **Figure 3.9 (A)**. The results showed that both gRNAs almost abolished the expression of SMAP1 in the cells **Figure 3.10 (B)**. Next, we generated clonal lines from the mass population of cells transfected with the CRISPR plasmids. 9 separate clones were isolated following selection with puromycin and scored for their SMAP1 expression levels by western blotting with the SMAP1 antibody **Figure 3.10 (C)**. As expected, all the clones generated, were successful SMAP1 bi-allelic knock-outs **Figure 3.9 (D)**.

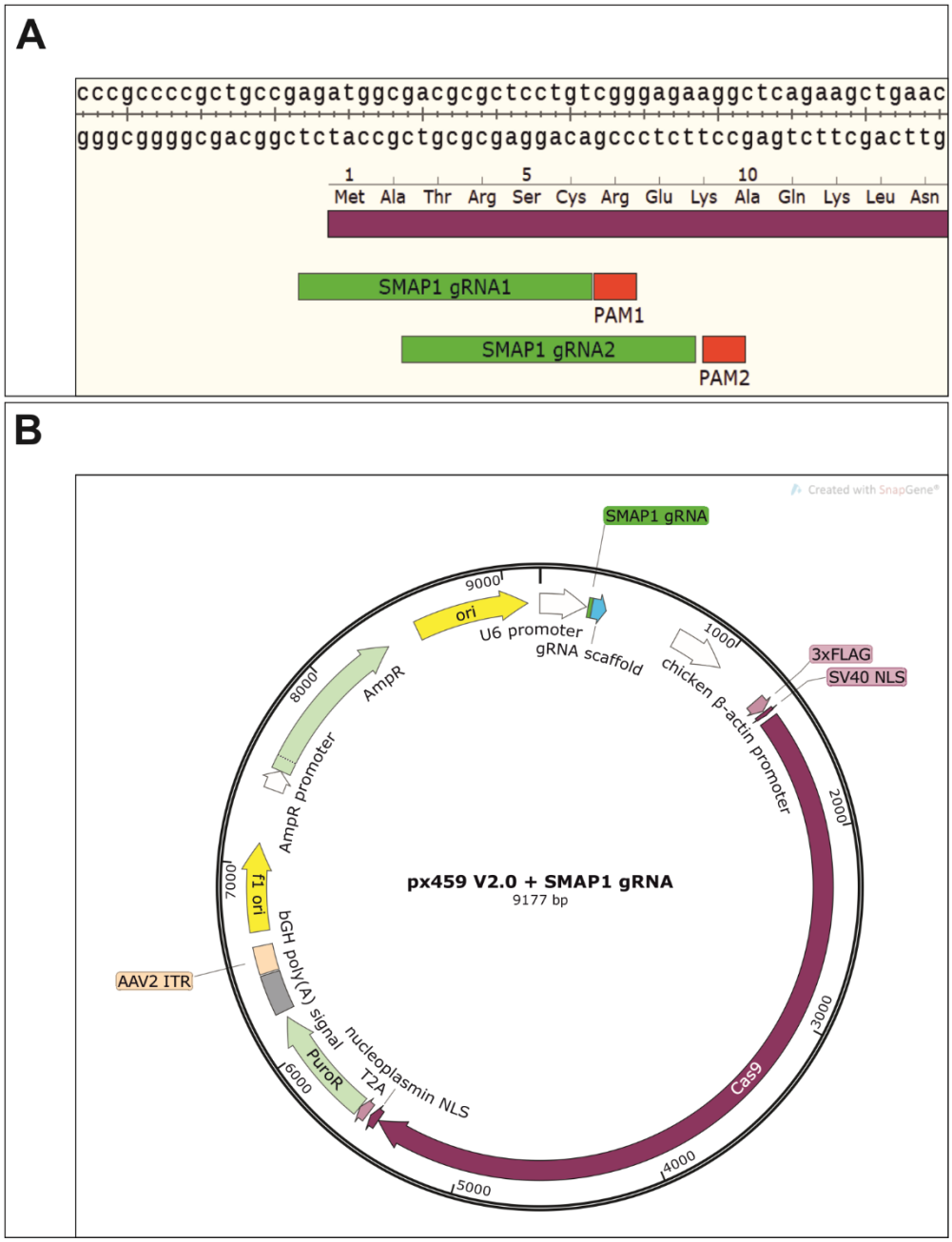


Figure 3.9: CRISPR/CAS9 Vector Design for the Knock-out of SMAP1

(A) gRNAs designed using the Sanger Institute CRISPR platform for the targeting of SMAP1. The gRNAs are 20nt long and target sequences close to the translation start site of the protein. (B) Construct used for generating HEK-293 SMAP1KO cell lines. The vector carries a FLAG and NLS-tagged CAS9 cDNA downstream of a CAG promoter and fused with puromycin via a T2A self-cleaving peptide. A U6 RNA promoter upstream of the CAG drives the transcription of the SMAP1 gRNA.

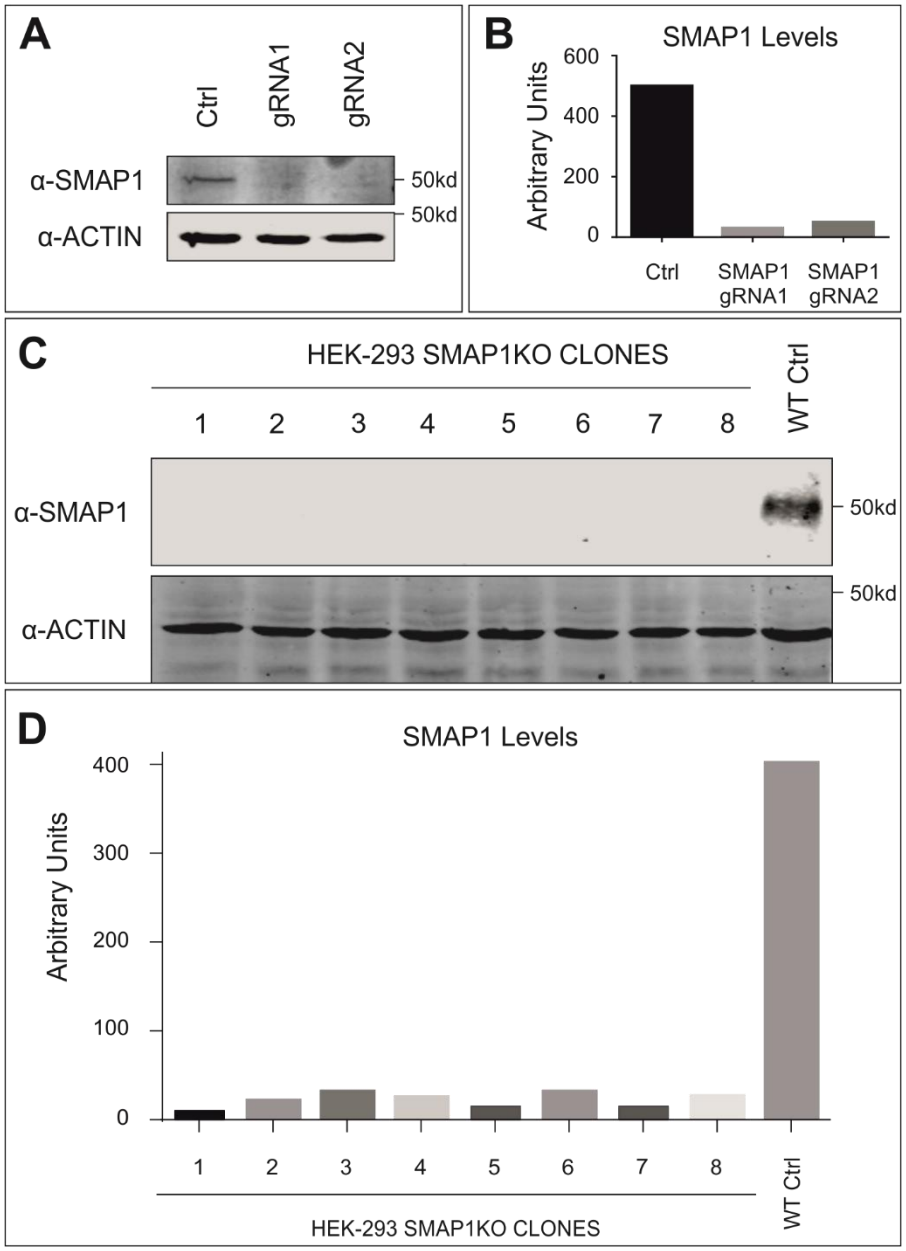


Figure 3.10: SMAP1 CRISPR Knock-out in HEK-293 cells

(A) HEK-293 cells were transiently transfected with CRISPR/CAS9 constructs carrying two different SMAP1 targeting gRNAs. After 48hrs, cells were lysed in 1% SDS lysis buffer, lysates were subjected to SDS-PAGE and immunoblotted with an α-SMAP1 antibody. Non-transfected HEK-293 cells were used as a negative control. (B) Quantitation of SMAP1 expression levels in HEK-293 cells transfected with the above constructs. Densitometry was performed using the Image Studio Lite software. (C) HEK-293 cells were transfected with a CRISPR/CAS9 construct carrying the SMAP1 targeting gRNA and selected with 1µg/mL of puromycin for 48hrs or until the control cells were dead. Positive colonies were manually picked with cloning rings and replated. The clones that emerged were lysed in 1% SDS lysis buffer, lysates were

subjected to SDS-PAGE and immunoblotted with an α-SMAP1 antibody. Non-transfected HEK-293 cells were used as a negative control. (D) Quantitation of SMAP1 expression levels in the above clones. Densitometry was performed using the Image Studio Lite software.

3.2.7 SMAP1 is Responsible for the Activin A / TGFβ Mediated ARF6 GTP – GDP Exchange

In section 3.2.6 we reported the generation and validation of SMAP1 Knock-out HEK-293 cells using the CRISPR technique. SMAP1 is a specific ARF6 GAP, which we found to interact with the wild-type ACVR1B receptor. Reasonably, we hypothesised that SMAP1 is the GAP that inactivates ARF6 in response to treatment with Activin A or TGFβ.

To confirm that hypothesis we carried out a pull-down assay using the SMAP1KO HEK-293s or wild-type cells as a negative control. Both cell lines were transiently transfected with a construct encoding the HA-tagged wild-type form of ARF6 and induced with TGFβ or Activin A for 40min prior to lysis. The GST-GAP protein reported previously (see section 3.2.4), was used as bait for ARF6-GTP.

The results indicated that in wild type cells ARF6 was inactivated after induction with the ligands. However, exactly the opposite occurred in the SMAP1KO cells, with the levels of ARF6-GTP rising significantly **Figure 3.11 (A)**. More specifically, in wild-type HEK-293 cells, induction with TGFβ results in a 1.4-fold ARF6 inactivation while treatment with Activin A in a 2.7-fold inactivation **Figure 3.11 (B)**. In SMAP1KO cells induction with TGFβ or Activin A results in a 1.4-fold ARF6 activation **Figure 3.11 (B)**. Taken together these results indicate that SMAP1 is the GAP responsible for the inactivation of ARF6 in the presence of TGFβ or Activin A.

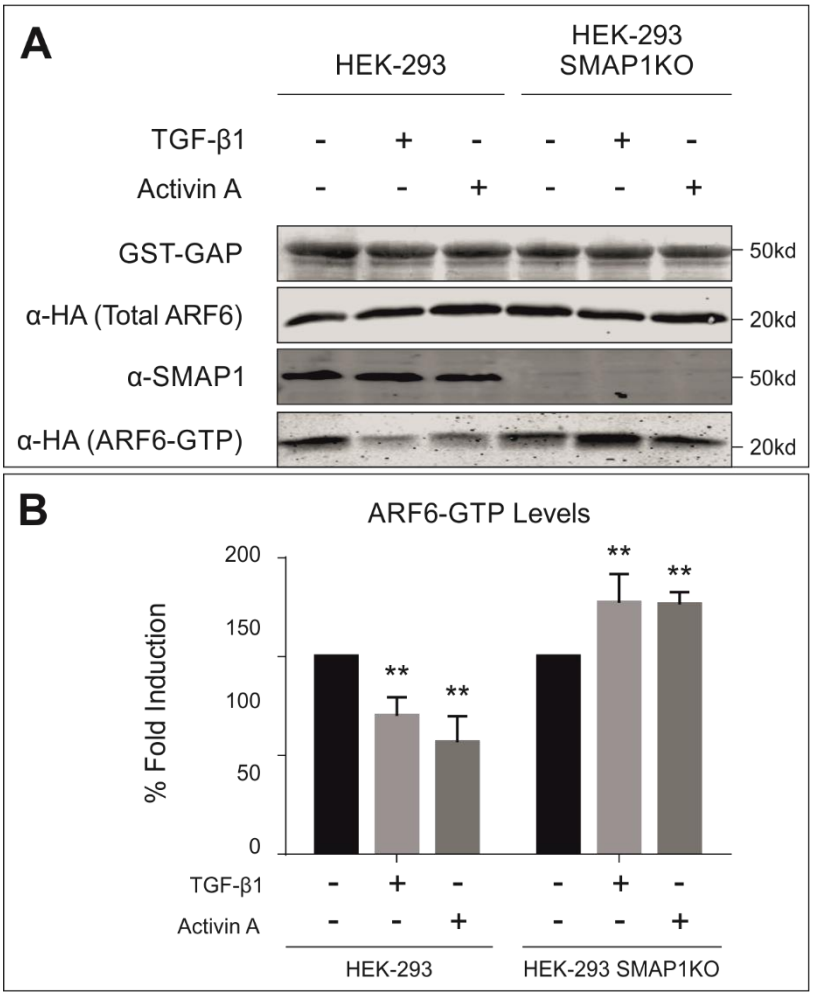


Figure 3.11: Effect of Activin A / TGFβ Signalling on ARF6-GTP Loading in SMAP1KO Cells

(A) The GTP binding domain of an ARF6GAP was tagged with GST and purified from *E. Coli BL21DE* bacteria. Wild type or SMAP1KO HEK-293 cells were transfected with HA-ARF6WT, subjected to 3hrs serum starvation and induced with TGF-β1 (2.5ng/ml) or Activin A (50ng/ml) for 40min. The cell lysates were incubated with GST-GAP for 1hr and GST beads were used to pull-down the ARF6-HA-GTP/GST-GAP complex. ARF6-GTP bound to the beads was detected by western blot using an α-HA antibody. (B) Quantitation of the ARF6-GTP levels in control and TGF-β1 or Activin A treated cells. Densitometry was performed using the Image Studio Lite software. Statistical significance was calculated in GraphPad Prism using the non-parametric Mann-Whitney test (N=3).

3.3 Discussion

In the present chapter we have established that ARF6 is directly implicated in TGFβ and Activin A signalling. The observations leading to this conclusion include that: (1) Activated ARF6 interacts with SMAD2/3 and SMAD4. (2) Activin A or TGFβ induction in the presence of activated ARF6 leads to increased R-SMAD phosphorylation. (3) Activin A or TGFβ induction in the absence of ARF6 leads to decreased R-SMAD phosphorylation. (4) Activin A or TGFβ induction leads to ARF6 inactivation. (5) SMAP1 interacts with ACVR1B and is responsible for the inactivation of ARF6 following Activin A or TGFβ induction.

SMAD2/3 and SMAD4 proteins have been found to interact specifically with activated ARF6 (Q67L) while showing no affinity for the activation resistant mutant (T27N). This observation suggests that ARF6 might regulate TGFβ signalling at multiple subcellular levels. ARF6-GTP is known to be associated with membranes because of its N-terminal amphipathic helix and myristoylation motif (Donaldson, 2003). Therefore, ARF6 activation could potentially facilitate SMAD translocation to the same compartments where TGFβ receptors are also situated and able to phosphorylate SMADs. In addition, the interactions uncovered above persist regardless of the R-SMADs phosphorylation state. This suggests that dissolution of the ARF6-SMAD complex is only possible after ARF6 GTP-GDP exchange. This might be a safeguarding mechanism to attenuate signalling, thus ensuring that SMAD complexes translocate to the nucleus only after ARF6 inactivation and normal receptor trafficking along the endocytic pathway **Figure 6.1**. A similar mechanism of R-SMAD cytoplasmic sequestration has been attributed to SnoN, a proto-oncoprotein that

retains phosphorylated SMADs in the cytoplasm, thus attenuating TGFβ signalling (Krakowski et al., 2005).

Several scientific publications suggest that activated ARF6 promotes CME by orchestrating the production of PI(4,5)P2 which leads to the recruitment of AP-2 (Wenk and De Camilli, 2004). In addition, CME of TGFβ ligand/receptor complexes into SARA positive endosomes promotes signalling (Hayes et al., 2002; Penheiter et al., 2002). Therefore, increased SMAD phosphorylation in the presence of activated ARF6 can be attributed to stimulation of the CME pathway. Reasonably, the opposite results observed by knocking-down ARF6 can be due to impaired CME and/or internalisation through Caveolin, leading to signalling attenuation (Di Guglielmo et al., 2003). Additionally, interaction of activated ARF6 with SMADs might also contribute to the differences in R-SMAD phosphorylation. As stated previously, activated ARF6 could potentially recruit SMADs to the membrane, thus facilitating their interaction with TGFβ receptors **Figure 6.1**.

ARF6 GTP-GDP exchange in response to Activin A or TGFβ stimulation was attributed to SMAP1, a GAP that was found to interact specifically with wild-type ACVR1B. The inability of SMAP1 to interact with activated or dominant negative mutants suggests that the interaction is associated with the kinase domain of the receptor. Therefore, ligand activation might lead to SMAP1 dissociation from the receptor and ARF6 hydrolysis, thus allowing the progression of physiological trafficking. A recently published study revealed two adjacent Serine and Threonine residues in SMAP1 that are phosphorylated by specific CDKs, during mitosis (Olsen et al., 2010). Being a Serine/Threonine kinase, ACVR1B might directly phosphorylate the GAP promoting its dissociation **Figure 6.1**. In agreement to this, analysis of SMAP1

sequence by NetPhorest predicts TGFβ receptors as kinases potentially responsible for phosphorylating the residues reported above (http://www.netphorest.info/). SMAP1 has also been identified as a partner of SMURF2 (Barrios-Rodiles et al., 2005). Even though the mechanism of action is not yet characterized, it might further implicate SMAP1 in the TGFβ pathway either by recruiting or sequestering the E3 ubiquitin ligase away. Interestingly, in SMAP1 knock-out cells ARF6 was activated in response to Activin A or TGFβ induction. This can be attributed to the sequential activity of an unidentified GEF and SMAP1. The GEF would be responsible for activating and recruiting ARF6 to the membrane and SMAP1 for inactivating the GTPase, thus allowing signalling and trafficking to progress.

To the best of our knowledge, this is the first study directly implicating ARF6 in the TGFβ signalling pathway. Nevertheless, ARF6 and SMAP1 have been associated with the internalisation of E-Cadherin through CME. Overexpression of SMAP1 was shown to inhibit the above process in MDCK cells. Interestingly, overexpression of a GAP-negative mutant of SMAP1 exhibited the same results (Kon et al., 2008). Even though seemingly contradictory, these results are in agreement with research showing that ARF6 cycling is indispensable for vesicle formation and trafficking, reviewed in: (D'Souza-Schorey and Chavrier, 2006).

CHAPTER 4

ELUCIDATING THE ROLE OF ARF6 IN HUMAN EMBRYONIC STEM CELL SIGNALLING

4.1 Introduction

Pluripotency in hES cells is known to be regulated primarily by components of the TGFβ superfamily. Activin A and TGFβ ligands act by activating SMAD2 and SMAD3 proteins which oligomerise with SMAD4 in the cytoplasm. The SMAD2/3/4 complex translocates to the nucleus and interacts with the promoter of *NANOG* (Xu et al., 2008). NANOG is a transcription factor involved in safeguarding pluripotency and attenuating differentiation. By physically interacting with SMAD2/3 proteins, NANOG reduces their transcriptional activity and suspends their drive for endodermal differentiation (Vallier et al., 2009). The BMP pathway effector proteins SMAD1/5/9 suppress genes implicated in hES cell pluripotency. SMAD1 interacts with the promoter of *NANOG* resulting in its downregulation (Xu et al., 2008). Although it is not clear if SMAD2/3 compete with SMAD1/5/9 proteins for the NANOG promoter interaction, a subtle balance between them seems to regulate the maintenance of pluripotency and the onset of differentiation.

In the previous chapter we provided evidence of the involvement of ARF6 in Activin A / TGFβ signalling. So far, ARF6 has been found to interact with SMAD2/3/4 proteins *in vitro.* Also, activation or knock-down of ARF6 affects the phosphorylation of SMAD2/3 proteins following induction with Activin A or TGFβ. The importance of this pathway in hES cells dictates that activation or knock-down of the GTPase should

affect pluripotency and/or differentiation. This is also supported by the fact that ARF6 ablation in mice leads to an embryonic lethal phenotype due to malformation of the hepatic cord (Suzuki et al., 2006).

Given all the above, in this chapter we attempted to decipher the role of ARF6 in hES cells. We investigated if the activation state of the GTPase affects SMAD phosphorylation and which the implications in pluripotency and differentiation are.

4.2 Results

4.2.1 Generation and Characterisation of the Fast Cycling ARF6 and GFP Control Stable H1 Cell Lines

hES cells are a versatile culture system for the study of signalling pathways related to embryogenesis and tissue specification. However, one of their important drawbacks is their limited transfection efficiency compared to other transformed or cancer cell lines. Since transient overexpression and RNA interference are not an option in this system, we needed to generate stable cell lines and knock-outs, in order to recapitulate the results that were presented in HEK-293s, in Chapter 3.

Initially, we obtained a construct from Dr. Ivana Barbaric (Sheffield University, UK) that expresses GFP under the control of a CAG promoter and contains a puromycin resistance copy after an IRES. The CAG promoter has been shown not to be silenced in stably transformed hES cells wherein it drives heterologous expression of downstream cDNA (Norrman et al., 2010). That construct was used intact for the generation of a GFP control stable H1 cell line. In addition, utilising the MCS in the 5' prime end of the GFP, we inserted the fast cycling mutant of ARF6 (T157A) into the vector, thus generating a C-terminally GFP tagged version of ARF6T157A **Figure 4.1 (A)**. That construct was subsequently used for the generation of an ARF6T157A-GFP stable H1 cell line that would be used for the study of the effects of ARF6 activation in hES cells, in pluripotency and differentiation.

We managed to isolate one GFP and two ARF6T157A-GFP H1 clones. In order to check the levels of ARF6 overexpression in these clones, we isolated whole cell lysates and analysed them by western blotting with an α-ARF6 antibody. The GFP

stable H1 cell line instead of wild-type H1 cells, was used as a control for the fast cycling clones, since ARF6T157A is C-terminally GFP tagged. In **Figure 4.1 (B)**, wild-type ARF6 appears at 20kd in all the lines at the same expression level. ARF6T157A-GFP, appears in the two clones just below the 50kd marker, which is expected since the added molecular weight of GFP is 27kd. Performing densitometry analysis, we quantified the expression levels of ARF6T157A relatively to the levels of wild-type ARF6. ARF6T157A expression was found to be 100 times more than wild-type ARF6 in ARF6 fast cycling clone 1, and 8 times more in fast cycling clone 2 **Figure 4.1 (C)**.

In order to use the fast cycling clones of ARF6 for subsequent experiments, we needed to validate their pluripotency. The first step was to characterise them based on the expression of major pluripotency factors. In that direction, we immunostained all the cell lines for E-Cadherin, NANOG, OCT4 and SOX2. Confocal microscopy revealed that all the lines retained the expression of the aforementioned markers **Figure 4.2 (A), (B), (C)**. E-Cadherin was localised mainly at the cell membrane, whereas NANOG, OCT4 and SOX2 were correctly situated in the nucleus. Fast cycling ARF6 was also localised mainly at the cell membrane, which is expected given that activation of the GTPase results in its association with membranes because of its N-terminus co-translational myristoylation (Donaldson and Jackson, 2011).

Furthermore, we quantified the expression levels of the major pluripotency factors between the two H1 ARF6T157A-GFP clones and the GFP control cell line by western blotting. Using primary antibodies against NANOG, E-Cadherin and OCT4 **Figure 4.3 (A)** we demonstrated by densitometry that activation of ARF6 has no significant effects on the expression levels of the aforementioned markers **Figure 4.3 (B), (C), (D)**.

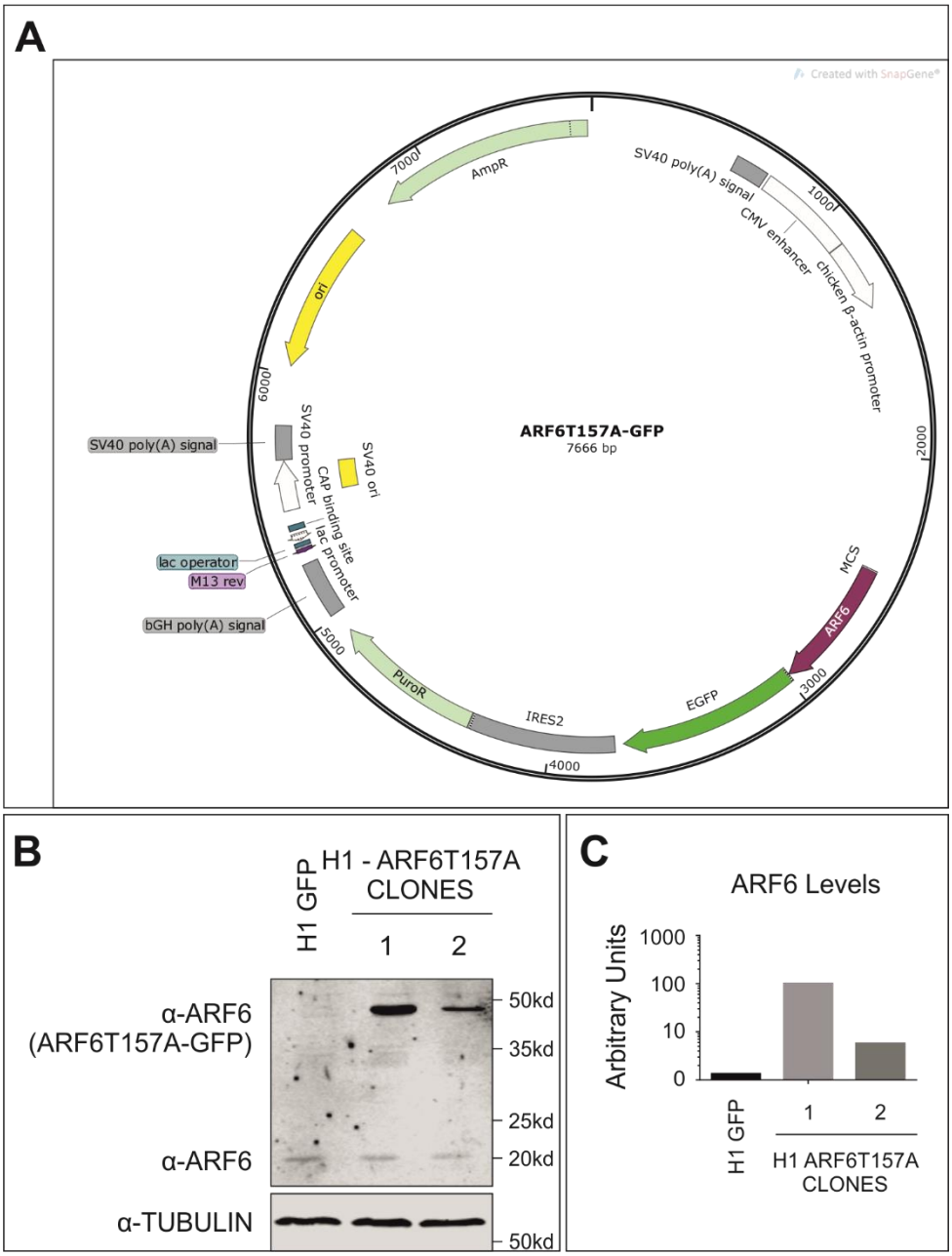
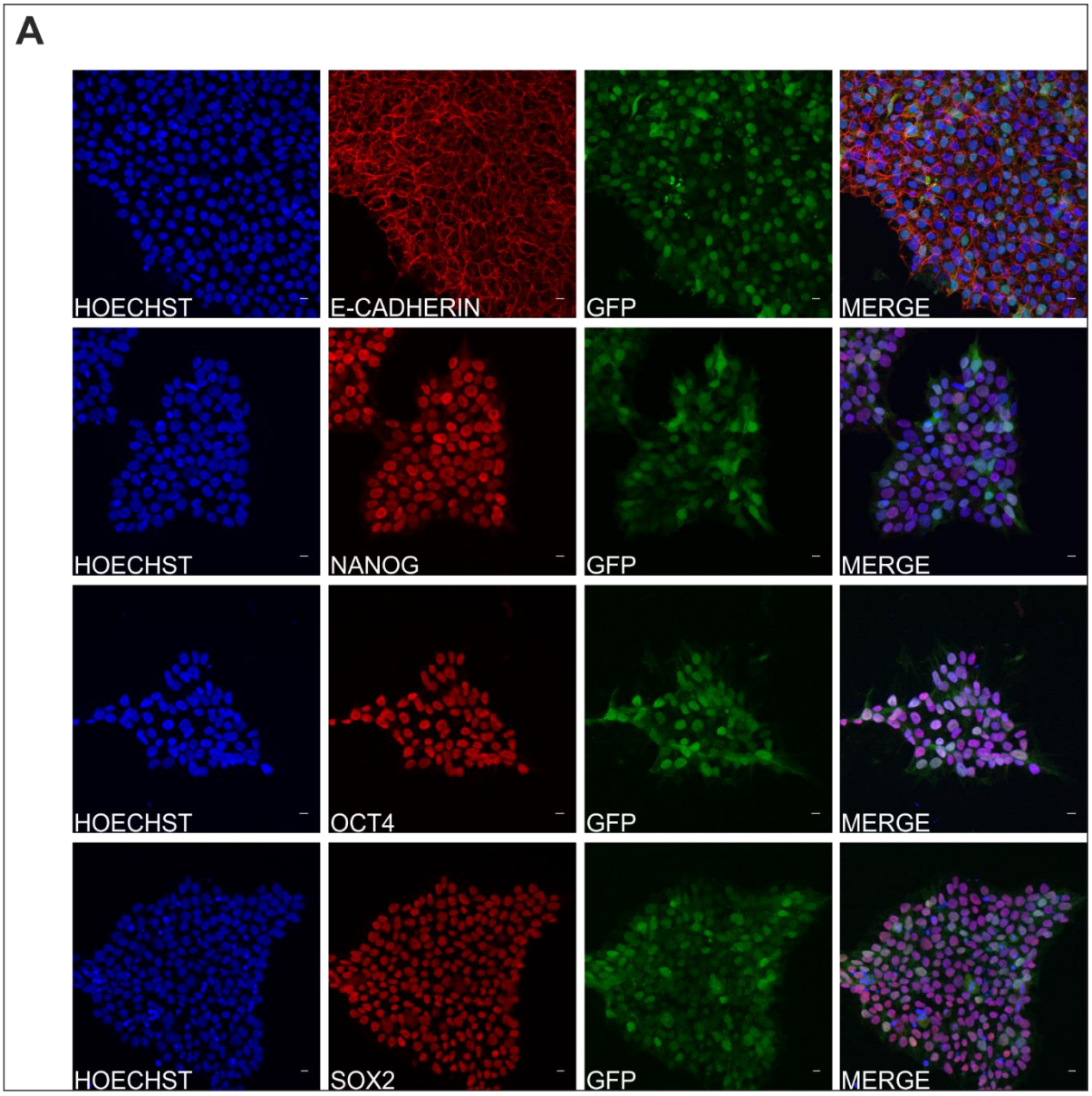
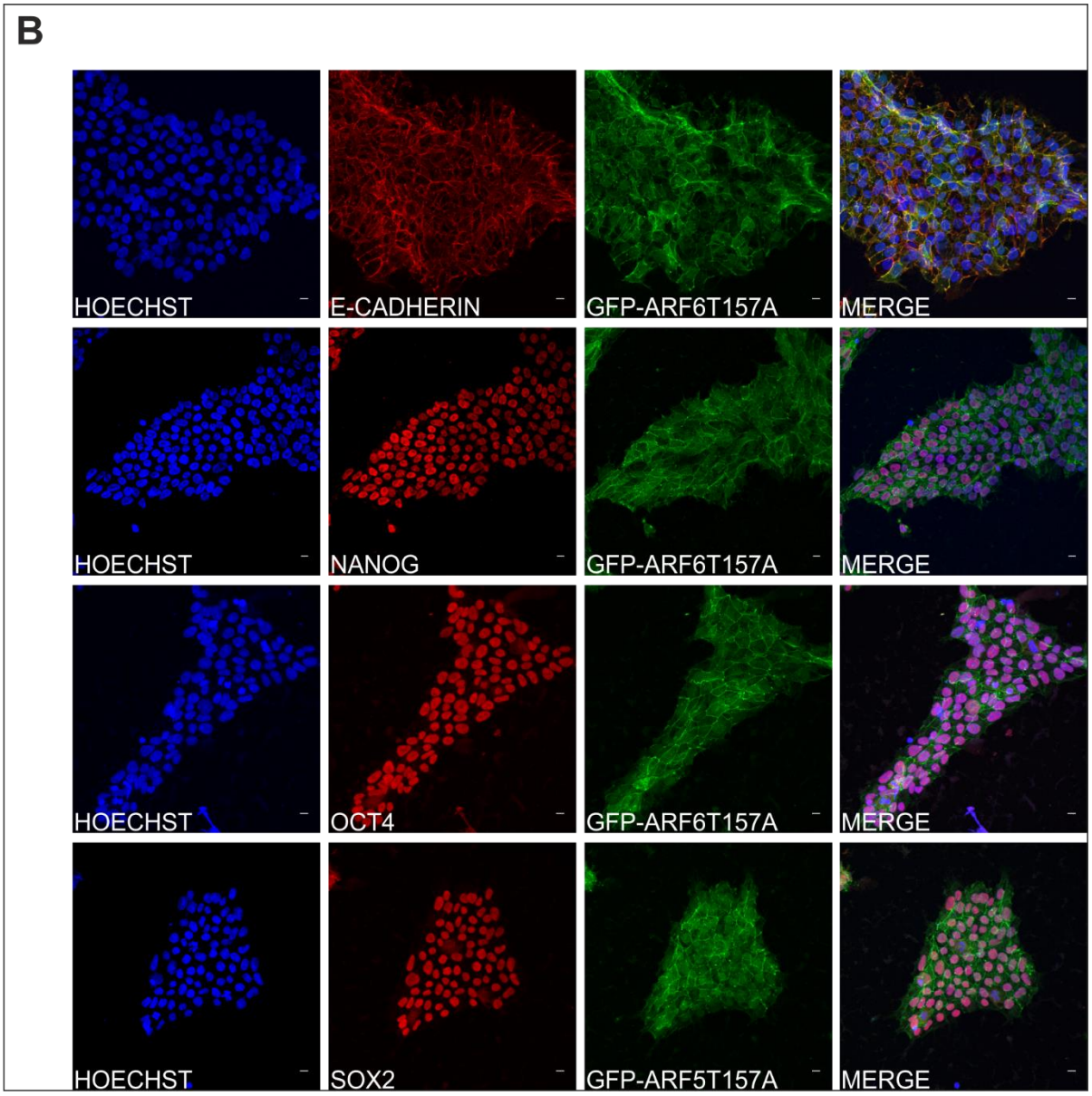


Figure 4.1: Design of H1 ARF6T157A-GFP Stable Cell Lines

(A) Construct used for generating stable H1 cell lines overexpressing the fast cycling form of ARF6 (ARF6T157A-GFP). The vector carries a GFP tagged ARF6 mutant downstream of a CAG promoter and fused with an IRES driving the expression of puromycin. H1 control GFP lines were generated with an identical vector that lacks the ARF6T157A cDNA. (B) H1 cells were transfected with the GFP or ARF6T157A-GFP vectors and selected with 250ng/mL of puromycin for 48hrs or until the control cells were dead. Positive colonies were manually picked with cloning rings, expanded, subjected to SDS-PAGE and immunoblotted with an α-ARF6 antibody. (C) ARF6 Levels were quantified by densitometry using the Image Studio Lite software.


A
HOECHST
E-CADHERIN
GFP
MERGE
HOECHST
NANOG
GFP
MERGE
HOECHST
OCT4
GFP
MERGE
HOECHST
SOX2
GFP
MERGE


B
HOECHST
E-CADHERIN
GFP-ARF6T157A
MERGE
HOECHST
NANOG
GFP-ARF6T157A
MERGE
HOECHST
OCT4
GFP-ARF6T157A
MERGE
HOECHST
SOX2
GFP-ARF5T157A
MERGE

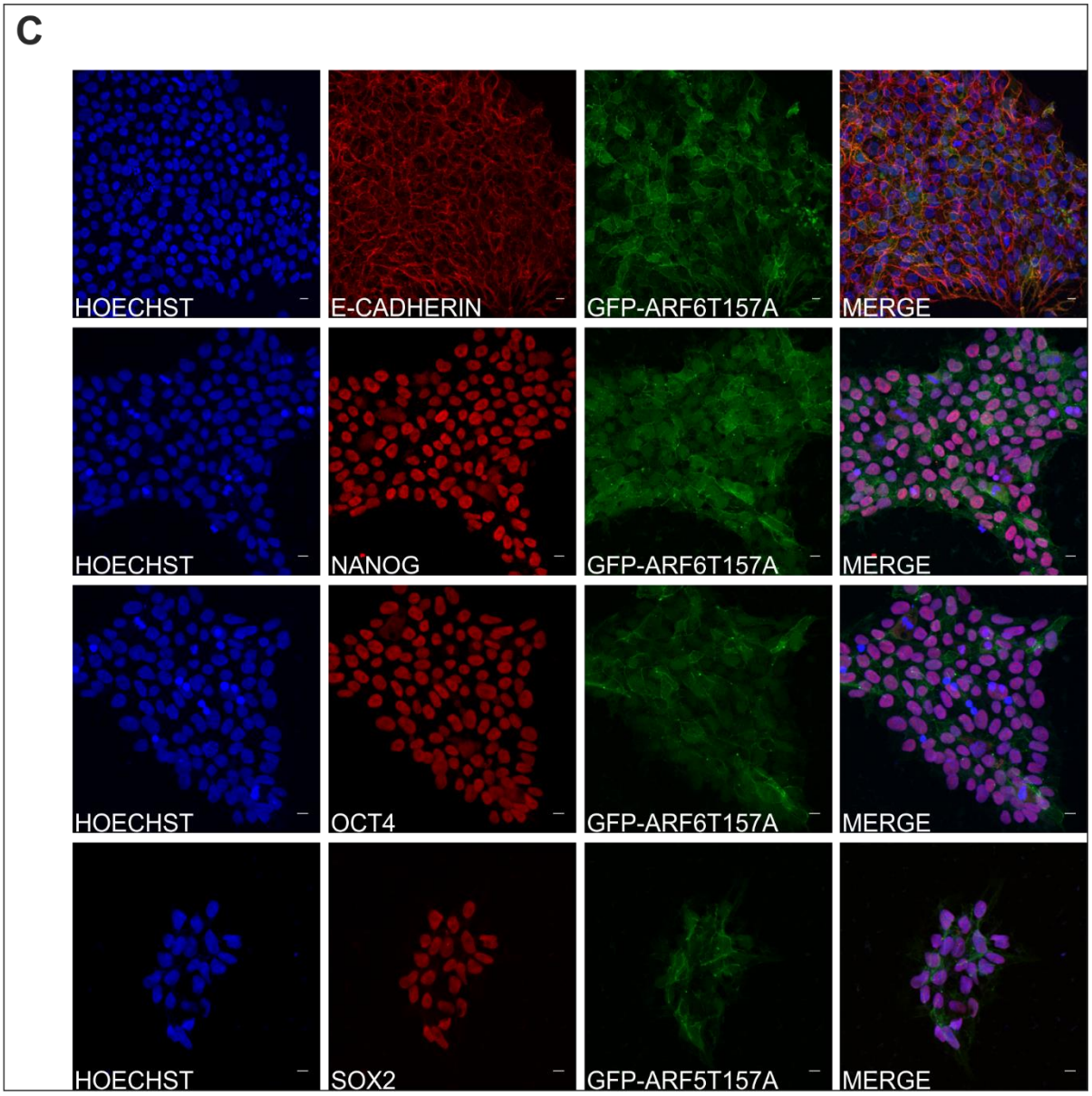


Figure 4.2: Expression of Pluripotency Factors in H1 ARF6T157A-GFP Cells and GFP Control Cells

(A) The H1 stable cell line overexpressing GFP or two H1 stable cell lines overexpressing the fast cycling form of ARF6 (ARF6T157A-GFP) (B), (C) were cultured to approximately 50% confluency in 8-well permanox chambers and immunostained with primary antibodies against E-Cadherin, NANOG, OCT4 and SOX2. All Images were obtained using a Leica SP8 Confocal Microscope and a 40X/1.30 NA objective. Scale bar size is 10μm. Images are maximum projections.

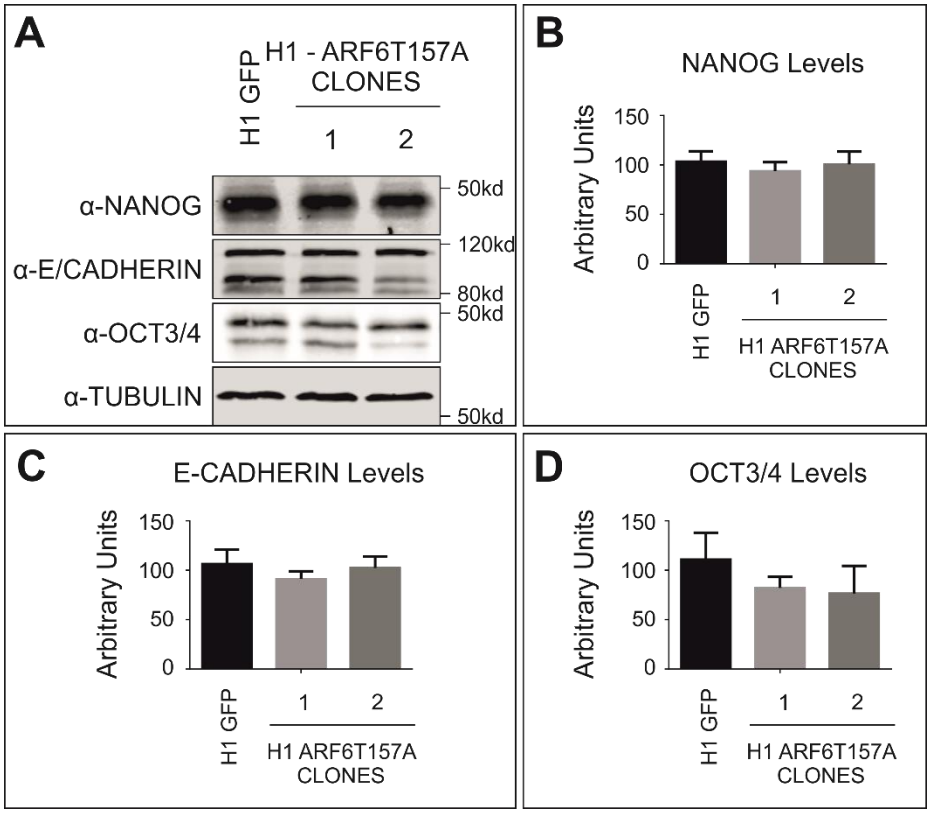


Figure 4.3: Levels of Pluripotency Factors in H1 ARF6T157A-GFP Cells

(A) Two H1 stable cell lines overexpressing the fast cycling form of ARF6 (ARF6T157A-GFP) were cultured to approximately 50% confluency and lysed using 1% SDS lysis buffer. The lysates were subjected to SDS-PAGE and immunoblotted with α-E/Cadherin, α-NANOG and α-OCT4 antibodies. The H1 stable cell line overexpressing GFP was used as a control. (B), (C), (D). The expression levels of the pluripotency factors were compared between the two ARF6T157A-GFP clones and the H1 GFP control cells by densitometry using the Image Studio Lite software. Statistical significance was calculated in GraphPad Prism using the non-parametric Mann-Whitney test (N=3).

4.2.2 ARF6 Activation Increases the Activin A Mediated SMAD2/3 Phosphorylation in H1 Cells

In section 3.2.3 we demonstrated that ARF6 activation raises the phosphorylation levels of SMAD2 and SMAD3 upon induction with Activin A or TGFβ, in HEK-293 cells. Given the importance of these pathways in hES cells, we needed to investigate whether a similar molecular mechanism exists and what its potential effects in pluripotency or differentiation.

In order to examine that, we used the fast cycling ARF6 and GFP control lines characterised in section 4.2.1. The cells were cultured in mTeSR1, a medium that preserves them in pluripotency based on the action of TGFβ and bFGF among other factors. The cells were subsequently serum starved for 4hrs in plain medium and induced with Activin A (50ng/mL) for 40min. The cell lysates were then analysed by western blotting using antibodies recognising the phosphorylated forms of SMAD2 and SMAD3. The total levels of SMAD2 and SMAD3 proteins remained the same after induction as revealed by probing with an antibody against total SMAD2/3. The results were normalised to ACTIN **Figure 4.4 (A)**.

Densitometry analysis showed that SMAD2 phosphorylation was increased by 1.55-fold and SMAD3 by 1.77-fold in ARF6 fast cycling clone 1 compared to the GFP control line **Figure 4.4 (B)**. In addition, SMAD2 phosphorylation was increased by 1.76-fold and SMAD3 by 2.03-fold in ARF6 fast cycling clone 2 compared to the GFP control line **Figure 4.4 (C)**.

Summarising, activation of ARF6 results in increased phosphorylation levels of SMAD2 and SMAD3 in hES cells upon activation with Activin A.

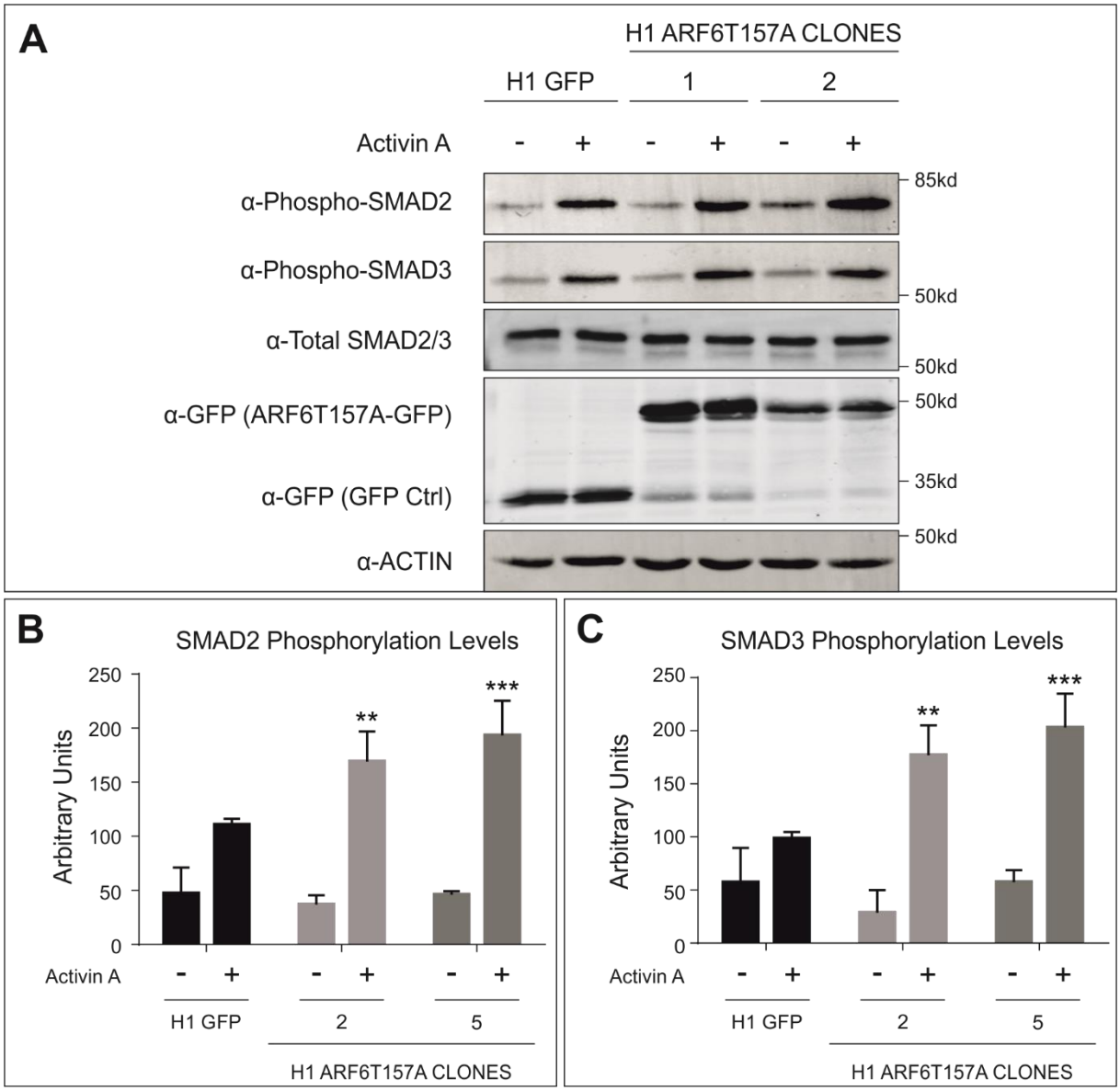


Figure 4.4: Effect of ARF6 Activation on SMAD2/3 Phosphorylation

(A) Two H1 stable cell lines overexpressing the fast cycling form of ARF6 (ARF6T157A-GFP) were cultured to approximately 50% confluency and subjected to 2hrs growth factor starvation in minimal medium followed by induction with 50ng/ml Activin A. Cells were lysed using 1% SDS, subjected to SDS-PAGE and immunoblotted with α-pSMAD2 and α-pSMAD3 antibodies to check the effect of ARF6 activation on the Activin A mediated SMAD2/3 phosphorylation. The H1 GFP stable cell line was used as a control. Changes in the phosphorylation levels of (B) SMAD2 and (C) SMAD3 in the presence of the fast cycling ARF6 mutant were assessed by densitometry using the Image Studio Lite software. Statistical significance was calculated in GraphPad Prism using the non-parametric Mann-Whitney test (N=6).

4.2.3 ARF6 Activation Increases the BMP4 Mediated SMAD1/5/9 Phosphorylation in H1 Cells

In the previous section we reported the effect of ARF6 activation in the phosphorylation of SMAD2/3 proteins in H1 cells. That effect revealed a role for the GTPase in the Activin A pathway which is implicated mainly in the pluripotency of hES cells. However, it has not yet been reported whether ARF6 status affects the BMP-SMAD1/5/9 pathway that is involved in differentiation.

In order to investigate that, we used the fast cycling ARF6 and GFP control lines characterised previously. Initially, we cultured these lines in mTeSR1 to preserve them in a pluripotent and self-renewal state. The cells were subsequently serum starved for 4hrs in plain medium and induced with BMP4 (50ng/mL) for 40min. The cell lysates were then analysed by western blotting using a single antibody that recognises the phosphorylated forms of SMAD1/5/9 proteins. The total levels of the R-SMADs remained the same after induction as revealed by probing with an antibody against total SMAD1/5/9. The results were normalised to ACTIN **Figure 4.5 (A)**.

Subsequently, we performed densitometry analysis and demonstrated that SMAD1/5/9 phosphorylation was increased by 1.72-fold in ARF6 fast cycling clone 1 compared to the GFP control line **Figure 4.5 (B)**. In addition, SMAD1/5/9 phosphorylation was increased by 1.3-fold in ARF6 fast cycling clone 2 compared to the GFP control line **Figure 4.5 (C)**.

Taken together, these results indicate that activation of ARF6 results in increased phosphorylation levels of SMAD1/5/9 in hES cells upon activation with BMP4.

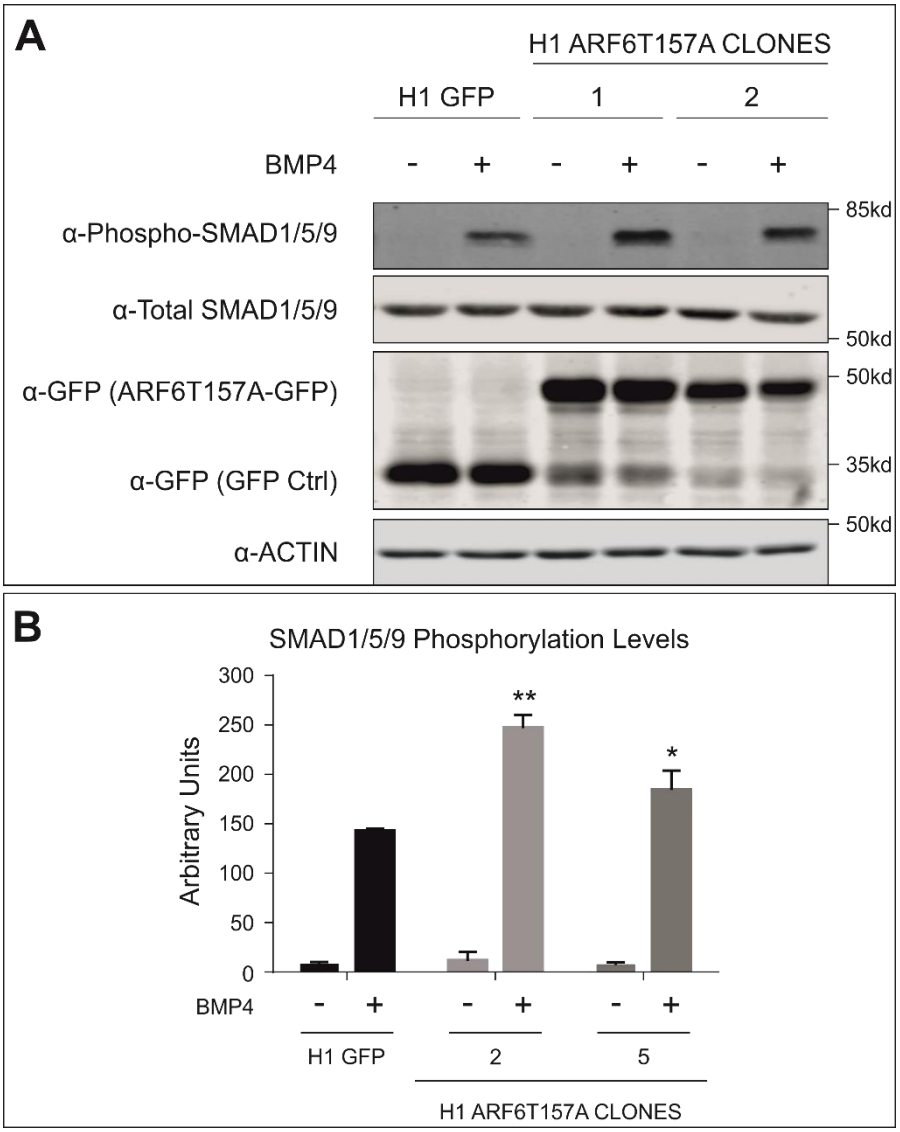


Figure 4.5: Effect of ARF6 Activation on SMAD1/5/9 Phosphorylation

(A) Two H1 stable cell lines overexpressing the fast cycling form of ARF6 (ARF6T157A-GFP) were cultured to approximately 50% confluency and subjected to 2hrs growth factor starvation in minimal medium followed by induction with 50ng/ml BMP4. Cells were lysed using 1% SDS lysis buffer, subjected to SDS-PAGE and immunoblotted with an α-pSMAD1/5/9 antibody to investigate the effect of ARF6 activation on the BMP4 mediated SMAD1/5/9 phosphorylation. The H1 GFP stable cell line was used as a control. (B) Changes in the phosphorylation levels of SMAD1/5/9 in the presence of the fast cycling ARF6 mutant were assessed by densitometry using the Image Studio Lite software. Statistical significance was calculated in GraphPad Prism using the non-parametric Mann-Whitney test (N=3).

4.2.4 ARF6 Activation Reduces the Expression of BRACHYURY upon Mesendoderm Induction

So far we have demonstrated that activation of ARF6 is implicated in the Activin A and BMP4 induced phosphorylation of proteins SMAD2/3 and SMAD1/5/9 in H1 cells, respectively. The next step was to investigate whether this leads to a different phenotype during differentiation.

In that direction we used the two H1 clones stably expressing the fast cycling ARF6 mutant along with the GFP control cell line in a differentiation assay towards mesendoderm. The differentiation protocol used was based on a medium containing Activin A (50ng/mL) and BMP4 (50ng/mL). Even though various different methods and media have been reported in the literature to guide cells to mesendoderm, we chose this particular one as it relies on the orchestrated effect of both pathways in which ARF6 was previously found to have an effect.

In brief, the cells were cultured in mTeSR1 medium until they reached 50% confluency. Next, differentiation to mesendoderm was initiated by incubation in the above medium for 48hrs. The cell lysates were analysed by western blotting with the outcome of differentiation being scored based on the expression levels of the early mesendodermal marker BRACHYURY. The levels of BRACHYURY were normalised to endogenous ACTIN **Figure 4.6 (A)**.

The results of the densitometry analysis demonstrated that BRACHYURY levels were reduced by 5-fold in the ARF6 fast cycling clone 1, and 1.75-fold in the ARF6 fast cycling clone 2, compared to the GFP control line **Figure 4.6 (B)**.

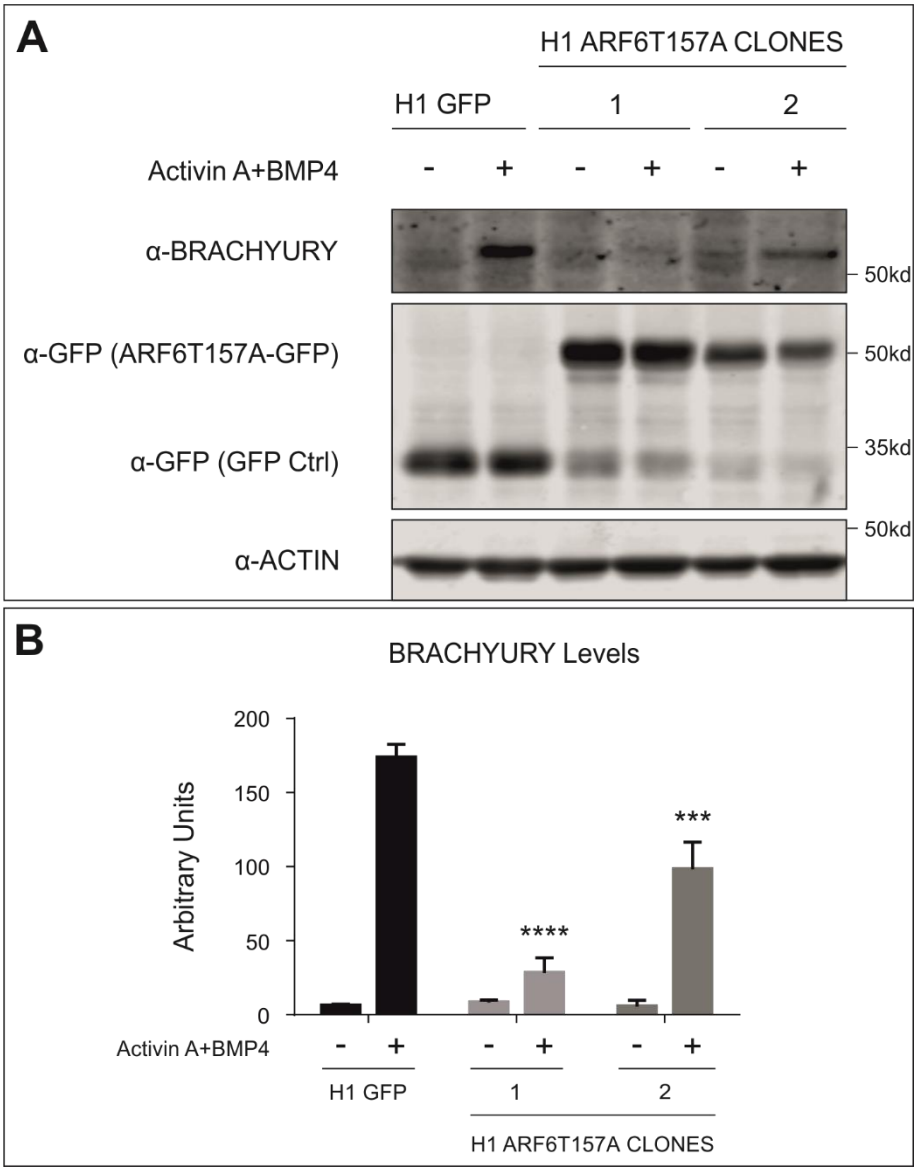


Figure 4.6: Effect of ARF6 Activation on BRACHYURY Expression upon Mesendoderm Induction

(A) Two H1 stable cell lines overexpressing the fast cycling form of ARF6 (ARF6T157A-GFP) were cultured to approximately 50% confluency. Differentiation to mesendoderm was initiated by substituting mTeSR1 with a medium containing Activin A (50ng/mL) and BMP4 (50ng/mL). After 48hrs cells were lysed using 1% SDS, subjected to SDS-PAGE and immunoblotted with an α-BRACHYURY antibody to investigate the effect of ARF6 activation in the expression levels of the mesendodermal marker. (B) Changes in the expression levels of BRACHYURY in the presence of the fast cycling ARF6 mutant were assessed by densitometry using the Image Studio Lite software. Statistical significance was calculated in GraphPad Prism using the non-parametric Mann-Whitney test (N=3).

Previously, we showed that ARF6 activation leads to increased expression of BRACYURY after 48hrs of mesendoderm differentiation with Activin A and BMP4. This can be attributed to a change on either the timing or the regulation of BRACHYURY's expression.

In order to investigate that, we used the same fast cycling ARF6 clones and the GFP control line in a differentiation assay towards mesendoderm in 3 different time points. The cells were cultured to approximately 50% confluency in mTeSR1 and were subsequently incubated in the differentiation medium characterised above for 48, 72 and 96hrs. Next, the cell lysates were analysed by western blotting with the outcome of differentiation being scored based on the expression levels of BRACHYURY at each time point. The levels of BRACHYURY were normalised to endogenous ACTIN **Figure 4.7 (A)**.

The results of the densitometry analysis demonstrated that BRACHYURY levels were reduced by 6.55-fold in the ARF6 fast cycling clone 1 and 1.85-fold in the ARF6 fast cycling clone 2 after 48hrs, 3.88-fold and 1.63-fold after 72hrs and 2.5-fold and 1.5-fold after 96hrs of differentiation **Figure 4.7 (B)**.

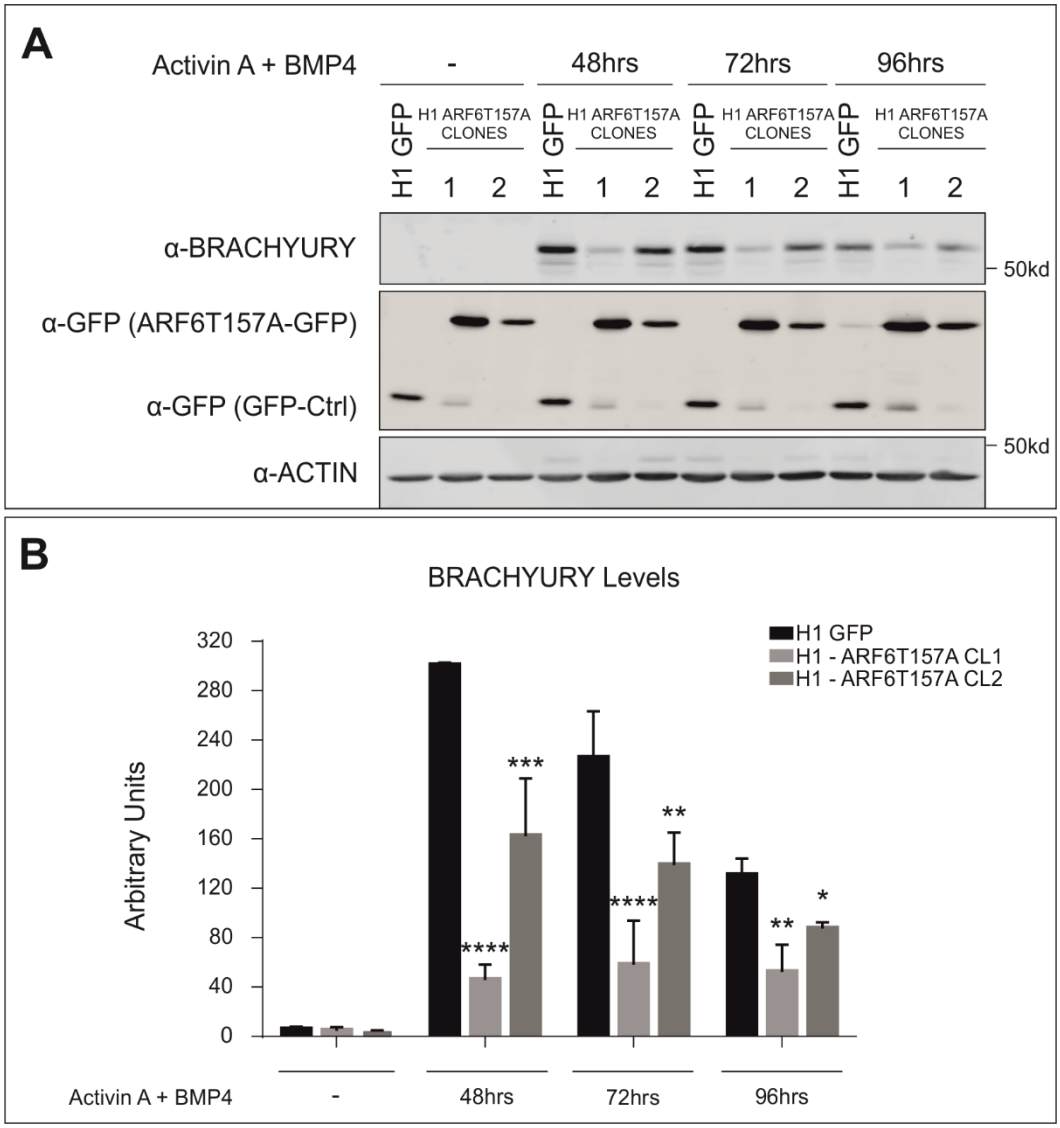


Figure 4.7: Effect of ARF6 Activation on the Timing of BRACHYURY Expression upon Mesendoderm Induction

(A) Two H1 stable cell lines overexpressing the fast cycling form of ARF6 (ARF6T157A-GFP) were cultured to approximately 50% confluency. Differentiation to mesendoderm was initiated by substituting mTeSR1 with a medium containing Activin A (50ng/mL) and BMP4 (50ng/mL). After 48, 72 and 96hrs cells were lysed using 1% SDS, subjected to SDS-PAGE and immunoblotted with an α-BRACHYURY antibody to investigate the effect of ARF6 activation in the expression levels of the mesendodermal marker in a time dependent manner. (B) Changes in the expression levels of BRACHYURY in the presence of the fast cycling ARF6 mutant were assessed by densitometry using the Image Studio Lite software. Statistical significance was calculated in GraphPad Prism using the non-parametric Mann-Whitney test (N=3).

4.2.5 Generation and Characterisation of ARF6 CRISPR Knock-Out H1 Cell Lines

In the previous sections of Chapter 4, we characterised the effect of ARF6 activation on SMAD2/3 and SMAD1/5/9 phosphorylation, as well as on the expression of BRACHYURY during mesendoderm differentiation. Here, we attempt to generate hES cell CRISPR Knock-out lines of ARF6 in order to investigate the impact of the absence of the GTPase on the pathways above. The CRISPR/CAS9 approach was chosen over RNA interference as the latter is impractical in hES cells due to limited transfection efficiency.

One ARF6 gRNA was chosen targeting a PAM close to the translation start site of the protein **Figure 4.8 (A)**. The gRNA designed exhibited minimum off-target effects based on the Sanger Institute CRISPR platform. The vector used for delivering the gRNAs and the CAS9 endonuclease in the cells, is depicted in **Figure 4.8 (B)**.

The construct encoding the gRNA for ARF6 was initially transfected in HEK-293 cells so that its efficiency is tested in an easily manipulated and cost-effective cell culture system. Out of the clones that emerged after treatment with puromycin, we isolated 6 different ones and scored them for their ARF6 expression levels by western blotting with an α-ARF6 antibody **Figure 4.9 (A)**. 2 out of the 6 clones that were generated were successful ARF6 knock-outs **Figure 4.9 (B)**. Wild-type HEK-293 cells were used as a negative control.

Having validated that the gRNA designed is indeed functional, we moved on to transfect H1 cells. Treatment with puromycin resulted in the isolation of 6 cell lines that were subsequently expanded and tested for ARF6 expression by western blotting

Figure 4.9 (C). 6 out of the 6 clones that were generated were successful ARF6 knock-outs **Figure 4.9 (D)**. Wild-type H1 cells were used as a negative control.

In order to use the H1 ARF6 knock-out clones for subsequent experiments, we needed to validate their pluripotency. The first step was to characterise them based on the expression of major pluripotency factors. In that direction, we immunostained 3 of the cell lines for E-Cadherin, NANOG, OCT4 and SOX2. Confocal microscopy revealed that all the lines tested retained the expression of all the aforementioned markers **Figure 4.10 (A), (B), (C)**. E-Cadherin was localised mainly at the cell membrane, whereas the transcription factors NANOG, OCT4 and SOX2 were correctly situated in the nucleus.

Furthermore, we quantified the expression levels of the major pluripotency factors between the three H1 ARF6KO clones and wild-type H1 cells by western blotting. Using primary antibodies against NANOG, E-Cadherin and OCT4 **Figure 4.11 (A)** we demonstrated by densitometry that knock-out of ARF6 has no significant effect on the expression levels of the aforementioned markers **Figure 4.11 (B), (C), (D)**.

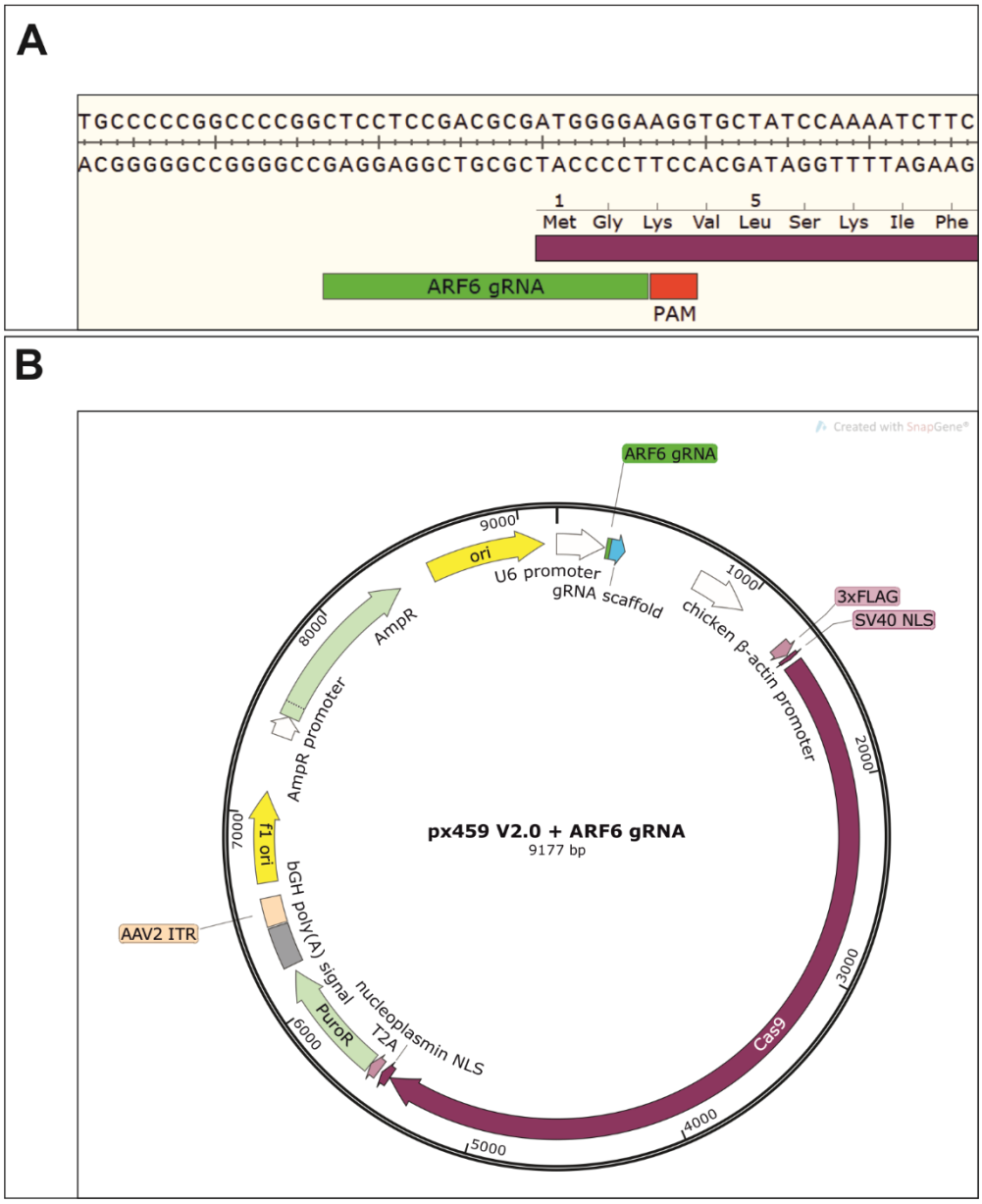


Figure 4.8: CRISPR/CAS9 Vector Design for the Knock-out of ARF6

(A) gRNA designed using the Sanger Institute CRISPR platform for the targeting of ARF6. The gRNA is 20nt long and targets a sequence close to the translation start site of the protein. (B) Construct used for generating HEK-293 and H1 ARF6KO cell lines. The vector carries a FLAG and NLS-tagged CAS9 cDNA downstream of a CAG promoter and fused with puromycin via a T2A self-cleaving peptide. A U6 RNA promoter upstream of the CAG drives the transcription of the ARF6 gRNA.

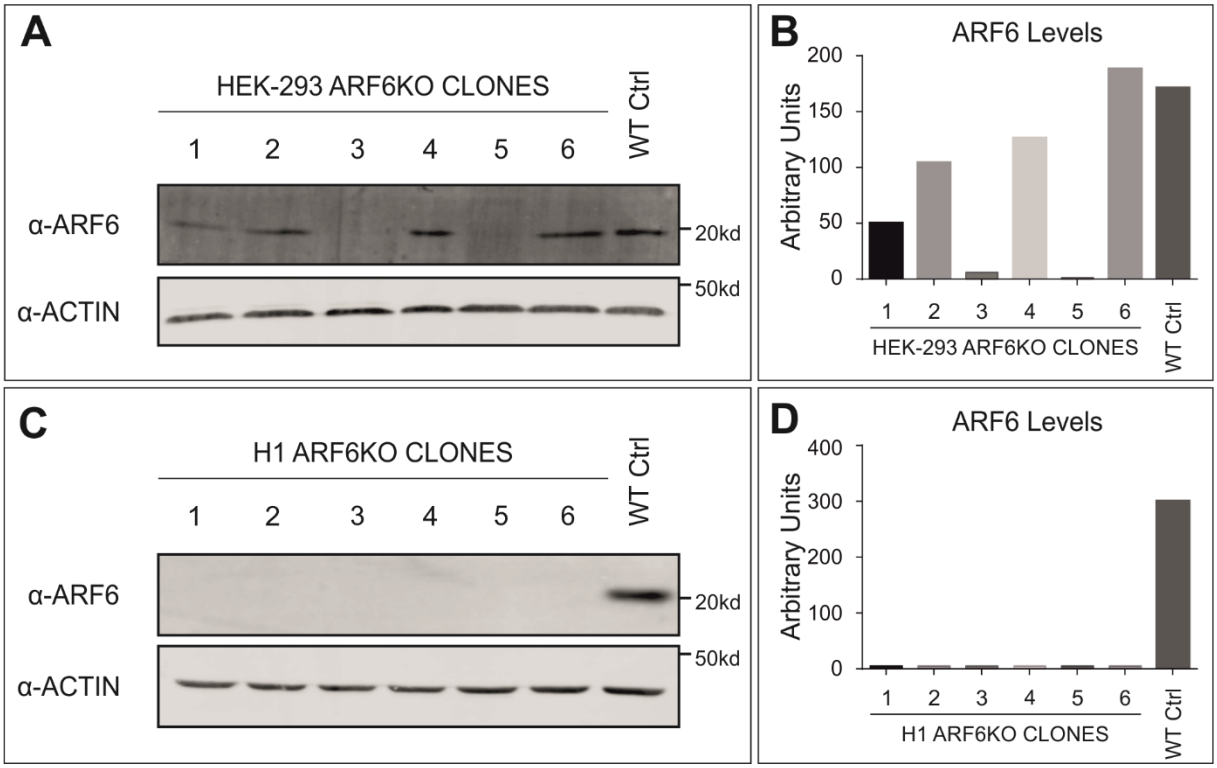
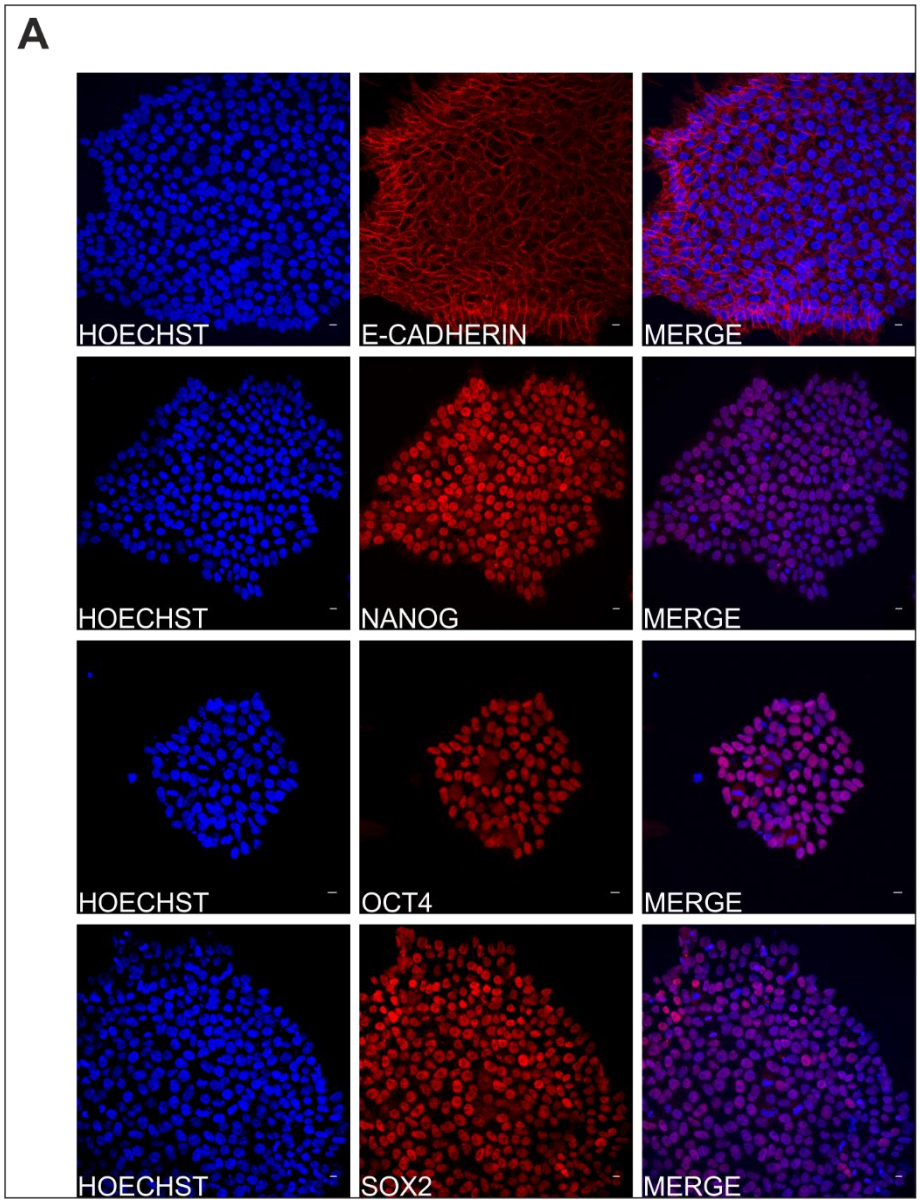
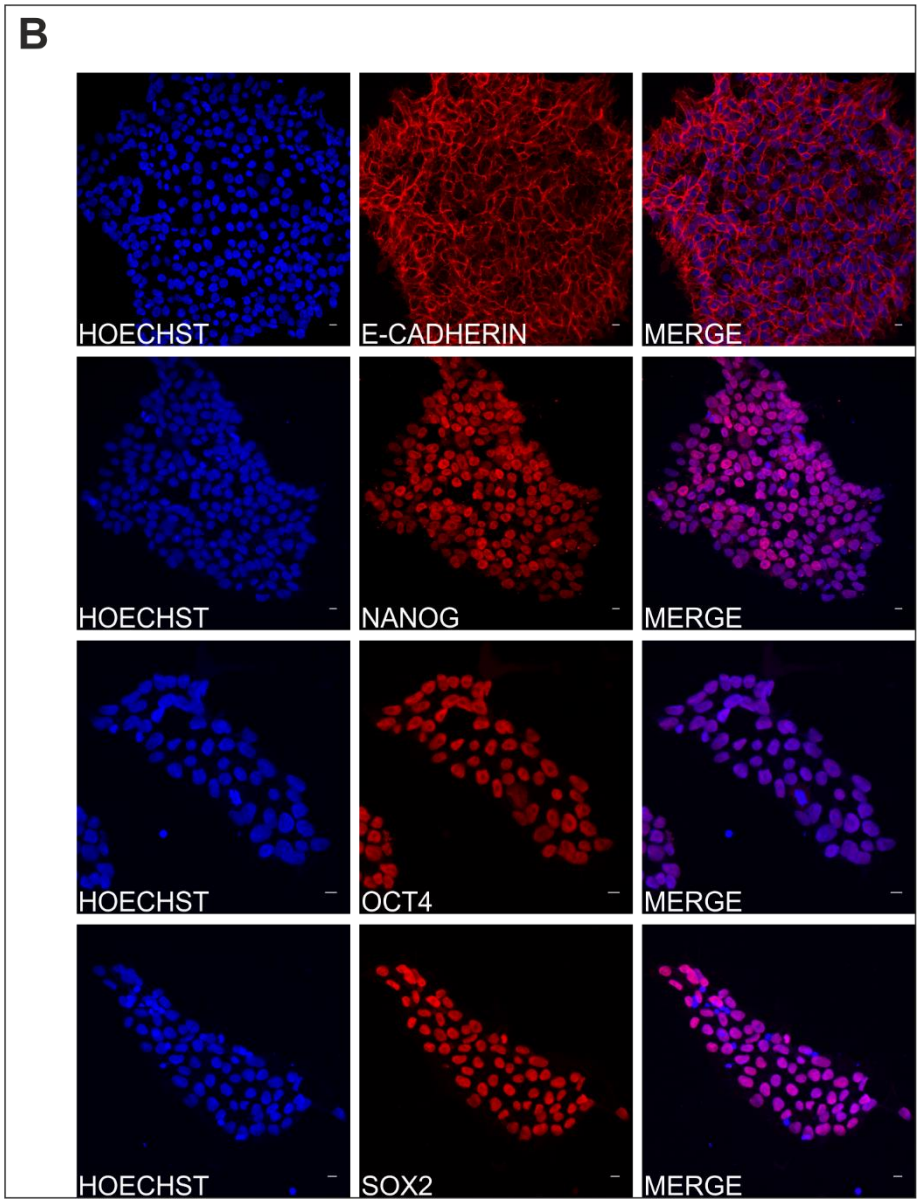


Figure 4.9: Generation of HEK-293 and H1 ARF6KO Cell Lines

(A) HEK-293 cells were transfected with a CRISPR/CAS9 construct carrying the ARF6 targeting gRNA and selected with 1µg/mL of puromycin for 48hrs or until the control cells were dead. Positive colonies were manually picked with cloning rings and replated. The clones that emerged were lysed with 1% SDS, lysates were subjected to SDS-PAGE and immunoblotted with an α-ARF6 antibody. Non-transfected HEK-293 cells were used as a negative control. (B) Quantitation of ARF6 expression levels in the above clones. Densitometry was performed using the Image Studio Lite software. (C) H1 cells were transfected with a CRISPR/CAS9 construct carrying the ARF6 targeting gRNA and selected with 250ng/mL of puromycin for 48hrs or until the control cells were dead. Positive colonies were manually picked with cloning rings and replated. The clones that emerged were lysed with 1% SDS, lysates were subjected to SDS-PAGE and immunoblotted with an α-ARF6 antibody. Non-transfected H1 cells were used as a negative control. (D) Quantitation of ARF6 expression levels in the above clones. Densitometry was performed using the Image Studio Lite software.


A
HOECHST
E-CADHERIN
MERGE
HOECHST
NANOG
MERGE
HOECHST
OCT4
MERGE
HOECHST
SOX2
MERGE


B
HOECHST
E-CADHERIN
MERGE
HOECHST
NANOG
MERGE
HOECHST
OCT4
MERGE
HOECHST
SOX2
MERGE

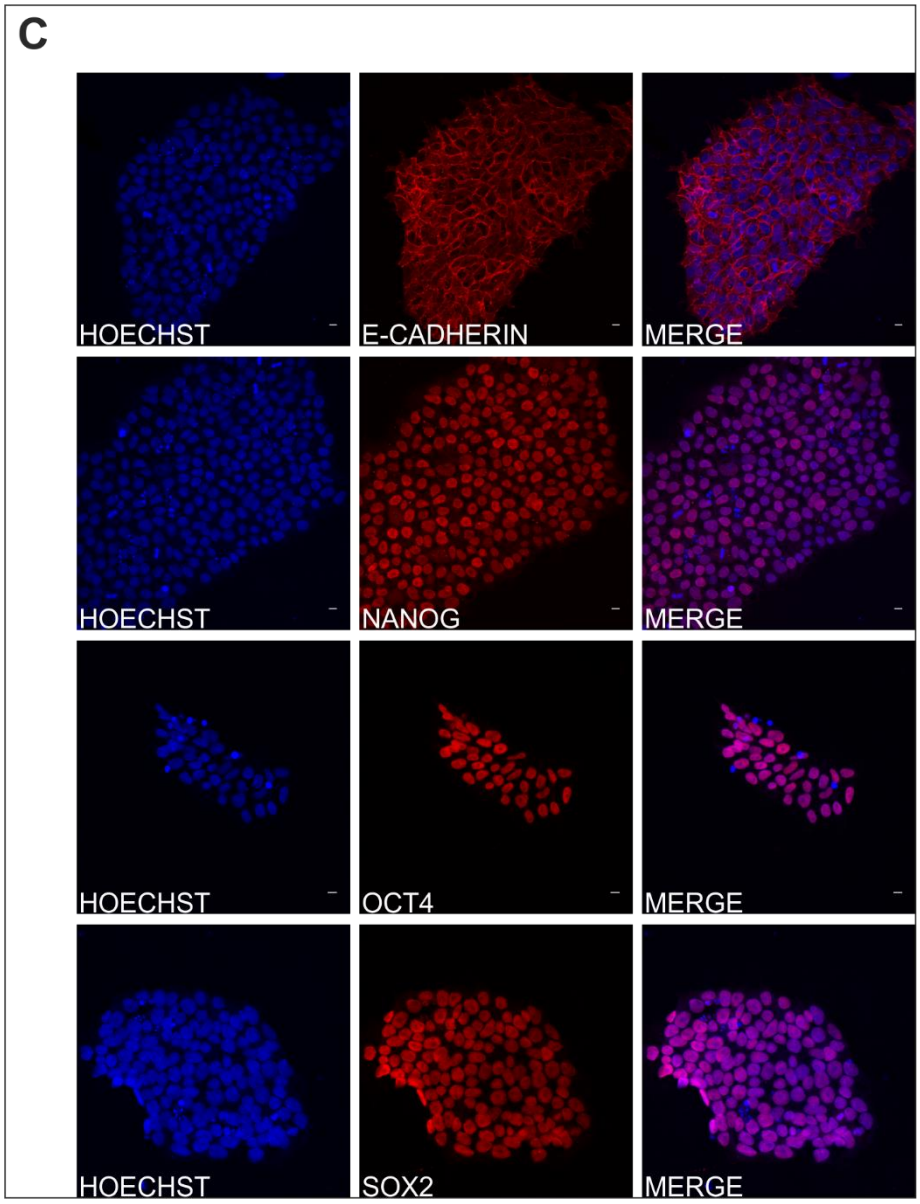


Figure 4.10: Expression of Pluripotency Factors in H1 ARF6KO Cells

(A) Wild type H1 cells or (B), (C) two H1 ARF6KO cell lines were cultured to approximately 50% confluency in 8-well permanox chambers and immunostained with primary antibodies against E-Cadherin, NANOG, OCT4 and SOX2. All Images were obtained using a Leica SP8 Confocal Microscope and a 40X/1.30 NA objective. Scale bar size is 10μm. Images are maximum projections.

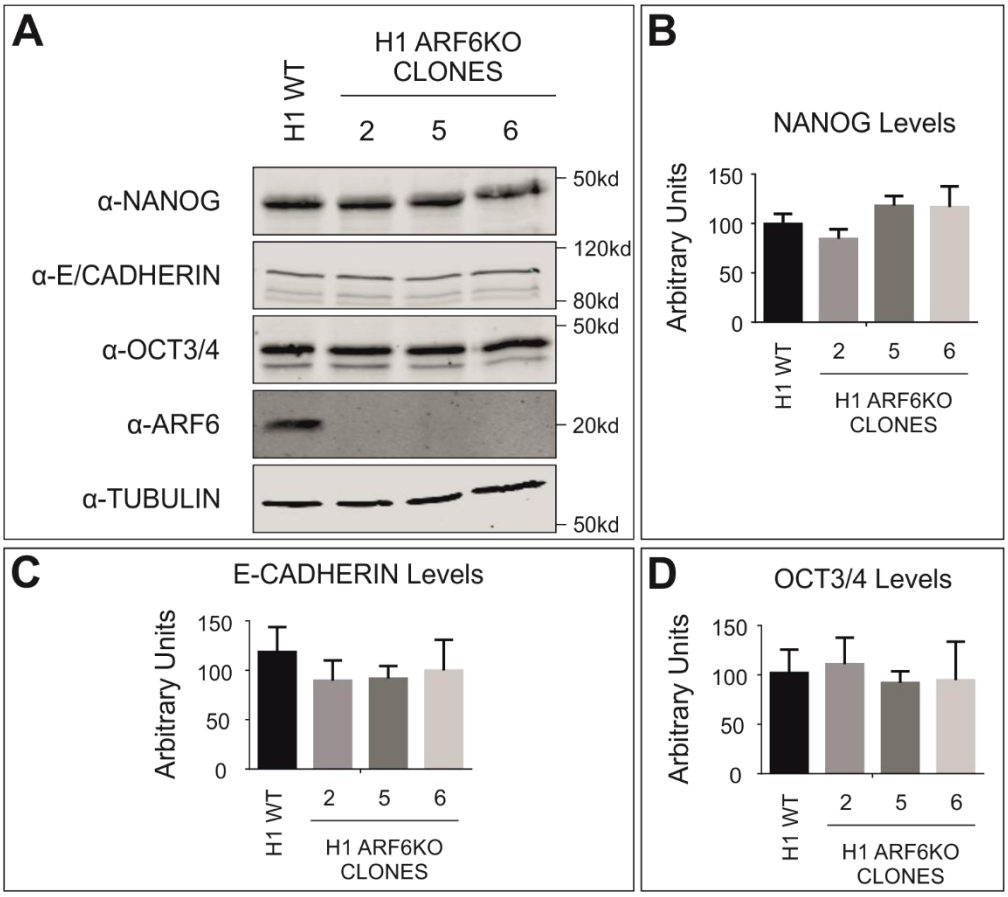


Figure 4.11: Levels of Pluripotency Factors in H1 ARF6KO Cells

(A) Three H1 ARF6KO cell lines were cultured to approximately 50% confluency and lysed using 1% SDS. The lysates were subjected to SDS-PAGE and immunoblotted with α-E/Cadherin, α-NANOG and α-OCT4 antibodies. Wild type H1 cells were used as a positive control. (B), (C), (D). The expression levels of the pluripotency factors were compared between the three ARF6KO clones and the H1 control cells by densitometry using the Image Studio Lite software. Statistical significance was calculated in GraphPad Prism using the non-parametric Mann-Whitney test (N=3).

4.2.6 ARF6 Knock-out Reduces the Activin A Mediated SMAD2/3 Phosphorylation in H1 Cells

In section 4.2.2 we demonstrated that ARF6 activation raises the phosphorylation levels of SMAD2 and SMAD3 upon induction with Activin A, in H1 cells. Here, we use the H1 ARF6 knock-out clones in order to address the impact on the phosphorylation of the R-SMADs in the absence of the GTPase.

Three different H1 ARF6 knock-out clones, along with wild-type H1 control cells were cultured in mTeSR1 until they reached approximately 50% confluency. Subsequently, the cells were serum starved for 4hrs in plain medium and induced with Activin A (50ng/mL) for 40min. The cell lysates were then analysed by western blotting using antibodies recognising the phosphorylated forms of SMAD2 and SMAD3 proteins. The total levels of SMAD2 and SMAD3 proteins remained the same after induction as revealed by probing with an antibody against total SMAD2/3. The results were normalised to ACTIN **Figure 4.12 (A)**.

Densitometry analysis revealed that SMAD2 phosphorylation was reduced by 1.85-fold in ARF6KO clone 2, 1.4-fold in ARF6KO clone 5 and 1.2-fold in ARF6KO clone 6 **Figure 4.12 (B)**. In addition, SMAD3 phosphorylation was also reduced in all the clones by 3.5-fold, 3.1-fold and 3.4-fold, respectively **Figure 4.12 (C)**.

Taken together, these results indicate that knock-out of ARF6 in hES cells results in reduced phosphorylation levels of SMAD2 and SMAD3 upon activation with Activin A.

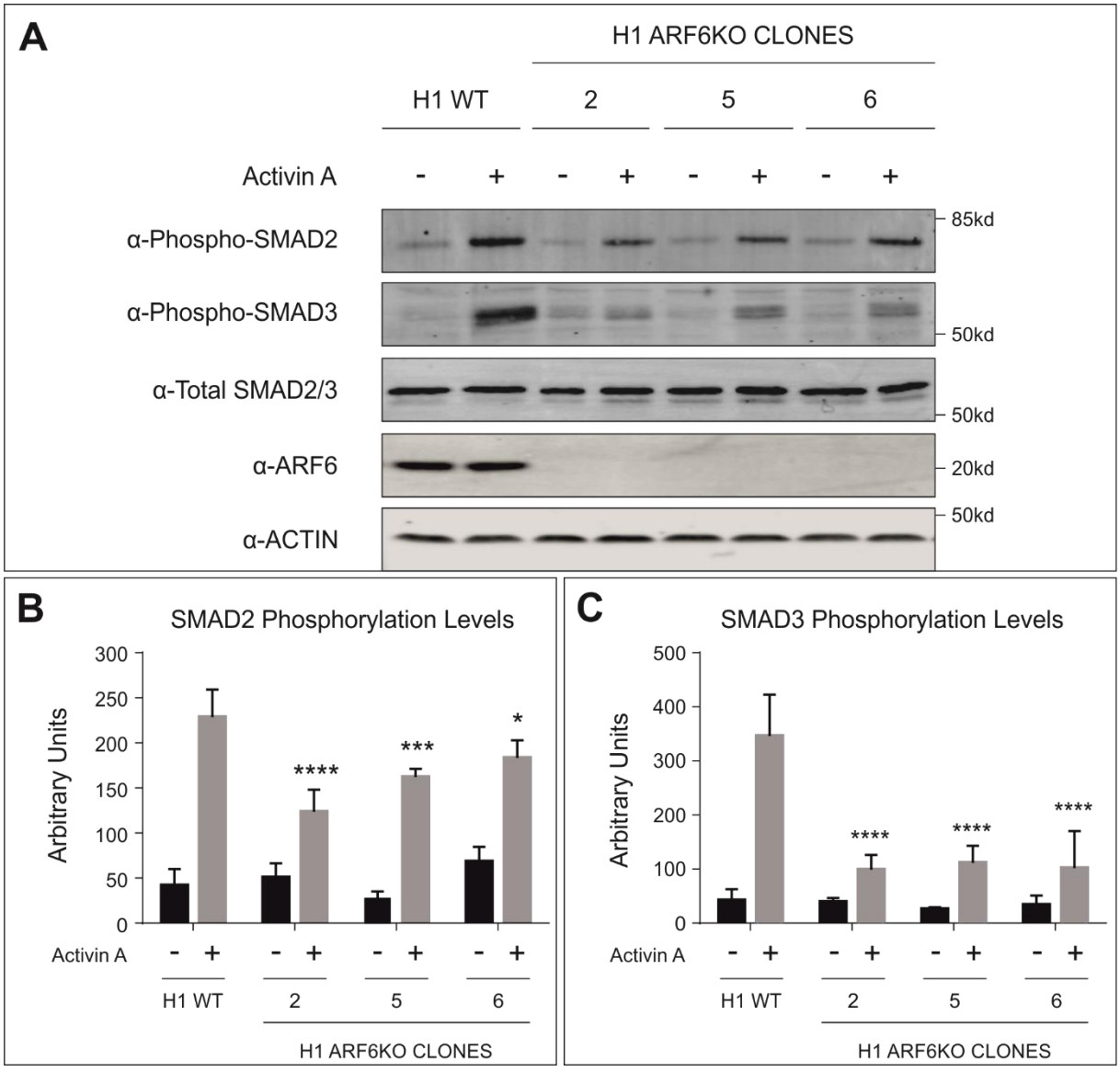


Figure 4.12: Effect of ARF6 Knock-out on SMAD2/3 Phosphorylation

(A) Three H1 ARF6KO cell lines were cultured to approximately 50% confluency and subjected to 2hrs of growth factor starvation in minimal medium followed by induction with 50ng/ml Activin A. Cells were lysed using 1% SDS, subjected to SDS-PAGE and immunoblotted with α-pSMAD2 and α-pSMAD3 antibodies to check the effect of ARF6 knock-out in the Activin A mediated SMAD2/3 phosphorylation. Wild type H1 cells were used as a control. Changes in the phosphorylation levels of (B) SMAD2 and (C) SMAD3 in the absence of ARF6 were assessed by densitometry using the Image Studio Lite software. Statistical significance was calculated in GraphPad Prism using the non-parametric Mann-Whitney test (N=6).

4.2.7 ARF6 Knock-out Reduces the BMP4 Mediated SMAD1/5/9 Phosphorylation in H1 Cells

In section 4.2.3 we reported the effect of ARF6 activation in the phosphorylation of SMAD1/5/9 proteins in H1 cells. That effect revealed a role for the GTPase in the BMP-SMAD1/5/9 pathway which is implicated mainly in the differentiation of hES cells. Here, we use the H1 ARF6 knock-out clones in order to address the impact on the phosphorylation of the R-SMADs in the absence of the GTPase.

Three different H1 ARF6 knock-out clones, along with wild-type H1 control cells were cultured in mTeSR1 until they reached approximately 50% confluency. Subsequently, the cells were serum starved for 4hrs in plain medium and induced with BMP4 (50ng/mL) for 40min. The cell lysates were then analysed by western blotting using a single antibody that recognises the phosphorylated forms of SMAD1/5/9 proteins. The total levels of the R-SMADs remained the same after induction as revealed by probing with an antibody against total SMAD1/5/9. The results were normalised to ACTIN **Figure 4.13 (A)**.

Subsequently, we performed densitometry analysis and demonstrated that SMAD1/5/9 phosphorylation was reduced by 1.43-fold in ARF6KO clone 2, 1.84-fold in ARF6KO clone 5 and 1.52-fold in ARF6KO clone 6 **Figure 4.13 (B)**.

Summarising, these results indicate that knock-out of ARF6 in hES cells results in reduced phosphorylation levels of SMAD1/5/9 upon induction with BMP4.

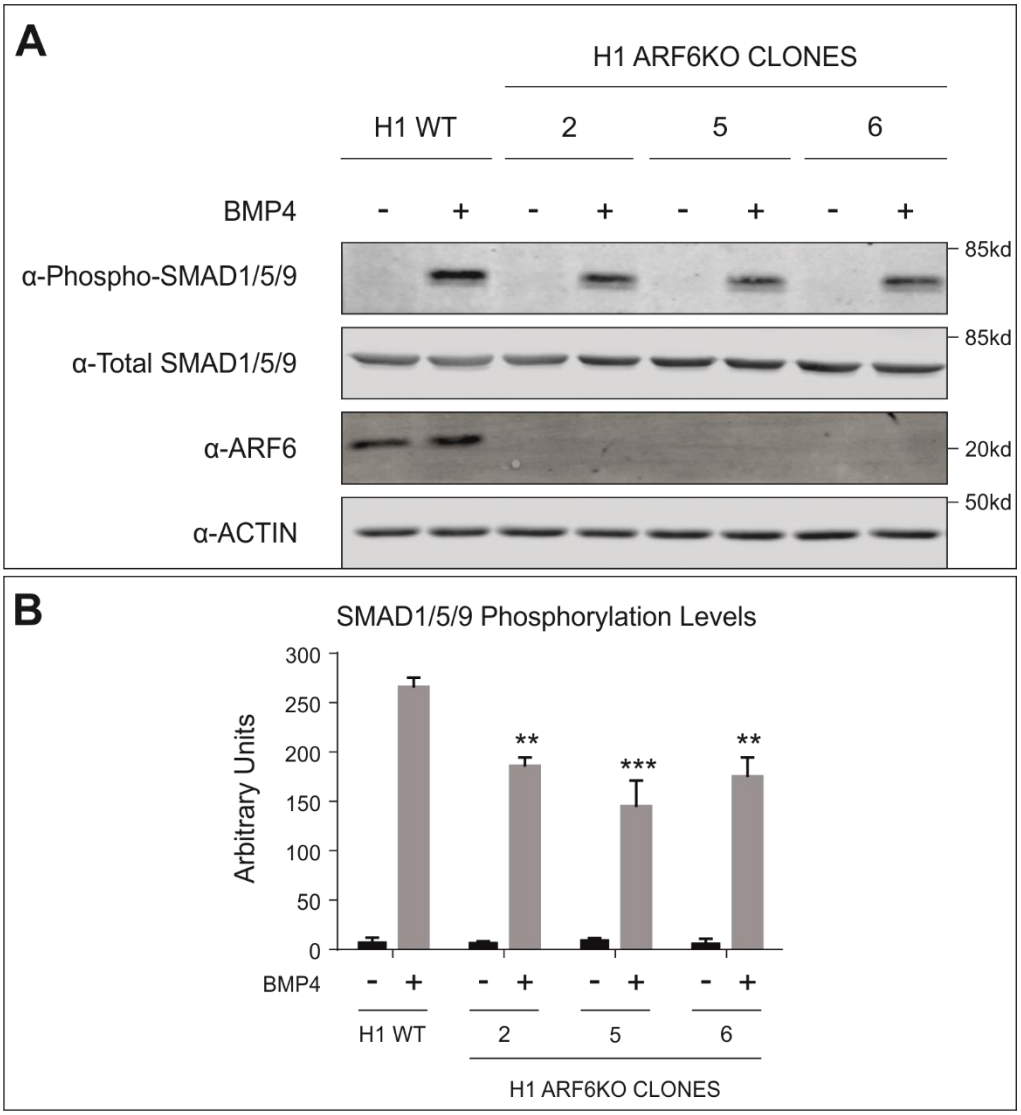


Figure 4.13: Effect of ARF6 Knock-out on SMAD1/5/9 Phosphorylation

(A) Three H1 ARF6KO cell lines were cultured to approximately 50% confluency and subjected to 2hrs of growth factor starvation in minimal medium followed by induction with 50ng/ml BMP4. Cells were lysed using 1% SDS, subjected to SDS-PAGE and immunoblotted with an α-pSMAD1/5/9 antibody to investigate the effect of ARF6 knock-out in the BMP4 mediated SMAD1/5/9 phosphorylation. Wild type H1 cells were used as a control. (B) Changes in the phosphorylation levels of SMAD1/5/9 in the absence of ARF6 were assessed by densitometry using the Image Studio Lite software. Statistical significance was calculated in GraphPad Prism using the non-parametric Mann-Whitney test (N=3).

4.2.8 ARF6 Knock-out Increases the Expression of BRACHYURY upon Mesendoderm Induction

So far we have demonstrated that ARF6 is implicated in the Activin A and BMP4 induced phosphorylation of proteins SMAD2/3 and SMAD1/5/9 in H1 cells. In addition, we have also shown that activation of the GTPase is involved in the regulation of BRACHYURY during mesendoderm differentiation. Here, we use the H1 knock-out clones of ARF6 in order to investigate whether BRACHYURY expression is altered in the absence of ARF6.

Three different H1 ARF6 knock-out clones, along with wild-type H1 control cells were cultured in mTeSR1 until they reached approximately 50% confluency. The differentiation protocol applied was based on a medium containing Activin A (50ng/mL) and BMP4 (50ng/mL). Differentiation to mesendoderm was initiated by incubation in the above medium for 48hrs. The cell lysates were analysed by western blotting with the outcome of differentiation being scored based on the expression levels of the early mesendodermal marker BRACHYURY. The levels of BRACHYURY were normalised to endogenous ACTIN **Figure 4.14 (A)**.

The results of the densitometry analysis demonstrated that BRACHYURY levels were increased by 1.8-fold in ARF6KO clone 2, 2.9-fold in ARF6KO clone 5 and 1.9-fold in ARF6KO clone 6 **Figure 4.14 (B)**.

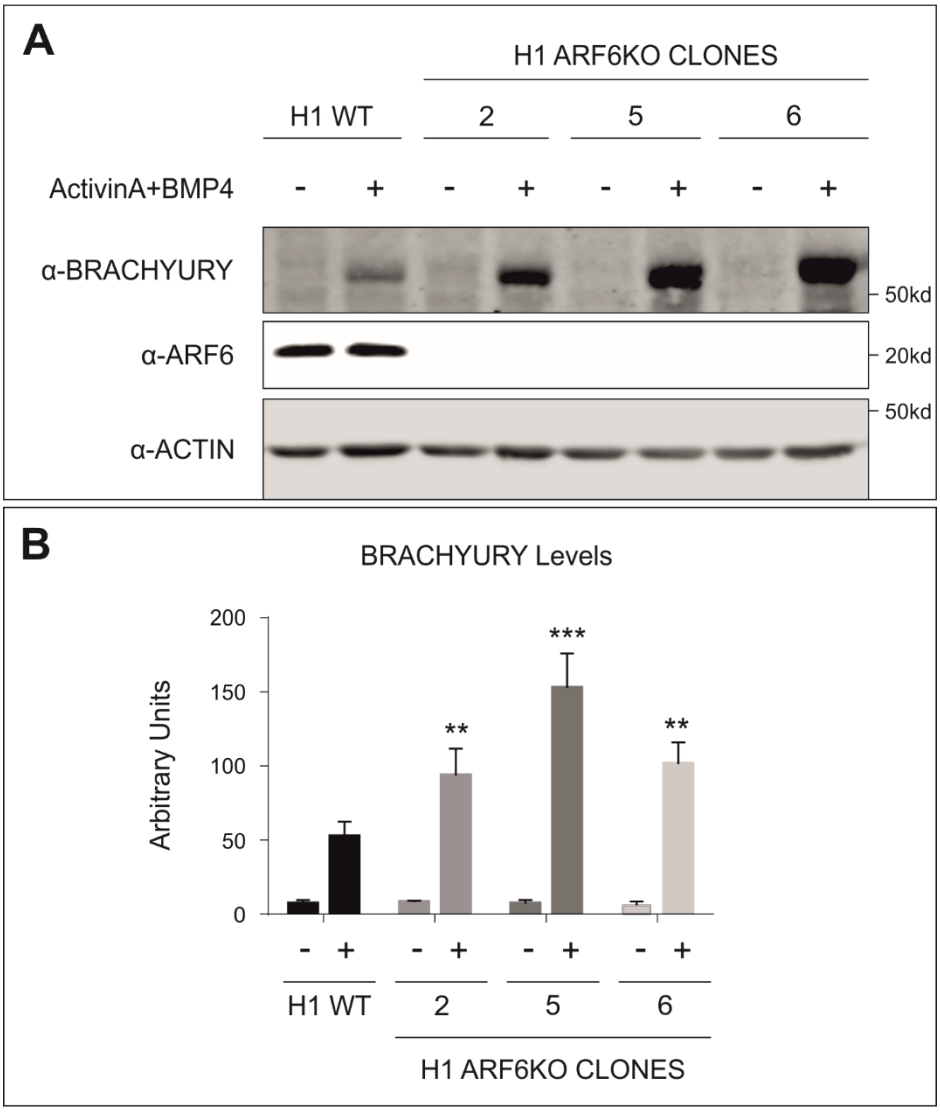
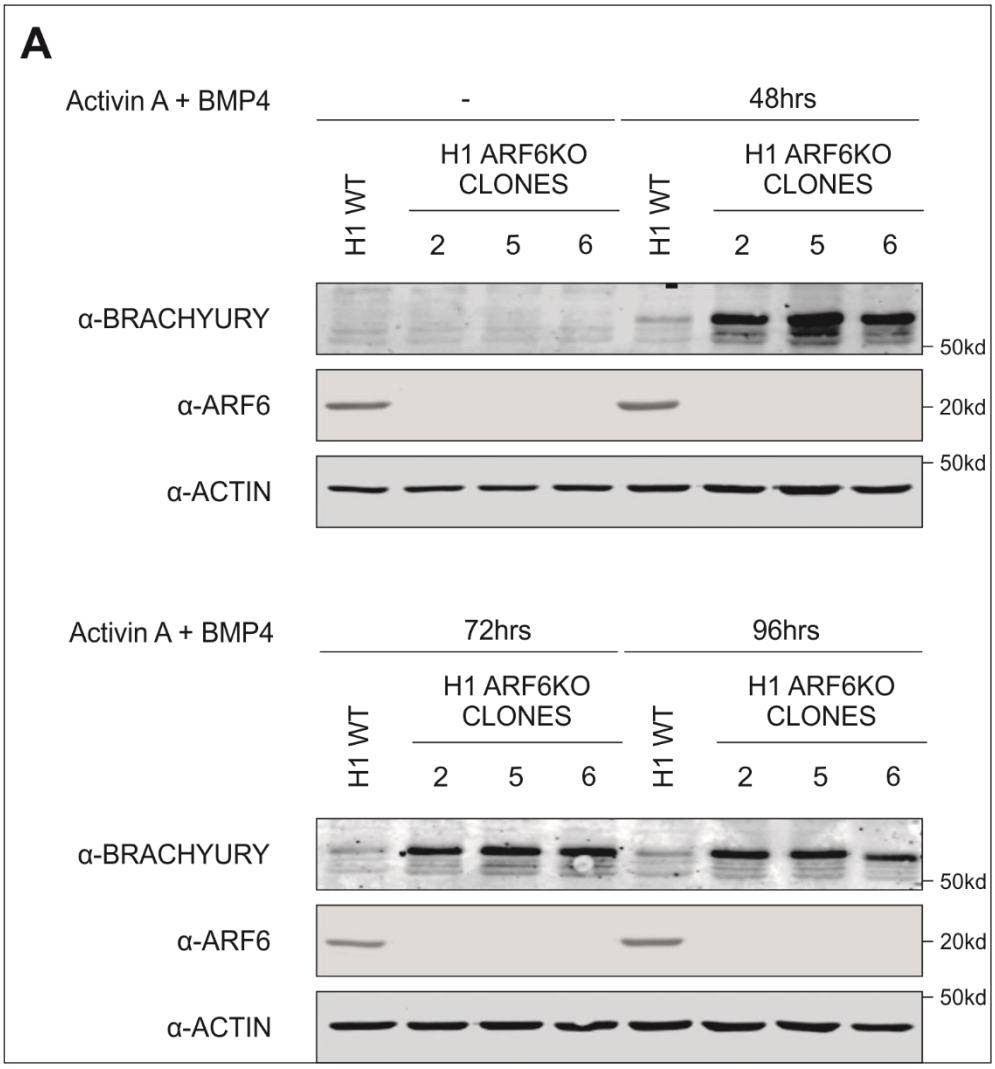


Figure 4.14: Effect of ARF6 Knock-out on BRACHYURY Expression upon Mesendoderm Induction

(A) Three H1 ARF6KO cell lines were cultured to approximately 50% confluency. Differentiation to mesendoderm was initiated by substituting mTeSR1 with a medium containing Activin A (50ng/mL) and BMP4 (50ng/mL). After 48hrs cells were lysed using 1% SDS, subjected to SDS-PAGE and immunoblotted with an α-BRACHYURY antibody to investigate the effect of ARF6 knock-out in the expression levels of the mesendodermal marker. (B) Changes in the expression levels of BRACHYURY in the absence of ARF6 were assessed by densitometry using the Image Studio Lite software. Statistical significance was calculated in GraphPad Prism using the non-parametric Mann-Whitney test (N=3).


A
Activin A + BMP4
-
48hrs
H1 WT
H1 ARF6KO CLONES
2
5
6
α-BRACHYURY
α-ARF6
α-ACTIN
50kd
20kd
72hrs
96hrs

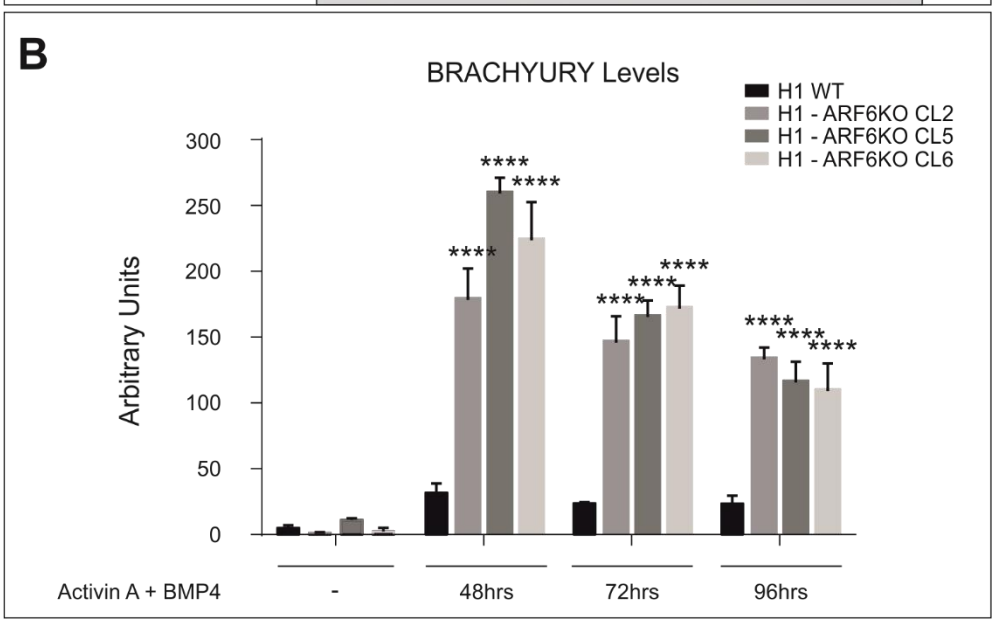

B
BRACHYURY Levels
H1 WT
H1 - ARF6KO CL2
H1 - ARF6KO CL5
H1 - ARF6KO CL6
Arbitrary Units
300
250
200
150
100
50
0
****
Activin A + BMP4
-
48hrs
72hrs
96hrs

Figure 4.15: Effect of ARF6 Knock-out on the Timing of BRACHYURY Expression upon Mesendoderm Induction

(A) Three H1 ARF6KO cell lines were cultured to approximately 50% confluency. Differentiation to mesendoderm was initiated by substituting mTeSR1 with a medium containing Activin A (50ng/mL) and BMP4 (50ng/mL). After 48, 72 and 96hrs cells were lysed using 1% SDS, subjected to SDS-PAGE and immunoblotted with an α-BRACHYURY antibody to investigate the effect of ARF6 knock-out in the expression levels of the mesendodermal marker in a time dependent manner. (B) Changes in the expression levels of BRACHYURY in the absence of the fast cycling ARF6 mutant were assessed by densitometry using the Image Studio Lite software. Statistical significance was calculated in GraphPad Prism using the non-parametric Mann-Whitney test (N=3).

Having demonstrated that in the absence of ARF6 differentiating H1 cells exhibit a higher expression of BRACHYURY, we needed to investigate whether that can be attributed to a change on the timing or the regulation of BRACHYURY's expression.

In that direction, we cultured three H1 ARF6 knock-out clones along with H1 wild-type cells in mTeSR1 until approximately 50% confluency. Subsequently, the cells were incubated in the differentiation medium reported above for 48, 72 and 96hrs. Next, the cell lysates were analysed by western blotting with the outcome of differentiation being scored based on the expression levels of BRACHYURY at each time point. The levels of BRACHYURY were normalised to endogenous ACTIN **Figure 4.15 (A)**.

The results of the densitometry analysis demonstrated that BRACHYURY levels were increased by 5.56-fold in ARF6KO clone 2, 8-fold in ARF6KO clone 5 and 7-fold in ARF6KO clone 6 after 48hrs, 6.3-fold, 7.2-fold and 7.4-fold after 72hrs and 5.8-fold, 5-fold and 4.8-fold after 96hrs of differentiation **Figure 4.15 (B)**.

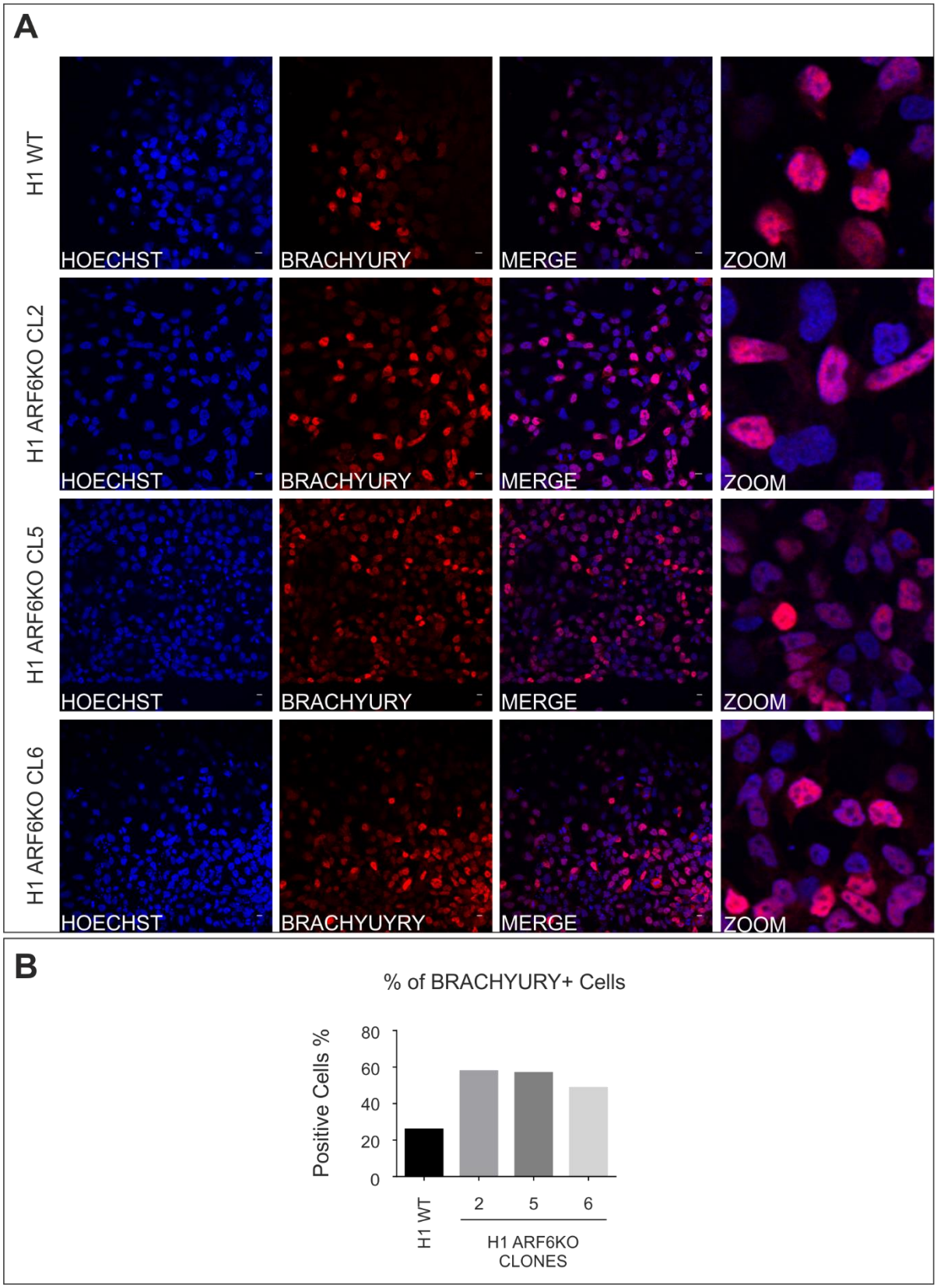

A
H1 WT
H1 ARF6KO CL2
H1 ARF6KO CL5
H1 ARF6KO CL6
HOECHST
BRACHYURY
MERGE
ZOOM
HOECHST
BRACHYURY
MERGE
ZOOM
HOECHST
BRACHYURY
MERGE
ZOOM
HOECHST
BRACHYUYRY
MERGE
ZOOM
B
% of BRACHYURY+ Cells
Positive Cells %
80
60
40
20
0
H1 WT
2
5
6
H1 ARF6KO
CLONES

Figure 4.16: Effect of ARF6 Knock-out on the Percentage of Cells Expressing BRACHYURY upon Mesendoderm Induction

(A) Wild type H1 cells and three H1 ARF6KO cell lines were cultured to approximately 50% confluency in 8-well permanox chambers. Differentiation to mesendoderm was initiated by substituting mTeSR1 with a medium containing Activin A (50ng/mL) and BMP4 (50ng/mL). After 48hrs cells were immunostained with an α-BRACHYURY antibody to investigate the effect of ARF6 knock-out on the percentage of cells expressing the mesendodermal marker within a colony. All Images were obtained using a Leica SP8 Confocal Microscope and a 40X/1.30 NA objective. Scale bar size is 10μm. Images are maximum projections. (B) Comparison of the percentage of BRACHYURY positive cells between the control H1 wild type cells and the three ARF6KO cell lines. The number of positive cells per condition was measured in ImageJ. A total number of approximately 1000 cells per condition was used to evaluate the percentage.

Taking the previous results into account, so far we have demonstrated that in the absence of ARF6, differentiating H1 cells towards mesendoderm express higher levels of BRACHYURY. Based on that, we hypothesised that more cells should be expressing the marker in the ARF6 knock-out clones compared to the wild-type control H1 cells.

In order to investigate that, we cultured the three H1 ARF6 knock-out clones, along with the wild-type control cells in permanox 8-well chambers, in mTeSR1. At approximately 50% confluency we started the differentiation to mesendoderm by incubating them in the Activin A / BMP4 medium that has been reported before. After 48hrs the cells were fixed and immunostained with a primary antibody against BRACHYURY. Confocal microscopy revealed that the percentage of BRACHYURY positive cells is significantly altered in the knock-out clones of ARF6 **Figure 4.16 (A)**. More specifically, in approximately 1000 cells counted, BRACHYURY expressing cells are increased by 2.23-fold in ARF6 knock-out clone 2, 2.20-fold in ARF6 knock-out clone 5 and 1.88-fold in ARF6 knock-out clone 6 **Figure 4.16 (B)**.

4.2.9 Activin A / BMP4 Signalling Promotes ARF6 GTP – GDP Exchange in H1 Cells

All the previous experiments in hES cells point out that ARF6 is implicated in Activin A and BMP4 signalling. In addition, in section 3.2.4 we provide evidence that activation of the Activin A or TGFβ pathway in HEK-293 cells leads to ARF6 inactivation. However, we have not yet examined if the same mechanism exists in hES cells or whether activation of the BMP4 pathway will lead to the same result.

In that direction, we generated a novel H1 cell line that stably overexpresses a wild-type, HA tagged ARF6 transcript. The process of generating this line was identical to what we report in section 4.2.1. Subsequently, this cell line was used in a pull-down experiment using the aforementioned GST-GAP protein as bait. In short, GST-GAP will bind only the GTP form of ARF6. Prior to lysis, cells were subjected to 4hrs serum starvation followed by induction with Activin A or BMP4. We examined 4 different time points. The cells were incubated with the ligands for 5, 10, 20 and 40min. Next, the cell lysates were analysed by western blotting with a primary antibody against the HA tag.

The results of the assay indicated that upon treatment with either ligand, GST-GAP binds a lower quantity of ARF6-GTP. That is the case for all the time points examined, with no significant difference in the quantity of ARF6-GTP detected **Figure 4.17 (A)**. More specifically, induction with either Activin A or BMP4, results in an approximate 1.5-fold ARF6 inactivation across all the time points examined **Figure 4.17 (B)**.

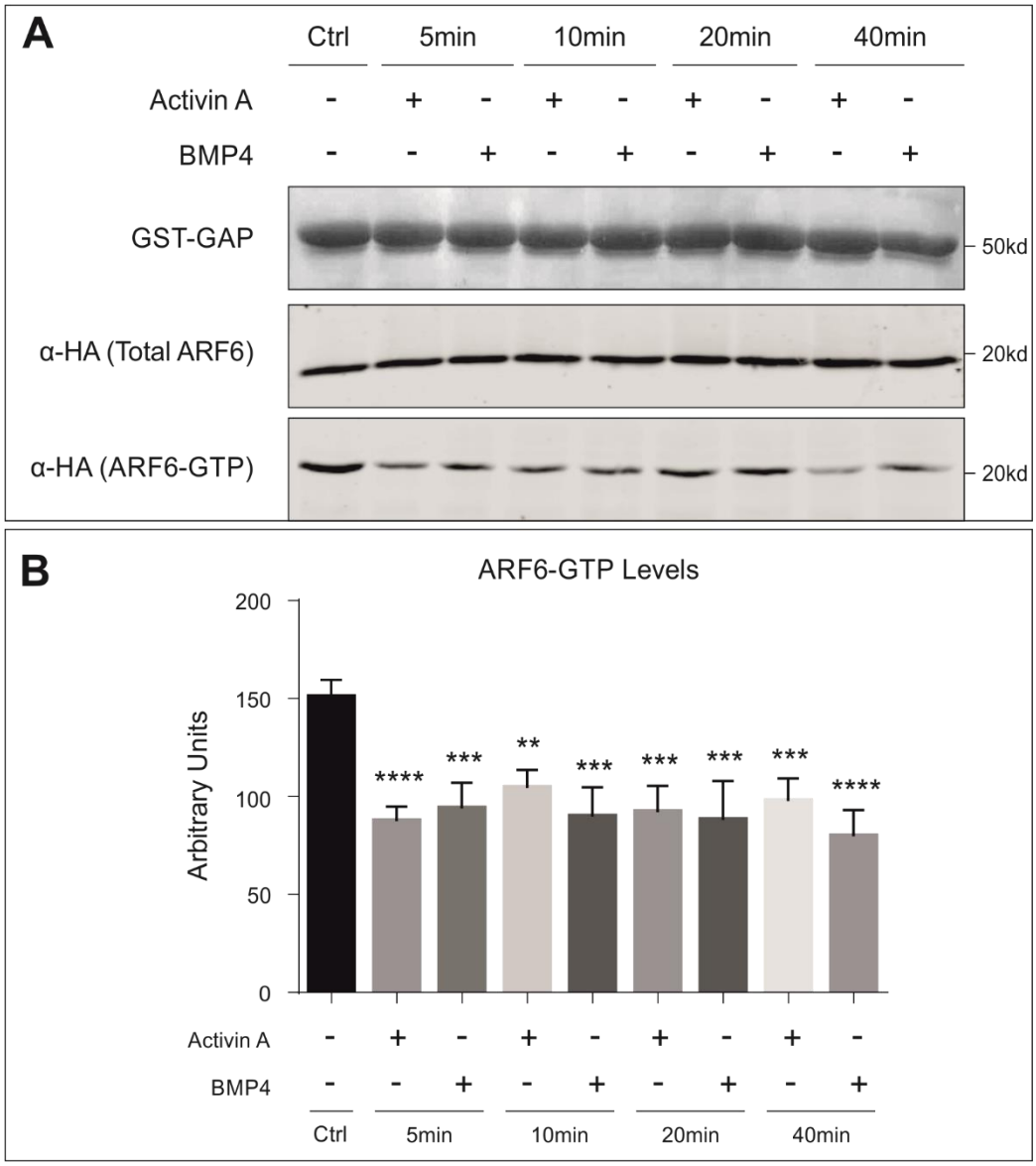


Figure 4.17: Effect of Activin A / BMP4 Signalling on ARF6-GTP Loading

(A) The GTP binding domain of an ARF6GAP was tagged with GST and purified from *E. Coli BL21DE* bacteria. H1 cells were transfected with a vector carrying HA-ARF6 and selected with 250ng/mL of puromycin for 48hrs or until the control cells were dead. Positive colonies were manually picked with cloning rings and expanded. One H1 HA-ARF6 stable cell line was subjected to 3hrs serum starvation and induced with Activin A (50ng/ml) or BMP4 (50ng/ml) for 5, 10, 20 and 40min. The cell lysates were incubated with GST-GAP for 1hr and GST beads were used to pull-down the ARF6/GST-GAP complex. ARF6-GTP bound to the beads was detected by western blot using an α-HA antibody. (B) Quantitation of the ARF6-GTP levels between control and Activin A or BMP4 treated cells. Densitometry was performed using the Image Studio Lite software. Statistical significance was calculated in GraphPad Prism using the non-parametric Mann-Whitney test (N=3).

4.3 Discussion

In the present chapter we have established that ARF6 is directly implicated in major signalling pathways regulating pluripotency and differentiation in hES cells. The observations leading to this conclusion include that: (1) Activin A or BMP4 induction in the presence of fast-cycling ARF6 leads to increased SMAD2/3 and SMAD1/5/9 phosphorylation, respectively. (2) Activin A or BMP4 induction in the absence of ARF6 leads to decreased SMAD2/3 and SMAD1/5/9 phosphorylation, respectively. (3) BRACHYUYRY expression is decreased during mesendoderm formation in the presence of fast-cycling ARF6. (4) BRACHYUYRY expression is increased during mesendoderm formation in the absence of ARF6. (5) Activin A or BMP4 induction leads to ARF6 inactivation.

To date, there is no scientific research investigating the role of ARF6 in hES cells. However, the importance of the GTPase during development has been outlined by the fact that its knock-out in mice is embryonic lethal. Interestingly, knock-out effects are apparent only at E10.5, during the formation of the hepatic cord (Suzuki et al., 2006). This can explain why ARF6 activation or ablation did not perturb the morphology, proliferation or expression of pluripotency markers in our system, which resembles an *in vitro* model of the epiblast.

Similarly to our results in HEK-293 cells, overexpression of fast-cycling ARF6 (T157A) increases Activin A induced SMAD2/3 phosphorylation, while ARF6 ablation leads to the opposite result. Interestingly, BMP4 induced SMAD1/5/9 phosphorylation also follows the same trend, suggesting that ARF6 might orchestrate TGFβ superfamily responses in a similar fashion, regardless of the subsequent SMAD cascade. Even

though a potential interaction of activated ARF6 with SMAD1/5/9 has not been demonstrated, SMAD1/5/9 C-terminal tails exhibit an even higher percentage of identity with SMAD4 compared to SMAD2/3 (62.5% vs 56.2%). Therefore, a mechanism of R-SMAD recruitment to receptors by ARF6-GTP might contribute to the differences observed in R-SMAD phosphorylation **Figure 6.1**.

ARF6 involvement in regulating endocytosis might also contribute to the observed differences. ARF6 is known to stimulate CME, an entry route that facilitates TGFβ signalling by forwarding receptors to EEA1 and SARA positive endosomes (Wenk and De Camilli, 2004; Hayes et al., 2002; Penheiter et al., 2002). Unpublished results from our lab concluded that Activin A internalisation in hES cell is partly Dynamin-dependent, as pharmacological inhibition of the GTPase resulted in a 40% decrease in SMAD2/3 phosphorylation, post ligand induction. In addition, ARF6 is known to regulate Dynamin cycling during CME by interacting with NM23-H1, a nucleoside diphosphate kinase which modulates GTP levels (Palacios et al., 2002). Consequently, we hypothesize that ARF6 activation facilitates CME of TGFβ components, thus promoting signalling. Ablation of ARF6 in hES cells perturbs the same process and results in decreased R-SMAD phosphorylation **Figure 6.1**.

Current scientific literature suggests that cooperative induction of BMP4 and Activin A pathways in the absence of FGF/IGF, leads to upregulation of primitive streak transcripts (Zhang et al., 2008). BMP4 acts through SMAD1/5/9 to enhance BRACHYURY, while Activin A through SMAD2/3 which coordinate with endogenous WNT signals, like β-catenin, to activate MIXL1 and others (Singh et al., 2012). In our system, expression of BRACHYURY following differentiation with Activin A and BMP4 was dependent on the activation state of ARF6. Interestingly, ARF6T157A Clone 1,

which demonstrated a 10-fold higher expression of ARF6T157A compared to Clone 2, exhibited higher levels of SMAD1/5/9 phosphorylation upon induction with BMP4. The same clone also exhibited lower levels of BRACHYURY when differentiated with Activin A and BMP4. These observations suggest an inversely proportional relation between SMAD1/5/9 phosphorylation and BRACHYURY induction that further supports a mechanism by which activated ARF6 sequesters phosphorylated SMAD2/3 and SMAD1/5/9 in the cytoplasm, prohibiting their nuclear translocation. This remains to be addressed experimentally **Figure 6.1**.

Furthermore, in physiological conditions where ARF6 cycling is permitted, both Activin A and BMP4 induction resulted in ARF6 inactivation. It should be noted that overexpression of wild-type ARF6 does not perturb its normal cellular function or localisation (Peters et al., 1995). Since ARF6 interacts with SMAD2/3 and possibly SMAD1/5/9 when activated, its inactivation in response to ligand stimulation might allow both trafficking to progress and R-SMADs to translocate to the nucleus and exert their signalling. In HEK-293 cells, SMAP1 was demonstrated to interact with ACVR1B and catalyze ARF6 hydrolysis upon Activin A or TGFβ induction. In addition, comparison of the intracellular domains of ACVR1B with ACVR1, BMPR1A and BMPR1B demonstrated 65%, 60% and 64% identity, respectively. Therefore, SMAP1 could potentially promote ARF6 inactivation in hES cells upon Activin A or BMP4 addition, by interacting with Activin and BMP type I receptors. However, as SMAP1 knock-out was not tolerated in hES cells, we were unable to definitively prove that it is the GAP involved in the process. In MDCK cells, overexpression of SMAP1 or a SMAP1 mutant with limited GAP activity, inhibited internalisation of E-Cadherin and EMT (Kon et al., 2008). This suggests that physiological ARF6 cycling is indispensable

in the process of E-Cadherin endocytosis and possibly explains why SMAP1 knock-out was not tolerated in hES cells. In addition, overexpression of activated ARF6 (Q67L) in hES cells also exhibited a lethal phenotype that can be attributed to a similar mechanism. More specifically, in MDCK cells, ARF6 activation in response to WNT signalling has been demonstrated to promote E-Cadherin internalisation and dissolution of adherens junctions, thus promoting EMT (Pellon-Cardenas et al., 2013). Since hES cells strongly depend on cell to cell interactions to maintain colony formation, ablation of E-Cadherin from the surface might be detrimental for self-renewal. In the fast-cycling ARF6 stable lines that we established, E-Cadherin levels and localisation were found similar to the GFP expressing, control cell line. This could be attributed to the ability of fast-cycling ARF6 to undergo hydrolysis, contrary to the constitutively active mutant.

CHAPTER 5

IDENTIFYING NOVEL MOLECULES IMPLICATED IN EARLY MESENDODERM SPECIFICATION BY A BROAD TRANSCRIPTOMIC APPROACH

5.1 Introduction

hES cells have been cultured routinely by separate labs under different conditions. Typically, the culture protocol involves a feeder layer of Mouse Embryonic Fibroblasts (MEFs), that metabolically supports the stem cell colonies and secretes indispensable growth factors, like Activin A (Beattie et al., 2005), which promote pluripotency and self-renewal. Also, the culture media utilised are usually supplemented with serum (Skottman and Hovatta, 2006; De Miguel et al., 2010). These culture conditions, though cost effective, limit the quality of data generated due to the presence of a vast number of unknown factors originating both from the serum and the MEFs secretome. Several feeder-free, chemically defined culture systems have been developed, offering a more controlled environment in which the study of individual pathways is feasible (Ludwig et al., 2006; Xu et al., 2005; International Stem Cell Initiative Consortium et al., 2010). The most commonly used system is mTeSR1 / Matrigel. In brief, stem cells are plated on matrigel coated dishes in a chemically defined medium that relies on TGFβ1 and bFGF to preserve pluripotency (Ludwig et al., 2006). The only drawback of the system is that research is limited on studying signalling events in the presence of these growth factors that activate and suppress specific cascades.

In the present chapter we describe the development of a novel, versatile system for the culture of hES cells. Initially, we adapted our cells to a custom made version of mTeSR1 that is stripped of growth factors, and supplemented with Activin A and bFGF exogenously. Cells were cultured for several passages under various concentrations of Activin A while being observed for phenotypic changes. Having pinpointed the appropriate concentration of the growth factor, we investigated for potential effects on the expression of pluripotency markers, karyotype and *in vivo* differentiating capacity.

Subsequently, H1 cells cultured in the aforementioned system where used in an RNA-sequencing assay in order to reveal the early events of mesendodermal differentiation. In that direction, the medium was supplemented with Activin A, bFGF and BMP4 (Yu et al., 2011). Total RNA was extracted from the cells after 1hr and 4hrs of BMP4 addition. The early time point revealed transcripts affected directly by the growth factor while the second, transcripts that pose secondary responses facilitating the progression of differentiation.

5.2 Results

5.2.1 H1 Cells Cultured in Activin A Based Media Remain Pluripotent

The well-established system for the culture of hES cells in our lab relies on incubation in mTeSR1 medium on matrigel coated dishes. In these conditions, we have been able to maintain H1 and other hES cell lines (e.g. HuES1) in a pluripotent, self-renewing state and differentiate them to all germ layers with a variety of published protocols. In addition, frequent karyotypic analysis showed that the cells exhibit no evident chromosomal aberrations.

In order to transition our culture to an Activin A dependent medium, we used a commercially available form of mTeSR1 that is stripped of TGFβ, bFGF, LiCl, GABA and Pipecolic Acid. We supplemented all the factors to the original quantities stated in section 7.1.2 and substituted TGFβ for 0.25ng/mL, 0.5ng/mL or 1ng/mL of Activin A. Using that formulation, we cultured H1 cells for several passages and observed that only the 0.5ng/mL Activin A version was able to sustain the culture with minimum observable differentiation.

Transitioning any hES cell culture to a new maintenance system can affect several parameters, the most important of them being pluripotency. In order to verify that H1 cells cultured in the Activin A based medium remained pluripotent, we examined their expression for major pluripotency related transcription factors. In that direction, cells were cultured for at least 10 passages in the new medium, before being seeded on 8-well permanox dishes and fixed. Immunofluorescence was carried out with primary antibodies against NANOG, OCT4 and SOX2. The results indicated that H1 cells cultured in the presence of Activin A maintained the expression of the

aforementioned factors. Their localisation remained nuclear, as seen by their overlap with the DNA stain DAPI **Figure 5.1 (A)**.

We also compared the expression levels of the transcription factors NANOG and OCT4 between H1 cells cultured in mTeSR1 and Activin A supplemented mTeSR. H1 cells were cultured for at least 10 passages in both media. Cell lysates were subjected to western blotting using primary antibodies against the transcription factors NANOG and OCT4 **Figure 5.1 (B)**. The results of the densitometry analysis indicated that there is no significant difference in the expression levels between the two cell groups **Figure 5.1 (C), (D)**.

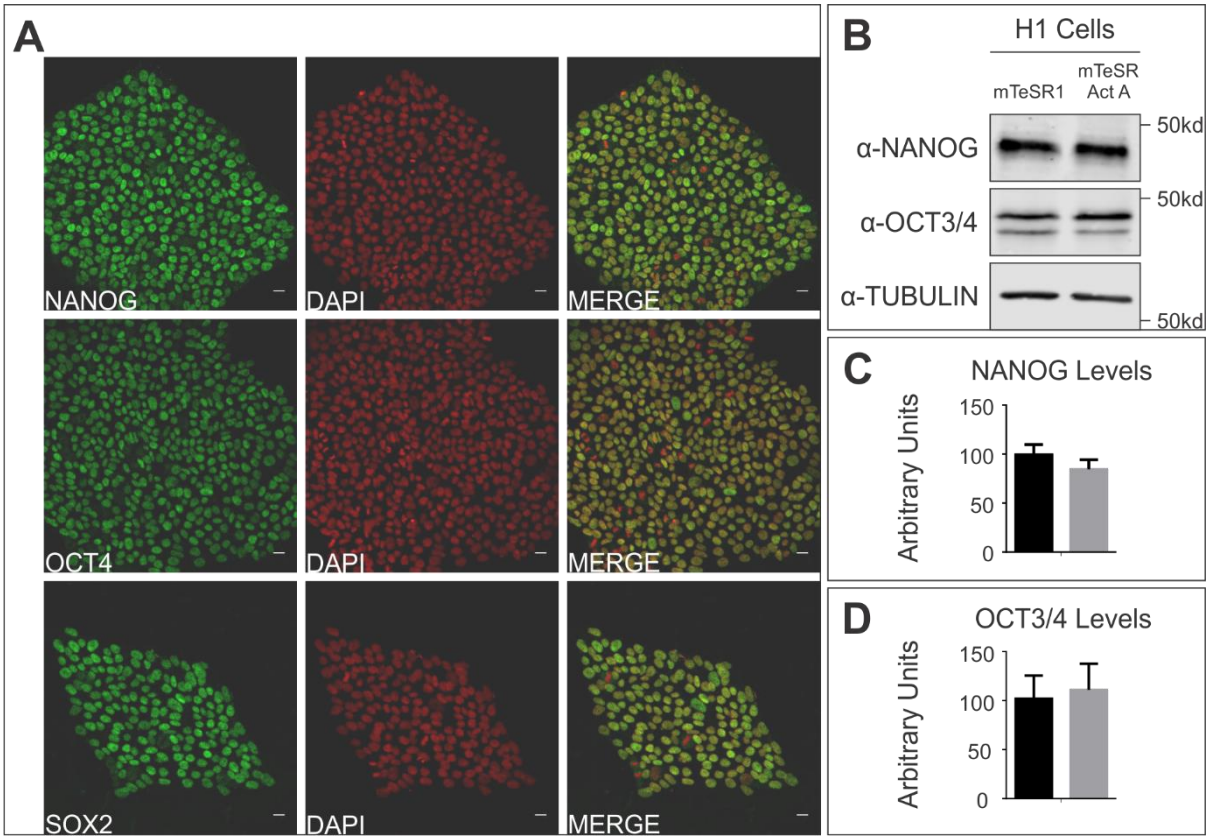


Figure 5.1: Expression Levels of Pluripotency Factors in H1 Cells Cultured in Activin A Based mTeSR

(A) H1 cells were cultured for 10 passages in custom mTeSR media with TGFβ substituted for Activin A. Cells were cultured in 35mm ibidi dishes to approximately 50% confluence and immunostained with primary antibodies against NANOG, OCT4 and SOX2. All Images were obtained using a Leica SP8 Confocal Microscope and a 40X/1.30 NA objective. Scale bar size is 10μm. Images are maximum projections. (B) H1 cells were cultured to approximately 50% confluency in Activin A based mTeSR and lysed using 1% SDS. The lysates were subjected to SDS-PAGE and immunoblotted with α-NANOG and α-OCT4 antibodies. H1 cells cultured in mTeSR1 were used as a positive control. (B), (C). The expression levels of the pluripotency factors were compared between the two cell groups by densitometry using the Image Studio Lite software. Statistical significance was calculated in GraphPad Prism using the non-parametric Mann-Whitney test (N=3).

5.2.2 H1 Cells in Activin A mTeSR are Karyotypically Normal and Form Teratomas in NOD/SCID Mice

In the previous section we verified that our novel Activin A dependent culture system for hES cells did not impact the expression or localisation of major pluripotency factors. However, in order to be able to use this system in subsequent experiments, we needed to verify that cells remain karyotypically normal and retain their differentiation capacity to all germ layers.

The karyotype of the cells was frequently analysed in order to ensure that the transition to the new culture conditions did not generate any chromosomal aberrations. The cells were initially adapted to the Activin A based media for over 10 passages. During the adaptation period, a certain degree of spontaneous differentiation was observed, but it was comparable to what is witnessed while culturing in the normal TGFβ1 based mTeSR1 media. The results indicated that karyotypic stability of the cells is maintained in the new culture conditions **Figure 5.2 (A)** H1 cells cultured in normal mTeSR1 were used as a positive control **Figure 5.2 (B)**.

In order to further validate that the cells transitioned to the Activin A based system remained pluripotent, we needed to demonstrate that they were able to differentiate into all germ layers *in vivo*. In that direction, H1 cells cultured in Activin A mTeSR for 10 passages along with H1 cells cultured in normal mTeSR1 were injected into immunodeficient NOD/SCID mice to test for their teratoma forming capacity.

Four mice were used in total, each injected with both cell lines **Figure 5.3 (Ai)**.The teratomas that formed were extracted after 6 weeks **Figure 5.3 (Aii)**. Next, the tissue was sectioned and stained with haematoxylin/eosin. Cell types originating

from all 3 different germ layers were present within the teratomas of both the control H1 cells and the Activin A. More specifically, we identified cartilage (Mesoderm [1]), melanin producing epithelial cells (Ectoderm [2]) and tubular glands (Endoderm [3]) **Figure 5.3 (B)**.

As a result, we can safely assume that the novel system we developed for the study of Activin A in pluripotency can substitute mTeSR1 efficiently with no apparent effects in the properties of the stem cell culture.

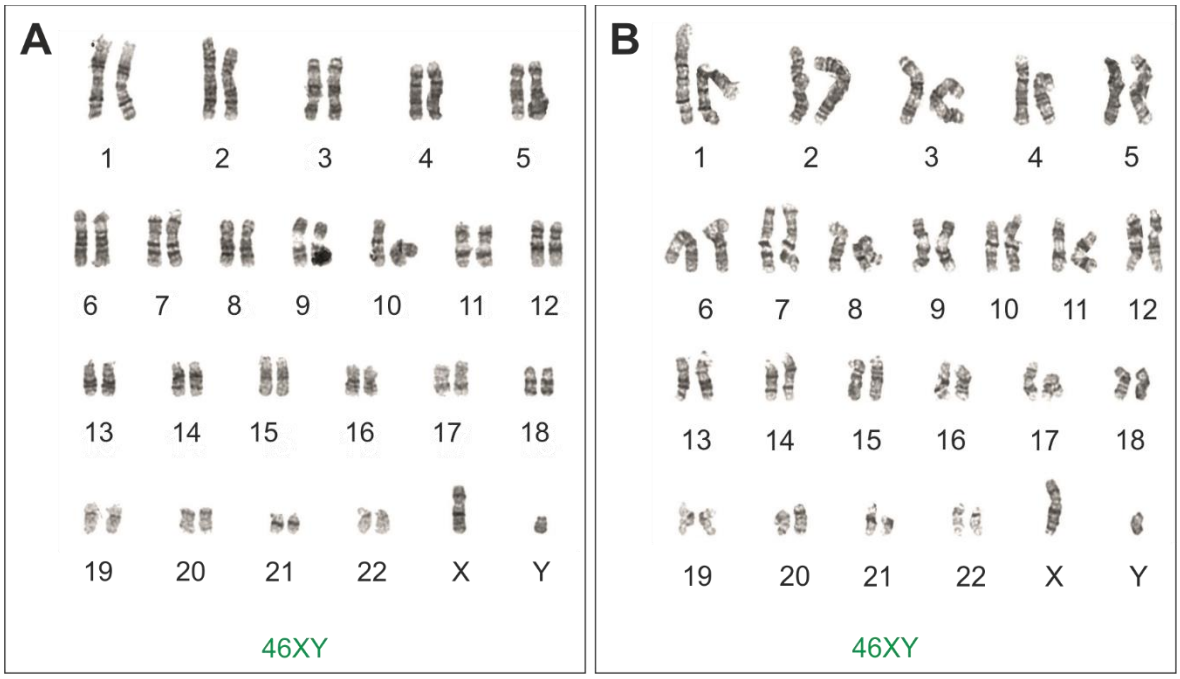


Figure 5.2: Karyotypic Analysis of H1 Cells Cultured in Activin A Based mTesR

(A) H1 cells cultured for 10 passages in Activin A based mTeSR and (B) H1 cells cultured in normal mTeSR1 were arrested in metaphasis using 0.04 µg/mL colcemid for 2hrs. Cells were lysed using a hypotonic buffer and the metaphasic chromosomes were extracted and stained with Giemsa reagent.

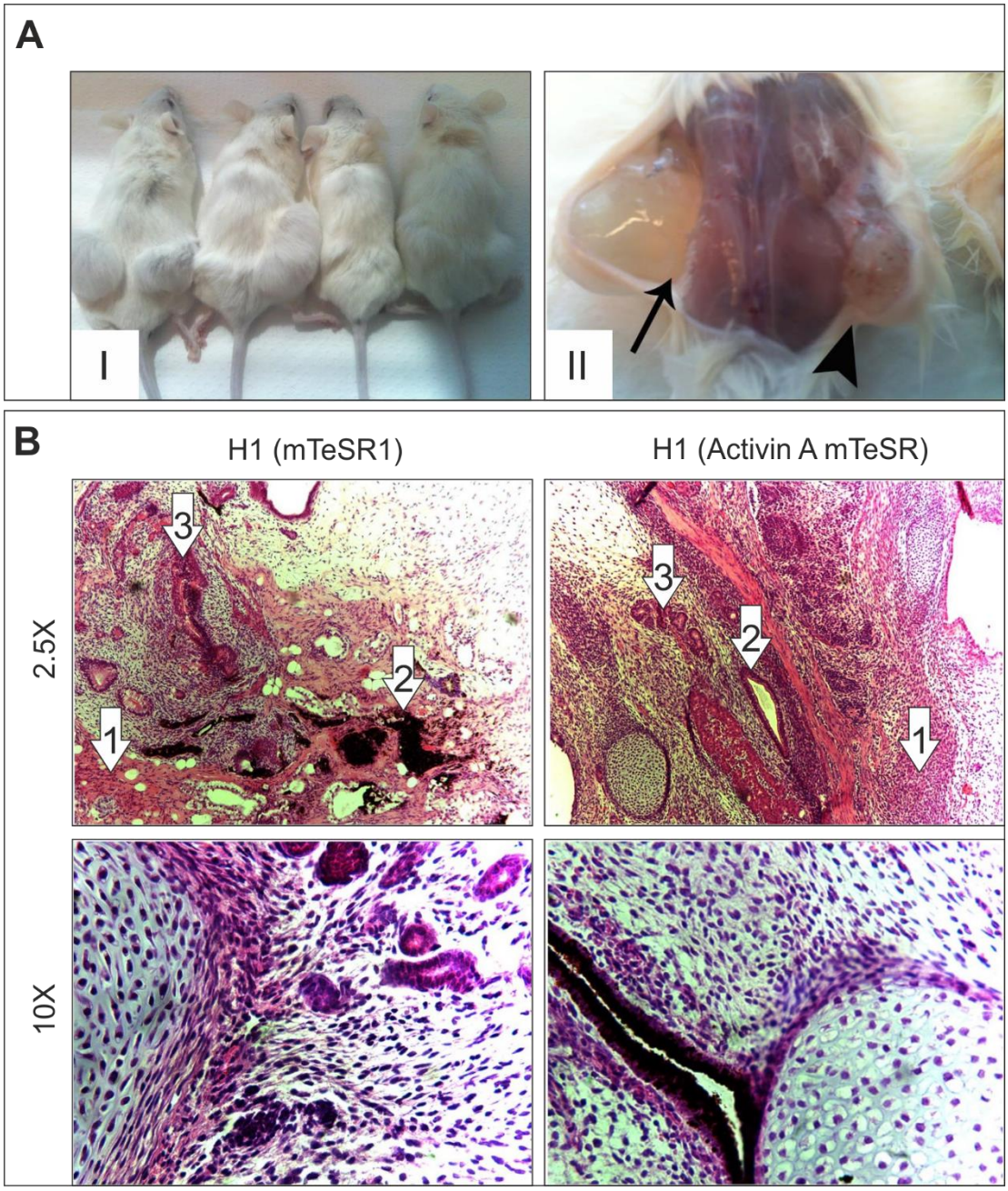


Figure 5.3: Teratoma Formation Assay of H1 Cells Cultured in Activin A mTeSR

(A) H1 cells cultured in Activin A based mTeSR for 10 passages and control H1 cells cultured in normal mTeSR1 were subcutaneously injected in immunodeficient NOD/SCID mice. Each mouse was injected with both cell lines to limit subject variability issues. After 6 weeks, the newly formed teratomas were removed, fixed, embedded in paraffin and stained with haematoxylin/eosin. (B) Among the cell types observed, there was (1) cartilage (Mesoderm), (2) melanin producing epithelial cells (Ectoderm) and (3) small glandular formations (Endoderm).

5.2.3 BMP4 Transcriptomics in H1 Cells Cultured in Activin A mTeSR

In the previous sections of the chapter we described the development of a novel, Activin A based medium, able to sustain H1 cells in pluripotency with no apparent effects in the expression levels of NANOG, OCT4 and SOX2, their karyotype or *in vivo* differentiating capacity. Using H1 cells adapted to this system, we carried out RNA sequencing upon addition of BMP4, in order to identify novel transcripts that are implicated in the early differentiation stages to mesendoderm.

More specifically, H1 cells were initially adapted to the Activin A based mTeSR for at least 10 passages. The cells were subsequently split in 3 full 6-well plates and incubated in the same medium until they reached approximately 50% confluency. At that point, the cells were induced with 50ng/mL BMP4 for 1hr or 4hrs. A full 6-well plate served as a non-induced control. RNA was extracted from all the conditions with the experiment being repeated 3 times using cells from three consecutive passages for statistical significance. The quantity and purity of the isolated RNAs per condition is summarized in **Table 7.1**.

RNA library preparation and subsequent RNA-Sequencing were carried out at The Oxford Genomics Centre (Wellcome Trust Centre for Human Genetics, Nuffield Department of Medicine, University of Oxford). After isolation, the samples were initially depleted for ribosomal RNA with the ribo-depleted fraction being isolated and converted to cDNA. A second strand cDNA synthesis was carried out to incorporate dUTPs. The cDNA was then end-repaired, A-tailed and adapter-ligated. Prior to amplification the samples underwent uridine digestion. The prepared libraries were multiplexed and paired-end sequenced twice over two lanes of a flow cell in an Illumina

HiSeq4000 sequencing system. The data generated was aligned to the GRCh37 reference human genome assembly.

Replicate	Sample Name	Concentration (ng/µL)	260/280	260/280
#1	Ctrl	604.8	2.06	2.07
#1	1hr BMP4	298.3	2.06	2.17
#1	4hrs BMP4	284.1	2.03	1.95
#2	Ctrl	257.9	2.04	2.06
#2	1hr BMP4	156.4	2.02	1.77
#2	4hrs BMP4	76.2	1.96	1.72
#3	Ctrl	131.8	2.02	1.74
#3	1hr BMP4	138.4	2.05	1.9
#3	4hrs BMP4	249.6	2.06	2.14

Table 5.1 Quantity and Purity of RNA Used for RNA-Sequencing

The acquired data were analysed in collaboration with Dr. Aditi Kanhere (School of Biosciences, University of Birmingham). The expression levels of transcripts in the two BMP4 treated groups were compared to the non-induced control. Only transcripts that presented a minimum of 2-fold up- or down- regulation were considered to be statistically significant. In **Figure 5.4** we depict in venn diagrams all the transcripts that were found to be significantly deregulated and their overlap between the BMP4 time point groups.

More specifically, 51 transcripts were found to be upregulated after 1hr of BMP4 treatment with the number rising to 143 after 4hrs. Out of the initial 51 transcripts, 33 remained upregulated after 4hrs, with the rest returning to their ground state. In addition, 17 transcripts were downregulated after 1hr of treatment with BMP4 and 33 after 4hrs. 8 out of the initial 17 transcripts remained downregulated at 4hrs of induction.

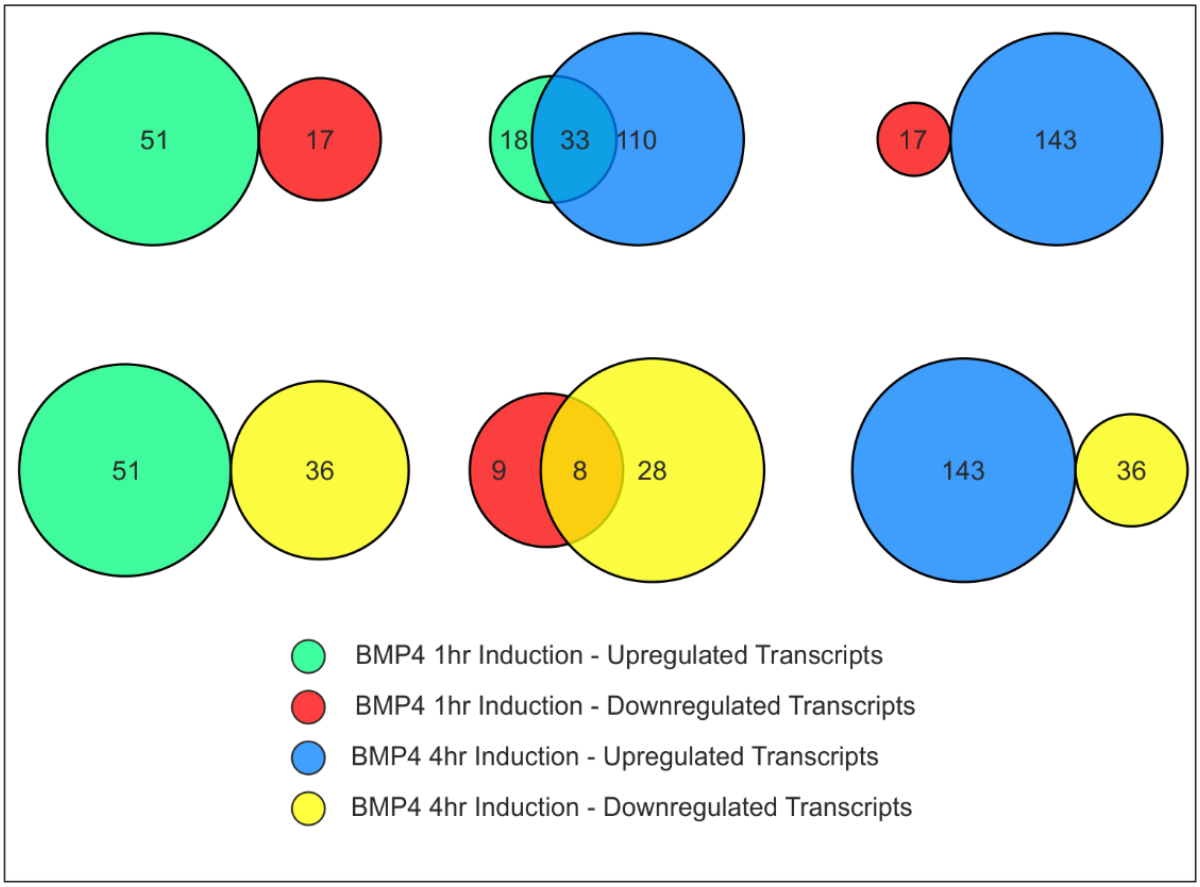


Figure 5.4: Overlap of Identified Transcripts

Differentially expressed transcripts between the control and BMP4 treated groups with a minimum of 2-fold up or downregulation. The BMP4 1hr upregulated group (N=51) shares 33 transcripts with the BMP4 4hrs upregulated group (N=143). The BMP4 1hr downregulated group (N=17) shares 8 transcripts with the BMP4 4hrs downregulated group (N=36). There are no common transcripts between groups with opposite direction of regulation.

5.2.4 Molecular Pathways and Functions Enriched after BMP4 Treatment

The RNA-sequencing results were evaluated based on the difference of expression between the control and the BMP4 induced groups. Only the transcripts that presented a minimum of 2-fold increase or decrease were taken into account. The significantly deregulated transcripts were uploaded into WebGestalt (WEB-based GEne SeT AnaLysis Toolkit) database and over-epresentation (OR) analysis was carried out. More specifically, we screened for enriched Biological Pathways (BPs) or Molecular Functions (MFs) and investigated affected KEGG (Kyoto Encyclopaedia of Genes and Genomes) pathways. The Gene Ontology (GO) terms that appeared to be enriched were run through ReViGO (Reduce & Visualise Gene Ontology) database for clustering into master categories.

After 1hr of BMP4 treatment, 51 transcripts were found to be significantly upregulated. OR analysis and subsequent clustering of the resulting GO terms revealed two significantly enriched categories of BPs. These are embryonic morphogenesis and regulation of transcription from RNA polymerase II promoter **Figure 5.5 (A)**. The most significantly enriched GO terms that clustered under these two categories are summarised in **Figure 5.5 (B)**. Among them, there are pathways involved in the development of tissues and systems of mesendodermal origin or in the response to BMP4 and other growth factors' signalling. Interestingly, the NOTCH pathway also seems to be activated, a finding that is in agreement with research claiming that NOTCH signalling is indispensable during differentiation to any germ layer (Yu et al., 2008). These results indicate that 1hr of BMP4 treatment is sufficient for the activation of pathways associated with mesendoderm.

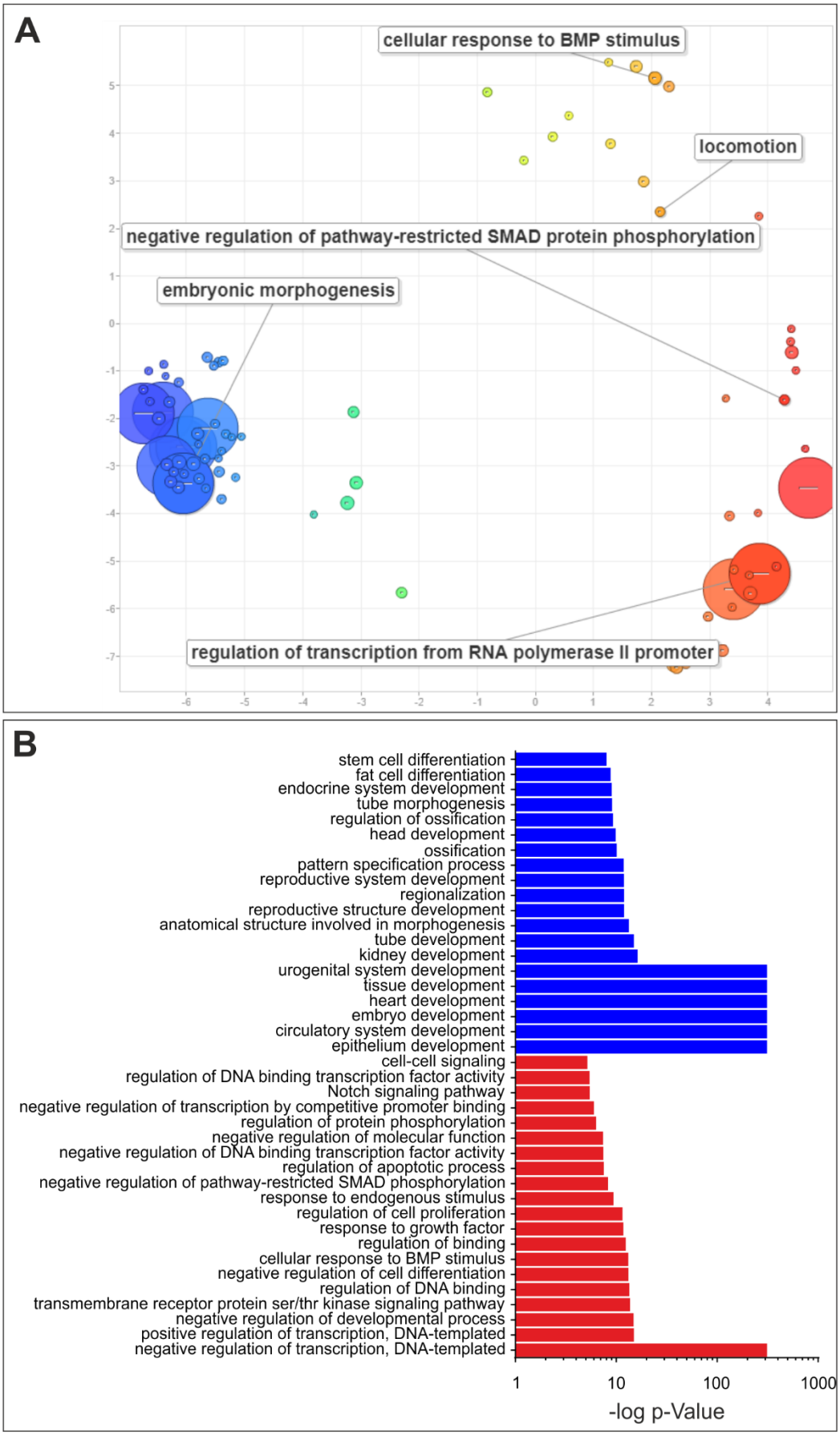

A
cellular response to BMP stimulus
locomotion
negative regulation of pathway-restricted SMAD protein phosphorylation
embryonic morphogenesis
regulation of transcription from RNA polymerase II promoter
B
stem cell differentiation
fat cell differentiation
endocrine system development
tube morphogenesis
regulation of ossification
head development
ossification
pattern specification process
reproductive system development
regionalization
reproductive structure development
anatomical structure involved in morphogenesis
tube development
kidney development
urogenital system development
tissue development
heart development
embryo development
circulatory system development
epithelium development
cell-cell signaling
regulation of DNA binding transcription factor activity
Notch signaling pathway
negative regulation of transcription by competitive promoter binding
regulation of protein phosphorylation
negative regulation of molecular function
negative regulation of DNA binding transcription factor activity
regulation of apoptotic process
negative regulation of pathway-restricted SMAD phosphorylation
response to endogenous stimulus
regulation of cell proliferation
response to growth factor
regulation of binding
cellular response to BMP stimulus
negative regulation of cell differentiation
regulation of DNA binding
transmembrane receptor protein ser/thr kinase signaling pathway
negative regulation of developmental process
positive regulation of transcription, DNA-templated
negative regulation of transcription, DNA-templated
1
10
100
1000
-log p-Value

Figure 5.5: Enriched Biological Pathways (1hr BMP4 – UP transcripts)

(A) Predominantly enriched categories of upregulated biological pathways after 1hr of BMP4 treatment. Transcripts that were upregulated by at least 2-fold were uploaded on WebGestalt database (http://www.webgestalt.org) and overrepresentation enrichment analysis of biological pathways was carried out. The resulting GO terms were run through REVIGO database (http://revigo.irb.hr/) in order to separate the predominant and redundant categories. The size of the clusters is proportional to the p-Value whereas the colours indicate a potential affinity between the pathways. (B) Statistically significant upregulated biological pathways that comprise the subcategories of the clusters depicted in (A).

OR analysis on the same 51 upregulated transcripts revealed several MFs that are significantly enriched. More specifically, there are functions that promote protein dimerization and others that involve DNA or protein binding in order to regulate transcription **Figure 5.6 (A)**. Among the members of the first group, an interesting function enriched is related to TGFβR binding **Figure 5.6 (B)**. The over-represented transcripts involved are BAMBI, INHBB, SMAD6 and SMAD7. BAMBI is known to negatively regulate TGF, Activin and BMP signalling (Lin et al., 2008). INHBB competes with Activin A for the binding to ACVRIIB (Namwanje and Brown, 2016). Proteins SMAD6/7 mitigate TGF, Activin and BMP signalling by competing with SMAD1/5/9 and SMAD2/3 for the binding of SMAD4 (Oshimori and Fuchs, 2012). All the above suggest that in response to BMP4 treatment, cells upregulate transcripts that oppose TGF signalling.

Two KEGG pathways are significantly enriched in response to BMP4 addition. The upregulated transcripts BAMBI, ID1, ID2, ID3, ID4, INHBB, SMAD6, SMAD7 and NOGGIN are implicated in the TGFβ signalling pathway **Figure 5.7 (A)**. Inhibitors of DNA-binding (ID) proteins heterodimerize with bHLH (basic Helix-Loop-Helix) transcription factors to mitigate DNA binding. They have also been reported to promote cardiac mesoderm formation in hES cells (Cunningham et al., 2017). NOGGIN

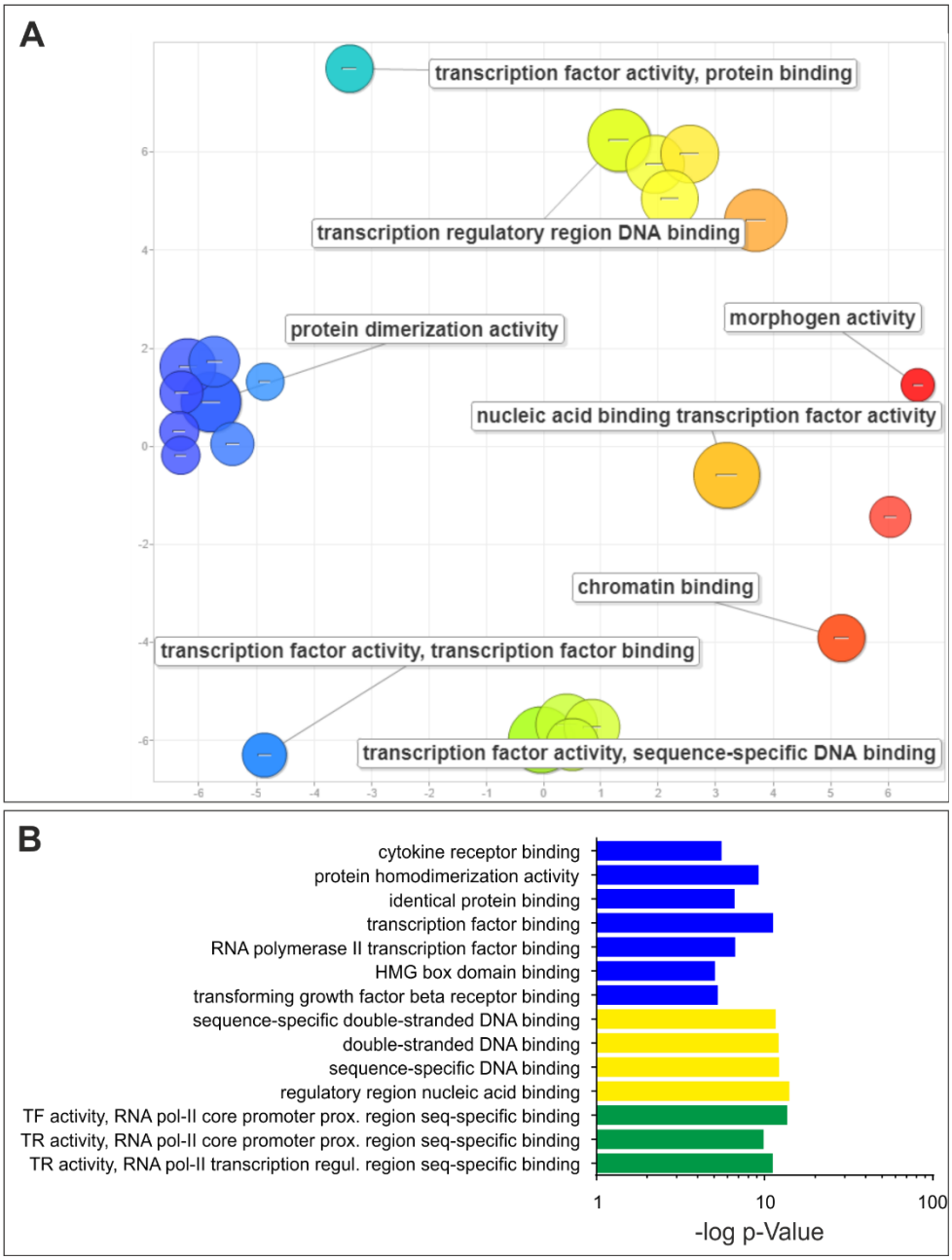


Figure 5.6: Enriched Molecular Functions (1hr BMP4 – UP transcripts)

(A) Predominantly enriched categories of upregulated molecular functions after 1hr of BMP4 treatment. Transcripts that were upregulated by at least 2-fold were uploaded on WebGestalt database (http://www.webgestalt.org) and overrepresentation enrichment analysis of molecular functions was carried out. The resulting GO terms were run through REVIGO database (http://revigo.irb.hr/) in order to separate the predominant and redundant categories. The size of the clusters is proportional to the p-Value whereas the colours indicate a potential affinity between the functions. (B) Statistically significant upregulated molecular functions that comprise the subcategories of the clusters depicted in (A).

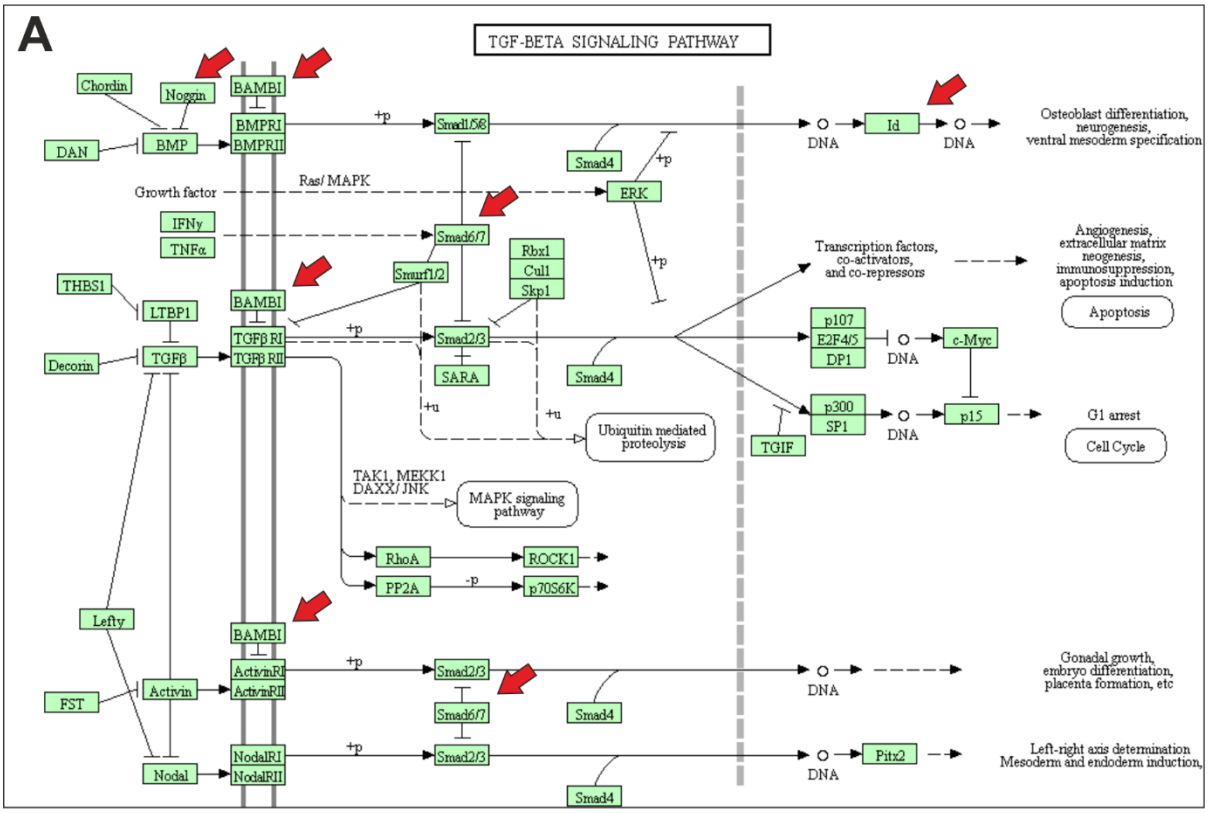
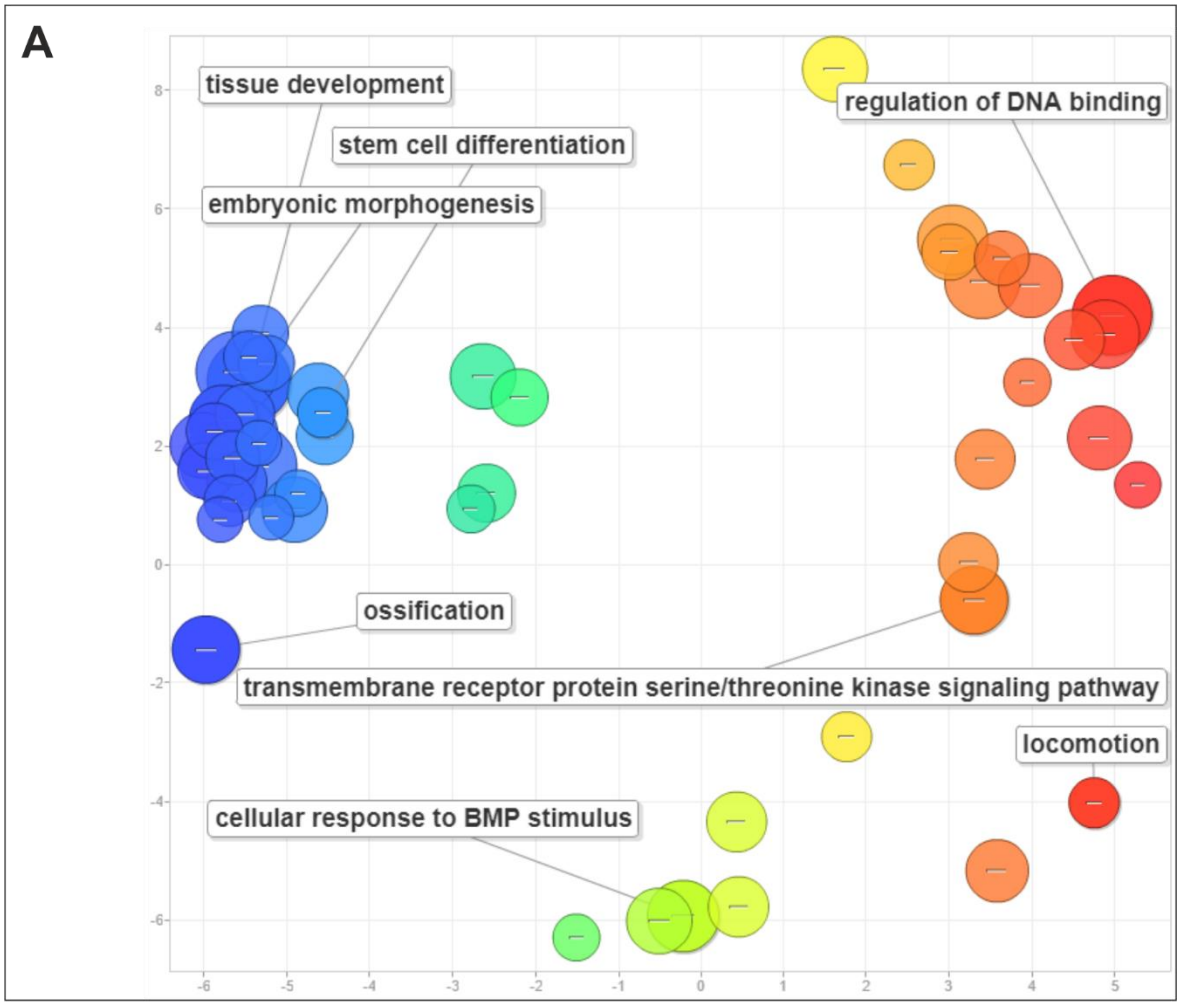

A
TGF-BETA SIGNALING PATHWAY
Chordin
Noggin
BAMBI
DAN
BMP
BMPRI
BMPRII
Smad1/5/8
Id
Osteoblast differentiation, neurogenesis, ventral mesoderm specification
Growth factor
Ras/ MAPK
ERK
Smad4
IFNγ
TNFα
Smad6/7
Rbx1
Cul1
Skp1
Smurf1/2
THBS1
LTBP1
Decorin
TGFβ
TGFβ RI
TGFβ RII
Smad2/3
SARA
Transcription factors, co-activators, and co-repressors
Angiogenesis, extracellular matrix neogenesis, immunosuppression, apoptosis induction
Apoptosis
p107
E2F4/5
DP1
c-Myc
p300
SP1
p15
G1 arrest
Cell Cycle
TGIF
Ubiquitin mediated proteolysis
TAK1, MEKK1
DAXX/ JNK
MAPK signaling pathway
RhoA
ROCK1
PP2A
p70S6K
Lefty
FST
Activin
ActivinRI
ActivinRII
Gonadal growth, embryo differentiation, placenta formation, etc
Nodal
NodalRI
NodalRII
Pitx2
Left-right axis determination
Mesoderm and endoderm induction
B
SIGNALING PATHWAYS REGULATING PLURIPOTENCY OF STEM CELLS
Naive stem cells
Mouse ES cells (mESCs)
Mouse iPS cells (miPSCs)
LIF (mESCs, miPSC)
LIFR
JAK
STAT3
Jak-STAT signaling pathway
Grb2
Mek
Erk1/2
MAPK signaling pathway
PI3K
Akt
Activin
Nodal (mESCs)
ACVRI/II
SMAD2/3
Proliferation
SMAD4
TGFβ signaling pathway
SMADs
BMP4 (mESCs, miPSC)
BMPRI/II
Erk1/2
p38
Wnt signaling pathway
Wnt (mESCs)
Frizzled
Dvl
GSK-3β
Axin
APC
β-catenin
TCF3
TCF1
Klf4
c-Myc
Tbx3
DUSP9
ID
Esrrb
Pluripotency-associated genes
Wnt target genes
Sox2
Nanog
Oct4
Self-renewal
DNA
OCT4, SOX2, and NANOG target genes in human and/or mouse ES cells
Key pluripotency genes
Oct4
Sox2
Nanog
ES cell transcription factors
Stat3
Hesx1
Zic3
Esrrb
ES cell signaling
Tcf3
Fgf2
Lefty2
Skil
Epigenetic regulators
Smarcad1
Myst3
Setdb1
Jarid2
Inhibitor of neurogenesis
Rest
Telomere-associated protein
Rif1
Totipotency
Pluripotency
Multipotency
Unipotency
(In vitro)
iPS cells
(In vivo)
Zygote
Blastocyst
Epiblast
Somatic stem cells
Functional differentiated cells
EpiS cells
Differentiated somatic cells
ES cells
In vitro-derived somatic stem cells
Primodial germ cells
Sperm and oocytes
Pluripotency maintenance
PcG
Ectoderm development
Pax6
Meis1
Hoxb1
Lhx5
Otx1
Neurog1
Mesoderm development
Hand1
Dlx5
Myf5
Onecut1
Endoderm development
Isl1
Atbf1
Extra-embryonic development
Esx1
Primed stem cells
Human ES cells (hESCs)
Human iPS cells (hiPSCs)
Mouse EpiS cells (mEpiSCs)
BMP4 (hESCs, hiPSC, mEpiSCs)
Activin
Nodal (hESCs, hiPSC, mEpiSCs)
FGF2 (hESCs, hiPSC, mEpiSCs)
FGFR
Ras
Raf
IGF (hESCs)
IGF-IR
PI3K-Akt signaling pathway
Core transcriptional network

Figure 5.7: Deregulated KEGG Pathways (1hr BMP4 – UP transcripts)

Transcripts that were upregulated by at least 2-fold after 1hr of BMP4 treatment, were uploaded on WebGestalt database (http://www.webgestalt.org) and overrepresentation enrichment analysis of KEGG pathways was carried out. The TGFβ (A) and the stem cell pluripotency signalling pathways (B) came up as being significantly altered. The pathways were run through Genome database (http://www.genome.jp) for visualisation and the upregulated transcripts were annotated with red arrows.

Is a secreted polypeptide that antagonizes BMP signalling by acting directly on the ligand (McMahon et al., 1998). All that taken together suggest that the TGF signalling pathway is negatively regulated in response to BMP4 induction. The second enriched KEGG pathway involves the regulatory signalling of pluripotency in stem cells. Along with the ID proteins and INHBB, transcripts KLF4 and HAND1 also appear to be upregulated in response to BMP4 **Figure 5.7 (B)**. KLF4 has been shown to regulate the expression of the pluripotency related gene NANOG (Chan et al., 2009) and HAND1 to be indispensable during mesoderm development (Richter et al., 2014).

After 4hrs of BMP4 treatment, 143 transcripts were found to be significantly upregulated. The GO terms revealed from the OR analysis clustered into three significantly enriched categories of BPs. These are embryonic morphogenesis, regulation of DNA binding and cellular response to BMP stimulus **Figure 5.8 (A)**. The most significantly enriched GO terms that clustered under these two categories are summarised in **Figure 5.8 (B)**. Among them, there are pathways involved in heart, muscle and skeletal tissue development. Interestingly, components of the WNT pathway are also enriched in response to BMP4 stimulation. That fact can be attributed to the action of FGF2, which is also present in the Activin A based mTeSR, and in


A
tissue development
stem cell differentiation
embryonic morphogenesis
regulation of DNA binding
ossification
transmembrane receptor protein serine/threonine kinase signaling pathway
locomotion
cellular response to BMP stimulus
8
6
4
2
0
-2
-4
-6
-6
-5
-4
-3
-2
-1
0
1
2
3
4
5

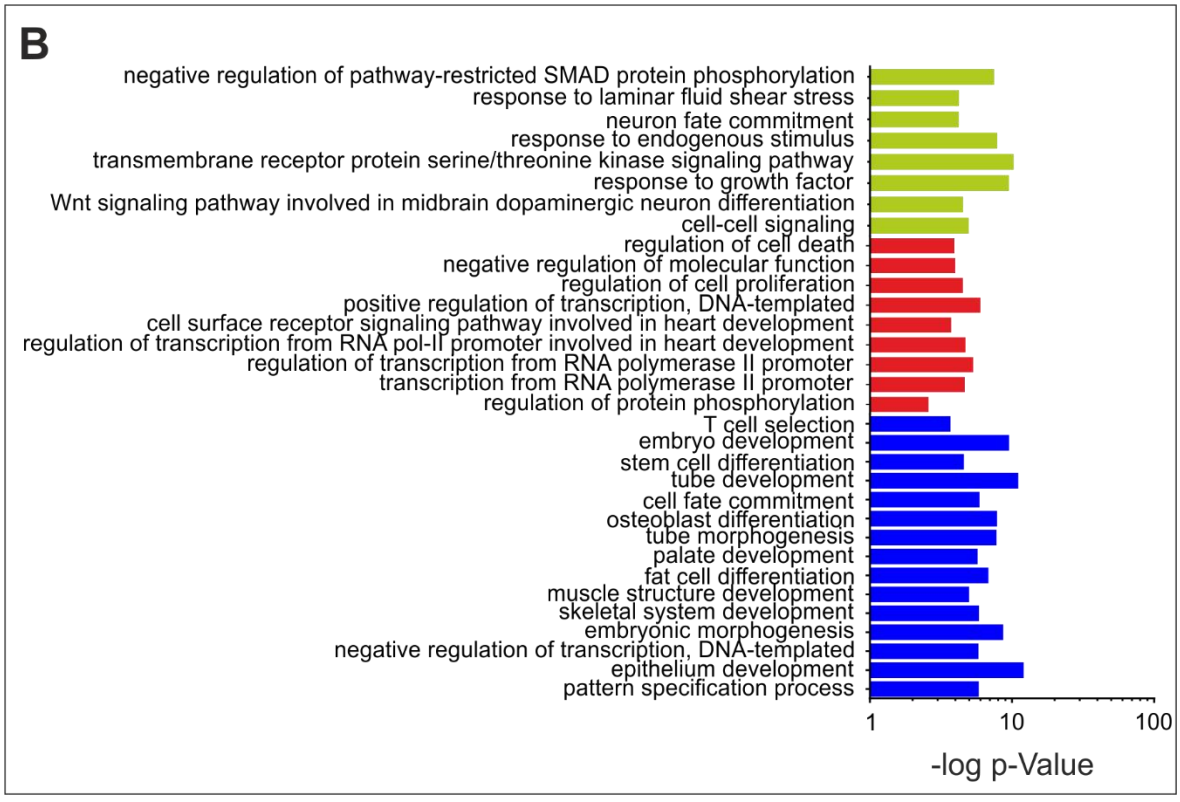

B
negative regulation of pathway-restricted SMAD protein phosphorylation
response to laminar fluid shear stress
neuron fate commitment
response to endogenous stimulus
transmembrane receptor protein serine/threonine kinase signaling pathway
response to growth factor
Wnt signaling pathway involved in midbrain dopaminergic neuron differentiation
cell-cell signaling
regulation of cell death
negative regulation of molecular function
regulation of cell proliferation
positive regulation of transcription, DNA-templated
cell surface receptor signaling pathway involved in heart development
regulation of transcription from RNA pol-II promoter involved in heart development
regulation of transcription from RNA polymerase II promoter
transcription from RNA polymerase II promoter
regulation of protein phosphorylation
T cell selection
embryo development
stem cell differentiation
tube development
cell fate commitment
osteoblast differentiation
tube morphogenesis
palate development
fat cell differentiation
muscle structure development
skeletal system development
embryonic morphogenesis
negative regulation of transcription, DNA-templated
epithelium development
pattern specification process
1
10
100
-log p-Value

Figure 5.8: Enriched Biological Pathways (4hrs BMP4 – UP transcripts)

(A) Predominantly enriched categories of upregulated biological pathways after 4hrs of BMP4 treatment. Transcripts that were upregulated by at least 2-fold were uploaded on WebGestalt database (http://www.webgestalt.org) and overrepresentation enrichment analysis of biological pathways was carried out. The resulting GO terms were run through REVIGO database (http://revigo.irb.hr/) in order to separate the predominant and redundant categories. The size of the clusters is proportional to the p-Value whereas the colours indicate a potential affinity between the pathways. (B) Statistically significant upregulated biological pathways that comprise the subcategories of the clusters depicted in (A).

concert with BMP4 leads to the upregulation of primitive streak related transcripts (Yu et al., 2011).

Three major clusters of MFs emerged by performing OR analysis on the 143 transcripts that are upregulated following 4hrs of BMP4 addition. These involve transcription factor or sequence specific DNA binding and RNA polymerase II transcription factor activity **Figure 5.9 (A)**. Among the members of the first group, two interesting functions enriched are related to TGFβR and FRIZZLED binding **Figure 5.9 (B)**. The former function is conserved between the two time points of BMP4 induction and consists of the same upregulated transcripts. That fact suggests that negative regulation of the TGF pathway may be an important step during the early differentiation stages following BMP4 addition. On the other hand, FRIZZLED binding is only enriched as a function after 4hrs of BMP4 induction. Above, we showed that WNT pathway components are also upregulated at the same time point. Taken together, all the above suggest that WNT signalling is a secondary response to BMP4 treatment, as it is activated only in the late time points of differentiation.

The KEGG pathways significantly enriched are the same between the two BMP4 induction time points. However, the regulatory signalling of pluripotency in stem

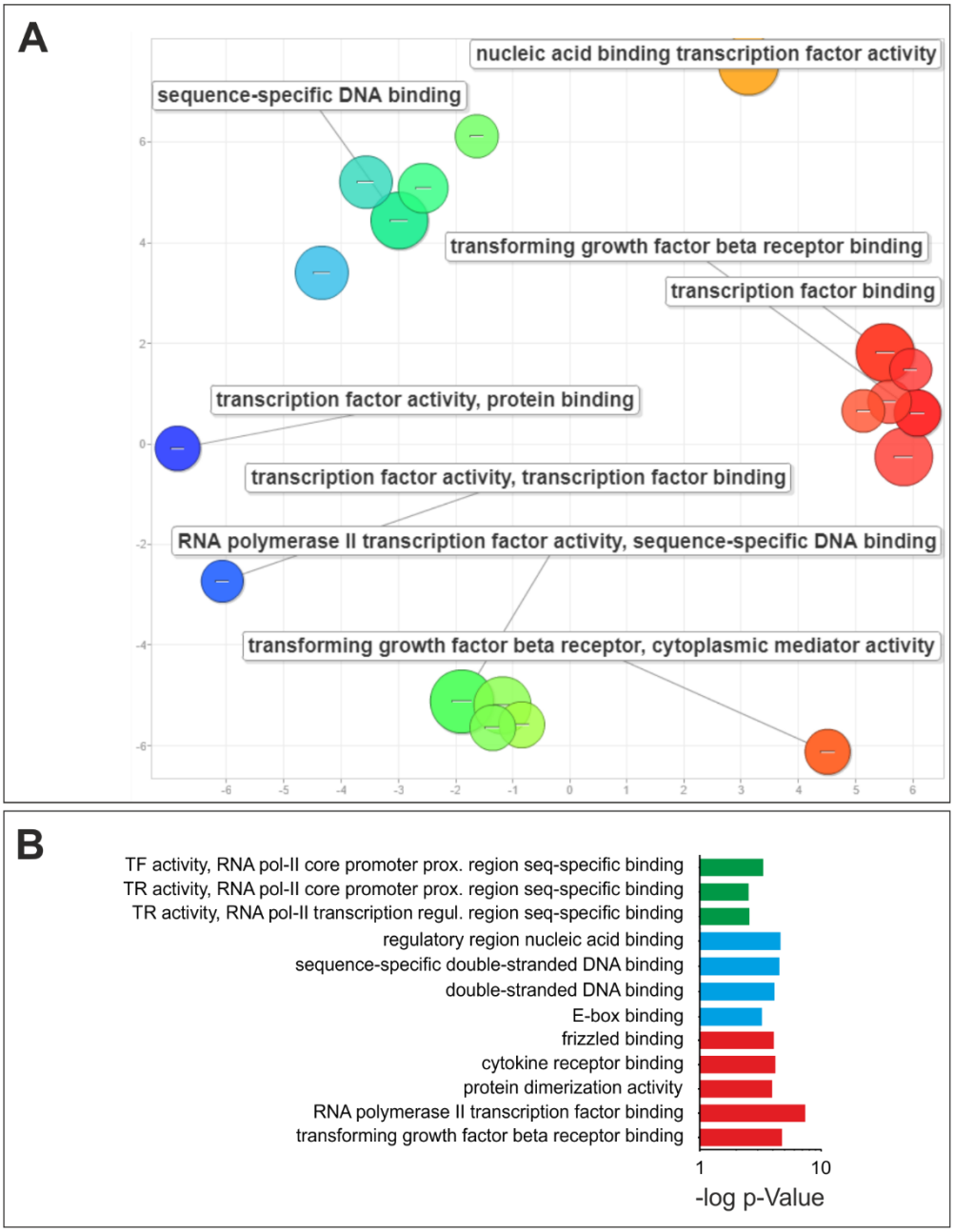
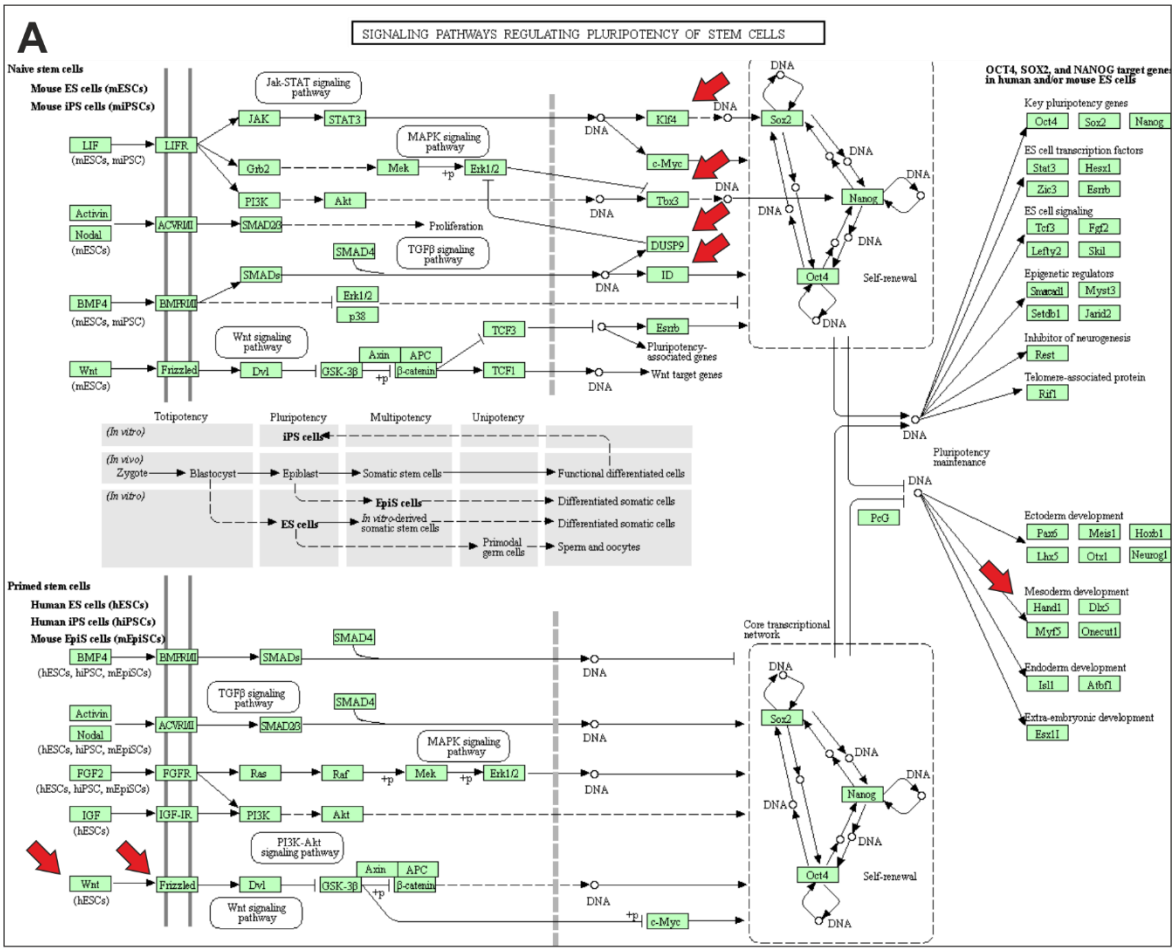


Figure 5.9: Enriched Molecular Functions (4hrs BMP4 – UP transcripts)

(A) Predominantly enriched categories of upregulated molecular functions after 4hrs of BMP4 treatment. Transcripts that were upregulated by at least 2-fold were uploaded on WebGestalt database (http://www.webgestalt.org) and overrepresentation enrichment analysis of molecular functions was carried out. The resulting GO terms were run through REVIGO database (http://revigo.irb.hr/) in order to separate the predominant and redundant categories. The size of the clusters is proportional to the p-Value whereas the colours indicate a potential affinity between the functions. (B) Statistically significant upregulated molecular functions that comprise the subcategories of the clusters depicted in (A).


A
SIGNALING PATHWAYS REGULATING PLURIPOTENCY OF STEM CELLS
Naive stem cells
Mouse ES cells (mESCs)
Mouse iPS cells (miPSCs)
LIF
(mESCs, miPSC)
LIFR
JAK
STAT3
Jak-STAT signaling pathway
Grb2
Mek
Erk1/2
MAPK signaling pathway
PI3K
Akt
Activin
Nodal
(mESCs)
ACVRIIB
SMAD2/3
Proliferation
SMAD4
TGFβ signaling pathway
BMP4
(mESCs, miPSC)
BMPRIB
SMADs
Erk1/2
p38
Wnt
(mESCs)
Frizzled
Dvl
Wnt signaling pathway
GSK-3β
Axin
APC
β-catenin
TCF3
TCF1
Klf4
c-Myc
Tbx3
DUSP9
ID
Esrrb
Pluripotency-associated genes
Wnt target genes
DNA
Sox2
Nanog
Oct4
Self-renewal
OCT4, SOX2, and NANOG target genes in human and/or mouse ES cells
Key pluripotency genes
Oct4
Sox2
Nanog
ES cell transcription factors
Stat3
Hesx1
Zic3
Esrrb
ES cell signaling
Tcf3
Fgf2
Lefty2
Skil
Epigenetic regulators
Smarcad1
Myst3
Setdb1
Jarid2
Inhibitor of neurogenesis
Rest
Telomere-associated protein
Rif1
Totipotency
Pluripotency
Multipotency
Unipotency
(In vitro)
iPS cells
(In vivo)
Zygote
Blastocyst
Epiblast
Somatic stem cells
Functional differentiated cells
EpiS cells
Differentiated somatic cells
ES cells
In vitro-derived somatic stem cells
Primordial germ cells
Sperm and oocytes
Pluripotency maintenance
PcG
Ectoderm development
Pax6
Meis1
Hoxb1
Lhx5
Otx1
Neurog1
Mesoderm development
Hand1
Dlx5
Myf5
Onecut1
Endoderm development
Isl1
Afbp1
Extra-embryonic development
Esx1l
Primed stem cells
Human ES cells (hESCs)
Human iPS cells (hiPSCs)
Mouse EpiS cells (mEpiSCs)
(hESCs, hiPSC, mEpiSCs)
(hESCs)
FGF2
FGFR
Ras
Raf
IGF
IGF-IR
PI3K-Akt signaling pathway
Core transcriptional network

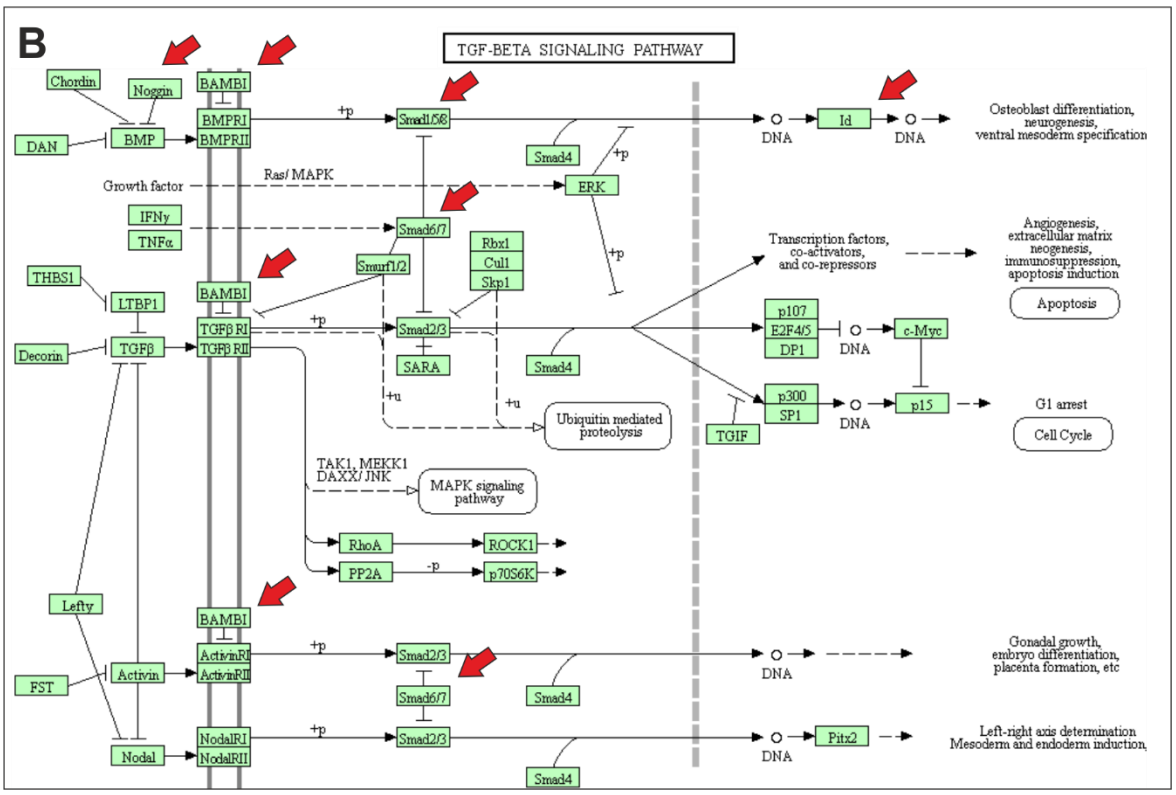
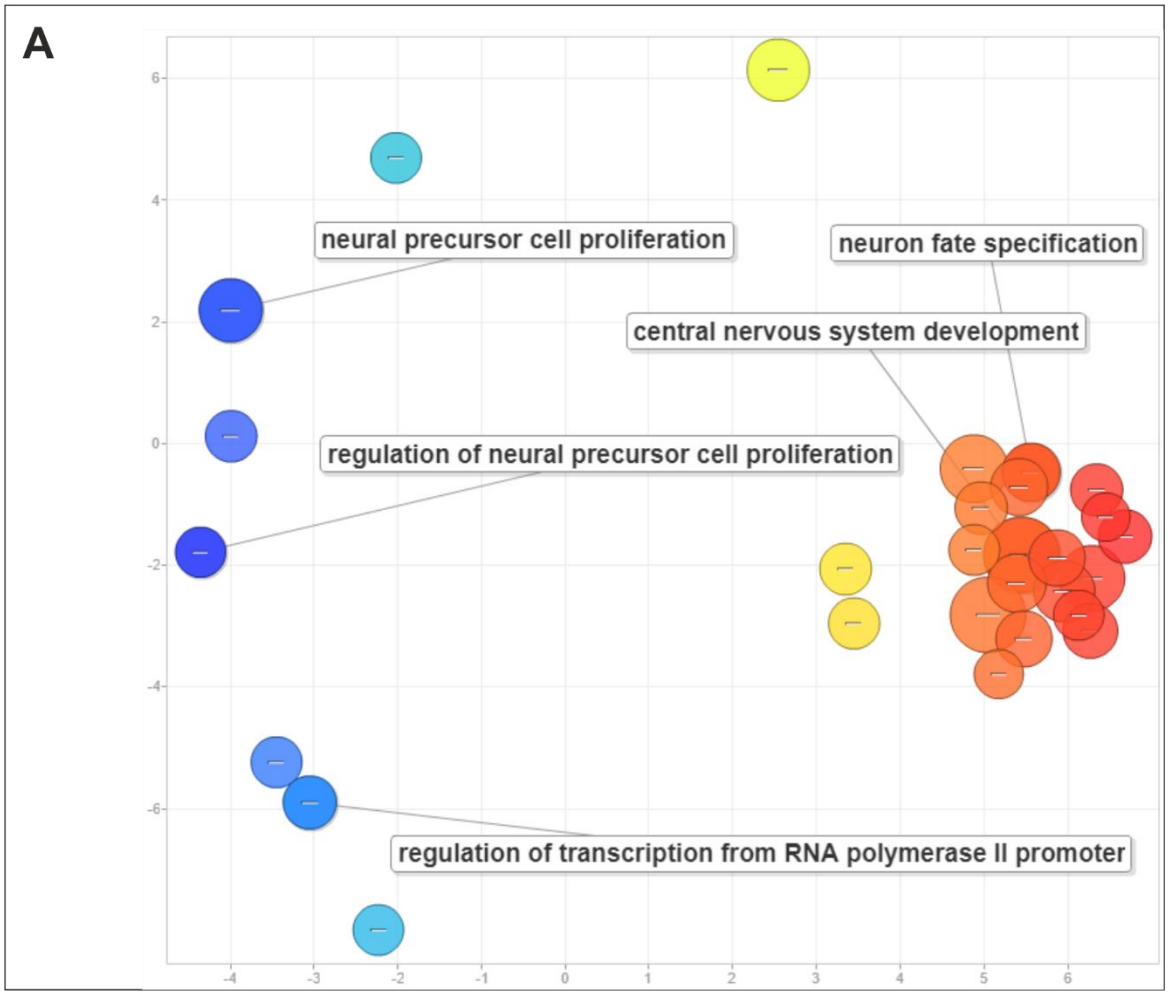

B
TGF-BETA SIGNALING PATHWAY
Chordin
Noggin
DAN
BMP
BAMBI
BMPRI
BMPRII
Smad1/5/8
Smad4
Id
DNA
Osteoblast differentiation, neurogenesis, ventral mesoderm specification
Growth factor
Ras/ MAPK
ERK
IFNγ
TNFα
Smad6/7
Smurf1/2
Rbx1
Cul1
Skp1
THBS1
LTBP1
Decorin
TGFβ
TGFβ RI
TGFβ RII
SARA
Transcription factors, co-activators, and co-repressors
Angiogenesis, extracellular matrix neogenesis, immunosuppression, apoptosis induction
Apoptosis
p107
E2F4/5
DP1
c-Myc
p300
SP1
p15
TGIF
G1 arrest
Cell Cycle
Ubiquitin mediated proteolysis
TAK1, MEKK1
DAXX/ JNK
MAPK signaling pathway
RhoA
ROCK1
PP2A
p70S6K
Lefty
FST
Activin
ActivinRI
ActivinRII
Nodal
NodalRI
NodalRII
Gonadal growth, embryo differentiation, placenta formation, etc
Pitx2
Left-right axis determination
Mesoderm and endoderm induction

Figure 5.10: Deregulated KEGG Pathways (4hrs BMP4 – UP transcripts)

Transcripts that were upregulated by at least 2-fold after 4hrs of BMP4 treatment, were uploaded on WebGestalt database (http://www.webgestalt.org) and overrepresentation enrichment analysis of KEGG pathways was carried out. The stem cell pluripotency (A) and the TGFβ signalling pathways (B) came up as being significantly altered. The pathways were run through Genome database (http://www.genome.jp) for visualisation and the upregulated transcripts were annotated with red arrows.

cells pathway is comprised of a higher number of members. In addition to the transcripts mentioned above, DUSP9, FGFR3, WNT3 and FZD1 are also upregulated **Figure 5.10 (A)**. DUSP9 and FGFR3 are members of the FGF/ERK signalling pathway. In mES cells DUSP9 has been found to reduce ERK phosphorylation in response to BMP4 signalling (Li et al., 2012). In hES cells, DUSP6 has been reported to attenuate ERK phosphorylation which leads to prolonged NANOG expression during BMP4 induction. That switches the outcome of differentiation to mesendoderm (Yu et al., 2011). However, very little is known about the role of DUSP9 in hES cell signalling. Last, as expected the KEGG pathway involving TGF signalling consisted of the same transcripts that remained upregulated for both BMP4 time points **Figure 5.10 (B)**.

Above we reported the enriched BPs, MFs and KEGG pathways following BMP4 addition after 1hr or 4hrs taking into account the upregulated transcripts. However, a considerable number of transcripts was significantly downregulated following treatment. More specifically, 17 were downregulated after the first and 36 after the second time point. Due to the small number of candidates, for most cases, OR analysis failed to provide a sufficient number of GO terms that would cluster into subcategories. Nevertheless, we obtained a cluster of BPs enriched after 4hrs of BMP4 addition, with pathways implicated mainly in neural differentiation **Figure 5.11 (A), (B)**.


A
neural precursor cell proliferation
neuron fate specification
central nervous system development
regulation of neural precursor cell proliferation
regulation of transcription from RNA polymerase II promoter
6
4
2
0
-2
-4
-6
-4
-3
-2
-1
0
1
2
3
4
5
6

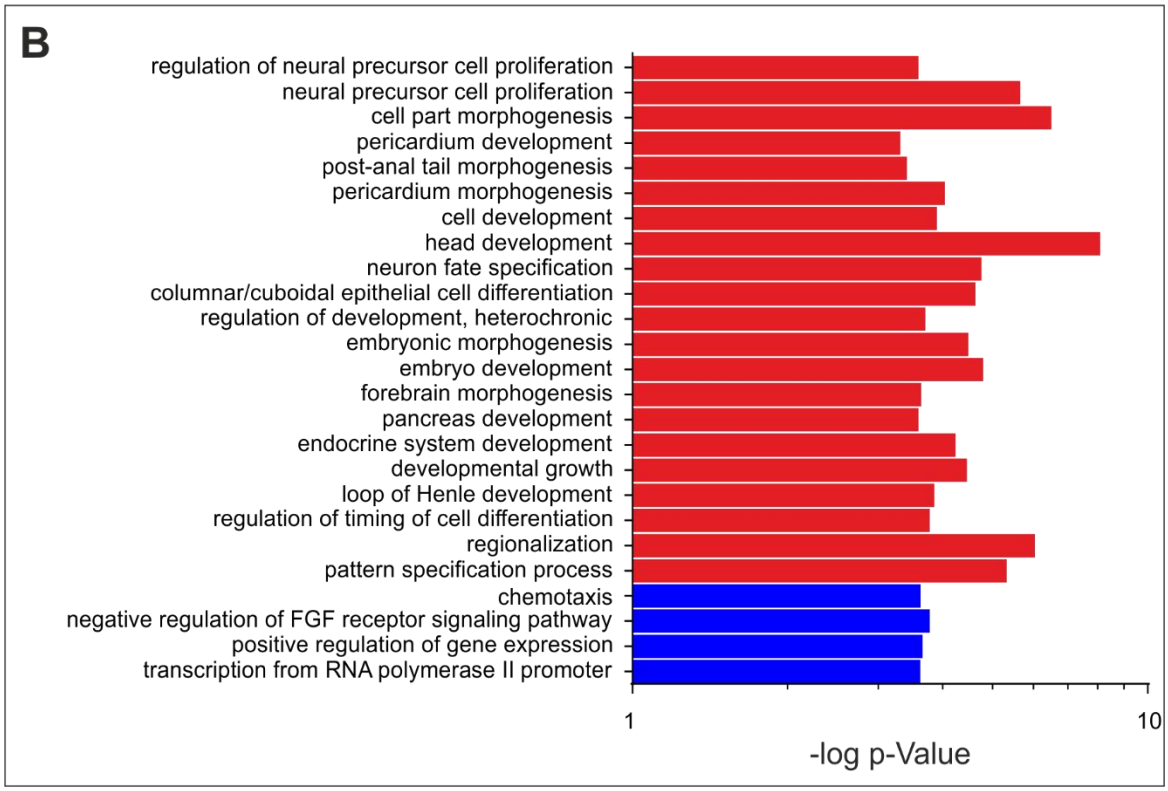

B
regulation of neural precursor cell proliferation
neural precursor cell proliferation
cell part morphogenesis
pericardium development
post-anal tail morphogenesis
pericardium morphogenesis
cell development
head development
neuron fate specification
columnar/cuboidal epithelial cell differentiation
regulation of development, heterochronic
embryonic morphogenesis
embryo development
forebrain morphogenesis
pancreas development
endocrine system development
developmental growth
loop of Henle development
regulation of timing of cell differentiation
regionalization
pattern specification process
chemotaxis
negative regulation of FGF receptor signaling pathway
positive regulation of gene expression
transcription from RNA polymerase II promoter
1
10
-log p-Value

Figure 5.11: Enriched Biological Pathways (4hrs BMP4 – DOWN transcripts)

(A) Predominantly enriched categories of downregulated biological pathways after 4hrs of BMP4 treatment. Transcripts that were downregulated by at least 2-fold were uploaded on WebGestalt database (http://www.webgestalt.org) and overrepresentation enrichment analysis of biological pathways was carried out. The resulting GO terms were run through REVIGO database (http://revigo.irb.hr/) in order to separate the predominant and redundant categories. The size of the clusters is proportional to the p-Value whereas the colours indicate a potential affinity between the pathways. (B) Statistically significant downregulated biological pathways that comprise the subcategories of the clusters depicted in (A).

5.3 Discussion

In the present chapter we established a novel, Activin A –based system for the culture of hES cells. H1 cells maintained in this system: (1) Express pluripotency factors NANOG and OCT4 at appropriate levels, (2) demonstrate an unaltered, normal karyotype and (3) retain the capacity to form teratomas, *in vivo*. Utilizing this novel culture system, we performed RNA sequencing to identify novel transcripts that are altered in response to BMP4 stimulation. The results of the assay indicated that: (1) Primary responses to BMP4 (1hr) induction include upregulation of BMP inhibitors and (2) initiation of mesoderm differentiation. (3) Later responses to BMP4 (4hr) include activation of WNT components and (4) suppression neural differentiation.

Early responses of H1 cells to BMP4 stimulation (1hr) demonstrated a negative feedback loop that opposes BMP4 signalling. This seemingly contradictory result is in complete agreement with research showing that BMP inhibitors are syn-expressed with ligands during development and modulate BMP-related embryonic patterning. More specifically, in *Drosophila* embryos, BMPs collaborate with Sog, a BMP inhibitor, and Tld, a protease that cleaves Sog, to modulate development of the dorso-ventral axis (Eldar et al., 2002). In *Xenopus*, development of the same axis is self-regulated by BMP levels. Low ligand concentration leads to the expression of BMP agonist ADMP, whereas increased levels upregulate the antagonist Crossveinless-2 (Ambrosio et al., 2008). BMP4-induced upregulation of BAMBI, and SMAD6/7 has been correlated with a dynamic output to different ligand doses. Knock-down of BAMBI in *Xenopus* embryos, reduced the expression range of developmental genes ventx1/2, causing them to saturate under lower ligand concentrations (Paulsen et al., 2011).

Research around BMP4 inhibitors in the context of hES cells is very limited. A recent study demonstrated that stimulation with BMP4 was sufficient to differentiate hES cells, cultured in micro-patterned surfaces, towards all the germ layers (Warmflash et al., 2014). In the same culture system, NOGGIN was shown to be upregulated in response to BMP4 induction and confine SMAD1 phosphorylation to the colony edges (Etoc et al., 2016). Our results verified NOGGIN upregulation in response to BMP4 and pinpointed the inhibitor to be upregulated after 1hr of BMP4 stimulation. Moreover, we have identified CER1 and GREM1 as transcripts directly regulated by BMP4, as well. Both factors are BMP antagonists that bind ligands and prohibit their association with receptors. Interestingly, CER1 is known to be regulated by WNT signalling (Katoh and Katoh, 2006). This is in agreement with our results that show CER1 to be downregulated in the later timepoint of BMP4 addition, coinciding with the upregulation of WNT components.

Furthermore, 4hrs of BMP4 stimulation was shown to activate the WNT pathway which is indispensable for the progression of mesoderm differentiation. Recent research demonstrated that in the presence of FZ8CRD, the soluble domain of FRIZZLED which binds and sequesters WNT ligands, BMP4 stimulation failed to upregulate MSX1 or BRACHYURY. Additionally, induction of hES cells with BMP4 in the presence of IWP2, a specific inhibitor of WNT ligand synthesis, lead to limited expression of the above mesodermal markers even though the BMP pathway was active, as verified by upregulation of its direct target gene *ID1* (Kurek et al., 2015). These results suggest that BMP4 activates WNT by stimulating the expression of endogenous ligands with differentiation progression relying on WNT thereafter. In agreement with the data above, WNT3 and WNT3A were found to be significantly

upregulated after 4hrs of BMP4 induction. In the present study we provide further evidence supporting that BMP4 activates endogenous WNT components to drive mesoderm differentiation. Also, we pinpoint for the first time the exact timepoint of WNT signalling initiation in response to BMP4 induction.

The limited number of downregulated transcripts post BMP4 treatment impeded the identification of negatively regulated pathways. Nevertheless, we did identify a cluster of transcripts that included OLIG3, PAX6 and POU3F2 which have been characterized as factors indispensable for neuron development, (Urban et al., 2015). Antagonism of neural specification by BMP signalling is a well characterised event during embryo patterning of different organisms, reviewed in: (Zirra et al., 2016) and several differentiation protocols rely on BMP inhibitors to drive hES cells towards that germ layer (Xu et al., 2011; Greber et al., 2011; Lupo et al., 2013). Experiments in mES cells demonstrated that BMP4 stimulation inhibits neural differentiation through upregulation of IDs, which are direct targets of BMP4 known to antagonise bHLH transcription factors in the central nervous system (Ying et al., 2003). In addition, a study in hES cells showed that neuroectodermal differentiation by NOGGIN-mediated inhibition of BMP signalling lead to downregulation of ID1 and ID2 proteins (Gerrard et al., 2005). The data above suggest the existence of a common mechanism of neuroectodermal inhibition that relies on BMP4 signalling.

Our results indicate that downregulation of neuroectodermal transcripts post 4hrs of BMP4 stimulation follow the activation of ID1/2/3/4 transcripts, which occurs as early as 1hr of treatment. At the later timepoint we also witness upregulation of DUSP9, a phosphatase that inhibits FGF signalling by de-phosphorylating ERK. In addition, chemical inhibition of FGF/ERK signalling has been shown to attenuate neural

differentiation by downregulating transcripts like SIX3 and PAX6 (Na et al., 2010). Therefore we hypothesize a mechanism that includes upregulation of ID proteins in combination with inhibition of FGF signalling to prevent neuroectodermal differentiation post BMP4 stimulation. To the best of our knowledge, this is the first study identifying the timepoint when cells deviate from pluripotency to a binary fate state. Further experiments should verify whether this is a reversible process.

CHAPTER 6

CONCLUSIONS AND FUTURE DIRECTIONS

In the present thesis we attempted to decipher the molecular mechanisms that regulate pluripotency and differentiation in hES cells. Scientific literature suggests that these processes are tightly modulated by a complex network of signalling factors in which TGFβ superfamily possesses a prominent role. The outcome of TGFβ signalling is subject to regulation at multiple levels, including internalisation route and subsequent intracellular trafficking of ligand/receptor complexes. Even though a plethora of different molecules is involved in regulating both processes, we focused on ARF6, a GTPase with undocumented roles in hES cells and TGFβ superfamily signalling.

In chapter 3 we discovered a novel implication of ARF6 in intracellular TGFβ superfamily signalling. Pilot experiments indicated an interaction of ARF6-GTP with SMAD4. This interaction was verified and mapped to a domain within the last 43 amino acids of SMAD4 C-terminal tail. Comparing the same domain of SMAD4 with SMAD2/3 proteins we observed 50% and 57% identity, respectively. In addition, a highly conserved 6 amino acid domain (T-P-C-W-I-E) is present in all SMADs. Therefore, we hypothesised that ARF6 might interact with SMAD2/3 and validated this with pull-down and immunoprecipitation assays. While exploring the significance of this interaction, we concluded that overexpression of hydrolysis resistant and fast-cycling mutants of ARF6 leads to increased SMAD2/3 phosphorylation. As expected, ARF6 knock-down yielded the opposite results. Effects of TGFβ signalling on ARF6 cycling were also investigated. In response to activating cells with Activin A or TGFβ we showed that ARF6 is hydrolyzed by SMAP1, an ARF6GAP that interacts with wild-type ACVR1B as

well as Clathrin heavy chains. Interestingly, in the absence of SMAP1, ARF6 appears to be activated in response to the same stimulation. Based on our and previous data, we propose the following model of ARF6 involvement in Activin A signalling **Figure 6.1**.

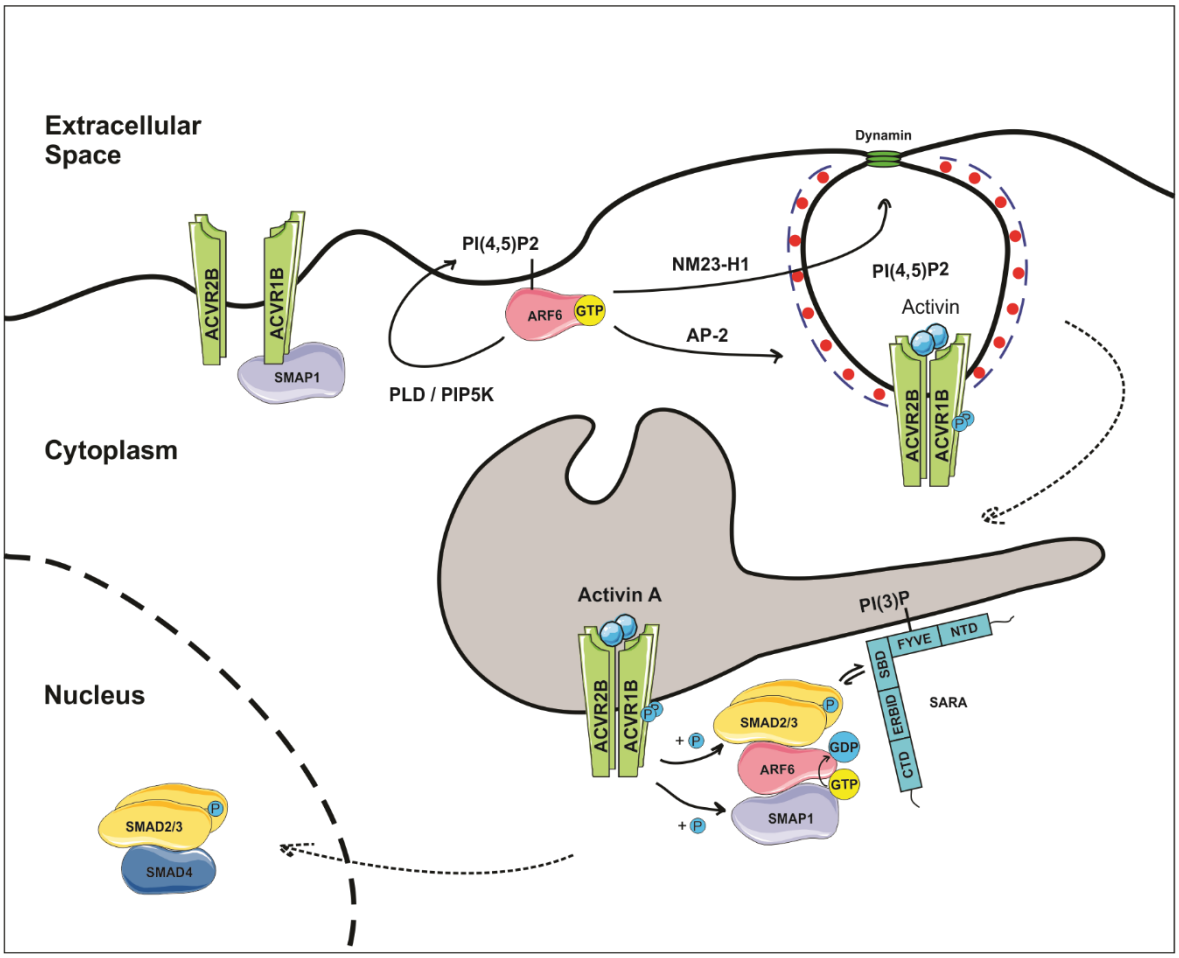


Figure 6.1: Proposed Model

ARF6-GTP stimulates CME of Activin A receptors by activating PLD and PIP5K to produce PI(4,5)P2 and recruiting AP-2 and NM23-H1 which promote formation of the Clathrin-coated pit and Dynamin-dependent vesicle fission, respectively. In the absence of ligand type I receptor ACVR1B is not phosphorylated and is associated with ARF6GAP, SMAP1. However, upon formation of the ligand-receptors complex, constitutive kinase ACVR2B phosphorylates ACVR1B releasing SMAP1 which is probably responsible for ARF6-GTP hydrolysis. As SMAD2/3/4 and pSMAD2/3 bind only ARF6-GTP, inactivation of the GTPase triggers SMAD dissociation from ARF6 and may facilitate their nuclear translocation. In addition, Activin A/ACVR2B/ACVR1B induced phosphorylation of SMAD2/3 causes their dissociation from the SBD of SARA. Whether there is cross-talk between ARF6-GTP and SARA bound SMADs is unclear.

Analysis of results presented in chapter 3, in combination with current literature investigation suggests that there are several unexplored directions that might further implicate ARF6 in TGFβ superfamily signalling. First of all, repeating the pull-down and immunoprecipitation assays between ARF6 and a mutated SMAD4 version that lacks the 6 amino acid domain (T-P-C-W-I-E) mentioned above should abolish the interaction. Furthermore, comparing the C-terminal tails of SMAD4 with SMAD1/5/9 we observed an even greater identity (62.5% vs 56.2%) than with SMAD2/3. Also, the same 6 amino acid domain is present in SMAD1/5/9, as well. Therefore, carrying out pull-down and immunoprecipitation assays between ARF6 and the C-terminal tails of SMAD1/5/9 should yield an interaction. Given that ARF6 activation and knock-down affected SMAD1/5/9 phosphorylation in hES cells, we anticipate similar effects in HEK-293 cells, as well. Furthermore, in section 3.3 we suggested a mechanism of pSMAD2/3 cytoplasmic sequestration by activated ARF6. Analysis of the localisation of phosphorylated SMADs in the presence of activated ARF6 by confocal microscopy should validate this hypothesis. The mechanism of ARF6 inactivation in response to TGFβ stimulation should also be examined. Comparing the kinase domain of ACVR1B and TGFβR1 we observed 90% identity. Therefore, co-immunoprecipitation of TGFβR1 with SMAP1 should indicate whether the mechanism of ARF6 inactivation is the same. Provided that ARF6 is implicated in BMP signalling, the same assay should be repeated between SMAP1 and BMPR1A, BMPR1B and ACVR1, as the kinase domains of type I BMP receptors exhibit a 60%, 64% and 65% identity to ACVR1B, respectively. Additionally, the mechanism of SMAP1 dissociation from the receptor in response to TGFβ signalling should also be investigated. Since SMAP1 includes two adjacent serine and threonine residues known to be phosphorylated, type I TGFβ

receptors might be responsible for this event (Olsen et al., 2010). Immunoprecipitation of SMAP1 and ACVR1B in Activin A stimulated and control cells in combination with subsequent mass spectrometry of the interactome should reveal whether ACVR1B phosphorylates SMAP1, causing its dissociation. Alternatively, mutation of the above residues of SMAP1 should limit its capacity to interact with wild-type ACVR1B. Last, activation of ARF6 by Activin A or TGFβ stimulation in the absence of SMAP1 suggests that a GEF might also be implicated. Knocking-down ARF6 GEFs in SMAP1KO cells and repeating the pull-down assay should indicate which is implicated in the pathway.

In chapter 4 we have uncovered an undocumented role for ARF6 in the major signalling pathways regulating pluripotency and differentiation of hES cells. Relying on the output of experiments conducted in HEK-293 cells, we generated stable hES cell lines with fast-cycling ARF6 and CRISPR knock-outs in order to study the effect of the GTPase in TGFβ signalling. Conclusions drawn from these assays indicated that activation of ARF6 in the presence of Activin A leads to increased SMAD2/3 phosphorylation. Interestingly, ARF6 activation also increased the BMP4-induced SMAD1/5/9 phosphorylation. As expected, ARF6 knock-out yielded the opposite results. In addition, perturbing ARF6 in hES cells affects mesendoderm specification. This was demonstrated by differentiating the above cell lines with Activin A and BMP4 and evaluating the expression of primitive streak marker BRACHYURY. Activation of ARF6 lead to decreased BRACHYURY expression, while knock-out of the GTPase had the exact opposite trend. Last, stimulation with either ligand resulted in ARF6 hydrolysis, suggesting a conserved mechanism between HEK-293 and hES cells.

There is a vast number of scientific publications concerned with the biology of ARF6 in both physiological and pathological conditions. However, this is the first study

outlining a clear role of the GTPase in TGFβ signalling and hES cells. Therefore, the cell lines generated and characterized in the present thesis will prove invaluable in determining potential implications of ARF6 in pluripotency and differentiation. Given the effect of ARF6 on BRACHYURY expression during mesendoderm specification and literature suggesting that its ablation is detrimental during liver formation in mice, we hypothesize additional effects during endoderm and mesoderm differentiation (Suzuki et al., 2006). Further experiments should include a broad transcriptomics approach to uncover deregulated transcripts during differentiation towards the above germ layers using these cell lines. The same approach can also be utilised in pluripotent conditions using wild-type cells as control, in order to investigate potentially affected pathways. Furthermore, in sections 3.3 and 4.3 we suggested a mechanism of cytoplasmic sequestration of phosphorylated SMADs by activated ARF6. This mechanism adequately explains how increased phosphorylation leads to decreased BRACHYURY expression. In order to verify this hypothesis, localisation of phosphorylated SMADs should be investigated by confocal microscopy after ligand stimulation in the above cell lines. Furthermore, as ARF6 is implicated in internalisation and trafficking processes, we would expect differences in the intracellular trafficking of TGFβ ligands and receptors in the above cell lines. Tracking the fate of fluorescently labelled Activin A / BMP4 and their receptors by confocal and video microscopy should uncover these differences. Activation of ARF6 has also been linked with E-Cadherin internalisation (Pellon-Cardenas et al., 2013). Even though total E-Cadherin levels are unaffected in the cell lines above, confocal microscopy after E-Cadherin labelling should reveal potential effects on protein localisation. Last, as ablation of SMAP1 was detrimental for cell survival we were not able to definitively pinpoint SMAP1 as the GAP

responsible for inactivating ARF6 following Activin A or BMP4 induction. However, overexpression of a SMAP1 mutant that is unable to hydrolyze ARF6 might be tolerated. Repeating the pull-down assay described in section 3.2 in such hES cell line should abolish ligands' ability to inactivate ARF6.

In chapter 5 we described the establishment of a novel, Activin A –based system for the culture of hES cells. Having assessed the expression of relevant pluripotency markers and retained capacity of the cells to form *in vivo* teratomas, we concluded that this system is able to preserve hES cell pluripotency. Next, cells cultured under these conditions were induced with BMP4 in two different timepoints (1hr / 4hrs) and total RNA was used for an RNA sequencing assay in order to uncover novel transcripts deregulated as primary and secondary targets of the BMP4 pathway. Results indicated that initial stages of induction are characterized by upregulation of BMP pathway inhibitors and mesendodermal transcripts. Interestingly, secondary events included activation of the WNT pathway and suppression of neuroectodermal markers.

RNA sequencing of BMP4 performed in hES cells yielded interesting results that open new investigation avenues of the differentiation process. To begin with, this assay was performed in a novel medium we established that relies on Activin A to preserve pluripotency. Therefore, comparing the transcriptional profile of our control condition with already published results obtained culturing cells in mTeSR1 should reveal whether Activin A and TGFβ preserve pluripotency acting through the same pathways. While upregulation of mesendodermal transcripts was expected after short BMP4 treatment, positive regulation of BMP4 inhibitors was a completely novel finding. In the literature there are hints that these inhibitors act by fine-tuning cells sensitivity to BMP4 stimulation (Paulsen et al., 2011). Therefore, future experiments should include

quantitation of their levels by qPCR after treatment with several BMP4 concentrations. In addition, since BAMBI and CER1 inhibit Activin A as well as BMP4 pathways, their upregulation might be dependent on the presence of Activin A in the medium. Repeating differentiation in mTeSR1 will clarify whether Activin A is implicated. Moreover, since BAMBI overexpression has been linked to activation of the WNT pathway (Kim et al., 2015) it is possible that repeating differentiation in a BAMBI knock-out system might inhibit its progression or direct cells to a specific fate. In addition, inhibiting endogenous WNT with specific antagonists after induction with BMP4 for different time intervals should reveal the implication of the pathway. Furthermore, downregulation of neuroectodermal markers after 4hrs of BMP4 treatment indicated for the first time that commitment to mesendoderm occurs early in the process. However, it is yet unclear whether cells retain the plasticity to populate all three layers post 4hrs of BMP4 addition. Therefore, inducing neuroectodermal differentiation after treatment with BMP4 for several time intervals should pinpoint the exact timepoint when cells abolish their capacity to form this layer, irreversibly.

CHAPTER 7

MATERIALS AND METHODS

7.1 Cellular Biology Methods

7.1.1 Transformed Cells

7.1.1.1 Cell Culture

HEK-293 cells were cultured in 10cm dishes (Sarstedt – 83.3902) at 37^0C, 5% CO_2 using DMEM (ThermoFisher Scientific – 11995065) supplemented with 10% FCS (ThermoFisher Scientific – 10270106) and 100 U/mL Penicillin/Streptomycin (ThermoFisher Scientific – 15140122). Cells were passaged every 3 days at a ratio of 1 to 5. During passaging, cells were washed with PBS (Sigma – D8537) and incubated with Trypsin (ThermoFisher Scientific – 25200056) for 1min at 37^0C. Subsequently, they were dissociated, resuspended in fresh media and transferred to new dishes.

Prior to freezing, HEK-293 cells were passaged from 10cm plates as described above and collected in 15mL falcon tubes (Sarstedt – 62.554.502). They were centrifuged at 100g for 3min at room temperature and resuspended in 1mL of FCS supplemented with 10% DMSO (Sigma – D2650). Next, they were transferred in cryo-vials (Sarstedt – 72.377) and stored for 24hrs at -80^0C before being transferred to liquid nitrogen. During thawing, HEK-293 cells were incubated in a 37^0C waterbath for 30sec and transferred to a 15mL falcon tube containing 10mL of fresh media. Next, cells were centrifuged at 100g for 3min at room temperature, collected with fresh media and plated in 10cm dishes as usual.

7.1.1.2 Plasmid / siRNA Transfections

One day prior to DNA transfection, HEK-293 cells were split as described in section 7.1.1.1. Cell number was determined using a haemocytometer and approximately $5x10^5$ cells were added in a 60mm dish. DNA transfections were carried out using the Calcium Phosphate method. A mixture of 125mM $CaCl_2$ (Sigma – 223506) and 15µg of midi-prepped (ThermoFisher Scientific – 12752663) plasmid DNA was added to 2XHBS buffer (50mM NaCl Acros Organics – S316065, 1.5mM Na_2HPO_4 Sigma – 30435, 280mM HEPES Sigma – H4034). The DNA precipitates were allowed to form for 20min at room temperature before being added dropwise, on top of the cells. Subsequently, the cells were incubated for 24hrs before being used in experimental assays.

One day prior to siRNA transfection, HEK-293 cells were split as described in section 7.1.1.1. Cell number was determined using a haemocytometer and approximately $5x10^4$ cells were added in each well of 24-well plates (Sarstedt – 83.3922). siRNA transfections were carried out using the Lipofectamine RNAiMAX transfection compound (ThermoFisher Scientific – 12323563) according to the manufacturer's protocol. In short, 1.5µl of lipid and 5pmol of siRNA were allowed to equilibrate at room temperature in separate eppendorf tubes containing 25µl of Opti-MEM™ I Reduced Serum Medium (ThermoFisher Scientific – 31985047). Lipid and siRNA were then combined in a single tube and the complexes were allowed to form for 10min at room temperature. Subsequently, siRNA-lipid complexes were added dropwise on the cells. Experimental assays were carried out after 48hrs.

Plasmid	Use
pSRa-ARF6-HA	Transient overexpression in HEK-293
pSRa-ARF6T27N-HA	Transient overexpression in HEK-293
pSRa-ARF6Q67L-HA	Transient overexpression in HEK-293
pGEX-4T1-SMAD4	GST-SMAD4 purification / Pull-Down
pGEX-6P1	GST control purification / Pull-Down
pEGFP-C3-SMAD4	Transient overexpression in HEK-293
pSRa-ARF1Q71L-HA	Transient overexpression in HEK-293
pcDNA3-ARF5Q71L-HA	Transient overexpression in HEK-293
pGEX-4T1-SMAD4 (N273-N552)	GST-SMAD4 (N273-N552) purification / Pull-Down
pGEX-4T1-SMAD4 (N520-N552)	GST-SMAD4 (N520-N552) purification / Pull-Down
pGEX-4T1-SMAD4 ΔC43	GST-SMAD4 ΔC43 purification / Pull-Down
pGEX-6P1-SMAD2 (N427-N467)	GST-SMAD2 (N427-N467) purification / Pull-Down
pGEX-6P1-SMAD2EDME(N427-N467)	GST-SMAD2EDME (N427-N467) purification / Pull-Down
pGEX-6P1-SMAD3 (N385-N425)	GST-SMAD3 (N385-N425) purification / Pull-Down
pGEX-6P1-SMAD3EDVE (N385-425)	GST-SMAD3EDVE (N385-N425) purification / Pull-Down
pRK5-SMAD2-myc	Transient overexpression in HEK-293
pRK5-SMAD2EDME-myc	Transient overexpression in HEK-293
pRK5-SMAD3-myc	Transient overexpression in HEK-293
pRK5-SMAD3EDVE-myc	Transient overexpression in HEK-293
pEGFP-N1-ARF6T157A-GFP	Transient overexpression in HEK-293
pEGFP-C1	GFP control - Transient overexpression in HEK-293
pGEX-4T1-ARHGAP10 (N885-N1096)	GST-ARF6GAP (N885-N1096) purification / Pull-Down
pRK5-ACVR1B-FLAG	Transient overexpression in HEK-293
pRK5-ACVR1BT206D-FLAG	Transient overexpression in HEK-293
pRK5-ACVR1BK234R-FLAG	Transient overexpression in HEK-293
pcDNA3-HA-SMAP1	Transient overexpression in HEK-293
px459-SMAP1gRNA	SMAP1 CRISPR-KO in HEK-293

Table 7.1 Summary of Plasmids Used in Chapter 3

7.1.2 Human Embryonic Stem Cells

7.1.2.1 Cell Culture

H1 cells (WiCell – WB0113) were obtained at passage 20 and cultured routinely in mTeSR1 medium (Stem Cell Technologies - 05851) or mTeSR without select factors (Stem Cell Technologies - 05896) supplemented with 100ng/mL bFGF (ImmunoTools – 11343627), 0,5ng/mL Activin A (by Dr Marko Hyvönen, Cambridge University), 1mM LiCl (Sigma – 62476), 1mM G-AminoButyric Acid (Sigma A5835) and 0.1mM Pipecolic Acid (Sigma – P2519) on matrigel (Corning – 354277) coated 6-well dishes (Sarstedt – 83.3920). Medium was exchanged every 24h and cells were passaged every 5 to 7 days at a ratio of 1 to 6. Prior to passaging, 200µL of frozen matrigel were diluted in 20mL of DMEM/F12 (ThermoFisher Scientific – 10770245) and used to coat new 6-well dishes (1.5mL/well). Matrigel was allowed to solidify for 45min at room temperature and the dishes were subsequently washed with DMEM/F12. Prior to passaging, differentiated cells or colonies were manually marked and removed by aspiration. H1 cells were incubated with dispase (ThermoFisher Scientific – 1710541) diluted to 1mg/mL in DMEM/F12 until the colony boarders were beginning to detach from the substrate (5-7min). Next, cells were washed twice with DMEM/F12 and fresh medium was added. Cells were gently dissociated with the pipette and transferred to the new 6-wells.

Prior to freezing, H1 cells were passaged from 6-well plates as described above and collected in15mL falcon tubes. They were centrifuged at 50g for 3min at room temperature and resuspended in 1mL of mFreSR reagent (Stem Cell Technologies – 05855). Next, they were transferred in cryo-vials and stored for 24hrs at -80^{0}C before being transferred to liquid nitrogen. During thawing, H1 cells were incubated in a 37^{0}C

waterbath for 30sec, and transferred to a 15mL falcon tube containing 10mL of fresh media. Next, cells were centrifuged at 50g for 3min at room temperature, collected with fresh media and plated in 6-well dishes in the presence of 5μM ROCK inhibitor (LC Laboratories – F4660).

7.1.2.2 Plasmid Transfections

One day prior to DNA transfection, H1 were passaged similarly to the method described in section 7.1.2.1, using Versene-EDTA 0.02% (Lonza – BE17-711E) instead of dispase, at a ratio of 1 to 6. In short, cells were incubated with Versene-EDTA for 7min at room temperature and were subsequently dissociated into small clumps (3-5 cells). The cell aggregates were transferred into new 6-well dishes and allowed to attach and proliferate for 24hrs in fresh media supplemented with 5μM ROCK inhibitor. DNA transfections were carried out using the X-tremeGENE™ 9 DNA Transfection Reagent (Roche – XTG9-RO). DNA/lipid complexes at a ratio of 1 to 3 were allowed to form for 5min at room temperature in Opti-MEM™ I Reduced Serum Medium. The complexes were then added dropwise on the cells and incubated with them for 24hrs. In order to generate stable or CRISPR knock-out cell lines, H1 cells were split with the same process 24hrs after transfection, at a ratio of 1 to 1, in new matrigel coated dishes with fresh media supplemented with 5μM ROCK inhibitor. After 24hrs the medium was exchanged for fresh, containing 250ng/mL puromycin (Sigma – P7255). Antibiotic resistant colonies were isolated with cloning rings, dissociated from the plates using the same Versene-EDTA passaging method and expanded in new plates. Puromycin was removed from the daily media changes of CRISPR knock-out clones so as to avoid CAS9 integration but was retained in the case of stable lines to ensure incorporation of the transgenes.

Plasmid	Use
pCAG-ARF6-HA	ARF6-HA H1 Stable cell line
pCAG-ARF6T157A-GFP	ARF6T157A-GFP H1 Stable cell line
pCAG-GFP	GFP H1 Stable cell line
px459-ARF6gRNA	ARF6 CRISPR-KO in H1

Table 7.2 Summary of Plasmids Used in Chapter 4

7.1.2.3 Cell Differentiation

Prior to differentiation, H1 cells were passaged according to the protocol described in the previous section and allowed to proliferate. The medium was exchanged daily until cells reached approximately 60% confluency. At this point normal mTeSR1 was substituted for mesendoderm differentiation medium that consists of RPMI 1640 (ThermoFisher Scientific – 21875034) supplemented with 1X Non Essential Aminoacids (ThermoFisher Scientific – 11140050), GlutaMax (ThermoFisher Scientific – 35050038), β-Mercaptoethanol (ThermoFisher Scientific – 21985023), insulin transferrin selenium (ThermoFisher Scientific – 41400045), 50ng/mL BMP4 and 50ng/mL Activin A. The medium was exchanged with fresh after 24hrs in order to remove dead cells. The outcome of differentiation was assessed by western blotting or immunofluorescence at different timepoints (24-48-72-96hrs).

7.2 Biochemical Methods

7.2.1 SDS-PAGE Electrophoresis and Western Blotting

Cells were washed twice with cold PBS and then lysed using SDS (Sigma – 75746) lysis buffer (1% SDS in PBS, 1mM PMSF). Cell lysates were sonicated 3 times for 10s at 5% amplitude, incubated at 100^0C for 5min and centrifuged at 14.000rpm for 15min. Protein concentration was determined using the BCA Protein Assay Kit (ThermoFisher Scientific - 23225). Samples were separated by SDS-PAGE electrophoresis and transferred to nitrocellulose membranes (GE Healthcare – 10600012). After blocking for 1hr in 5% milk/TBS-T, membranes were incubated overnight at 4^0C with the primary antibodies that are summarized below. Subsequently, membranes were washed 3 times for 10min in TBS-T and incubated for 1hr with HRP conjugated secondary antibodies that are summarized below. The Enhanced Chemiluminescence Western Blotting Detection Reagent (Amersham - RPN2209) was used to develop the films in a standard developing machine. Alternatively, membranes were incubated with near-infrared fluorescent secondary antibodies that are summarized below and visualized using the LI-COR Odyssey imaging system.

Antibody	Company	Cat No	Working Concentration
α-HA	Roche	11867423001	100ng/mL
α-GFP	Millipore	06896	200ng/mL
α-myc	DSHB	9E10	100ng/mL
α-pSMAD2	Cell Signalling	3101S	100ng/mL
α-pSMAD3	Rockland	600401919	100ng/mL
α-SMAD2/3	Cell Signalling	8685S	100ng/mL
α-ACTIN	Millipore	MAB1501	100ng/mL
α-ARF6	Origene	TA310193	1µg/mL
α-NANOG	Cell Signalling	3580s	100ng/mL
α-E/CADHERIN	Novus Biologicals	AF648-SP	200ng/mL
α-OCT4	Santa Cruz	sc5279	200ng/mL
α-TUBULIN	DSHB	E7	100ng/mL
α-BRACHYURY	R&D Systems	AF2085	200ng/mL

Table 7.3 Western Blotting Primary Antibodies

Antibody	Company	Cat No	Working Concentration
IRDye® 800CW α-Rat	LI-COR	925-32218	100ng/mL
IRDye® 800CW α-Mouse	LI-COR	925-32212	200ng/mL
IRDye® 800CW α-Rabbit	LI-COR	925-32211	100ng/mL
IRDye® 800CW α-Goat	LI-COR	925-32214	100ng/mL
α-Rat HRP	Jackson	712-035-15	100ng/mL
α-Mouse HRP	Jackson	115-035-062	100ng/mL
α-Rabbit HRP	Jackson	115-035-008	100ng/mL

Table 7.4 Western Blotting Secondary Antibodies

7.2.2 GST Protein Amplification and Purification

A single colony of *E. Coli BL21DE* bacteria transformed with a plasmid encoding the GST fused protein of interest was inoculated overnight at 37^0C at 180rpm in 2mL of LB broth (Sigma – L3522) plus 50µg/mL ampicillin (ThermoFisher Scientific – 10193433). 1L of LB broth plus 50µg/mL ampicillin was inoculated with 1mL of the above culture and incubated at 37^0C at 180rpm until the OD at 600nm reached 0.5. At that point IPTG (ThermoFisher Scientific – 10725471) was added to the colony at a final concentration of 0.3mM and the incubation continued for 2hrs. The bacteria were then pelleted by centrifugation at 5000g for 30min at 4^0C and lysed through a French press at 1000psi in a lysis buffer containing 20 mM Tris–HCl pH 7.8 and 100 mM NaCl and protease inhibitors (Roche –04693159001). The cell lysate was subsequently centrifuged at 12000g for 30min at 4^0C, and the supernatant containing the GST protein was incubated with 300µL of glutathione Sepharose 4B beads (GE Healthcare - 17-0756-01) that had been equilibrated in the above lysis buffer. The beads were then retained in a Poly-Prep chromatography column (BioRad – 7311550) and washed 3 times with the lysis buffer above. The GST fused protein was eluted from the beads with an elution buffer containing 10 mM reduced glutathione (ThermoFisher Scientific – 252110), 20 mM Tris–HCl pH 7.8, 100 mM NaCl, and protease inhibitors with an adjusted pH at 7.8. The eluate was then dialysed against a buffer containing 20 mM Tris–HCl pH 7.5, 150 mM NaCl overnight at 4^0C and the protein concentration was estimated with a Bradford assay.

7.2.3 GST Pull - Down

Glutathione Sepharose 4B beads were equilibrated in a buffer containing 150 mM NaCl and 20 mM Tris–HCl pH 7.5. They were incubated with 1% BSA (Sigma - A2153) for 1hr at 4^0C to block non-specific binding of proteins. Next, beads were incubated with 15μg GST protein alone or GST fusion protein at a final volume of 200 μL for 1hr at 4^0C. Following, the bead - GST complexes were washed with the buffer mentioned above and incubated for 3hrs at 4^0C with cell lysates that overexpressed the protein of interest. Cells were previously lysed in a buffer containing 1% Triton X-100, 150 mM NaCl, 20 mM, Tris–HCl pH 7.5 and complete protease inhibitors (Roche - 11836153001). After a final washing step, complexes were eluted from the beads with Laemmli buffer and subjected to SDS-PAGE electrophoresis and Western Blotting to detect the protein of interest.

7.2.4 Co-Immunoprecipitation

HEK-293 cells cultured in 60mm dishes were transfected with constructs expressing the two proteins of interest according to the protocol above. Cells were lysed on ice in a buffer containing 1% Triton X-100, 150 mM NaCl, 20 mM, Tris–HCl pH 7.5, 1mM EDTA 8,0 and complete protease inhibitors. Protein G Sepharose beads (GE Healthcare - 17-0618-01) were washed in the above buffer and 10μL were added in the cell lysate and incubated for 1hr at 4^0C to bind non-specific proteins. Protein concentration of the lysates was determined using the BCA Protein Assay Kit and 400μg were incubated overnight at 4^0C with 10μg of primary antibody or the appropriate IgG control. Subsequently, the complexes were incubated for 4hrs at 4^0C with 20μL of Protein G Sepharose beads. The beads were washed, the complexes

were eluted with Laemmli buffer and subjected to SDS-PAGE electrophoresis and Western Blotting to verify the interaction.

7.2.5 Immunofluorescence

H1 cells were cultured on matrigel coated ibidi dishes (Thistle Scientific – IB81151) or 8-well permanox chambers (ThermoFisher Scientific – 154534). At approximately 50% confluency, cells were washed twice with PBS, fixed in 3.7% PFA (Sigma – P6148) for 15 min and quenched with 50mM NH_4Cl (Sigma – A4514) for 15min. Subsequently, cells were permeabilised with 0.5% Triton X-100 (ThermoFisher Scientific – 10254583) for 4min, blocked in 10% FCS for 20min and incubated for 1 hour with primary antibodies. Next, cells were washed 3 times for 5min in PBS and incubated with secondary antibodies for 45min. Cells were washed 3 times for 5min in PBS and treated with RNAse (Sigma - R6513) 1mg/ml for 15min. The nuclei were stained with Propidium Iodide (Sigma - 81845) or Hoechst 33342 (Cell Signalling Technology – 4082s) and the samples were mounted in Prolong® Diamond Antifade Mountant (ThermoFisher Scientific - 15218243). Imaging was carried out using a Leica SP5 Inverted Confocal Microscope or a Leica SP8 Upright Confocal Microscope.

Antibody	Company	Cat No	Working Concentration
α-NANOG	Cell Signalling	3580s	100ng/mL
α-E/CADHERIN	Novus Biologicals	AF648-SP	200ng/mL
α-OCT4	Santa Cruz	sc5279	200ng/mL
α-SOX2	R&D Systems	MAB2018	1µg/mL
α-BRACHYURY	R&D Systems	AF2085	1µg/mL

Table 7.6 Immunofluorescence Primary Antibodies

Antibody	Company	Cat No	Working Concentration
AlexaFluor® 488 α-Rabbit	Jackson	711-545-152	500ng/mL
FITC α-Mouse	Jackson	715-095-151	500ng/mL
TRITC α-Rabbit	Jackson	711-025-152	500ng/mL
Alexa Fluor® 594 α-Mouse	Jackson	715-585-151	500ng/mL
Alexa Fluor® 594 α-Goat	Jackson	705-585-147	500ng/mL

Table 7.7 Immunofluorescence Secondary Antibodies

7.2.6 Karyotype Analysis

H1 cells were incubated with 0,04ug/ml Karyomax Colcemid (ThermoFisher Scientific - 15212) for 2hrs at 37^0C. Subsequently, cells were dissociated with Trypsin-EDTA (ThermoFisher Scientific – 25300096) for 3min at 37^0C and the enzyme was deactivated using an equal volume of trypsin inhibitor (Sigma – T6414). Cells were centrifuged for 10min at 100g and incubated with a hypotonic KCl buffer 0.56w/v (Sigma – P9541) for 6min at 37^0C. In order to be fixed, a methanol/acetic acid (3:1) buffer was added on top and incubated for 5min at room temperature. Cells were centrifuged for 5min at 100g, diluted in fresh fixative solution and stored overnight at -20^0C. The following day, the fixed cells were resuspended in 200uL of fresh fixative and dropped from a height of 15-20cm on a slide to extract the chromosomes. They were stained with a Giemsa reagent (Sigma – G5637) and visualized under a phase contrast microscope.

7.3 In Vivo Assays

7.3.1 Teratoma Formation

Immune-deficient NOD/SCID mice, maintained under SPF conditions in the Animal facility of the Academy of Athens, Greece, were used to perform teratoma assays. H1 cells were maintained for more than 10 passages in normal mTeSR1 or mTeSR containing Activin A instead of TGFβ. The cells were dissociated from the substrate using dispase, as detailed in section 7.1.2.1 and collected in 15mL falcon tubes. Subsequently, cells were centrifuged at 50g for 3min and resuspended in 150uL of matrigel. The cell/matrigel mixture was then injected subcutaneously in the hind legs of the mice. The tumours that emerged were removed, sectioned and embedded in paraffin. Following that, the tissue sections were stained with hematoxylin/eosin in order to study the different germ layers.

LIST OF REFERENCES

Abranches, E., Guedes, A.M. V, Moravec, M., et al. (2014) Stochastic NANOG fluctuations allow mouse embryonic stem cells to explore pluripotency. *Development (Cambridge, England)*, 141 (14): 2770–9. doi:10.1242/dev.108910.

Aghion, J., Gueth-Hallonet, C., Antony, C., et al. (1994) Cell adhesion and gap junction formation in the early mouse embryo are induced prematurely by 6-DMAP in the absence of E-cadherin phosphorylation. *Journal of cell science*, 107 (Pt 5: 1369–79. Available at: http://www.ncbi.nlm.nih.gov/pubmed/7929642.

Ambrosio, A.L., Taelman, V.F., Lee, H.X., et al. (2008) Crossveinless-2 Is a BMP feedback inhibitor that binds Chordin/BMP to regulate Xenopus embryonic patterning. *Developmental cell*, 15 (2): 248–60. doi:10.1016/j.devcel.2008.06.013.

Amita, M., Adachi, K., Alexenko, A.P., et al. (2013) Complete and unidirectional conversion of human embryonic stem cells to trophoblast by BMP4. *Proceedings of the National Academy of Sciences of the United States of America*, 110 (13): E1212-21. doi:10.1073/pnas.1303094110.

Amsalem, A.R., Marom, B., Shapira, K.E., et al. (2016) Differential regulation of translation and endocytosis of alternatively spliced forms of the type II bone morphogenetic protein (BMP) receptor. *Molecular biology of the cell*, 27 (4): 716–30. doi:10.1091/mbc.E15-08-0547.

Antonny, B., Beraud-Dufour, S., Chardin, P., et al. (1997) N-terminal hydrophobic residues of the G-protein ADP-ribosylation factor-1 insert into membrane phospholipids upon GDP to GTP exchange. *Biochemistry*, 36 (15): 4675–84. doi:10.1021/bi962252b.

Armstrong, L., Hughes, O., Yung, S., et al. (2006) The role of PI3K/AKT, MAPK/ERK and NFkappabeta signalling in the maintenance of human embryonic stem cell pluripotency and viability highlighted by transcriptional profiling and functional analysis. *Human molecular genetics*, 15 (11): 1894–913. doi:10.1093/hmg/ddl112.

Babst, M. (2011) MVB vesicle formation: ESCRT-dependent, ESCRT-independent and everything in between. *Current opinion in cell biology*, 23 (4): 452–7. doi:10.1016/j.ceb.2011.04.008.

Bai, M., Gad, H., Turacchio, G., et al. (2011) ARFGAP1 promotes AP-2-dependent endocytosis. *Nature cell biology*, 13 (5): 559–67. doi:10.1038/ncb2221.

Bakkebø, M., Huse, K., Hilden, V.I., et al. (2012) SARA is dispensable for functional TGF-β signaling. *FEBS letters*, 586 (19): 3367–72. doi:10.1016/j.febslet.2012.07.027.

Balasubramanian, N., Scott, D.W., Castle, J.D., et al. (2007) Arf6 and microtubules in adhesion-dependent trafficking of lipid rafts. *Nature cell biology*, 9 (12): 1381–91. doi:10.1038/ncb1657.

Barrios-Rodiles, M., Brown, K.R., Ozdamar, B., et al. (2005) High-throughput mapping of a dynamic signaling network in mammalian cells. *Science (New York, N.Y.)*, 307 (5715): 1621–5. doi:10.1126/science.1105776.

Bastiani, M., Liu, L., Hill, M.M., et al. (2009) MURC/Cavin-4 and cavin family members form tissue-specific caveolar complexes. *The Journal of cell biology*, 185 (7): 1259–73. doi:10.1083/jcb.200903053.

Beattie, G.M., Lopez, A.D., Bucay, N., et al. (2005) Activin A maintains pluripotency of human embryonic stem cells

in the absence of feeder layers. *Stem cells (Dayton, Ohio)*, 23 (4): 489–95. doi:10.1634/stemcells.2004-0279.

Behfar, A., Yamada, S., Crespo-Diaz, R., et al. (2010) Guided cardiopoiesis enhances therapeutic benefit of bone marrow human mesenchymal stem cells in chronic myocardial infarction. *Journal of the American College of Cardiology*, 56 (9): 721–34. doi:10.1016/j.jacc.2010.03.066.

Bellamy, V., Vanneaux, V., Bel, A., et al. (2015) Long-term functional benefits of human embryonic stem cell-derived cardiac progenitors embedded into a fibrin scaffold. *The Journal of heart and lung transplantation : the official publication of the International Society for Heart Transplantation*, 34 (9): 1198–207. doi:10.1016/j.healun.2014.10.008.

Bentzinger, C.F., Wang, Y.X., von Maltzahn, J., et al. (2013) The emerging biology of muscle stem cells: implications for cell-based therapies. *BioEssays : news and reviews in molecular, cellular and developmental biology*, 35 (3): 231–41. doi:10.1002/bies.201200063.

van den Berg, D.L.C., Snoek, T., Mullin, N.P., et al. (2010) An Oct4-centered protein interaction network in embryonic stem cells. *Cell stem cell*, 6 (4): 369–81. doi:10.1016/j.stem.2010.02.014.

Bernabeu, C., Lopez-Novoa, J.M. and Quintanilla, M. (2009) The emerging role of TGF-beta superfamily coreceptors in cancer. *Biochimica et biophysica acta*, 1792 (10): 954–73. doi:10.1016/j.bbadis.2009.07.003.

Bianconi, E., Piovesan, A., Facchin, F., et al. (2014) An estimation of the number of cells in the human body. *Annals of human biology*, 40 (6): 463–71. doi:10.3109/03014460.2013.807878.

Bischof, P. and Campana, A. (1996) A model for implantation of the human blastocyst and early placentation. *Human reproduction update*, 2 (3): 262–70. doi:10.1093/humupd/2.3.262.

Le Blanc, K., Rasmusson, I., Sundberg, B., et al. (2004) Treatment of severe acute graft-versus-host disease with third party haploidentical mesenchymal stem cells. *Lancet (London, England)*, 363 (9419): 1439–41. doi:10.1016/S0140-6736(04)16104-7.

Blin, G., Nury, D., Stefanovic, S., et al. (2010) A purified population of multipotent cardiovascular progenitors derived from primate pluripotent stem cells engrafts in postmyocardial infarcted nonhuman primates. *The Journal of clinical investigation*, 120 (4): 1125–39. doi:10.1172/JCI40120.

Bonifacino, J.S. and Glick, B.S. (2004) The mechanisms of vesicle budding and fusion. *Cell*, 116 (2): 153–66. doi:10.1016/S0092-8674(03)01079-1.

Bonor, J., Adams, E.L., Bragdon, B., et al. (2012) Initiation of BMP2 signaling in domains on the plasma membrane. *Journal of cellular physiology*, 227 (7): 2880–8. doi:10.1002/jcp.23032.

Boucrot, E., Ferreira, A.P.A., Almeida-Souza, L., et al. (2015) Endophilin marks and controls a clathrin-independent endocytic pathway. *Nature*, 517 (7535): 460–5. doi:10.1038/nature14067.

Boyer, L. a, Lee, T.I., Cole, M.F., et al. (2005) Core transcriptional regulatory circuitry in human embryonic stem cells. *Cell*, 122 (6): 947–956. doi:10.1016/j.cell.2005.08.020.

Bragdon, B., Thinakaran, S., Bonor, J., et al. (2009) FRET reveals novel protein-receptor interaction of bone morphogenetic proteins receptors and adaptor protein 2 at the cell surface. *Biophysical journal*, 97 (5): 1428–35. doi:10.1016/j.bpj.2009.05.061.

Brehm, a, Ohbo, K. and Schöler, H. (1997) The carboxy-terminal transactivation domain of Oct-4 acquires cell specificity through the POU domain. *Molecular and cellular biology*, 17 (1): 154–62. doi:10.1128/MCB.17.1.154.

Brown, F.D., Rozelle, A.L., Yin, H.L., et al. (2001) Phosphatidylinositol 4,5-bisphosphate and Arf6-regulated membrane traffic. *The Journal of cell biology*, 154 (5): 1007–17. doi:10.1083/jcb.200103107.

Burd, C. and Cullen, P.J. (2014) Retromer: a master conductor of endosome sorting. *Cold Spring Harbor perspectives in biology*, 6 (2). doi:10.1101/cshperspect.a016774.

de Caestecker, M.P., Yahata, T., Wang, D., et al. (2000) The Smad4 activation domain (SAD) is a proline-rich, p300-dependent transcriptional activation domain. *The Journal of biological chemistry*, 275 (3): 2115–22. Available at: http://www.ncbi.nlm.nih.gov/pubmed/10636916 (Accessed: 1 February 2018).

Campolo, F., Gori, M., Favaro, R., et al. (2013) Essential role of Sox2 for the establishment and maintenance of the germ cell line. *Stem cells (Dayton, Ohio)*, 31 (7): 1408–21. doi:10.1002/stem.1392.

Carson, D.D., Tang, J.P. and Julian, J. (1993) Heparan sulfate proteoglycan (perlecan) expression by mouse embryos during acquisition of attachment competence. *Developmental biology*, 155 (1): 97–106. doi:10.1006/dbio.1993.1010.

Casanova, J.E. (2007) Regulation of Arf activation: the Sec7 family of guanine nucleotide exchange factors. *Traffic (Copenhagen, Denmark)*, 8 (11): 1476–85. doi:10.1111/j.1600-0854.2007.00634.x.

Chambers, I., Colby, D., Robertson, M., et al. (2003) Functional expression cloning of Nanog, a pluripotency sustaining factor in embryonic stem cells. *Cell*, 113 (5): 643–655. doi:10.1016/S0092-8674(03)00392-1.

Chan, K.K.-K., Zhang, J., Chia, N.-Y., et al. (2009) KLF4 and PBX1 directly regulate NANOG expression in human embryonic stem cells. *Stem cells (Dayton, Ohio)*, 27 (9): 2114–25. doi:10.1002/stem.143.

Chazaud, C., Yamanaka, Y., Pawson, T., et al. (2006) Early lineage segregation between epiblast and primitive endoderm in mouse blastocysts through the Grb2-MAPK pathway. *Developmental cell*, 10 (5): 615–24. doi:10.1016/j.devcel.2006.02.020.

Chen, E.H., Pryce, B.A., Tzeng, J.A., et al. (2003) Control of myoblast fusion by a guanine nucleotide exchange factor, loner, and its effector ARF6. *Cell*, 114 (6): 751–62. doi:10.1016/S0092-8674(03)00720-7.

Chen, P.-W., Jian, X., Yoon, H.-Y., et al. (2013) ARAP2 signals through Arf6 and Rac1 to control focal adhesion morphology. *The Journal of biological chemistry*, 288 (8): 5849–60. doi:10.1074/jbc.M112.415778.

Chen, Y.-G. (2009) Endocytic regulation of TGF-beta signaling. *Cell research*, 19 (1): 58–70. doi:10.1038/cr.2008.315.

Chen, Y.G., Hata, A., Lo, R.S., et al. (1998) Determinants of specificity in TGF-beta signal transduction. *Genes & development*, 12 (14): 2144–52. doi:10.1101/gad.12.14.2144.

Cherfils, J. and Zeghouf, M. (2013) Regulation of small GTPases by GEFs, GAPs, and GDIs. *Physiological reviews*, 93 (1): 269–309. doi:10.1152/physrev.00003.2012.

Chiu, F.-L., Lin, J.-T., Chuang, C.-Y., et al. (2015) Elucidating the role of the A2A adenosine receptor in neurodegeneration using neurons derived from Huntington's disease iPSCs. *Human molecular genetics*, 24 (21):

6066–79. doi:10.1093/hmg/ddv318.

Choi, S.-C., Kim, G.-H., Lee, S.J., et al. (2008) Regulation of activin/nodal signaling by Rap2-directed receptor trafficking. *Developmental cell*, 15 (1): 49–61. doi:10.1016/j.devcel.2008.05.004.

Claude, A., Zhao, B.P., Kuziemsky, C.E., et al. (1999) GBF1: A novel Golgi-associated BFA-resistant guanine nucleotide exchange factor that displays specificity for ADP-ribosylation factor 5. *The Journal of cell biology*, 146 (1): 71–84. doi:10.1083/jcb.146.1.71.

Collins, B.M., McCoy, A.J., Kent, H.M., et al. (2002) Molecular architecture and functional model of the endocytic AP2 complex. *Cell*, 109 (4): 523–35. doi:10.1016/S0092-8674(02)00735-3.

Condic, M.L. (2014) Totipotency: what it is and what it is not. *Stem cells and development*, 23 (8): 796–812. doi:10.1089/scd.2013.0364.

Connick, P., Kolappan, M., Crawley, C., et al. (2012) Autologous mesenchymal stem cells for the treatment of secondary progressive multiple sclerosis: an open-label phase 2a proof-of-concept study. *The Lancet. Neurology*, 11 (2): 150–6. doi:10.1016/S1474-4422(11)70305-2.

Constam, D.B. (2014) Regulation of TGFβ and related signals by precursor processing. *Seminars in cell & developmental biology*, 32: 85–97. doi:10.1016/j.semcdb.2014.01.008.

Cunningham, T.J., Yu, M.S., McKeithan, W.L., et al. (2017) Id genes are essential for early heart formation. *Genes & development*, 31 (13): 1325–1338. doi:10.1101/gad.300400.117.

D'Souza-Schorey, C. and Chavrier, P. (2006) ARF proteins: roles in membrane traffic and beyond. *Nature reviews. Molecular cell biology*, 7 (5): 347–58. doi:10.1038/nrm1910.

D'Souza-Schorey, C., Li, G., Colombo, M.I., et al. (1995) A regulatory role for ARF6 in receptor-mediated endocytosis. *Science (New York, N.Y.)*, 267 (5201): 1175–8. doi:10.1126/science.7855600.

Dard, N., Louvet-Vallée, S. and Maro, B. (2009) Orientation of mitotic spindles during the 8- to 16-cell stage transition in mouse embryos. *PloS one*, 4 (12): e8171. doi:10.1371/journal.pone.0008171.

Davidson, K.C., Adams, A.M., Goodson, J.M., et al. (2012) Wnt/β-catenin signaling promotes differentiation, not self-renewal, of human embryonic stem cells and is repressed by Oct4. *Proceedings of the National Academy of Sciences of the United States of America*, 109 (12): 4485–90. doi:10.1073/pnas.1118777109.

Davidson, K.C., Mason, E.A. and Pera, M.F. (2015) The pluripotent state in mouse and human. *Development (Cambridge, England)*, 142 (18): 3090–9. doi:10.1242/dev.116061.

Davies, M., Robinson, M., Smith, E., et al. (2005) Induction of an epithelial to mesenchymal transition in human immortal and malignant keratinocytes by TGF-beta1 involves MAPK, Smad and AP-1 signalling pathways. *Journal of cellular biochemistry*, 95 (5): 918–31. doi:10.1002/jcb.20458.

Ding, V.M.Y., Ling, L., Natarajan, S., et al. (2010) FGF-2 modulates Wnt signaling in undifferentiated hESC and iPS cells through activated PI3-K/GSK3beta signaling. *Journal of cellular physiology*, 225 (2): 417–28. doi:10.1002/jcp.22214.

Donaldson, J.G. (2003) Multiple roles for Arf6: sorting, structuring, and signaling at the plasma membrane. *The*

Journal of biological chemistry, 278 (43): 41573–6. doi:10.1074/jbc.R300026200.

Donaldson, J.G. and Jackson, C.L. (2011) ARF family G proteins and their regulators: roles in membrane transport, development and disease. *Nature reviews. Molecular cell biology*, 12 (6): 362–75. doi:10.1038/nrm3117.

Dubois, T., Paléotti, O., Mironov, A.A., et al. (2005) Golgi-localized GAP for Cdc42 functions downstream of ARF1 to control Arp2/3 complex and F-actin dynamics. *Nature cell biology*, 7 (4): 353–64. doi:10.1038/ncb1244.

Duinsbergen, D., Salvatori, D., Eriksson, M., et al. (2009) Tumors originating from induced pluripotent stem cells and methods for their prevention. *Annals of the New York Academy of Sciences*, 1176: 197–204. doi:10.1111/j.1749-6632.2009.04563.x.

Eldar, A., Dorfman, R., Weiss, D., et al. (2002) Robustness of the BMP morphogen gradient in Drosophila embryonic patterning. *Nature*, 419 (6904): 304–8. doi:10.1038/nature01061.

Ellis, P.S., Burbridge, S., Soubes, S., et al. (2015) ProNodal acts via FGFR3 to govern duration of Shh expression in the prechordal mesoderm. *Development (Cambridge, England)*, 142 (22): 3821–32. doi:10.1242/dev.119628.

Enders, A.C. and King, B.F. (1988) Formation and differentiation of extraembryonic mesoderm in the rhesus monkey. *The American journal of anatomy*, 181 (4): 327–40. doi:10.1002/aja.1001810402.

Etoc, F., Metzger, J., Ruzo, A., et al. (2016) A Balance between Secreted Inhibitors and Edge Sensing Controls Gastruloid Self-Organization. *Developmental cell*, 39 (3): 302–315. doi:10.1016/j.devcel.2016.09.016.

Feng, X.-H. and Derynck, R. (2005) Specificity and Versatility in Tgf-B Signaling Through Smads. *Annual Review of Cell and Developmental Biology*, 21 (1): 659–693. doi:10.1146/annurev.cellbio.21.022404.142018.

Foletta, V.C., Lim, M.A., Soosairajah, J., et al. (2003) Direct signaling by the BMP type II receptor via the cytoskeletal regulator LIMK1. *The Journal of cell biology*, 162 (6): 1089–98. doi:10.1083/jcb.200212060.

Fong, H., Hohenstein, K.A. and Donovan, P.J. (2008) Regulation of self-renewal and pluripotency by Sox2 in human embryonic stem cells. *Stem cells (Dayton, Ohio)*, 26 (8): 1931–8. doi:10.1634/stemcells.2007-1002.

Ford, M.G.J., Mills, I.G., Peter, B.J., et al. (2002) Curvature of clathrin-coated pits driven by epsin. *Nature*, 419 (6905): 361–6. doi:10.1038/nature01020.

Ford, M.G.J., Pearse, B.M.F., Higgins, M.K., et al. (2001) Simultaneous binding of PtdIns(4,5)P2 and clathrin by AP180 in the nucleation of clathrin lattices on membranes. *Science (New York, N.Y.)*, 291 (5506): 1051–5. doi:10.1126/science.291.5506.1051.

Franco, M. (1999) EFA6, a sec7 domain-containing exchange factor for ARF6, coordinates membrane recycling and actin cytoskeleton organization. *The EMBO Journal*, 18 (6): 1480–1491. doi:10.1093/emboj/18.6.1480.

Fuchs, E. (2009) The tortoise and the hair: slow-cycling cells in the stem cell race. *Cell*, 137 (5): 811–9. doi:10.1016/j.cell.2009.05.002.

Fuentealba, L.C., Eivers, E., Ikeda, A., et al. (2007) Integrating patterning signals: Wnt/GSK3 regulates the duration of the BMP/Smad1 signal. *Cell*, 131 (5): 980–93. doi:10.1016/j.cell.2007.09.027.

Fusaki, N., Ban, H., Nishiyama, A., et al. (2009) Efficient induction of transgene-free human pluripotent stem cells using a vector based on Sendai virus, an RNA virus that does not integrate into the host genome. *Proceedings of*

the Japan Academy. Series B, Physical and biological sciences, 85 (8): 348–62. doi:10.2183/pjab.85.348.

Gadir, N., Lee, E., Garcia, A., et al. (2007) Suppression of TGF-beta signaling by phospholipase D. *Cell cycle (Georgetown, Tex.)*, 6 (22): 2840–5. doi:4921 [pii].

Gafni, O., Weinberger, L., Mansour, A.A., et al. (2013) Derivation of novel human ground state naive pluripotent stem cells. *Nature*, 504 (7479): 282–6. doi:10.1038/nature12745.

Gagliardi, A., Mullin, N.P., Ying Tan, Z., et al. (2013) A direct physical interaction between Nanog and Sox2 regulates embryonic stem cell self-renewal. *The EMBO journal*, 32 (16): 2231–47. doi:10.1038/emboj.2013.161.

Gary C Schoenwolf, Steven B Bleyl, Philip R Brauer, P.H.F.-W. (2015) *Larsen's Human Embriology*.

Gehring, W.J., Qian, Y.Q., Billeter, M., et al. (1994) Homeodomain-DNA recognition. *Cell*, 78 (2): 211–23. doi:10.1016/0092-8674(94)90292-5.

Gerrard, L., Rodgers, L. and Cui, W. (2005) Differentiation of human embryonic stem cells to neural lineages in adherent culture by blocking bone morphogenetic protein signaling. *Stem cells (Dayton, Ohio)*, 23 (9): 1234–41. doi:10.1634/stemcells.2005-0110.

Gleason, R.J., Akintobi, A.M., Grant, B.D., et al. (2014) BMP signaling requires retromer-dependent recycling of the type I receptor. *Proceedings of the National Academy of Sciences of the United States of America*, 111 (7): 2578–83. doi:10.1073/pnas.1319947111.

Goldberg, J. (1999) Structural and functional analysis of the ARF1-ARFGAP complex reveals a role for coatomer in GTP hydrolysis. *Cell*, 96 (6): 893–902. doi:10.1016/S0092-8674(00)80598-X.

Gordon, K.J. and Blobe, G.C. (2008) Role of transforming growth factor-beta superfamily signaling pathways in human disease. *Biochimica et biophysica acta*, 1782 (4): 197–228. doi:10.1016/j.bbadis.2008.01.006.

Goto, K., Kamiya, Y., Imamura, T., et al. (2007) Selective inhibitory effects of Smad6 on bone morphogenetic protein type I receptors. *The Journal of biological chemistry*, 282 (28): 20603–11. doi:10.1074/jbc.M702100200.

Greber, B., Coulon, P., Zhang, M., et al. (2011) FGF signalling inhibits neural induction in human embryonic stem cells. *The EMBO journal*, 30 (24): 4874–84. doi:10.1038/emboj.2011.407.

Groppe, J., Hinck, C.S., Samavarchi-Tehrani, P., et al. (2008) Cooperative Assembly of TGF-β Superfamily Signaling Complexes Is Mediated by Two Disparate Mechanisms and Distinct Modes of Receptor Binding. *Molecular Cell*, 29 (2): 157–168. doi:10.1016/j.molcel.2007.11.039.

Grskovic, M., Javaherian, A., Strulovici, B., et al. (2011) Induced pluripotent stem cells--opportunities for disease modelling and drug discovery. *Nature reviews. Drug discovery*, 10 (12): 915–29. doi:10.1038/nrd3577.

Di Guglielmo, G.M., Le Roy, C., Goodfellow, A.F., et al. (2003) Distinct endocytic pathways regulate TGF-beta receptor signalling and turnover. *Nature cell biology*, 5 (5): 410–21. doi:10.1038/ncb975.

Hanyu, A., Ishidou, Y., Ebisawa, T., et al. (2001) The N domain of Smad7 is essential for specific inhibition of transforming growth factor-beta signaling. *The Journal of cell biology*, 155 (6): 1017–27. doi:10.1083/jcb.200106023.

Harrison, C.A., Al-Musawi, S.L. and Walton, K.L. (2011) Prodomains regulate the synthesis, extracellular

localisation and activity of TGF-β superfamily ligands. *Growth factors (Chur, Switzerland)*, 29 (5): 174–86. doi:10.3109/08977194.2011.608666.

Hartung, A., Bitton-Worms, K., Rechtman, M.M., et al. (2006) Different Routes of Bone Morphogenic Protein (BMP) Receptor Endocytosis Influence BMP Signaling. *Molecular and Cellular Biology*, 26 (20): 7791–7805. doi:10.1128/MCB.00022-06.

Hashimoto, A., Hashimoto, S., Ando, R., et al. (2011) GEP100-Arf6-AMAP1-cortactin pathway frequently used in cancer invasion is activated by VEGFR2 to promote angiogenesis. *PloS one*, 6 (8): e23359. doi:10.1371/journal.pone.0023359.

Hayes, S., Chawla, A. and Corvera, S. (2002) TGF beta receptor internalization into EEA1-enriched early endosomes: role in signaling to Smad2. *The Journal of cell biology*, 158 (7): 1239–49. doi:10.1083/jcb.200204088.

Heining, E., Bhushan, R., Paarmann, P., et al. (2011) Spatial segregation of BMP/Smad signaling affects osteoblast differentiation in C2C12 cells. *PloS one*, 6 (10): e25163. doi:10.1371/journal.pone.0025163.

Heldin, C.-H. and Moustakas, A. (2016) Signaling Receptors for TGF-β Family Members. *Cold Spring Harbor perspectives in biology*, 8 (8). doi:10.1101/cshperspect.a022053.

Henne, W.M., Boucrot, E., Meinecke, M., et al. (2010) FCHo proteins are nucleators of clathrin-mediated endocytosis. *Science (New York, N.Y.)*, 328 (5983): 1281–4. doi:10.1126/science.1188462.

Hinck, A.P. (2012) Structural studies of the TGF-βs and their receptors - insights into evolution of the TGF-β superfamily. *FEBS letters*, 586 (14): 1860–70. doi:10.1016/j.febslet.2012.05.028.

Hinshaw, J.E. and Schmid, S.L. (1995) Dynamin self-assembles into rings suggesting a mechanism for coated vesicle budding. *Nature*, 374 (6518): 190–2. doi:10.1038/374190a0.

Hocevar, B.A., Smine, A., Xu, X.X., et al. (2001) The adaptor molecule Disabled-2 links the transforming growth factor beta receptors to the Smad pathway. *The EMBO journal*, 20 (11): 2789–801. doi:10.1093/emboj/20.11.2789.

Hongu, T., Funakoshi, Y., Fukuhara, S., et al. (2015) Arf6 regulates tumour angiogenesis and growth through HGF-induced endothelial β1 integrin recycling. *Nature communications*, 6: 7925. doi:10.1038/ncomms8925.

Honmou, O., Houkin, K., Matsunaga, T., et al. (2011) Intravenous administration of auto serum-expanded autologous mesenchymal stem cells in stroke. *Brain : a journal of neurology*, 134 (Pt 6): 1790–807. doi:10.1093/brain/awr063.

Huang, H.M., Chang, T.W. and Liu, J.C. (2004) Basic fibroblast growth factor antagonizes activin A-mediated growth inhibition and hemoglobin synthesis in K562 cells by activating ERK1/2 and deactivating p38 MAP kinase. *Biochemical and Biophysical Research Communications*, 320 (4): 1247–1252. doi:10.1016/j.bbrc.2004.06.083.

Huse, M., Muir, T.W., Xu, L., et al. (2001) The TGF beta receptor activation process: an inhibitor- to substrate-binding switch. *Molecular cell*, 8 (3): 671–82. doi:10.1016/S1097-2765(01)00332-X.

Hyman, T., Shmuel, M. and Altschuler, Y. (2006) Actin is required for endocytosis at the apical surface of Madin-Darby canine kidney cells where ARF6 and clathrin regulate the actin cytoskeleton. *Molecular biology of the cell*, 17 (1): 427–37. doi:10.1091/mbc.E05-05-0420.

Inman, G.J., Nicolás, F.J. and Hill, C.S. (2002) Nucleocytoplasmic shuttling of Smads 2, 3, and 4 permits sensing of TGF-beta receptor activity. *Molecular cell*, 10 (2): 283–94. doi:S1097276502005853 [pii].

International Stem Cell Initiative Consortium, Akopian, V., Andrews, P.W., et al. (2010) Comparison of defined culture systems for feeder cell free propagation of human embryonic stem cells. *In vitro cellular & developmental biology. Animal*, 46 (3–4): 247–58. doi:10.1007/s11626-010-9297-z.

Itoh, S., Thorikay, M., Kowanetz, M., et al. (2003) Elucidation of Smad requirement in transforming growth factor-beta type I receptor-induced responses. *The Journal of biological chemistry*, 278 (6): 3751–61. doi:10.1074/jbc.M208258200.

Jackson, T.R., Brown, F.D., Nie, Z., et al. (2000a) ACAPs are arf6 GTPase-activating proteins that function in the cell periphery. *The Journal of cell biology*, 151 (3): 627–38. doi:10.1083/jcb.151.3.627.

Jackson, T.R., Kearns, B.G. and Theibert, A.B. (2000b) Cytohesins and centaurins: mediators of PI 3-kinase-regulated Arf signaling. *Trends in biochemical sciences*, 25 (10): 489–95. doi:10.1016/S0968-0004(00)01644-3.

James, D., Levine, A.J., Besser, D., et al. (2005) TGFbeta/activin/nodal signaling is necessary for the maintenance of pluripotency in human embryonic stem cells. *Development (Cambridge, England)*, 132 (6): 1273–82. doi:10.1242/dev.01706.

Jovanovic, O.A., Brown, F.D. and Donaldson, J.G. (2006) An effector domain mutant of Arf6 implicates phospholipase D in endosomal membrane recycling. *Molecular biology of the cell*, 17 (1): 327–35. doi:10.1091/mbc.E05-06-0523.

Julien, S., Puig, I., Caretti, E., et al. (2007) Activation of NF-kappaB by Akt upregulates Snail expression and induces epithelium mesenchyme transition. *Oncogene*, 26 (53): 7445–56. doi:10.1038/sj.onc.1210546.

Jullien, J. and Gurdon, J. (2005) Morphogen gradient interpretation by a regulated trafficking step during ligand-receptor transduction. *Genes & development*, 19 (22): 2682–94. doi:10.1101/gad.341605.

Kang, H.B., Kim, J.S., Kwon, H.-J., et al. (2005) Basic fibroblast growth factor activates ERK and induces c-fos in human embryonic stem cell line MizhES1. *Stem cells and development*, 14 (4): 395–401. doi:10.1089/scd.2005.14.395.

Kang, M.H., Oh, S.C., Lee, H.J., et al. (2011) Metastatic function of BMP-2 in gastric cancer cells: the role of PI3K/AKT, MAPK, the NF-κB pathway, and MMP-9 expression. *Experimental cell research*, 317 (12): 1746–62. doi:10.1016/j.yexcr.2011.04.006.

Katoh, M. and Katoh, M. (2006) CER1 is a common target of WNT and NODAL signaling pathways in human embryonic stem cells. *International journal of molecular medicine*, 17 (5): 795–9. doi:10.3892/ijmm.17.5.795.

Kawagishi, R., Tahara, M., Sawada, K., et al. (2004) Na+ / H+ exchanger-3 is involved in mouse blastocyst formation. *Journal of experimental zoology. Part A, Comparative experimental biology*, 301 (9): 767–75. doi:10.1002/jez.a.90.

Kfoury, Y. and Scadden, D.T. (2015) Mesenchymal cell contributions to the stem cell niche. *Cell stem cell*, 16 (3): 239–53. doi:10.1016/j.stem.2015.02.019.

Kim, J., Johnson, K., Chen, H.J., et al. (1997) Drosophila Mad binds to DNA and directly mediates activation of

vestigial by Decapentaplegic. *Nature*, 388 (6639): 304–8. doi:10.1038/40906.

Kim, M.-S., Horst, A., Blinka, S., et al. (2015) Activin-A and Bmp4 levels modulate cell type specification during CHIR-induced cardiomyogenesis. *PloS one*, 10 (2): e0118670. doi:10.1371/journal.pone.0118670.

Kimbrel, E.A. and Lanza, R. (2016) Pluripotent stem cells: the last 10 years. *Regenerative medicine*, 11 (8): 831–847. doi:10.2217/rme-2016-0117.

Klarlund, J.K., Guilherme, A., Holik, J.J., et al. (1997) Signaling by phosphoinositide-3,4,5-trisphosphate through proteins containing pleckstrin and Sec7 homology domains. *Science (New York, N.Y.)*, 275 (5308): 1927–30. doi:10.1126/science.275.5308.1927.

Kolios, G. and Moodley, Y. (2013) Introduction to stem cells and regenerative medicine. *Respiration; international review of thoracic diseases*, 85 (1): 3–10. doi:10.1159/000345615.

Kon, S., Tanabe, K., Watanabe, T., et al. (2008) Clathrin dependent endocytosis of E-cadherin is regulated by the Arf6GAP isoform SMAP1. *Experimental cell research*, 314 (7): 1415–28. doi:10.1016/j.yexcr.2007.11.006.

Kopp, J.L., Ormsbee, B.D., Desler, M., et al. (2008) Small increases in the level of Sox2 trigger the differentiation of mouse embryonic stem cells. *Stem cells (Dayton, Ohio)*, 26 (4): 903–11. doi:10.1634/stemcells.2007-0951.

Krakowski, A.R., Laboureau, J., Mauviel, A., et al. (2005) Cytoplasmic SnoN in normal tissues and nonmalignant cells antagonizes TGF-beta signaling by sequestration of the Smad proteins. *Proceedings of the National Academy of Sciences of the United States of America*, 102 (35): 12437–42. doi:10.1073/pnas.0504107102.

Kretzschmar, M., Doody, J. and Massagué, J. (1997) Opposing BMP and EGF signalling pathways converge on the TGF-beta family mediator Smad1. *Nature*, 389 (6651): 618–22. doi:10.1038/39348.

Kretzschmar, M. and Massagué, J. (1998) SMADs: mediators and regulators of TGF-beta signaling. *Current opinion in genetics & development*, 8 (1): 103–11. doi:10.1016/S0959-437X(98)80069-5.

Kroon, E., Martinson, L.A., Kadoya, K., et al. (2008) Pancreatic endoderm derived from human embryonic stem cells generates glucose-responsive insulin-secreting cells in vivo. *Nature biotechnology*, 26 (4): 443–52. doi:10.1038/nbt1393.

Krugmann, S., Andrews, S., Stephens, L., et al. (2006) ARAP3 is essential for formation of lamellipodia after growth factor stimulation. *Journal of cell science*, 119 (Pt 3): 425–32. doi:10.1242/jcs.02755.

Kühl, S.J. and Kühl, M. (2013) On the role of Wnt/β-catenin signaling in stem cells. *Biochimica et biophysica acta*, 1830 (2): 2297–306. doi:10.1016/j.bbagen.2012.08.010.

Kumari, S. and Mayor, S. (2008) ARF1 is directly involved in dynamin-independent endocytosis. *Nature cell biology*, 10 (1): 30–41. doi:10.1038/ncb1666.

Kurek, D., Neagu, A., Tastemel, M., et al. (2015) Endogenous WNT signals mediate BMP-induced and spontaneous differentiation of epiblast stem cells and human embryonic stem cells. *Stem cell reports*, 4 (1): 114–28. doi:10.1016/j.stemcr.2014.11.007.

Labbé, E., Silvestri, C., Hoodless, P.A., et al. (1998) Smad2 and Smad3 positively and negatively regulate TGF beta-dependent transcription through the forkhead DNA-binding protein FAST2. *Molecular cell*, 2 (1): 109–20.

Available at: http://www.ncbi.nlm.nih.gov/pubmed/9702197 (Accessed: 1 February 2018).

Lafourcade, C., Sobo, K., Kieffer-Jaquinod, S., et al. (2008) Regulation of the V-ATPase along the endocytic pathway occurs through reversible subunit association and membrane localization. *PloS one*, 3 (7): e2758. doi:10.1371/journal.pone.0002758.

Lai, C.-F. and Cheng, S.-L. (2002) Signal transductions induced by bone morphogenetic protein-2 and transforming growth factor-beta in normal human osteoblastic cells. *The Journal of biological chemistry*, 277 (18): 15514–15522. doi:10.1074/jbc.M200794200.

Lamouille, S., Connolly, E., Smyth, J.W., et al. (2012) TGF-β-induced activation of mTOR complex 2 drives epithelial-mesenchymal transition and cell invasion. *Journal of cell science*, 125 (Pt 5): 1259–73. doi:10.1242/jcs.095299.

Lamouille, S. and Derynck, R. (2007) Cell size and invasion in TGF-beta-induced epithelial to mesenchymal transition is regulated by activation of the mTOR pathway. *The Journal of cell biology*, 178 (3): 437–51. doi:10.1083/jcb.200611146.

Laroche, G., Giguère, P.M., Dupré, E., et al. (2007) The N-terminal coiled-coil domain of the cytohesin/ARNO family of guanine nucleotide exchange factors interacts with Galphaq. *Molecular and cellular biochemistry*, 306 (1–2): 141–52. doi:10.1007/s11010-007-9564-9.

Lazarus, H.M., Haynesworth, S.E., Gerson, S.L., et al. (1995) Ex vivo expansion and subsequent infusion of human bone marrow-derived stromal progenitor cells (mesenchymal progenitor cells): implications for therapeutic use. *Bone marrow transplantation*, 16 (4): 557–64. Available at: http://www.ncbi.nlm.nih.gov/pubmed/8528172.

Li, H.-S., Shome, K., Rojas, R., et al. (2003) The guanine nucleotide exchange factor ARNO mediates the activation of ARF and phospholipase D by insulin. *BMC cell biology*, 4: 13. doi:10.1186/1471-2121-4-13.

Li, Z., Fei, T., Zhang, J., et al. (2012) BMP4 Signaling Acts via dual-specificity phosphatase 9 to control ERK activity in mouse embryonic stem cells. *Cell stem cell*, 10 (2): 171–82. doi:10.1016/j.stem.2011.12.016.

Liao, J., Wu, Z., Wang, Y., et al. (2008) Enhanced efficiency of generating induced pluripotent stem (iPS) cells from human somatic cells by a combination of six transcription factors. *Cell research*, 18 (5): 600–3. doi:10.1038/cr.2008.51.

Lin, Z., Gao, C., Ning, Y., et al. (2008) The pseudoreceptor BMP and activin membrane-bound inhibitor positively modulates Wnt/beta-catenin signaling. *The Journal of biological chemistry*, 283 (48): 33053–8. doi:10.1074/jbc.M804039200.

Liu, P., Chen, M., Liu, Y., et al. (2018) CRISPR-Based Chromatin Remodeling of the Endogenous Oct4 or Sox2 Locus Enables Reprogramming to Pluripotency. *Cell Stem Cell*, pp. 1–10. doi:10.1016/j.stem.2017.12.001.

De Los Angeles, A., Ferrari, F., Xi, R., et al. (2015) Hallmarks of pluripotency. *Nature*, 525 (7570): 469–78. doi:10.1038/nature15515.

Ludwig, T.E., Bergendahl, V., Levenstein, M.E., et al. (2006) Feeder-independent culture of human embryonic stem cells. *Nature methods*, 3 (8): 637–46. doi:10.1038/nmeth902.

Lundmark, R., Doherty, G.J., Howes, M.T., et al. (2008) The GTPase-activating protein GRAF1 regulates the

CLIC/GEEC endocytic pathway. *Current biology : CB*, 18 (22): 1802–8. doi:10.1016/j.cub.2008.10.044.

Lupo, G., Novorol, C., Smith, J.R., et al. (2013) Multiple roles of Activin/Nodal, bone morphogenetic protein, fibroblast growth factor and Wnt/β-catenin signalling in the anterior neural patterning of adherent human embryonic stem cell cultures. *Open biology*, 3 (4): 120167. doi:10.1098/rsob.120167.

Martin, G.R. (1981) Isolation of a pluripotent cell line from early mouse embryos cultured in medium conditioned by teratocarcinoma stem cells. *Proceedings of the National Academy of Sciences of the United States of America*, 78 (12): 7634–8. doi:10.1073/pnas.78.12.7634.

Massagué, J. (2008) TGFbeta in Cancer. *Cell*, 134 (2): 215–30. doi:10.1016/j.cell.2008.07.001.

Maxfield, F.R. and McGraw, T.E. (2004) Endocytic recycling. *Nature reviews. Molecular cell biology*, 5 (2): 121–32. doi:10.1038/nrm1315.

Maxfield, F.R. and Yamashiro, D.J. (1987) Endosome acidification and the pathways of receptor-mediated endocytosis. *Advances in experimental medicine and biology*, 225: 189–98. doi:10.1007/978-1-4684-5442-0_16.

McMahon, J.A., Takada, S., Zimmerman, L.B., et al. (1998) Noggin-mediated antagonism of BMP signaling is required for growth and patterning of the neural tube and somite. *Genes & development*, 12 (10): 1438–52. doi:10.1101/gad.12.10.1438.

Mellman, I. (1996) Endocytosis and molecular sorting. *Annual review of cell and developmental biology*, 12 (1): 575–625. doi:10.1146/annurev.cellbio.12.1.575.

Mellman, I., Fuchs, R. and Helenius, A. (1986) Acidification of the endocytic and exocytic pathways. *Annual review of biochemistry*, 55: 663–700. doi:10.1146/annurev.bi.55.070186.003311.

Mercer, J., Schelhaas, M. and Helenius, A. (2010) Virus entry by endocytosis. *Annual review of biochemistry*, 79: 803–33. doi:10.1146/annurev-biochem-060208-104626.

De Miguel, M.P., Fuentes-Julián, S. and Alcaina, Y. (2010) Pluripotent stem cells: origin, maintenance and induction. *Stem cell reviews*, 6 (4): 633–649. doi:10.1007/s12015-010-9170-1.

Mitchell, H., Choudhury, A., Pagano, R.E., et al. (2004) Ligand-dependent and -independent transforming growth factor-beta receptor recycling regulated by clathrin-mediated endocytosis and Rab11. *Molecular biology of the cell*, 15 (9): 4166–78. doi:10.1091/mbc.E04-03-0245.

Mitsui, K., Tokuzawa, Y., Itoh, H., et al. (2003) The homeoprotein nanog is required for maintenance of pluripotency in mouse epiblast and ES cells. *Cell*, 113 (5): 631–642. doi:10.1016/S0092-8674(03)00393-3.

Miyazawa, K. and Miyazono, K. (2017) Regulation of TGF-β Family Signaling by Inhibitory Smads. *Cold Spring Harbor perspectives in biology*, 9 (3): 1–26. doi:10.1101/cshperspect.a022095.

Morikawa, M., Koinuma, D., Mizutani, A., et al. (2016) BMP Sustains Embryonic Stem Cell Self-Renewal through Distinct Functions of Different Krüppel-like Factors. *Stem cell reports*, 6 (1): 64–73. doi:10.1016/j.stemcr.2015.12.004.

Morikawa, M., Koinuma, D., Tsutsumi, S., et al. (2011) ChIP-seq reveals cell type-specific binding patterns of BMP-specific Smads and a novel binding motif. *Nucleic Acids Research*, 39 (20): 8712–8727. doi:10.1093/nar/gkr572.

Morishige, M., Hashimoto, S., Ogawa, E., et al. (2008) GEP100 links epidermal growth factor receptor signalling to Arf6 activation to induce breast cancer invasion. *Nature cell biology*, 10 (1): 85–92. doi:10.1038/ncb1672.

Moustakas, A. and Heldin, C.-H. (2009) The regulation of TGFbeta signal transduction. *Development (Cambridge, England)*, 136 (22): 3699–714. doi:10.1242/dev.030338.

Mueller, T.D. and Nickel, J. (2012) Promiscuity and specificity in BMP receptor activation. *FEBS letters*, 586 (14): 1846–59. doi:10.1016/j.febslet.2012.02.043.

Müller, M.P. and Goody, R.S. (2017) Molecular control of Rab activity by GEFs, GAPs and GDI. *Small GTPases*, pp. 1–17. doi:10.1080/21541248.2016.1276999.

Na, J., Furue, M.K. and Andrews, P.W. (2010) Inhibition of ERK1/2 prevents neural and mesendodermal differentiation and promotes human embryonic stem cell self-renewal. *Stem cell research*, 5 (2): 157–69. doi:10.1016/j.scr.2010.06.002.

Nakashima, S., Morinaka, K., Koyama, S., et al. (1999) Small G protein Ral and its downstream molecules regulate endocytosis of EGF and insulin receptors. *The EMBO journal*, 18 (13): 3629–42. doi:10.1093/emboj/18.13.3629.

Namwanje, M. and Brown, C.W. (2016) Activins and Inhibins: Roles in Development, Physiology, and Disease. *Cold Spring Harbor perspectives in biology*, 8 (7). doi:10.1101/cshperspect.a021881.

Naslavsky, N., Weigert, R. and Donaldson, J.G. (2004) Characterization of a nonclathrin endocytic pathway: membrane cargo and lipid requirements. *Molecular biology of the cell*, 15 (8): 3542–52. doi:10.1091/mbc.E04-02-0151.

Natsume, W., Tanabe, K., Kon, S., et al. (2006) SMAP2, a novel ARF GTPase-activating protein, interacts with clathrin and clathrin assembly protein and functions on the AP-1-positive early endosome/trans-Golgi network. *Molecular biology of the cell*, 17 (6): 2592–603. doi:10.1091/mbc.E05-10-0909.

Niakan, K.K. and Eggan, K. (2013) Analysis of human embryos from zygote to blastocyst reveals distinct gene expression patterns relative to the mouse. *Developmental biology*, 375 (1): 54–64. doi:10.1016/j.ydbio.2012.12.008.

Nichols, J., Zevnik, B., Anastassiadis, K., et al. (1998) Formation of pluripotent stem cells in the mammalian embryo depends on the POU transcription factor Oct4. *Cell*, 95 (3): 379–91. doi:10.1016/S0092-8674(00)81769-9.

Nishioka, N., Inoue, K., Adachi, K., et al. (2009) The Hippo signaling pathway components Lats and Yap pattern Tead4 activity to distinguish mouse trophectoderm from inner cell mass. *Developmental cell*, 16 (3): 398–410. doi:10.1016/j.devcel.2009.02.003.

Niwa, H., Miyazaki, J. and Smith, A.G. (2000) Quantitative expression of Oct-3/4 defines differentiation, dedifferentiation or self-renewal of ES cells. *Nature genetics*, 24 (4): 372–6. doi:10.1038/74199.

Norrman, K., Fischer, Y., Bonnamy, B., et al. (2010) Quantitative comparison of constitutive promoters in human ES cells. *PloS one*, 5 (8): e12413. doi:10.1371/journal.pone.0012413.

O'Connor, M.B., Umulis, D., Othmer, H.G., et al. (2006) Shaping BMP morphogen gradients in the Drosophila embryo and pupal wing. *Development (Cambridge, England)*, 133 (2): 183–93. doi:10.1242/dev.02214.

Obokata, H., Wakayama, T., Sasai, Y., et al. (2014) Stimulus-triggered fate conversion of somatic cells into

pluripotency. *Nature*, 505 (7485): 641–7. doi:10.1038/nature12968.

Ogihara, T., Watada, H., Kanno, R., et al. (2003) p38 MAPK is involved in activin A- and hepatocyte growth factor-mediated expression of pro-endocrine gene neurogenin 3 in AR42J-B13 cells. *The Journal of biological chemistry*, 278 (24): 21693–700. doi:10.1074/jbc.M302684200.

Olsen, J. V., Vermeulen, M., Santamaria, A., et al. (2010) Quantitative phosphoproteomics reveals widespread full phosphorylation site occupancy during mitosis. *Science signaling*, 3 (104): ra3. doi:10.1126/scisignal.2000475.

Olsson, N., Piek, E., Sundström, M., et al. (2001) Transforming growth factor-beta-mediated mast cell migration depends on mitogen-activated protein kinase activity. *Cellular signalling*, 13 (7): 483–90. doi:S0898656801001760 [pii].

Onel, S., Bolke, L. and Klämbt, C. (2004) The Drosophila ARF6-GEF Schizo controls commissure formation by regulating Slit. *Development (Cambridge, England)*, 131 (11): 2587–94. doi:10.1242/dev.01147.

Onichtchouk, D., Chen, Y.G., Dosch, R., et al. (1999) Silencing of TGF-beta signalling by the pseudoreceptor BAMBI. *Nature*, 401 (6752): 480–5. doi:10.1038/46794.

Oshimori, N. and Fuchs, E. (2012) The harmonies played by TGF-β in stem cell biology. *Cell stem cell*, 11 (6): 751–64. doi:10.1016/j.stem.2012.11.001.

Ozdamar, B., Bose, R., Barrios-Rodiles, M., et al. (2005) Regulation of the polarity protein Par6 by TGFbeta receptors controls epithelial cell plasticity. *Science (New York, N.Y.)*, 307 (5715): 1603–9. doi:10.1126/science.1105718.

Paarmann, P., Dörpholz, G., Fiebig, J., et al. (2016) Dynamin-dependent endocytosis of Bone Morphogenetic Protein2 (BMP2) and its receptors is dispensable for the initiation of Smad signaling. *The international journal of biochemistry & cell biology*, 76: 51–63. doi:10.1016/j.biocel.2016.04.010.

Le Page, C., Puiffe, M.-L., Meunier, L., et al. (2009) BMP-2 signaling in ovarian cancer and its association with poor prognosis. *Journal of ovarian research*, 2 (1): 4. doi:10.1186/1757-2215-2-4.

Palacios, F., Schweitzer, J.K., Boshans, R.L., et al. (2002) ARF6-GTP recruits Nm23-H1 to facilitate dynamin-mediated endocytosis during adherens junctions disassembly. *Nature cell biology*, 4 (12): 929–36. doi:10.1038/ncb881.

Di Paolo, G. and De Camilli, P. (2006) Phosphoinositides in cell regulation and membrane dynamics. *Nature*, 443 (7112): 651–7. doi:10.1038/nature05185.

Paris, S., Béraud-Dufour, S., Robineau, S., et al. (1997) Role of protein-phospholipid interactions in the activation of ARF1 by the guanine nucleotide exchange factor Arno. *The Journal of biological chemistry*, 272 (35): 22221–6. doi:10.1074/jbc.272.35.22221.

Parton, R.G. and del Pozo, M.A. (2013) Caveolae as plasma membrane sensors, protectors and organizers. *Nature reviews. Molecular cell biology*, 14 (2): 98–112. doi:10.1038/nrm3512.

Parton, R.G. and Simons, K. (2007) The multiple faces of caveolae. *Nature reviews. Molecular cell biology*, 8 (3): 185–94. doi:10.1038/nrm2122.

Pasqualato, S., Ménétrey, J., Franco, M., et al. (2001) The structural GDP/GTP cycle of human Arf6. *EMBO Reports*, 2 (3): 234–238. doi:10.1093/embo-reports/kve043.

Pasqualato, S., Renault, L. and Cherfils, J. (2002) Arf, Arl, Arp and Sar proteins: a family of GTP-binding proteins with a structural device for "front-back" communication. *EMBO reports*, 3 (11): 1035–41. doi:10.1093/embo-reports/kvf221.

Passier, R. and Mummery, C. (2003) Origin and use of embryonic and adult stem cells in differentiation and tissue repair. *Cardiovascular research*, 58 (2): 324–35. doi:10.1016/S0008-6363(02)00770-8.

Paulsen, M., Legewie, S., Eils, R., et al. (2011) Negative feedback in the bone morphogenetic protein 4 (BMP4) synexpression group governs its dynamic signaling range and canalizes development. *Proceedings of the National Academy of Sciences of the United States of America*, 108 (25): 10202–7. doi:10.1073/pnas.1100179108.

Pellon-Cardenas, O., Clancy, J., Uwimpuhwe, H., et al. (2013) ARF6-regulated endocytosis of growth factor receptors links cadherin-based adhesion to canonical Wnt signaling in epithelia. *Molecular and cellular biology*, 33 (15): 2963–75. doi:10.1128/MCB.01698-12.

Penheiter, S.G., Mitchell, H., Garamszegi, N., et al. (2002) Internalization-dependent and -independent requirements for transforming growth factor beta receptor signaling via the Smad pathway. *Molecular and cellular biology*, 22 (13): 4750–9. doi:10.1128/MCB.22.13.4750.

Pesce, M. and Schöler, H.R. (2000) Oct-4: control of totipotency and germline determination. *Molecular reproduction and development*, 55 (4): 452–7. doi:10.1002/(SICI)1098-2795(200004)55:4<452::AID-MRD14>3.0.CO;2-S.

Peters, P.J., Hsu, V.W., Ooi, C.E., et al. (1995) Overexpression of wild-type and mutant ARF1 and ARF6: distinct perturbations of nonoverlapping membrane compartments. *The Journal of cell biology*, 128 (6): 1003–17. doi:10.1083/jcb.128.6.1003.

Pierreux, C.E., Nicolás, F.J. and Hill, C.S. (2000) Transforming growth factor beta-independent shuttling of Smad4 between the cytoplasm and nucleus. *Molecular and cellular biology*, 20 (23): 9041–54. doi:10.1128/MCB.20.23.9041-9054.2000.

Pietras, E.M., Warr, M.R. and Passegué, E. (2011) Cell cycle regulation in hematopoietic stem cells. *The Journal of cell biology*, 195 (5): 709–20. doi:10.1083/jcb.201102131.

Premont, R.T., Claing, A., Vitale, N., et al. (1998) beta2-Adrenergic receptor regulation by GIT1, a G protein-coupled receptor kinase-associated ADP ribosylation factor GTPase-activating protein. *Proceedings of the National Academy of Sciences of the United States of America*, 95 (24): 14082–7. doi:10.1073/pnas.95.24.14082.

Raftery, L.A., Twombly, V., Wharton, K., et al. (1995) Genetic screens to identify elements of the decapentaplegic signaling pathway in Drosophila. *Genetics*, 139 (1): 241–54. Available at: http://www.ncbi.nlm.nih.gov/pubmed/7705627.

Ratajczak, M.Z., Zuba-Surma, E., Kucia, M., et al. (2012) Pluripotent and multipotent stem cells in adult tissues. *Advances in medical sciences*, 57 (1): 1–17. doi:10.2478/v10039-012-0020-z.

Reményi, A., Lins, K., Nissen, L.J., et al. (2003) Crystal structure of a POU/HMG/DNA ternary complex suggests

differential assembly of Oct4 and Sox2 on two enhancers. *Genes & development*, 17 (16): 2048–59. doi:10.1101/gad.269303.

Richter, A., Valdimarsdottir, L., Hrafnkelsdottir, H.E., et al. (2014) BMP4 promotes EMT and mesodermal commitment in human embryonic stem cells via SLUG and MSX2. *Stem cells (Dayton, Ohio)*, 32 (3): 636–48. doi:10.1002/stem.1592.

Robertson, S.E., Setty, S.R.G., Sitaram, A., et al. (2006) Extracellular signal-regulated kinase regulates clathrin-independent endosomal trafficking. *Molecular biology of the cell*, 17 (2): 645–57. doi:10.1091/mbc.E05-07-0662.

Römer, W., Pontani, L.-L., Sorre, B., et al. (2010) Actin dynamics drive membrane reorganization and scission in clathrin-independent endocytosis. *Cell*, 140 (4): 540–53. doi:10.1016/j.cell.2010.01.010.

Roode, M., Blair, K., Snell, P., et al. (2012) Human hypoblast formation is not dependent on FGF signalling. *Developmental biology*, 361 (2): 358–63. doi:10.1016/j.ydbio.2011.10.030.

Rossant, J. and Tam, P.P.L. (2017) New Insights into Early Human Development: Lessons for Stem Cell Derivation and Differentiation. *Cell stem cell*, 20 (1): 18–28. doi:10.1016/j.stem.2016.12.004.

Saharinen, J., Hyytiäinen, M., Taipale, J., et al. (1999) Latent transforming growth factor-beta binding proteins (LTBPs)--structural extracellular matrix proteins for targeting TGF-beta action. *Cytokine & growth factor reviews*, 10 (2): 99–117. doi:S1359610199000106 [pii].

Sakagami, H. (2008) The EFA6 family: guanine nucleotide exchange factors for ADP ribosylation factor 6 at neuronal synapses. *The Tohoku journal of experimental medicine*, 214 (3): 191–8. doi:10.1620/tjem.214.191.

Sakurai, A., Jian, X., Lee, C.J., et al. (2011) Phosphatidylinositol-4-phosphate 5-kinase and GEP100/Brag2 protein mediate antiangiogenic signaling by semaphorin 3E-plexin-D1 through Arf6 protein. *The Journal of biological chemistry*, 286 (39): 34335–45. doi:10.1074/jbc.M111.259499.

Sangar, F., Schreurs, A.S., Umaña-Diaz, C., et al. (2014) Involvement of small ArfGAP1 (SMAP1), a novel Arf6-specific GTPase-activating protein, in microsatellite instability oncogenesis. *Oncogene*, 33 (21): 2758–2767. doi:10.1038/onc.2013.211.

Santy, L.C. (2002) Characterization of a fast cycling ADP-ribosylation factor 6 mutant. *The Journal of biological chemistry*, 277 (43): 40185–8. doi:10.1074/jbc.C200481200.

Sato, N., Meijer, L., Skaltsounis, L., et al. (2004) Maintenance of pluripotency in human and mouse embryonic stem cells through activation of Wnt signaling by a pharmacological GSK-3-specific inhibitor. *Nature medicine*, 10 (1): 55–63. doi:10.1038/nm979.

Saunders, A., Faiola, F. and Wang, J. (2013) Concise review: pursuing self-renewal and pluripotency with the stem cell factor Nanog. *Stem cells (Dayton, Ohio)*, 31 (7): 1227–36. doi:10.1002/stem.1384.

Schmid, B., Fürthauer, M., Connors, S. a, et al. (2000) Equivalent genetic roles for bmp7/snailhouse and bmp2b/swirl in dorsoventral pattern formation. *Development (Cambridge, England)*, 127 (5): 957–67. Available at: http://www.ncbi.nlm.nih.gov/pubmed/10662635.

Schmierer, B. and Hill, C.S. (2007) TGFbeta-SMAD signal transduction: molecular specificity and functional flexibility. *Nature reviews. Molecular cell biology*, 8 (12): 970–82. doi:10.1038/nrm2297.

Schöler, H.R. (1991) Octamania: the POU factors in murine development. *Trends in genetics : TIG*, 7 (10): 323–9. doi:10.1016/0168-9525(91)90422-M.

Schwab, E.H., Pohl, T.L.M., Haraszti, T., et al. (2015) Nanoscale control of surface immobilized BMP-2: toward a quantitative assessment of BMP-mediated signaling events. *Nano letters*, 15 (3): 1526–34. doi:10.1021/acs.nanolett.5b00315.

Schwartz, S.D., Hubschman, J.-P., Heilwell, G., et al. (2012) Embryonic stem cell trials for macular degeneration: a preliminary report. *Lancet (London, England)*, 379 (9817): 713–20. doi:10.1016/S0140-6736(12)60028-2.

Schweitzer, J.K. and D'Souza-Schorey, C. (2002) Localization and activation of the ARF6 GTPase during cleavage furrow ingression and cytokinesis. *The Journal of biological chemistry*, 277 (30): 27210–6. doi:10.1074/jbc.M201569200.

Sekelsky, J.J., Newfeld, S.J., Raftery, L.A., et al. (1995) Genetic characterization and cloning of mothers against dpp, a gene required for decapentaplegic function in Drosophila melanogaster. *Genetics*, 139 (3): 1347–58. Available at: http://www.ncbi.nlm.nih.gov/pubmed/7768443.

Senju, Y., Rosenbaum, E., Shah, C., et al. (2015) Phosphorylation of PACSIN2 by protein kinase C triggers the removal of caveolae from the plasma membrane. *Journal of cell science*, 128 (15): 2766–80. doi:10.1242/jcs.167775.

Seshagiri, P.B., Sen Roy, S., Sireesha, G., et al. (2009) Cellular and molecular regulation of mammalian blastocyst hatching. *Journal of reproductive immunology*, 83 (1–2): 79–84. doi:10.1016/j.jri.2009.06.264.

Shapira, K.E., Gross, A., Ehrlich, M., et al. (2012) Coated pit-mediated endocytosis of the type I Transforming Growth Factor-β (TGF-β) receptor depends on a Di-leucine family signal and is not required for signaling. *Journal of Biological Chemistry*, 287 (32): 26876–26889. doi:10.1074/jbc.M112.362848.

Shi, Y. (2001) Structural insights on Smad function in TGFbeta signaling. *BioEssays : news and reviews in molecular, cellular and developmental biology*, 23 (3): 223–32. doi:10.1002/1521-1878(200103)23:3<223::AID-BIES1032>3.0.CO;2-U.

Shi, Y. and Massagué, J. (2003) Mechanisms of TGF-beta signaling from cell membrane to the nucleus. *Cell*, 113 (6): 685–700. doi:10.1016/S0092-8674(03)00432-X.

Shi, Y., Wang, Y.F., Jayaraman, L., et al. (1998) Crystal structure of a Smad MH1 domain bound to DNA: insights on DNA binding in TGF-beta signaling. *Cell*, 94 (5): 585–94. Available at: http://www.ncbi.nlm.nih.gov/pubmed/9741623 (Accessed: 1 February 2018).

Shibuya, H., Iwata, H., Masuyama, N., et al. (1998) Role of TAK1 and TAB1 in BMP signaling in early Xenopus development. *The EMBO journal*, 17 (4): 1019–28. doi:10.1093/emboj/17.4.1019.

Shimmi, O., Umulis, D., Othmer, H., et al. (2005) Facilitated transport of a Dpp/Scw heterodimer by Sog/Tsg leads to robust patterning of the Drosophila blastoderm embryo. *Cell*, 120 (6): 873–86. doi:10.1016/j.cell.2005.02.009.

Shoji, H., Tsuchida, K., Kishi, H., et al. (2000) Identification and characterization of a PDZ protein that interacts with activin type II receptors. *The Journal of biological chemistry*, 275 (8): 5485–92. doi:10.1074/jbc.275.8.5485.

Shu, Q., Lennemann, N.J., Sarkar, S.N., et al. (2015) ADAP2 Is an Interferon Stimulated Gene That Restricts RNA

Virus Entry. *PLoS pathogens*, 11 (9): e1005150. doi:10.1371/journal.ppat.1005150.

Simeone, D.M., Zhang, L., Graziano, K., et al. (2001) Smad4 mediates activation of mitogen-activated protein kinases by TGF-beta in pancreatic acinar cells. *American journal of physiology. Cell physiology*, 281 (1): C311-9. doi:10.1152/ajpcell.2001.281.1.C311.

Simonsson, M., Kanduri, M., Grönroos, E., et al. (2006) The DNA binding activities of Smad2 and Smad3 are regulated by coactivator-mediated acetylation. *The Journal of biological chemistry*, 281 (52): 39870–80. doi:10.1074/jbc.M607868200.

Singh, A.M., Reynolds, D., Cliff, T., et al. (2012) Signaling network crosstalk in human pluripotent cells: a Smad2/3-regulated switch that controls the balance between self-renewal and differentiation. *Cell stem cell*, 10 (3): 312–26. doi:10.1016/j.stem.2012.01.014.

Skottman, H. and Hovatta, O. (2006) Culture conditions for human embryonic stem cells. *Reproduction (Cambridge, England)*, 132 (5): 691–8. doi:10.1530/rep.1.01079.

Sorkin, A. and von Zastrow, M. (2009) Endocytosis and signalling: intertwining molecular networks. *Nature reviews. Molecular cell biology*, 10 (9): 609–22. doi:10.1038/nrm2748.

Staun-Ram, E. and Shalev, E. (2005) Human trophoblast function during the implantation process. *Reproductive biology and endocrinology : RB&E*, 3: 56. doi:10.1186/1477-7827-3-56.

Stoeber, M., Stoeck, I.K., Hänni, C., et al. (2012) Oligomers of the ATPase EHD2 confine caveolae to the plasma membrane through association with actin. *The EMBO journal*, 31 (10): 2350–64. doi:10.1038/emboj.2012.98.

Strumpf, D., Mao, C.-A., Yamanaka, Y., et al. (2005) Cdx2 is required for correct cell fate specification and differentiation of trophectoderm in the mouse blastocyst. *Development (Cambridge, England)*, 132 (9): 2093–102. doi:10.1242/dev.01801.

Sugimori, K., Matsui, K., Motomura, H., et al. (2005) BMP-2 prevents apoptosis of the N1511 chondrocytic cell line through PI3K/Akt-mediated NF-kappaB activation. *Journal of bone and mineral metabolism*, 23 (6): 411–9. doi:10.1007/s00774-005-0622-7.

Sumi, T., Tsuneyoshi, N., Nakatsuji, N., et al. (2008) Defining early lineage specification of human embryonic stem cells by the orchestrated balance of canonical Wnt/beta-catenin, Activin/Nodal and BMP signaling. *Development (Cambridge, England)*, 135 (17): 2969–79. doi:10.1242/dev.021121.

Sun, P.D. and Davies, D.R. (1995) The cystine-knot growth-factor superfamily. *Annual review of biophysics and biomolecular structure*, 24 (1): 269–91. doi:10.1146/annurev.bb.24.060195.001413.

Suzuki, T., Kanai, Y., Hara, T., et al. (2006) Crucial role of the small GTPase ARF6 in hepatic cord formation during liver development. *Molecular and cellular biology*, 26 (16): 6149–56. doi:10.1128/MCB.00298-06.

Takahashi, K. and Yamanaka, S. (2006) Induction of Pluripotent Stem Cells from Mouse Embryonic and Adult Fibroblast Cultures by Defined Factors. *Cell*, 126 (4): 663–676. doi:10.1016/j.cell.2006.07.024.

Tanabe, K., Torii, T., Natsume, W., et al. (2005) A novel GTPase-activating protein for ARF6 directly interacts with clathrin and regulates clathrin-dependent endocytosis. *Molecular biology of the cell*, 16 (4): 1617–28. doi:10.1091/mbc.E04-08-0683.

Teo, A.K.K., Arnold, S.J., Trotter, M.W.B., et al. (2011) Pluripotency factors regulate definitive endoderm specification through eomesodermin. *Genes and Development*, 25 (3): 238–250. doi:10.1101/gad.607311.

Thomson, J. a, Itskovitz-Eldor, J., Shapiro, S.S., et al. (1998) Embryonic stem cell lines derived from human blastocysts. *Science (New York, N.Y.)*, 282 (5391): 1145–7. doi:10.1126/science.282.5391.1145.

Tse, W.T., Pendleton, J.D., Beyer, W.M., et al. (2003) Suppression of allogeneic T-cell proliferation by human marrow stromal cells: implications in transplantation. *Transplantation*, 75 (3): 389–97. doi:10.1097/01.TP.0000045055.63901.A9.

Tsuchida, K., Nakatani, M., Matsuzaki, T., et al. (2004) Novel factors in regulation of activin signaling. *Molecular and cellular endocrinology*, 225 (1–2): 1–8. doi:10.1016/j.mce.2004.02.006.

Tsukazaki, T., Chiang, T.A., Davison, A.F., et al. (1998) SARA, a FYVE domain protein that recruits Smad2 to the TGFbeta receptor. *Cell*, 95 (6): 779–91. Available at: http://www.ncbi.nlm.nih.gov/pubmed/9865696 (Accessed: 1 February 2018).

Umulis, D., O'Connor, M.B. and Blair, S.S. (2009) The extracellular regulation of bone morphogenetic protein signaling. *Development (Cambridge, England)*, 136 (22): 3715–28. doi:10.1242/dev.031534.

Urban, S., Kobi, D., Ennen, M., et al. (2015) A Brn2-Zic1 axis specifies the neuronal fate of retinoic-acid-treated embryonic stem cells. *Journal of cell science*, 128 (13): 2303–18. doi:10.1242/jcs.168849.

Vallier, L., Mendjan, S., Brown, S., et al. (2009) Activin/Nodal signalling maintains pluripotency by controlling Nanog expression. *Development (Cambridge, England)*, 136 (8): 1339–49. doi:10.1242/dev.033951.

Venkateswarlu, K., Brandom, K.G. and Lawrence, J.L. (2004) Centaurin-alpha1 is an in vivo phosphatidylinositol 3,4,5-trisphosphate-dependent GTPase-activating protein for ARF6 that is involved in actin cytoskeleton organization. *The Journal of biological chemistry*, 279 (8): 6205–8. doi:10.1074/jbc.C300482200.

Vigano, M.A. and Staudt, L.M. (1996) Transcriptional activation by Oct-3: evidence for a specific role of the POU-specific domain in mediating functional interaction with Oct-1. *Nucleic acids research*, 24 (11): 2112–8. doi:10.1093/nar/24.11.2112.

Villa-Diaz, L.G., Pacut, C., Slawny, N.A., et al. (2009) Analysis of the factors that limit the ability of feeder cells to maintain the undifferentiated state of human embryonic stem cells. *Stem cells and development*, 18 (4): 641–51. doi:10.1089/scd.2008.0010.

Vitale, N., Patton, W.A., Moss, J., et al. (2000) GIT proteins, A novel family of phosphatidylinositol 3,4, 5-trisphosphate-stimulated GTPase-activating proteins for ARF6. *The Journal of biological chemistry*, 275 (18): 13901–6. doi:10.1074/jbc.275.18.13901.

Wang, Z., Oron, E., Nelson, B., et al. (2012) Distinct lineage specification roles for NANOG, OCT4, and SOX2 in human embryonic stem cells. *Cell stem cell*, 10 (4): 440–54. doi:10.1016/j.stem.2012.02.016.

Warmflash, A., Sorre, B., Etoc, F., et al. (2014) A method to recapitulate early embryonic spatial patterning in human embryonic stem cells. *Nature methods*, 11 (8): 847–54. doi:10.1038/nmeth.3016.

Warren, L., Manos, P.D., Ahfeldt, T., et al. (2010) Highly efficient reprogramming to pluripotency and directed differentiation of human cells with synthetic modified mRNA. *Cell stem cell*, 7 (5): 618–30.

doi:10.1016/j.stem.2010.08.012.

Watt, F.M. and Hogan, B.L. (2000) Out of Eden: stem cells and their niches. *Science (New York, N.Y.)*, 287 (5457): 1427–30. doi:10.1126/science.287.5457.1427.

van Weering, J.R.T., Sessions, R.B., Traer, C.J., et al. (2012) Molecular basis for SNX-BAR-mediated assembly of distinct endosomal sorting tubules. *The EMBO journal*, 31 (23): 4466–80. doi:10.1038/emboj.2012.283.

Weiss, A. and Attisano, L. (2013) The TGFbeta superfamily signaling pathway. *Wiley interdisciplinary reviews. Developmental biology*, 2 (1): 47–63. doi:10.1002/wdev.86.

Wenk, M.R. and De Camilli, P. (2004) Protein-lipid interactions and phosphoinositide metabolism in membrane traffic: insights from vesicle recycling in nerve terminals. *Proceedings of the National Academy of Sciences of the United States of America*, 101 (22): 8262–9. doi:10.1073/pnas.0401874101.

Wrana, J.L. (2013) Signaling by the TGFβ superfamily. *Cold Spring Harbor perspectives in biology*, 5 (10): a011197. doi:10.1101/cshperspect.a011197.

Wrighton, K.H. and Feng, X.-H. (2008) To (TGF)beta or not to (TGF)beta: fine-tuning of Smad signaling via post-translational modifications. *Cellular signalling*, 20 (9): 1579–91. doi:10.1016/j.cellsig.2008.02.003.

Wu, G., Chen, Y.G., Ozdamar, B., et al. (2000) Structural basis of Smad2 recognition by the Smad anchor for receptor activation. *Science (New York, N.Y.)*, 287 (5450): 92–7. doi:10.1126/SCIENCE.287.5450.92.

Wu, J. and Izpisua Belmonte, J.C. (2016) Stem Cells: A Renaissance in Human Biology Research. *Cell*, 165 (7): 1572–85. doi:10.1016/j.cell.2016.05.043.

Wu, J.W., Hu, M., Chai, J., et al. (2001) Crystal structure of a phosphorylated Smad2. Recognition of phosphoserine by the MH2 domain and insights on Smad function in TGF-beta signaling. *Molecular cell*, 8 (6): 1277–89. Available at: http://www.ncbi.nlm.nih.gov/pubmed/11779503 (Accessed: 1 February 2018).

Xiao, L., Yuan, X. and Sharkis, S.J. (2006) Activin A maintains self-renewal and regulates fibroblast growth factor, Wnt, and bone morphogenic protein pathways in human embryonic stem cells. *Stem cells (Dayton, Ohio)*, 24 (6): 1476–86. doi:10.1634/stemcells.2005-0299.

Xing, Y., Böcking, T., Wolf, M., et al. (2010) Structure of clathrin coat with bound Hsc70 and auxilin: mechanism of Hsc70-facilitated disassembly. *The EMBO journal*, 29 (3): 655–65. doi:10.1038/emboj.2009.383.

Xu, J.S., Lee, Y.L., Lee, K.F., et al. (2004) Embryotrophic factor-3 from human oviductal cells enhances proliferation, suppresses apoptosis and stimulates the expression of the beta1 subunit of sodium-potassium ATPase in mouse embryos. *Human reproduction (Oxford, England)*, 19 (12): 2919–26. doi:10.1093/humrep/deh497.

Xu, L., Frankel, P., Jackson, D., et al. (2003) Elevated phospholipase D activity in H-Ras- but not K-Ras-transformed cells by the synergistic action of RalA and ARF6. *Molecular and cellular biology*, 23 (2): 645–54. doi:10.1128/MCB.23.2.645-654.2003.

Xu, L., Kang, Y., Cöl, S., et al. (2002) Smad2 nucleocytoplasmic shuttling by nucleoporins CAN/Nup214 and Nup153 feeds TGFbeta signaling complexes in the cytoplasm and nucleus. *Molecular cell*, 10 (2): 271–82. Available at: http://www.ncbi.nlm.nih.gov/pubmed/12191473 (Accessed: 1 February 2018).

Xu, R.-H., Peck, R.M., Li, D.S., et al. (2005) Basic FGF and suppression of BMP signaling sustain undifferentiated proliferation of human ES cells. *Nature methods*, 2 (3): 185–90. doi:10.1038/nmeth744.

Xu, R.-H., Sampsell-Barron, T.L., Gu, F., et al. (2008) NANOG is a direct target of TGFbeta/activin-mediated SMAD signaling in human ESCs. *Cell stem cell*, 3 (2): 196–206. doi:10.1016/j.stem.2008.07.001.

Xu, X., Browning, V.L. and Odorico, J.S. (2011) Activin, BMP and FGF pathways cooperate to promote endoderm and pancreatic lineage cell differentiation from human embryonic stem cells. *Mechanisms of development*, 128 (7–10): 412–27. doi:10.1016/j.mod.2011.08.001.

Xue, G., Restuccia, D.F., Lan, Q., et al. (2012) Akt/PKB-mediated phosphorylation of Twist1 promotes tumor metastasis via mediating cross-talk between PI3K/Akt and TGF-β signaling axes. *Cancer discovery*, 2 (3): 248–59. doi:10.1158/2159-8290.CD-11-0270.

Yagi, K., Goto, D., Hamamoto, T., et al. (1999) Alternatively spliced variant of Smad2 lacking exon 3. Comparison with wild-type Smad2 and Smad3. *The Journal of biological chemistry*, 274 (2): 703–9. Available at: http://www.ncbi.nlm.nih.gov/pubmed/9873005 (Accessed: 1 February 2018).

Yamashita, M., Fatyol, K., Jin, C., et al. (2008) TRAF6 mediates Smad-independent activation of JNK and p38 by TGF-beta. *Molecular cell*, 31 (6): 918–24. doi:10.1016/j.molcel.2008.09.002.

Yang, J., Plikus, M. V. and Komarova, N.L. (2015) The Role of Symmetric Stem Cell Divisions in Tissue Homeostasis. *PLoS computational biology*, 11 (12): e1004629. doi:10.1371/journal.pcbi.1004629.

Yao, D., Ehrlich, M., Henis, Y.I., et al. (2002) Transforming growth factor-beta receptors interact with AP2 by direct binding to beta2 subunit. *Molecular biology of the cell*, 13 (11): 4001–12. doi:10.1091/mbc.02-07-0104.

Yi, J.Y., Shin, I. and Arteaga, C.L. (2005) Type I transforming growth factor beta receptor binds to and activates phosphatidylinositol 3-kinase. *The Journal of biological chemistry*, 280 (11): 10870–6. doi:10.1074/jbc.M413223200.

Yin, X., Murphy, S.J., Wilkes, M.C., et al. (2013) Retromer maintains basolateral distribution of the type II TGF-β receptor via the recycling endosome. *Molecular biology of the cell*, 24 (14): 2285–98. doi:10.1091/mbc.E13-02-0093.

Ying, Q.L., Nichols, J., Chambers, I., et al. (2003) BMP induction of Id proteins suppresses differentiation and sustains embryonic stem cell self-renewal in collaboration with STAT3. *Cell*, 115 (3): 281–92. doi:10.1016/S0092-8674(03)00847-X.

Yu, J., Hu, K., Smuga-Otto, K., et al. (2009) Human induced pluripotent stem cells free of vector and transgene sequences. *Science (New York, N.Y.)*, 324 (5928): 797–801. doi:10.1126/science.1172482.

Yu, J., Vodyanik, M. a, Smuga-Otto, K., et al. (2007) Induced pluripotent stem cell lines derived from human somatic cells. *Science (New York, N.Y.)*, 318 (5858): 1917–20. doi:10.1126/science.1151526.

Yu, P., Pan, G., Yu, J., et al. (2011) FGF2 sustains NANOG and switches the outcome of BMP4-induced human embryonic stem cell differentiation. *Cell stem cell*, 8 (3): 326–34. doi:10.1016/j.stem.2011.01.001.

Yu, X., Zou, J., Ye, Z., et al. (2008) Notch signaling activation in human embryonic stem cells is required for embryonic, but not trophoblastic, lineage commitment. *Cell stem cell*, 2 (5): 461–71.

doi:10.1016/j.stem.2008.03.001.

Zawel, L., Dai, J.L., Buckhaults, P., et al. (1998) Human Smad3 and Smad4 are sequence-specific transcription activators. *Molecular cell*, 1 (4): 611–7. Available at: http://www.ncbi.nlm.nih.gov/pubmed/9660945 (Accessed: 1 February 2018).

Zhang, L., Deng, M., Parthasarathy, R., et al. (2005) MEKK1 transduces activin signals in keratinocytes to induce actin stress fiber formation and migration. *Molecular and cellular biology*, 25 (1): 60–5. doi:10.1128/MCB.25.1.60-65.2005.

Zhang, P., Li, J., Tan, Z., et al. (2008) Short-term BMP-4 treatment initiates mesoderm induction in human embryonic stem cells. *Blood*, 111 (4): 1933–41. doi:10.1182/blood-2007-02-074120.

Zhang, S. and Cui, W. (2014) Sox2, a key factor in the regulation of pluripotency and neural differentiation. *World journal of stem cells*, 6 (3): 305–11. doi:10.4252/wjsc.v6.i3.305.

Zhang, Z.-N., Chung, S.-K., Xu, Z., et al. (2014) Oct4 maintains the pluripotency of human embryonic stem cells by inactivating p53 through Sirt1-mediated deacetylation. *Stem cells (Dayton, Ohio)*, 32 (1): 157–65. doi:10.1002/stem.1532.

Zhang, Z., Lin, H., Shi, M., et al. (2012) Human umbilical cord mesenchymal stem cells improve liver function and ascites in decompensated liver cirrhosis patients. *Journal of gastroenterology and hepatology*, 27 Suppl 2: 112–20. doi:10.1111/j.1440-1746.2011.07024.x.

Zhao, H. and Jin, Y. (2017) Signaling networks in the control of pluripotency. *Current opinion in genetics & development*, 46: 141–148. doi:10.1016/j.gde.2017.07.013.

Zhou, H., Wu, S., Joo, J.Y., et al. (2009) Generation of induced pluripotent stem cells using recombinant proteins. *Cell stem cell*, 4 (5): 381–4. doi:10.1016/j.stem.2009.04.005.

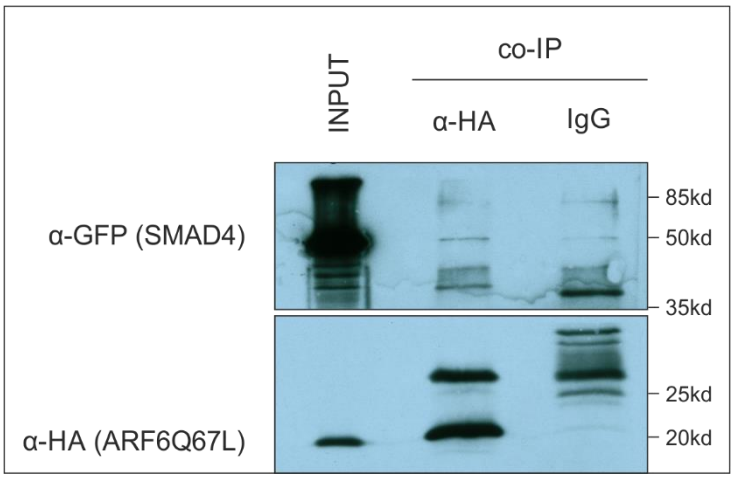
Zhou, Q., Heinke, J., Vargas, A., et al. (2007) ERK signaling is a central regulator for BMP-4 dependent capillary sprouting. *Cardiovascular research*, 76 (3): 390–9. doi:10.1016/j.cardiores.2007.08.003.

Zhou, Y., Scolavino, S., Funderburk, S.F., et al. (2004) Receptor internalization-independent activation of Smad2 in activin signaling. *Molecular endocrinology (Baltimore, Md.)*, 18 (7): 1818–26. doi:10.1210/me.2004-0079.

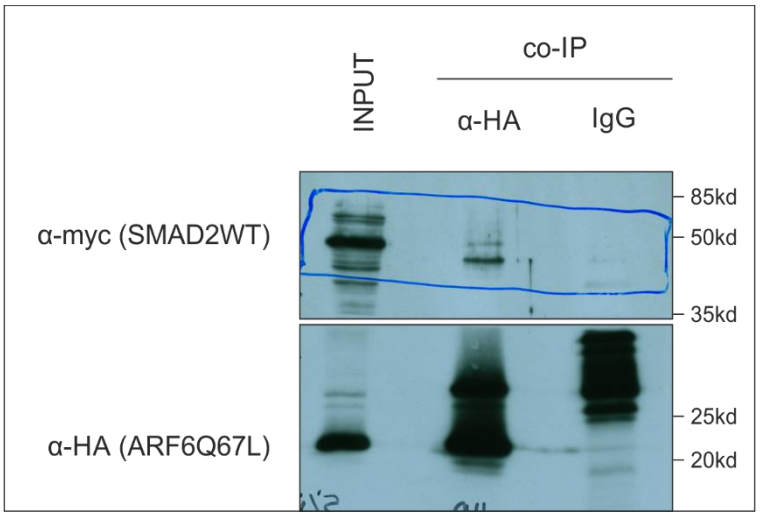
Zimmermann, P., Zhang, Z., Degeest, G., et al. (2005) Syndecan recycling [corrected] is controlled by syntenin-PIP2 interaction and Arf6. *Developmental cell*, 9 (3): 377–88. doi:10.1016/j.devcel.2005.07.011.

Zirra, A., Wiethoff, S. and Patani, R. (2016) Neural Conversion and Patterning of Human Pluripotent Stem Cells: A Developmental Perspective. *Stem cells international*, 2016: 8291260. doi:10.1155/2016/8291260.

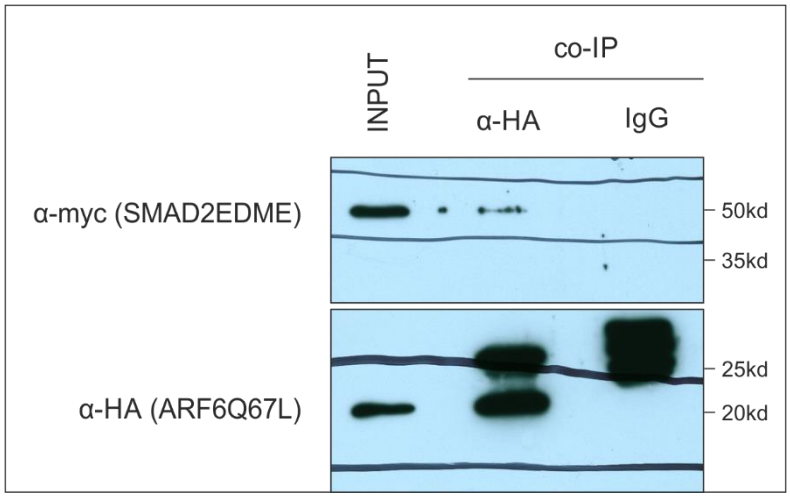
APPENDIX



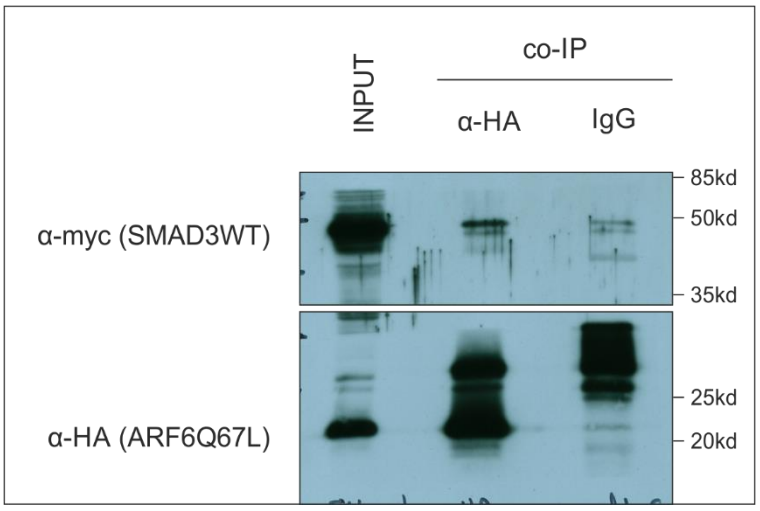
Supplementary Figure 1: Raw Data of Figure 3.1 (B)



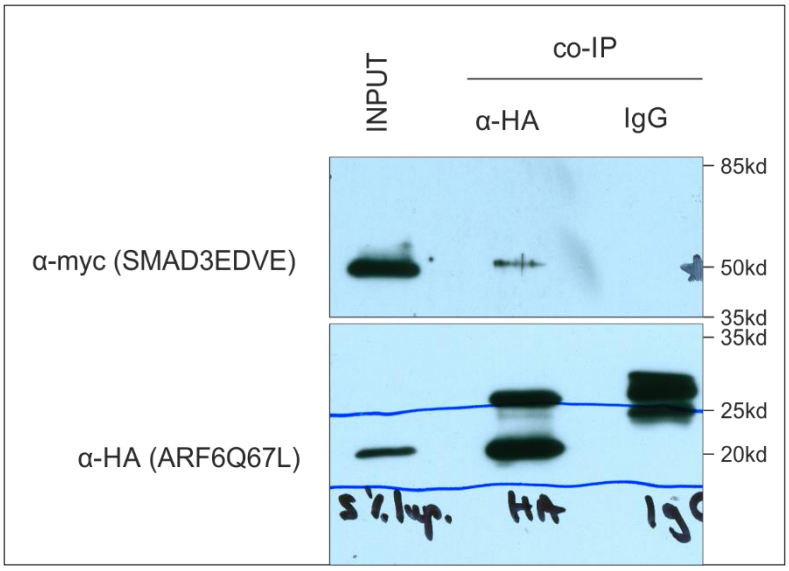
Supplementary Figure 2: Raw Data of Figure 3.4 (A)



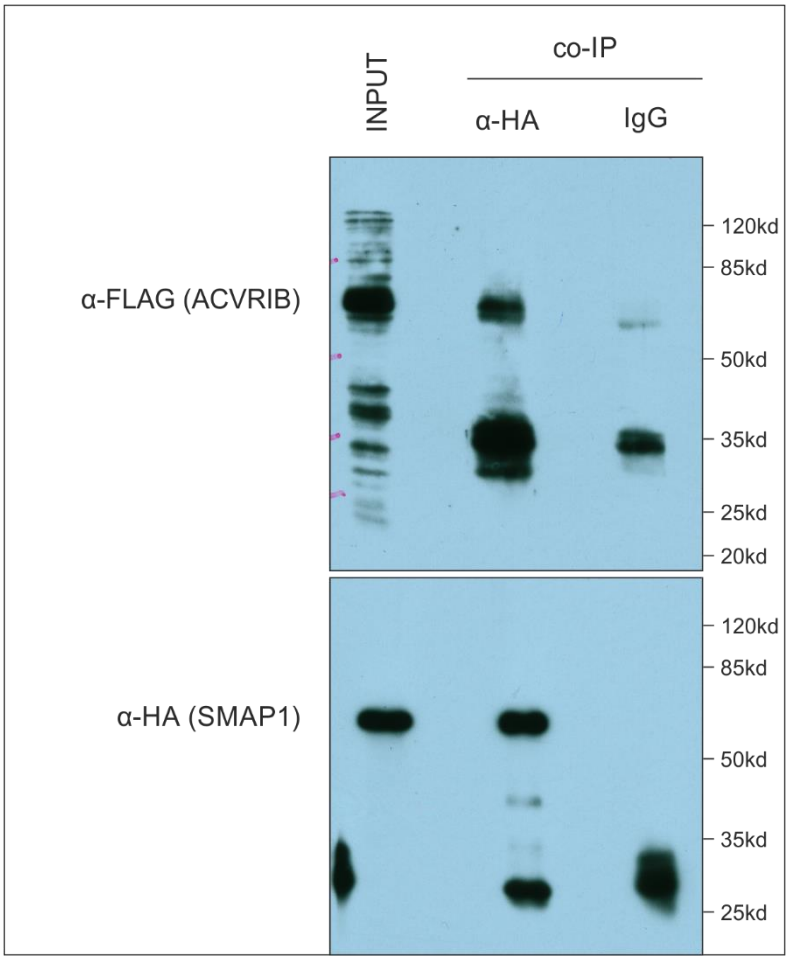
Supplementary Figure 3: Raw Data of Figure 3.4 (B)



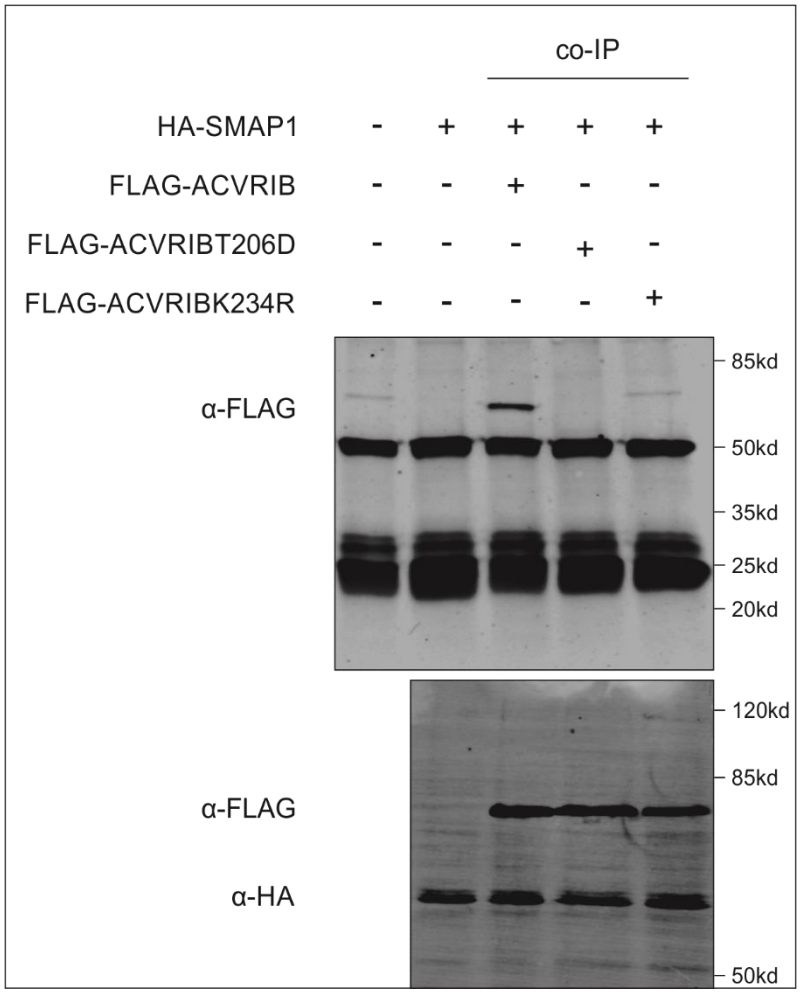
Supplementary Figure 4: Raw Data of Figure 3.4 (C)



Supplementary Figure 5: Raw Data of Figure 3.4 (D)



Supplementary Figure 6: Raw Data of Figure 3.8 (B)



Supplementary Figure 7: Interaction of SMAP1 with the Wild Type ACVR1B

HEK-293 cells overexpressing HA-SMAP1 and FLAG-ACVR1B, FLAG-ACVR1BK234R or FLAG-ACVR1BT206D were lysed using 1% Triton X-100 lysis buffer, and subjected to immunoprecipitation using α-HA antibody. Immunocomplexes were washed, subjected to SDS-PAGE and immunoblotted with an α-FLAG antibody to confirm the immunoprecipitations. In the 1st lane of the upper panel only α-HA antibody is loaded.